BioMed Research International

Application of Biotechnology for the Production of Biomass-Based Fuels

Lead Guest Editor: Liandong Zhu
Guest Editors: Ningbo Gao and Rong-Gang Cong

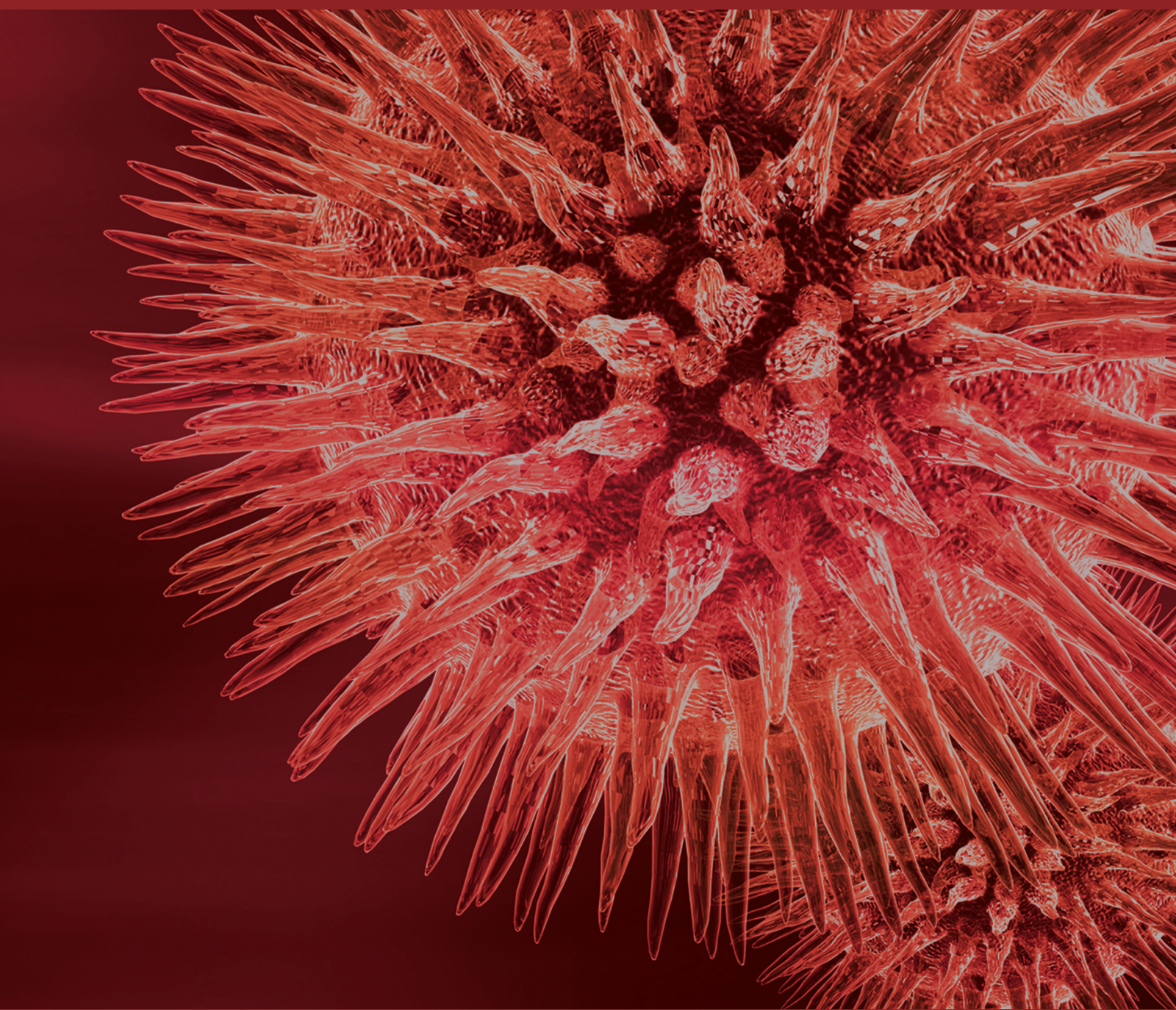

Application of Biotechnology for the Production of Biomass-Based Fuels

BioMed Research International

Application of Biotechnology for the Production of Biomass-Based Fuels

Lead Guest Editor: Liandong Zhu
Guest Editors: Ningbo Gao and Rong-Gang Cong

Contents

Hindawi
BioMed Research International
Volume 2017, Article ID 3896505, 2 pages
https://doi.org/10.1155/2017/3896505

Editorial

Application of Biotechnology for the Production of Biomass-Based Fuels

Liandong Zhu,[1] Ningbo Gao,[2] and Rong-Gang Cong[3]

[1]*Department of Energy Technology, University of Vaasa, 65101 Vaasa, Finland*
[2]*School of Energy and Power Engineering, Xi'an Jiaotong University, Xi'an 710049, China*
[3]*Department of Environmental Science, Aarhus University, 4000 Roskilde, Denmark*

Correspondence should be addressed to Liandong Zhu; zliand@uva.fi

Received 4 January 2017; Accepted 5 January 2017; Published 23 May 2017

In response to the energy crisis, global warming, and climate changes, biomass has received a great deal of interest as a promising feedstock for the production of biofuels. Biofuels derived from biomass are renewable and sustainable energies with the potential to replace fossil fuels. In addition, the development of biofuels might reduce a country's reliance on crude oil imports, mitigate greenhouse gas emissions, and increase regional incomes. To determine the stand of the latest available biotechnologies and keep the global academic communities up to date to the current advances in the conversion of biomass to biofuels, this special issue is publishing 10 quality papers with the focus on the application of biotechnology for the production of biomass-based fuels.

The paper titled "Isoprene Production on Enzymatic Hydrolysate of Peanut Hull Using Different Pretreatment Methods" by S. Wang et al. described the work on the use of peanut hull for isoprene production. The authors applied two pretreatment methods, hydrogen peroxide-acetic acid (HPAC) and popping, prior to enzymatic hydrolysis. Results demonstrated that the isoprene production on enzymatic hydrolysate with HPAC pretreatment was about 1.9-fold higher than that of popping pretreatment. The amount and category of inhibitors such as formic acid, acetic acid, and HMF varied among different enzymatic hydrolysates. In addition, results showed that the enzymatic hydrolysate of HPAC was detoxified by activated carbon.

The paper titled "Studies on the Ecological Adaptability of Growing Rice with Floating Bed on the Dilute Biogas Slurry" by Q. Kang et al. assessed the adaptability and possibility of growing rice on floating beds with diluted biogas slurry. The authors discovered that the growth stage, rice plant height, and rice yield and quality were significantly affected by multiple dilutions. It is found that the rice plants cultivated with 45 multiple dilutions had better ecological adaptability than others. Their study showed that it is possible and safe to cultivate rice plants with diluted biogas slurry. The yield, milled rice rate, and crude protein of the rice cultivated with slurry are not as much as those of rice cultivated with regular way in soil.

The paper titled "Strategies for Lipid Production Improvement in Microalgae as a Biodiesel Feedstock" by L. D. Zhu et al. presents a review on the application of the strategies to activate lipid accumulation, which opens the door for lipid overproduction in microalgae. The review highlights the main approaches for microalgal lipid accumulation induction to expedite the application of microalgal biodiesel as an alternative to fossil diesel for sustainable environment. To promote microalgal biodiesel production during the scale-up process, the achievement of lipid overproduction is essential, and certain appropriate strategies can help realize the goal. But, in practice, the lipid-inducing strategies can also be combined in an effort to achieve lipid production optimization.

The paper titled "Simultaneous Saccharification and Fermentation of Sugar Beet Pulp for Efficient Bioethanol Production" by J. Berłowska et al. explored an approach to investigate the effects of pretreatment, the dosage of cellulase and hemicellulase enzyme, and aeration on the release of fermentable sugars and ethanol yield during the simultaneous saccharification and fermentation (SSF) of sugar beet pulp-based worts. The results showed that a 6 h interval for enzymatic activation between the application of enzyme preparations and inoculation with ethanol red could further

improve the fermentation performances, with the highest ethanol concentration reaching 26.9 g/L and 86.5% fermentation, compared to the theoretical yield.

The paper titled "Application of the Initial Rate Method in Anaerobic Digestion of Kitchen Waste" by L. Feng et al. developed a method of methane production through the determination of the hydrolysis constants and reaction orders at both low total solid (TS) concentrations and high TS concentrations. The results showed that the first-order hydrolysis model better reflected the kinetic process of gas production. During the experiment, all the influential factors of anaerobic fermentation retained their optimal values. For a long reaction time, the authors believed that the hydrolysis involved in anaerobic fermentation of kitchen waste could be regarded as a first-order reaction in terms of reaction kinetics.

The paper titled "Outdoor Growth Characterization of an Unknown Microalga Screened from Contaminated Chlorella Culture" by S. Huo et al. used 18 s rDNA molecular technology to isolate and identify one wild strain *Scenedesmus* sp. F. S. from the culture of *Chlorella zofingiensis*. The authors discovered that *Scenedesmus* sp. F. S. showed good alkali resistance and robust adaption to the stress of the outdoor environment. Furthermore, under normal conditions, the oil content of *Scenedesmus* sp. F. S. could reach more than 22.0%, and C16–C18 content could reach up to 79.7%, showing that it had great potential as a large-scale cultivation strain for biodiesel production.

The paper authored by C. Quan and N. Gao provides a review on the copyrolysis of coal and biomass and then compares their results with those obtained using coal and biomass pyrolysis in detail. They also discuss the effects of reaction parameters such as feedstock types, blending ratio, heating rate, temperature, and reactor types on the occurrence of synergy and point out the main properties of the copyrolytic products.

The paper written by K. T. Dasa et al. examined the inhibitory effects of LCFAs (palmitic, stearic, and oleic acid) on biogas production as well as the protective effect of a membrane bioreactor (MBR) against LCFAs. Their findings showed that palmitic and oleic acid with concentrations of 3.0 and 4.5 g/L resulted in >50% inhibition on the biogas production, while stearic acid had an even stronger inhibitory effect. The encased cells in the MBR system were found to be able to perform better in the presence of LCFAs.

The paper authored by I. Masin and M. Petru dealt with the complex approach to design specification that could bring new innovative concepts to the design of mechanical machines for oil extraction. Their presented case study as the main part of the paper focused on the new concept of the screw of machine mechanically extracting oil from *Jatropha curcas* L. seeds.

The paper written by Wang et al. conducted the FTIR analysis which showed that the chemical structure of lignin was broken down in the LHW process. In addition, they also explored the impact of untreated and treated lignin on the enzymatic hydrolysis of cellulose. They also found that the LHW-treated lignin had little impact on the cellulase adsorption and enzyme activities and somehow could improve the enzymatic hydrolysis of cellulose.

Acknowledgments

We would like to thank all the authors for their excellent contributions to this special issue.

Liandong Zhu
Ningbo Gao
Rong-Gang Cong

Hindawi
BioMed Research International
Volume 2017, Article ID 3808521, 7 pages
https://doi.org/10.1155/2017/3808521

Research Article

Application of the Initial Rate Method in Anaerobic Digestion of Kitchen Waste

Lei Feng,[1] Yuan Gao,[1] Wei Kou,[2] Xianming Lang,[3] Yiwei Liu,[3] Rundong Li,[1] Meiling Yu,[2] Lijie Shao,[2] and Xiaoming Wang[2]

[1]*Liaoning Province Clean Energy Key Laboratory, Shenyang Aerospace University, Shenyang Daoyi Street 37, Shenyang 110136, China*
[2]*Liaoning Institute of Energy Resources, 65# Yingquan St., Yingkou, Liaoning, China*
[3]*Liaoning Academy of Environmental Sciences, 30# Shuangyuan St., Shenyang, Liaoning 115003, China*

Correspondence should be addressed to Wei Kou; kouwei6@126.com

Received 16 June 2016; Revised 28 November 2016; Accepted 15 December 2016; Published 4 May 2017

Academic Editor: Liandong Zhu

This article proposes a methane production approach through sequenced anaerobic digestion of kitchen waste, determines the hydrolysis constants and reaction orders at both low total solid (TS) concentrations and high TS concentrations using the initial rate method, and examines the population growth model and first-order hydrolysis model. The findings indicate that the first-order hydrolysis model better reflects the kinetic process of gas production. During the experiment, all the influential factors of anaerobic fermentation retained their optimal values. The hydrolysis constants and reaction orders at low TS concentrations are then employed to demonstrate that the first-order gas production model can describe the kinetics of the gas production process. At low TS concentrations, the hydrolysis constants and reaction orders demonstrated opposite trends, with both stabilizing after 24 days at 0.99 and 1.1252, respectively. At high TS concentrations, the hydrolysis constants and the reaction orders stabilized at 0.98 (after 18 days) and 0.3507 (after 14 days), respectively. Given sufficient reaction time, the hydrolysis involved in anaerobic fermentation of kitchen waste can be regarded as a first-order reaction in terms of reaction kinetics. This study serves as a good reference for future studies regarding the kinetics of anaerobic digestion of kitchen waste.

1. Introduction

Kitchen waste constitutes a key part of municipal waste, making up as much as 30% to 50% of municipal solid waste according to the National Environment Bulletin [1]. In China alone in 2012, the amount of kitchen waste produced was 110 million tons [2]. Kitchen waste is sometimes used as animal feed [3, 4], but it is also deposited in landfills, resulting in reduced landfill capacity and environmental issues [5–7]. Consisting of organics containing starch, protein, fiber, and fat, kitchen waste is characterized by high water content, high organic content, and exposure to acidification [8]. Therefore, anaerobic digestion is regarded as an effective way to recycle kitchen waste, as it disposes of the waste without producing contaminants. Meanwhile, methane, a clean energy source, can be produced by anaerobic digestion, making this process an example of good resource utilization [9, 10]. Additionally, solid waste produced by anaerobic digestion contains high nitrogen and phosphorus contents, such that it can be used as organic fertilizer [11, 12] or feed for microalgae that produces biodiesels [13]. In this way, addressing kitchen waste with anaerobic digestion can promote recovery and reuse of resources.

The first step in investigating reaction kinetics is to determine the order of the reaction, which is an indicator of the effect of reactant concentrations on reaction rates, as well as a key parameter for studying the reaction mechanism. Four approaches have so far been proposed for determining reaction order: the integration method, the differential method, the half-life method, and the initial rate method [14, 15]. The initial rate method is an easy and effective method for determining reaction order. Defined as the transient rate at the beginning of a reaction under certain conditions, the initial rate is recognized as a good indicator of the relationship between reactant concentrations and reaction rates as reverse reactions and side reactions are negligible at

this stage. Wanasolo et al. determined the hydrolysis constant and reaction order in anaerobic digestion of fruits using the initial rate method [16]. This study investigates trends of the hydrolysis constant and reaction order in anaerobic digestion of kitchen waste during experimental periods based on the initial rate method and the methane yield. The results demonstrate that anaerobic digestion of kitchen waste can be described and predicted by the first-order reaction model.

2. Materials and Methods

2.1. Raw Materials and Inoculum. Kitchen waste was obtained from the canteen of a local university. Nondegradable substances such as fishbone and disposable chopsticks were removed, and the waste was then cut into 1 cm × 1 cm × 0.5 cm cubes and stored at 4°C. The total solid (TS) concentration and volatile solid (VS) concentration were 23.31% and 92.84%, respectively. Sewage sludge used as inoculum was obtained from a local sewage plant and treated at mild temperatures. The TS concentration, VS concentration, and carbon-to-nitrogen (C/N) ratio of the sewage sludge were 11.26%, 77.79%, and 7.41, respectively.

2.2. Equipment and Methods. The customized reactor consisted of three 1 L wide mouth bottles used as a reaction bottle, gas collection bottle, and water collection bottle. For the three low TS concentration tests, 17.8 g, 60.7 g, and 103.6 g raw materials were mixed with 300 mL sludge in the reaction bottle. Water was added as needed so that the solutions in all reaction bottles reached 1 L. In these cases, the initial TS concentrations were 4%, 5%, and 6%, respectively. For the three high TS concentration tests, 330.7 g, 352.1 g, and 373.6 g raw materials were mixed with 150 mL sludge in the reaction bottle. Water was added as needed so that solutions in all reaction bottles reached 500 mL. In these cases, the initial TS concentrations were 19%, 20%, and 21%, respectively. High purity N_2 was then injected into each reactor for 5 min to eject air. The reaction bottles and gas collection bottles were connected by glass tubes and pretreated latex tubes, followed by sealing using rubber stoppers and sealant. Thermostatic water baths were used to maintain the designated temperature. Each experiment was designed to group 3 parallel samples. After adding water to the fermentation reactor to the level (1L), all reaction bottles were incubated at 37°C in the water bath for 30 d, during which period stirring was conducted twice a day. The pH values of the solutions and gas produced were measured daily to avoid issues such as the inhibition phenomenon.

During the anaerobic fermentation process, all of the influential factors retained their optimal values. Specifically, the fermentation tank was heated in water to maintain an internal temperature of 37°C, which is ideal for anaerobic fermentation. The pH values of the solutions were adjusted to fall within a range of 6.8 to 7.2. In addition, the fermentation tank was shaken twice a day for purposes of stirring, and it was sealed at all times.

2.3. Analytical Methods. The products in the TS concentration group and the VS concentration group were heated to 103–105°C and 600°C, respectively. The pH values of the solutions were determined using a digital pH meter. The volume of the produced gas was measured using the saturated salt water replacement method.

2.4. Anaerobic Fermentation Kinetic Model

2.4.1. Population Growth Model. The logistic equation is written as follows:

$$P = \frac{P_{\max}}{1 + \exp\left[\left(4R_{\max}\left(\lambda - t\right)/P_{\max}\right) + 2\right]}, \quad (1)$$

where P is the accumulated amount of methane produced per unit volatile organics at t moment (mL/gVS), $P_{\max}$ is the maximum production potential of methane (mL/gVS), $R_{\max}$ is the maximum production rate of methane (mL/gVS/d), t is the reaction period (d), and λ is the delay time (d).

The modified Gompertz equation is copied as follows:

$$M = P \times \exp\left\{-\exp\left[\frac{R_m \times e}{P}\left(\lambda - t\right) + 1\right]\right\}, \quad (2)$$

where M is the accumulated amount of methane produced per unit volatile organics at t moment (mL/gVS), P is the ultimate amount of methane produced per unit volatile organics (mL/gVS), R_m is the maximum production rate of methane (mL/gVS/d), t is the reaction period (d), and λ is the delay time (d).

The P, $P_{\max}$, and $P_{\max}$ values in the logistic equation are identical to the kinetic parameters M, P, and R_m in the modified Gompertz equation. This study adopted the nonlinear regression method using the Origin 8.0 software to carry out the kinetic parametric analysis for the logistic equation and modified Gompertz equation.

2.4.2. First-Order Gas Production Model. A first-order gas production model [17] was developed based on previous studies demonstrating that biodegradable organics convert into methane in certain ratios [18]:

$$\frac{1}{t}\ln\left(\frac{\mathrm{d}y_t}{\mathrm{d}t}\right) = \frac{1}{t}\left(\ln\left(y_m\right) + \ln k\right) - k, \quad (3)$$

where y_m is the theoretical amount of methane produced per unit volatile organics (mL/gVS), y_t is the practical amount of methane produced per unit volatile organics at t moment (mL/gVS), t is the reaction period (d), and k is the hydrolysis constant (d − 1).

In this way, $\ln\left(y_m\right) + \ln k$ and k of the corresponding organics can be identified.

2.5. Initial Rate Method. The procedures of the initial rate method are as follows: Assuming the reaction follows $bB + cC = dA$, the reaction rate (r) can be obtained by

$$r = -kc\left(B\right)^m c\left(C\right)^n = kc\left(A\right)^o, \quad (4)$$

where $c(B)$ and $c(C)$ are the initial concentrations of reactants B and C, while $c(A)$ is the concentration of product A at the end of the reaction; m, n, and o represent the reaction orders of B, C, and A, respectively [16].

Table 1: Standard Gibbs free energy change when using glucose as fermentation substrate and bacteria for hydrolysis, acid production, and fermentation.

Reaction equation (pH = 7, T = 298.15 K)	ΔG^{θ} (kJ/mol)	ΔS
$C_6H_{12}O_6 + 4H_2O + 2NAD^+ \longrightarrow 2CH_3COO^- + 2HCO_3^- + 2NADH + 2H_2 + 6H^+$	−215.67 < 0	>0
$C_6H_{12}O_6 + 2NADH \longrightarrow 2CH_3CH_2COO^- + 2H_2O + 2NAD^+$	−357.87 < 0	>0
$C_6H_{12}O_6 + 4H_2O \longrightarrow 2CH_3COO^- + 2HCO_3^- + 4H_2 + 4H^+$	−184.20 < 0	>0
$C_6H_{12}O_6 + 2H_2O \longrightarrow CH_3CH_2CH_2COO^- + 2HCO_3^- + 2H_2 + 3H^+$	−261.46 < 0	>0
$C_6H_{12}O_6 + 2H_2O + 2NADH \longrightarrow 2CH_3CH_2OH + 2HCO_3^- + 2NAD^+ + 2H_2$	−234.83 < 0	>0
$C_6H_{12}O_6 \longrightarrow 2CH_3CHOHCOO^- + 2H^+$	−217.70 < 0	>0

Table 2: Standard Gibbs free energy change when using hydrogen-producing acetogens for metabolism of organic acids and alcohols.

Reaction equation (pH = 7, T = 298.15 K)	ΔG^{θ} (kJ/mol)	ΔS
$CH_3CH_2OH + H_2O \longrightarrow CH_3COO^- + 2H_2 + 2H^+$	+9.6 > 0	<0
$CH_3CH_2COO^- + 3H_2O \longrightarrow CH_3COO^- + HCO_3^- + H^+ + 3H_2$	+76.1 > 0	<0
$CH_3CH_2COO^- + 2HCO_3^- \longrightarrow CH_3COO^- + H^+ + 3HCOO^-$	+72.4 > 0	<0
$CH_3CH_2CH_2COO^- + 2H_2O \longrightarrow 2CH_3COO^- + H + 2H_2$	+48.1 > 0	<0
$CH_3CH_2CH_2COO^- + 2HCO_3^- \longrightarrow 2CH3COO^- + H^+ + 2HCOO^-$	+45.5 > 0	<0
$CH_3CH_2CH_2CH_2COO^- + 2H_2O \longrightarrow CH_3COO^- + CH_3CH_2COO^- + H^+ + 2H_2$	+25.1 > 0	<0
$CH_3CHOHCOO^- + 2H_2O \longrightarrow CH_3COO^- + HCO_3^- + H^+ + 2H_2$	−4.2 < 0	>0

The initial rate method is based on different concentrations of reactants. In this study, the concentration of one reactant was assigned three different values for each group, while the concentrations of the other reactants remained constant. As the experiments proceeded, the concentrations of reactants and products were measured regularly.

Anaerobic fermentation refers to a process in which methane is produced from organics; therefore, the amount of methane produced can be recorded and used to investigate the hydrolysis constant and reaction order through the initial rate method. If $C \rightarrow A$ represents the conversion of VS to methane, then $r = -kc^n$, where c denotes the concentration of the reactant, namely, the mass of VS at the beginning. Define the groups with 1, 2, and 3 times the initial TS concentrations as Groups A, B, and C, respectively. Assuming they show consistent hydrolysis constants, then $r_1 = -kc_1^n$ and $r_2 = -kc_2^n$, where r_1/r_2 can be replaced by A_1/A_2 (the ratio of gas produced at a specific moment); then, $A_1/A_2 = {c_1}^n/{c_2}^n$, which can be rearranged as $n = (\ln(A_1/A_2))/(\ln(c_1/c_2))$, from which n can be determined.

3. Results and Discussion

3.1. Entropy Change Analysis of Anaerobic Fermentation Process. Entropy is a state function used to describe and characterize the degree of chaos in a system. The entropy change of a process is only related to the system's initial state and final state, regardless of the approach or method. ΔG denotes the Gibbs free energy change, and $\Delta G = \Delta H - T\Delta S$. Under conditions of constant temperature and pressure, the following associations are true: if $\Delta S > 0$ and $\Delta G < 0$, then a reaction spontaneously occurs; if $\Delta S < 0$ and $\Delta G > 0$, then a reaction occurs nonspontaneously; if $\Delta S = 0$ and $\Delta G = 0$, then the reaction is at an equilibrium state [19]. The entropy change analysis of the anaerobic fermentation process evaluates the process from a new perspective, providing a reliable scientific theory for the development and perfection of anaerobic fermentation technology, as well as the evaluation of treatment effects.

The complicated composition of kitchen waste makes the complete ΔG analysis of the fermentation process difficult; therefore, the digestion substrate of kitchen waste is simplified to glucose for convenience of analysis. In the process of anaerobic fermentation, glucose is first hydrolyzed and acidized into organic acids or alcohols with no less than 2C, then converted into acetic acid, H_2, and CO_2 by hydrogen-producing acetogens, and finally transformed to CH_4 under the action of methanogens. Table 1 elaborates the standard Gibbs free energy change when using glucose as the fermentation substrate and bacteria for hydrolysis, acid production, and fermentation [20, 21].

The data in Table 1 indicate that the standard Gibbs free energy changes for reactions in the hydrolysis, acid production, and fermentation phases are all smaller than zero, which implies that all the reactions take place spontaneously from left to right under standard conditions.

Therefore, the entropy values of these reactions are all greater than zero, and the processes increase entropy.

The standard Gibbs free energy change when using hydrogen-producing acetogens for the metabolism of organic acids and alcohols is shown in Table 2 [20, 22].

According to Table 2, the standard Gibbs free energy changes for most of the reactions at the hydrogen and acetic acid production phases are greater than zero, indicating that most of the reactions do not take place spontaneously from left to right under standard conditions. Therefore, the entropy of these phases is less than zero, indicating an entropy reduction process.

Table 3: Standard Gibbs free energy change when using methanogens for metabolism of intermediates.

Reaction equation (pH = 7, T = 298.15 K)	ΔG^{θ} (kJ/mol)	ΔS
$4CH_3CH_2COO^- + 3H_2O \longrightarrow 4CH_3COO^- + HCO_3^- + H^+ + 3CH_4$	−102.0 < 0	>0
$2CH_3CH_2CH_2COO^- + HCO_3^- + H_2O \longrightarrow 4CH_3COO^- + H^+ + CH_4$	−39.4 < 0	>0
$CH_3COOH \longrightarrow CO_2 + CH_4$	−31.0 < 0	>0
$4HCOOH \longrightarrow 3CO_2 + 2H_2O + CH_4$	−130.1 < 0	>0
$4H_2 + HCO_3^- + H^+ \longrightarrow 3H_2O + CH_4$	−135.6 < 0	>0
$2CH_3CH_2OH + CO_2 \longrightarrow 2CH_2COOH + CH_4$	−116.3 < 0	>0
$CH_3OH + H_2 \longrightarrow H_2O + CH_4$	−112.5 < 0	>0
$4CH_3OH \longrightarrow CO_2 + 2H_2O + 3CH_4$	−104.9 < 0	>0
$4CH_3NH_2 + 2H_2O \longrightarrow CO_2 + 4NH_3 + 3CH_4$	−75.0 < 0	>0
$2(CH_3)_2NH + 2H_2O \longrightarrow CO_2 + 2NH_3 + 3CH_4$	−73.2 < 0	>0
$4(CH_3)_3N + 6H_2O \longrightarrow 3CO_2 + 4NH_3 + 9CH_4$	−74.3 < 0	>0
$2(CH_3)_2S + 2H_2O \longrightarrow CO_2 + 2H_2S + 3CH_4$	−73.8 < 0	>0

Table 4: Fitting parameters for logistic equation.

TS/%	P_{max} (mL/gVS)	R_{max} (mL/gVS/d)	λ (d)	R^2
4	480.60	21.91	−7.42	0.95125
5	534.81	42.48	−1.18	0.97202
6	503.78	32.24	−1.17	0.99414

Furthermore, the numerical values of ΔG^{θ} are generally small. By appropriately modifying some of the reaction conditions, the energy change ΔG^{θ} can be adjusted to fall below 0, prompting the reactions that happen from left to right.

The standard Gibbs free energy change when using methanogens for the metabolism of intermediates is explained in Table 3 [20, 23].

The data in Table 3 show that the standard Gibbs free energy change values for reactions at the methane production phase are all less than zero, signifying that all of the reactions occur spontaneously from left to right under standard conditions. Therefore, the entropy in this phase is greater than zero, meaning that it is an entropy increasing process.

3.2. Result Discussion on Models for Anaerobic Digestion at Low TS Concentrations

3.2.1. Result Discussion on Population Growth Model. The anaerobic fermentation process of kitchen waste with initial TS concentrations of 4%, 5%, and 6% was analyzed using a population growth model. Nonlinear fitting with the software Origin established the fitting parameters for the logistic equation and modified Gompertz equation describing the anaerobic fermentation of kitchen waste at different initial TS concentrations (see Tables 4 and 5).

Tables 4 and 5 reveal that although the values of R^2 differ for different TS concentrations, they all fall between 0.95 and 1. This proves that the population growth model is suitable for simulating anaerobic fermentation and biogas production of kitchen waste at low TS concentrations. For different TS concentrations, the results also certify that the logistic equation and modified Gompertz equation are the right methods for the fitting process of anaerobic fermentation and biogas production of kitchen waste at various TS concentrations. In particular, the modified Gompertz equation shows the greatest gas production potential (540.94 mL/gVS) when applied to kitchen waste at 5% TS concentration, followed by the potentials for kitchen waste at 6% and 4% TS concentrations, which are 513.09 mL/gVS and 485.10 mL/gVS, respectively.

Table 5: Fitting parameters for modified Gompertz equation.

TS (%)	P (mL/gVS)	R_m (mL/gVS/d)	λ (d)	R^2
4	485.10	26.52	−5.53	0.95981
5	540.94	32.18	−4.95	0.98597
6	513.09	23.67	−6.34	0.99705

Because kitchen waste contains a great deal of readily decomposable organic starches like rice and steamed buns, as well as a moderate amount of organic protein like lean meat and eggs, the ratio between carbon and nitrogen during the anaerobic fermentation process is always appropriate. This not only accelerates the hydrolysis reaction but also benefits the growth and reproduction of microbes, thereby ensuring that the reaction proceeds smoothly. In this way, the experiment can generate biogas from the beginning, without any time delay.

3.2.2. Result Discussion of First-Order Gas Production Model. Table 6 shows k and $\ln(y_m) + \ln k$ at different TS concentrations, as predicted by the proposed first-order gas production model. The results show that $R^2 > 0.99$ is valid for all initial TS concentrations, indicating good effectiveness on the part of the proposed model for anaerobic fermentation of kitchen

Table 6: Parameters of anaerobic fermentation of kitchen waste at different TS concentrations predicted by the proposed first-order gas production model.

Initial TS concentration	Parameter		
	$\ln(y_m) + \ln k$	k	R^2
4%	4.8109	0.2179	0.9930
5%	4.1292	0.1170	0.9938
6%	4.2131	0.1430	0.9965

waste at low TS concentrations. Hence, this model was used for theoretical analysis of experimentally obtained data.

k is an indicator of the proportion of biodegradable substances that have been digested, and large k values indicate high reaction rates. While k reflects the rate at which the methane is produced, y_m reflects the amount of gas produced. Therefore, $\ln y_m + \ln k$ combines the overall amount of gas produced and the rate at which it is produced, making it a good indicator of the utilization of the biodegradable substances in the raw material. In other words, $\ln y_m + \ln k$ is a characteristic parameter of the gas production reaction. A large $\ln y_m + \ln k$ value indicates high gas production capacity for the raw materials. Therefore, k values obtained in this study indicate the rates at which organic macromolecules were converted into compounds, while $\ln y_m + \ln k$ values obtained in this study indicate the conversion efficiency of organic macromolecules into methane.

The results revealed that the hydrolysis constants corresponding to TS concentrations of 4%, 5%, and 6% were 0.2179, 0.1170, and 0.1430, respectively. Meanwhile, the values of $\ln y_m + \ln k$ corresponding to TS concentrations of 4%, 5%, and 6% were 4.8109, 4.1292, and 4.2131, respectively, suggesting that the reaction rate was maximized at TS = 4% and minimized at TS = 5%. Additionally, R^2 values of all the groups exceeded 0.99, demonstrating good efficacy of the proposed first-order gas production model in predicting anaerobic fermentation of kitchen waste.

According to the formulas and experimental data from the population growth model and first-order gas production model, both models achieve a satisfying fitting effect for the anaerobic fermentation and biogas production process of kitchen waste with low TS concentrations. In this study, the population growth model always yielded correlation coefficient R^2 values between 0.95 and 1, while the first-order gas production model yielded correlation coefficient R^2 values greater than 0.99. These results indicate that, for kitchen waste with low TS concentrations, the first-order gas production model has the best outcome in fitting the anaerobic fermentation and biogas production process, and it can therefore be used for the theoretical analysis of the experiments in general.

3.3. The Initial Rate Method for Anaerobic Digestion at Low TS Concentrations. Let the groups whose initial TS concentrations are 4%, 5%, and 6% be defined as Groups A, B, and C, respectively. Assuming they show consistent hydrolysis constants, then $r_1 = -kc_1^n$, $r_2 = -kc_2^n$, $n = (\ln(A_1/A_2))/(\ln(c_1/c_2))$. In this way, n can be obtained. During the tests, the hydrolysis constants and the reaction orders of all groups were measured daily, and the average values were recorded and shown in Figure 1.

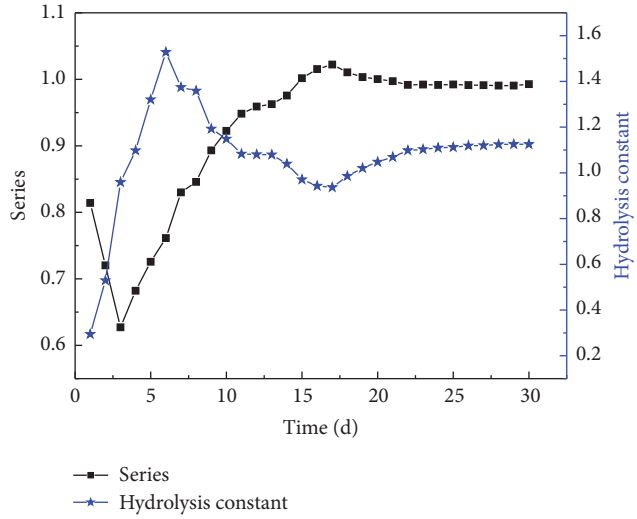

Figure 1: Hydrolysis constant and reaction order of anaerobic fermentation of kitchen waste at low TS concentrations.

The data indicates that the hydrolysis constant and reaction order exhibit opposite trends, although both stabilize eventually. The reaction order decreased during the first three days to a minimum at 0.6822, increased from Day 4 to Day 17, and finally decreased gradually until stabilizing at 0.99 from Day 24. The hydrolysis constant increased during the first six days, decreased from Day 7 to Day 17, and then increased steadily until stabilizing at 1.1252 from Day 24. Therefore, the hydrolysis of kitchen waste with initial TS concentrations of 4%, 5%, and 6% can be described by the first-order hydrolysis dynamic equations proposed.

3.4. The Initial Rate Method for Anaerobic Digestion at High TS Concentrations. In most studies concerning kitchen waste digestion, the first-order hydrolysis constant is obtained based on continuous dry fermentation. For instance, Wu et al. investigated anaerobic digestion of kitchen waste mixed with pig manure at mild temperatures [24]. In that study, feeding of organic matters increased gradually. Li et al. investigated the effects of loading rate on anaerobic digestion of kitchen waste during gradually increasing organic feeding [25]. In contrast to these studies, Lai et al. proposed a gas production model based on semicontinuous anaerobic digestion of kitchen waste mixed with pig manure during gradually increasing organic feeding [26]. Linke investigated the effects of organic loading rate on anaerobic digestion of tomato-based solid waste and obtained k based on first-order hydrolysis reactions [17]. Mähnert and Linke investigated the dynamics of first-order anaerobic digestion of energy crops mixed with animal manure and determined gas production both theoretically and practically, as well as identifying concentrations of volatile solids in the reactor, concentrations of

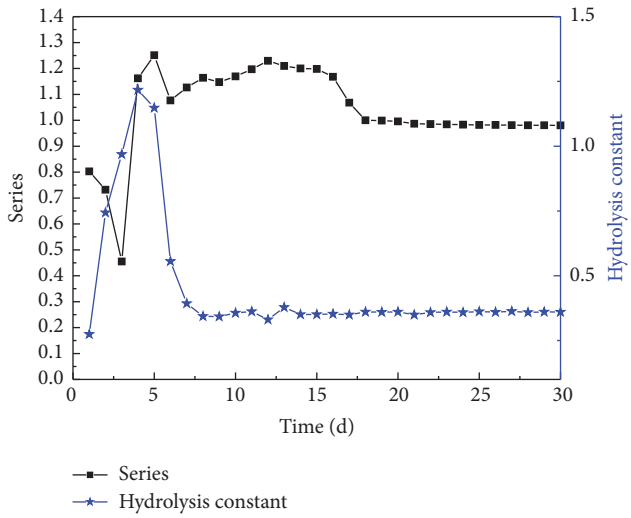

Figure 2: Hydrolysis constant and reaction order of anaerobic fermentation of kitchen waste at high TS concentrations.

outflow liquids, and the reaction rate constant [27]. However, none of these studies demonstrated the first-order model on the anaerobic digestion of kitchen waste alone. This study investigated the orders of sequenced reactions for waste with initial TS concentrations of 19%, 20%, and 21% using the initial rate method in order to provide reference for determining the reaction orders of dry fermentation of kitchen waste, as well as modelling continuous dry fermentation processes.

The average hydrolysis constants and reaction orders for anaerobic digestion of kitchen waste with initial TS concentrations of 19%, 20%, and 21%, from the initial moment to a specific point, were obtained and shown in Figure 2.

As the data shows, the reaction order dropped from 0.8027 to 0.4552 during the first three days and then increased to 1.2511 on Day 5. Afterwards, the hydrolysis constant fluctuated and stabilized at 0.98 after Day 18. In contrast, the hydrolysis constant increased during the first four days until it reached 1.1479; then, it decreased from Day 5 to Day 8, increased again, and stabilized at 0.3507 after Day 14. These results suggest that hydrolysis of kitchen waste with initial TS concentrations of 19%, 20%, and 21% can be described by the first-order hydrolysis dynamic equations proposed.

4. Conclusions

(1) This paper analyzed the entropy changes corresponding to each phase of the anaerobic biological treatment process. In the hydrolysis and acidification phases, the standard Gibbs free energy change $\Delta G^{\theta} < 0$, and the reactions happen spontaneously; therefore, it is an entropy increasing process. In contrast, in the hydrogen and acetic acid production phases, $\Delta G^{\theta} > 0$ for most of the reactions; therefore, it is an entropy reduction process. In the methane production phase, $\Delta G^{\theta} < 0$, and the reactions take place spontaneously; therefore, it is an entropy increasing process. Most of the reactions are spontaneous during the anaerobic biological treatment process; only the hydrogen and acetic acid production phases are nonspontaneous. From the perspective of thermodynamics, these phases require additional energy and matter supply.

(2) This study determined the hydrolysis constants and reaction orders for anaerobic digestion of kitchen waste using the initial rate method, in addition to examining the population growth model and first-order hydrolysis model. The results prove that the first-order hydrolysis model can better reflect the kinetic process of gas production. The results demonstrate the application of the proposed first-order gas production model in anaerobic digestion of kitchen waste.

(3) During 30 days of anaerobic digestion of kitchen waste with low TS concentrations, the hydrolysis constants and the reaction orders demonstrated opposite trends, and both stabilized after 24 days at 0.99 and 1.1252, respectively.

(4) During 30 days of anaerobic digestion of kitchen wastes with high TS concentrations, the hydrolysis constants and reaction orders stabilized at 0.98 (after 18 days) and 0.3507 (after 14 days), respectively. These results demonstrate that hydrolysis of kitchen waste with both low TS concentrations and high TS concentrations can be described using the proposed first-order hydrolysis dynamic equations.

(5) Given sufficient reaction time, the hydrolysis involved in anaerobic fermentation of kitchen waste can be regarded as a first-order reaction in terms of reaction kinetics.

Conflicts of Interest

The authors declare that they have no conflicts of interest.

Acknowledgments

This work was funded by the National Science and Technology support (no. 2014BAC24B01) and the Cultivation Plan for Youth Agricultural Science and Technology Innovative Talents of Liaoning Province support (no. 2014016).

References

[1] W. P. Xie, Y. J. Liang, D. W. He et al., "Food waste of resources technology status and progress," *Environmental Sanitation Engineering*, vol. 16, no. 2, pp. 43–46, 2008.

[2] C.-H. Yin, X. Dong, L. Lv et al., "Economic production of probiotics from kitchen waste," *Food Science and Biotechnology*, vol. 22, no. 1, pp. 59–63, 2013.

[3] S. Ribbens, J. Dewulf, F. Koenen et al., "A survey on biosecurity and management practices in Belgian pig herds," *Preventive Veterinary Medicine*, vol. 83, no. 3-4, pp. 228–241, 2008.

[4] S. Y. Yang, K. S. Ji, Y. H. Baik, W. S. Kwak, and T. A. McCaskey, "Lactic acid fermentation of food waste for swine feed," *Bioresource Technology*, vol. 97, no. 15, pp. 1858–1864, 2006.

[5] S. Manfredi and R. Pant, "Improving the environmental performance of bio-waste management with life cycle thinking (LCT) and life cycle assessment (LCA)," *International Journal of Life Cycle Assessment*, vol. 18, no. 1, pp. 285–291, 2013.

[6] A. Hanc, J. Szakova, and P. Svehla, "Effect of composting on the mobility of arsenic, chromium and nickel contained in kitchen and garden waste," *Bioresource Technology*, vol. 126, pp. 444–452, 2012.

[7] E. den Boer, J. den Boer, J. Jaroszyńska, and R. Szpadt, "Monitoring of municipal waste generated in the city of Warsaw," *Waste Management and Research*, vol. 30, no. 8, pp. 772–780, 2012.

[8] G. Liu, X. Liu, Y. Li, Y. He, and R. Zhang, "Influence of pH adjustment and inoculum on anaerobic digestion of kitchen waste for biogas producing," *Journal of Biobased Materials and Bioenergy*, vol. 5, no. 3, pp. 390–395, 2011.

[9] S. M. Tauseef, T. Abbasi, and S. A. Abbasi, "Energy recovery from wastewaters with high-rate anaerobic digesters," *Renewable and Sustainable Energy Reviews*, vol. 19, pp. 704–741, 2013.

[10] I. M. Nasir, T. I. M. Ghazi, and R. Omar, "Production of biogas from solid organic wastes through anaerobic digestion: a review," *Applied Microbiology and Biotechnology*, vol. 95, no. 2, pp. 321–329, 2012.

[11] A. J. Wang, W. W. Li, and H. Q. Yu, "Advances in biogas technology," *Advances in Biochemical Engineering Biotechnology*, vol. 128, pp. 119–141, 2012.

[12] C. H. Song, Z. M. Wei, B. D. Xi et al., "Effect of heavy metals biogas mixed material composting," *Safety and Environment*, vol. 13, no. 2, pp. 62–66, 2013.

[13] Z. Q. Liu, *Optimize Microalgae Culture, Harvesting and Cultivation of Microalgae Biogas Research*, Zhejiang University, 2012.

[14] J. Y. Chen, "Determination of the reaction order with respect to," *Chemistry of University*, vol. 15, no. 6, pp. 49–50, A Method for Determining Reaction Series, 2000.

[15] X. Yan, Y. H. Zhang, and Z. Li, "Experience teaching method for determining the reaction order," *Xinjiang Normal University*, vol. 31, no. 4, pp. 96–98, 2012.

[16] W. Wanasolo, S. V. Manyele, and J. Makunza, "A kinetic study of anaerobic biodegradation of food and fruit residues during biogas generation using initial rate method," *Engineering*, vol. 5, no. 7, pp. 577–586, 2013.

[17] B. Linke, "Kinetic study of thermophilic anaerobic digestion of solid wastes from potato processing," *Biomass and Bioenergy*, vol. 30, no. 10, pp. 892–896, 2006.

[18] L. Feng, H. L. Kou, W. Kou et al., "A hydrolysis of food waste and its components dynamics model," *Environmental Pollution and Control*, vol. 37, no. 8, pp. 17–20, 2015.

[19] Department of Inorganic Chemistry Dalian University of Technology, *Inorganic Chemistry*, Higher Education Press, Beijing, China, 5th edition, 2006.

[20] N.-Q. Ren, A.-J. Wang, and F. Ma, *Physiological Ecology of Acidogenic Fermention Microbial*, Science Press, Beijing, China, 2005.

[21] S.-K. Han and H.-S. Shin, "Performance of an innovative two-stage process converting food waste to hydrogen and methane," *Journal of the Air and Waste Management Association*, vol. 54, no. 2, pp. 242–249, 2004.

[22] Q. Wang, M. Kuninobu, H. I. Ogawa, and Y. Kato, "Degradation of volatile fatty acids in highly efficient anaerobic digestion," *Biomass and Bioenergy*, vol. 16, no. 6, pp. 407–416, 1999.

[23] J. B. Van Lier, K. C. Grolle, C. T. Frijters, A. J. Stams, and G. Lettinga, "Effects of acetate, propionate, and butyrate on the thermophilic anaerobic degradation of propionate by methanogenic sludge and defined cultures," *Applied and Environmental Microbiology*, vol. 59, no. 4, pp. 1003–1011, 1993.

[24] Y. Wu, W. Y. Zhang, Y. Pang et al., "Semi-continuous mixing food waste and manure anaerobic fermentation kinetics of," *Anhui Agricultural Sciences*, vol. 39, no. 20, pp. 12278–12280, 2011.

[25] L. Q. Li, X. J. Li, M. X. Zheng et al., "Tomato waste semi-continuous anaerobic fermentation experiment and kinetic model," *China Biogas*, vol. 27, no. 2, pp. 18–20, 2009.

[26] X. Lai, W. Zhang, L. Zhang, and J. Chen, "Prediction of gas production of semi-continuous anaerobic co-digestion based on artificial neural network," *Chinese Journal of Environmental Engineering*, vol. 9, no. 1, pp. 459–463, 2015.

[27] P. Mähnert and B. Linke, "Kinetic study of biogas production from energy crops and animal waste slurry: effect of organic loading rate and reactor size," *Environmental Technology*, vol. 30, no. 1, pp. 93–99, 2009.

Hindawi
BioMed Research International
Volume 2017, Article ID 5681617, 7 pages
https://doi.org/10.1155/2017/5681617

Research Article

Outdoor Growth Characterization of an Unknown Microalga Screened from Contaminated *Chlorella* Culture

Shuhao Huo,[1,2,3] Changhua Shang,[2,4] Zhongming Wang,[2] Weizheng Zhou,[2] Fengjie Cui,[1] Feifei Zhu,[1] Zhenhong Yuan,[2] and Renjie Dong[3]

[1]*School of Food and Biological Engineering, Jiangsu University, Zhenjiang 212013, China*
[2]*Guangzhou Institute of Energy Conversion, Chinese Academy of Sciences, Guangzhou 510640, China*
[3]*College of Engineering, China Agricultural University, Beijing 100083, China*
[4]*Institute of New Energy and New Materials, South China Agricultural University, Guangzhou, China*

Correspondence should be addressed to Zhongming Wang; wangzm@ms.giec.ac.cn and Renjie Dong; rjdong@cau.edu.cn

Received 17 March 2016; Revised 29 July 2016; Accepted 14 December 2016; Published 5 March 2017

Academic Editor: Atanas Atanassov

Outdoor microalgae cultivation process is threatened by many issues, such as pest pollution and complex, changeable weather. Therefore, it is difficult to have identical growth rate for the microalgae cells and to keep their continuous growth. Outdoor cultivation requires the algae strains not only to have a strong ability to accumulate oil, but also to adapt to the complicated external environment. Using 18S rRNA technology, one wild strain *Scenedesmus* sp. FS was isolated and identified from the culture of *Chlorella zofingiensis*. Upon contamination by *Scenedesmus* sp., the species could quickly replace *Chlorella zofingiensis* G1 and occupy ecological niche in the outdoor column photobioreactors. The results indicated that *Scenedesmus* sp. FS showed high alkali resistance. It also showed that even under the condition of a low inoculum rate (OD_{680}, 0.08), *Scenedesmus* sp. FS could still grow in the outdoor raceway pond under a high alkaline environment. Even under unoptimized conditions, the oil content of *Scenedesmus* sp. FS could reach more than 22% and C16–C18 content could reach up to 79.68%, showing that this species has the potential for the biodiesel production in the near future.

1. Introduction

Due to the exorbitant cost input into nutritive salts such as chemical fertilizers and high energy consumption in microalgae harvest, the microalgal biodiesel has not yet been successfully applied in commercial production [1–4]. Utilizing sunlight to magnify the cultivation of microalgae under outdoor conditions is an effective way to reduce the cost of microalgal cultivation. The current studies on energy microalgae are mainly carried out at indoor labs as there are many difficulties in outdoor cultivation [5–7]. In outdoor cultivation, the microalga of interest is often vulnerable to contamination with viruses, bacteria, fungi, insect pupae, rotifers, protozoa, or other unwanted algal species. Among them, rotifers and protozoa are the two organisms that are able to seize ecosystem niche quickly due to their small body, simple structure, and fast reproduction speed. They prey on microalgae cells, resulting in a great reduction of microalgae cell concentration, and exceedingly threatening the microalgae production. Meanwhile, the complex and changeable outdoor weather conditions make the cultivation of microalgae have an uneven growth rate and thus production is often difficult to be carried out [8–10].

Excellent microalgal strain is crucial to the realization of microalgal biodiesel production. Outdoor cultivation requires the selected algal strain not only to have a strong ability to accumulate oil but also to adapt to the external environment. The lipid accumulation of microalgae can be improved by changing the element content in the culture medium such as the deprivation of nitrogen, phosphorus, or other elements, while the outdoor adaptability of microalgae is more difficult to be improved in a short time. Through the amplification of 18S rRNA sequences of unknown algal strains, the wild microalgal strain screened from contaminated *Chlorella zofingiensis* G1 in an outdoor column photobioreactor was preliminarily identified in this

Figure 1: The wild microalgal strain in the outdoor pond observed with light microscope at ×400 magnification.

paper. *Chlorella zofingiensis* G1 could be quickly replaced by the wild microalgal strain (Figure 1), which could occupy ecological niche quickly, showing high alkali resistance and antipollution performances. The wild microalgal fronds are unicellular ellipse in shape with a smooth surface, and the cell size is approximately 5.0–7.0 μm in length and 2.0–4.0 μm in width under light microscope. At the same time, this paper also examined the possibility for large-scale cultivation in the outdoor raceway pond.

2. Materials and Methods

2.1. Materials. Colonies of microalgae were isolated from contaminated *Chlorella zofingiensis* G1 in an outdoor photobioreactor in the district of Sanshui, Foshan city, China (23°03′N–112°09′E). The isolated algal cells were cultured and maintained in a BG11 medium [11] at 25°C under continuous illumination by cool-white fluorescent lamps (light intensity: 2000 lux) in a 500 mL Erlenmeyer flask. Aeration and mixing were achieved by the sparging air with 6.0% CO_2 through a glass-filter, which was inserted to the bottom of the reactor and the flow rate of gas was 0.5 vvm, regulated by the gas flow meter (Model G, Aalborg Instruments & Controls, Inc., Orangeburg, NY, USA). The temperature of the culture media was 25 ± 1°C, regulated by the room air conditioner (Gree Electric Appliances Inc., Zhuhai, Guangdong, China). After 6 days of cultivation, when the cells were in the logarithmic phase, the cultures were used for outdoor experiments.

A 40 L vertical tubular outdoor photobioreactor (8.7 cm × 160 cm = diameter × height) was used to cultivate the above-mentioned strain as seed cultures for the outdoor raceway pond amplification cultivation.

rTaq, pMD18–T, and T4 DNA Ligase were obtained from Takara Biotech Co., Ltd., China. EasyPure Quick Gel Extraction Kit was obtained from Beijing TransGen Biotech Co., Ltd., China. The nucleotide sequences of these primers (Table 1) were synthesized by Sangon Biotech Co., Ltd., China. DNA sequencing was analyzed by Shanghai Life Technologies Corporation, China. The primers NS1 and NS8 were used to clone the 18S rRNA sequence of microalgae. The primers M13 (−40) Forward and M13 Reverse were used to clone the inserted gene fragment in pMD18-T and confirm the success of TA cloning.

Table 1: Oligonucleotide primers used in this work.

Primer	Sequence (5′ → 3′)
NS1	GTAGTCATATGCTTGTCTC
NS8	TCCGCAGGTTCACCTACGGA
M13 (−40) Forward	GTTTTCCCAGTCACGAC
M13 Reverse	CAGGAAACAGCTATGAC

2.2. Identification Methods

2.2.1. Microscopic Observation. After shaking evenly, a drop of 0.05 mL microalgae sample was dripped onto the slide, and the sample was covered by glass (18 × 24 mm) and observed with polarizing microscope from Nikon Instruments Eclipse LV100 POL at ×400 magnification.

2.2.2. Isolation of Genomic DNA of the Wild Microalgal Strain. Wild microalgal strain was harvested during logarithmic phase after 3-4 days of cultivation in a BG11 medium, frozen in liquid nitrogen, and grounded using a pestle and mortar. The genomic DNA was isolated by the CTAB method [12].

2.2.3. PCR Amplification of 18S rRNA from the Wild Microalgal Strain. The 18S rRNA was amplified by PCR using the NS1 and NS8 universal primers as shown in Table 1 and the genomic DNA was used as a template for PCR amplification. PCR amplification was carried out in 0.2 mL tubes. The PCR mixture included 10x PCR Buffer (Mg^{2+} plus) 5 μL, dNTPs (2.5 mM) 4 μL, NS1 (20 μM) 1 μL, NS8 (20 μM) 1 μL, genomic DNA 1 μL, rTaq (5 U/μL) 0.2 μL, and deionized water 37.8 μL, with a total volume of 50 μL. Amplification conditions were as follows: 30 cycles at 94°C for 30 s, 50°C for 30 s, and 72°C for 2 min, followed by a final extension at 72°C for 5 min. PCR products were fractionated in 2% (w/v) agarose gels and stained with ethidium bromide.

2.2.4. The Purification, Ligation, and Transformation of PCR Product. The PCR product was recovered using EasyPure Quick Gel Extraction Kit (Trans, Beijing), according to the instruction book. The amplification products were ligated into pMD18-T vector (Takara) and then transformed and sequenced, according to standard procedures described by Sambrook et al. [13].

2.2.5. The Identification of Positive Transformants. Amplified fragments with resistance to ampicillin were picked from the medium, they were cultured in 3 mL LB liquid medium at 150 rpm for about 20 h, and the colony was identified through PCR using 1 μL culture. Transformed *E. coli* DH5α were picked from the medium containing 100 μg/mL ampicillin. The PCR mixture included 10x PCR Buffer (Mg^{2+} plus) 5 μL, dNTPs (2.5 mM) 4 μL, M13 (−40) Forward (20 μM) 1 μL, M13 Reverse (20 μM) 1 μL, liquid culture 1 μL, rTaq (5 U/μL) 0.2 μL, and deionized water 37.8 μL, with a total volume of

Table 2: The quality of mountain spring water*.

Elements	Content (μg/L)
Mn	5.99 ± 3.46
Fe	22.37 ± 17.52
P	128.28 ± 1.50
Si	3481.00 ± 9.90
Na	28.27 ± 0.64
K	160.05 ± 6.12
Mg	1174.60 ± 9.33
Zn	26.84 ± 4.02
Ca	1979.60 ± 12.16
Mo	n. d.
Cu	n. d.

*Note: average values of water samples collected in two different locations; n.d.: not detected.

Figure 2: Photograph of outdoor ponds for wild microalgae cultivation (8 m × 50 m).

50 μL. Amplification conditions were as follows: 30 cycles at 94°C for 30 s, 46°C for 30 s, and 72°C for 2 min, followed by a final extension at 72°C for 5 min. PCR products were size fractionated in 2% (w/v) agarose gels and stained with ethidium bromide. Volume of 1.5 mL culture was selected for sequencing analysis (Life Technology, Shanghai).

2.2.6. Lipid Content and Fatty Acid Composition Analysis. Bigogno's method (2002) was applied to quantify the amount of total lipid content [14]. Fatty acid composition analysis was carried out by the saponification reaction with the participation of base catalyst [15].

2.3. Outdoor Raceway Pond Cultivation of the Wild Microalgae. The outdoor raceway ponds (brick cement ponds) were located in Sanshui district, Foshan city, China (23°03′N–112°09′E). The ponds were 50 cm in height, 8 m in width, and 50 m in length from north to south with semicircular arc at both ends and had average of 23–25 cm depth of water (Figure 2). Paddle wheel device was installed to circulate the pool liquid, which was operated at about 10 cm depth and rotated at the speed of 15 rpm. Cultivation water was mountain spring water (Table 2). Nutrient composition was specified in Table 2. A large amount of chemical fertilizer was added to the outdoor raceway pond, including 300 mg/L of CO $(NH_2)_2$, 60 mg/L of KH_2PO_4, and 60 mg/L of $MgSO_4$. The initial optical density (OD_{680}) of the culture was controlled between 0.3 and 0.5 when appropriate amount preculture broths were inoculated into the 25 m long small pond during the logarithmic phase. In the process of cultivation, the pH value was not adjusted. The pH, temperature, and light intensity were recorded 4 times a day (8:00, 11:00, 14:00, and 17:00). The biomass concentration was determined by measuring the OD_{680} value of the sample in the pond at 17:00. After 7 days of cultivation, the wild microalgae were harvested.

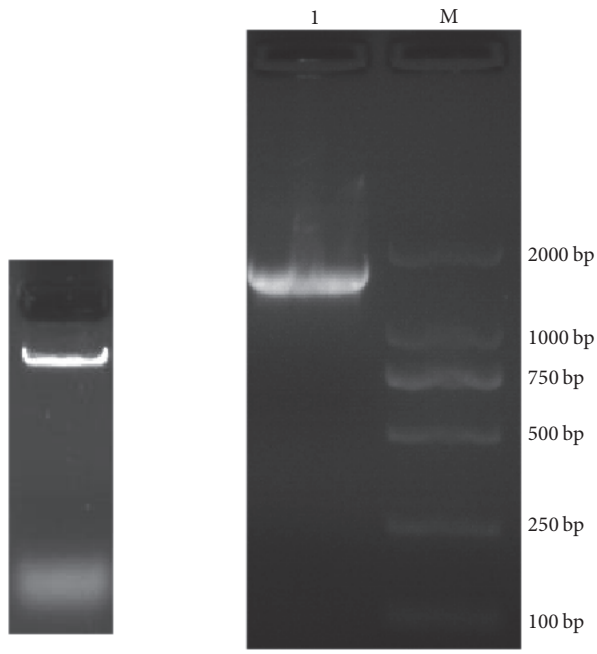

Figure 3: Genomic DNA from wild microalgal strains (left) and amplification results of 18S rRNA of wild microalgal strain (1: 18S rRNA band; M: DL2000 DNA marker) (right).

3. Results and Discussion

3.1. Wild Algae Identification Using 18S rDNA Technology. The CTAB method was used to extract the genomic DNA of wild microalgae strains. The results in Figure 3 showed that the genomic DNA sample was complete and no degradation phenomenon was found in 1% (w/v) agarose gels electrophoresis stained with ethidium bromide.

By using universal primers NS1 and NS8 and the wild algae genomic DNA as a template for PCR amplification, a 1767 bp band was obtained, as shown in Figure 3. A total of 12 positive transformants of *E. coli* DH5α were identified using primers M13 (−40) Forward and M13 Reverse using 1 μL culture as template. Electropherogram of PCR products was from 12 positive transformants of *E. coli* DH5α containing recombinant pMD18-T. The bands were identified by electrophoresis. As shown in Figure 4, the results suggested that all 18S rRNA fragments with approximate length of 2 kb were successfully connected to the pMD18-T vector. The 12 positive transformants were named as 18S-1~18S-12. Of them,

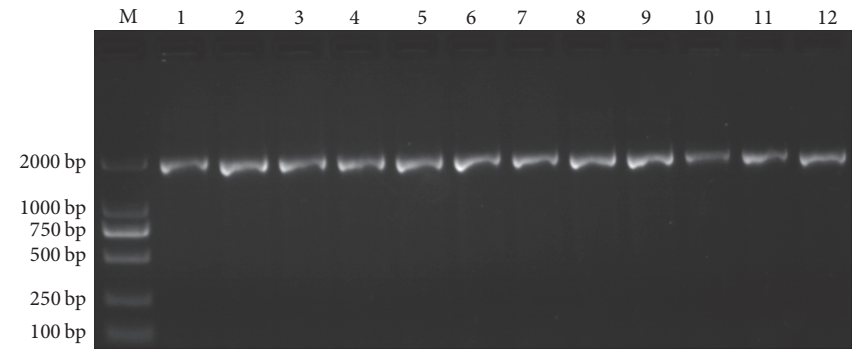

Figure 4: Electropherogram of PCR products from 12 positive transformants, carrying pMD18–T in which the 18S rRNA gene sequence of the wild alga was cloned. M13 primers were used for identification.

TCTAGAGATTGTAGTCATATGCTTGTCTCAAAGATTAAGCCATGCATGTCTAAGTATAAACTGCTTATACTGTGAAACTG
CGAATGGCTCATTAAATCAGTTATAGTTTATTTGGTGGTACCTTACTACTCGGATAACCGTAGTAATTCTAGAGCTAATA
CGTGCGTAAATCCCGACTTCTGGAAGGGACGTATATATTAGATAAAAGGCCGACCGAGCTTTGCTCGACCCGCGGTGA
ATCATGATATCTTCACGAAGCGCATGGCCTTGTGCCGGCGCTGTTCCATTCAAATTTCTGCCCTATCAACTTTCGATGGT
AGGATAGAGGCCTACCATGGTGGTAACGGGTGACGGAGGATTAGGGTTCGATTCCGGAGAGGGAGCCTGAGAAACG
GCTACCACATCCAAGGAAGGCAGCAGGCGCGCAAATTACCCAATCCTGATACGGGGAGGTAGTGACAATAAATAACA
ATACCGGGCATTTCATGTCTGGTAATTGGAATGAGTACAATCTAAATCCCTTAACGAGGATCCATTGGAGGGCAAGTCT
GGTGCCAGCAGCCGCGGTAATTCCAGCTCCAATAGCGTATATTTAAGTTGTTGCAGTTAAAAAGCTCGTAGTTGGATTT
CGGGTGGGTTCTAGCGGTCCGCCTATGGTGAGTACTGCTATGGCCTTCCTTTCTGTCGGGGACGGGCTTCTGGGCTTC
ACTGTCCGGGACTCGGAGTCGACGTGGTTACTTTGAGTAAATTAGAGTGTTCAAAGCAGGCTTACGCCAGAATACTTT
AGCATGGAATAACACGATAGGACTCTGGCCTATCTTGTTGGTCTGTAGGACCGGAGTAATGATTAAGAGGGACAGTCG
GGGGCATTCGTATTTCATTGTCAGAGGTGAAATTCTTGGATTTATGAAAGACGAACTACTGCGAAAGCATTTGCCAAG
GATGTTTTCATTAATCAAGAACGAAAGTTGGGGGCTCGAAGACGATTAGATACCGTCGTAGTCTCAACCATAAACGAT
GCCGACTAGGGATTGGCGAATGTTTTTTTAATGACTTCGCCAGCACCTTATGAGAAATCAAAGTTTTTGGGTTCCGGG
GGGAGTATGGTCGCAAGGCTGAAACTTAAAGGAATTGACGGAAGGGCACCACCAGGCGTGGAGCCTGCGGCTTAAT
TTGACTCAACACGGGAAAACTTACCAGGTCCAGACATAGTGAGGATTGACAGATTGAGAGCTCTTTCTTGATTCTATG
GGTGGTGGTGCATGGCCGTTCTTAGTTGGTGGGTTGCCTTGTCAGGTTGATTCCGGTAACGAACGAGACCTCAGCCT
GCTAAATAGTCTCAGTTGCTTTTTGCAGCTGGCTGACTTCTTAGAGGGACTATTGGCGTTTAGTCAATGGAAGTATGAG
GCAATAACAGGTCTGTGATGCCCTTAGATGTTCTGGGCCGCACGCGCGCTACACTGATGCATTCAACAAGCCTATCCT
TGACCGAAGGGTCTGGGTAATCTTTGAAACTGCATCGTGATGGGGATAGATTATTGCAATTATTAGTCTTCAACGAGG
AATGCCTAGTAAGCGCAAGTCATCAGCTTGCGTTGATTACGTCCCTGCCCTTTGTACACACCGCCCGTCGCTCCTACC
GATTGGGTGTGCTGGTGAAGTGTTCGGATTGGCAGCTTAGGGTGGCAACACCTCAGGTCTGCCGAGAAGTTCATTAA
ACCCTCCCACCTAGAGGAAGGAGAAGTCGTAACAAGGTTTCCGTAGGTGAACCTGCGGAAATCGTCGACC

Figure 5: 18S rDNA gene sequence of the wild strain.

18S-1~18S-5 were selected for sequencing and the results were completely consistent (analyzed by Shanghai Life Biotech Co., Ltd.).

The 18S rRNA gene sequence amplified from this strain is 1767 bp in length (Figure 5), which showed similarities with other known sequences from green algae based on the BLAST *n* results, with homology above 99% to *Scenedesmus obliquus* and *Scenedesmus acutus*. The phylogenetic analysis indicated that this strain has a close relationship with *Scenedesmus* sp., named *Scenedesmus* sp. FS (Figure 6). The sequences of 18S rRNA gene (fragment) of those microalgae in NCBI GenBank were as follows: *Scenedesmus obliquus*: FR865738.1; *Scenedesmus acutus*: AJ249512.1; *Scenedesmus subspicatus*: AJ249514.1; *Neochloris vigenis*: M74496.1; *Chlorella vulgaris* strain CCAP 211/11F: AY591515.1; *Chlorococcum oleofaciens*: KM020101.1; *Chlamydomonas* sp. A-SIO: AF517100.1; *Chlamydomonas segnis*: U70593.1; *Chlorococcum hypnosporum*: U41173.1; *Chlamydomonas cribrum*: LC086333.1; *Chlamydomonas mexicana*: AF395434.1; *Scenedesmus* sp. FS: KY268297.

3.2. Cultivation of Scenedesmus sp. FS in the Outdoor Raceway Pond. As shown in Figure 7, the optical density of inoculum was very low (OD_{680}, 0.08), and the raceway pond had a large surface area to volume ratio, which could inhibit the

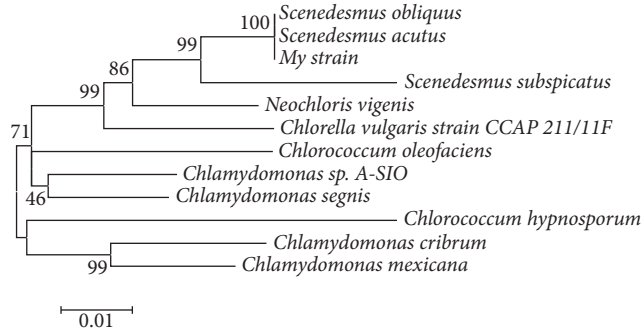

Figure 6: Phylogenetic tree constructed based on the 18S rRNA gene sequences of 11 strains of green algae and the experimental microalga (Bootstrap values are indicated as percentages at the nodes).

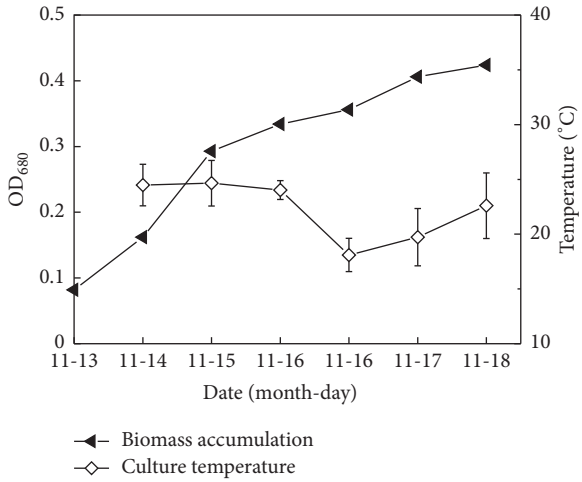

Figure 7: Growth curve and fluctuation of culture temperature (an average value from 8:00 am to 5:00 pm each day).

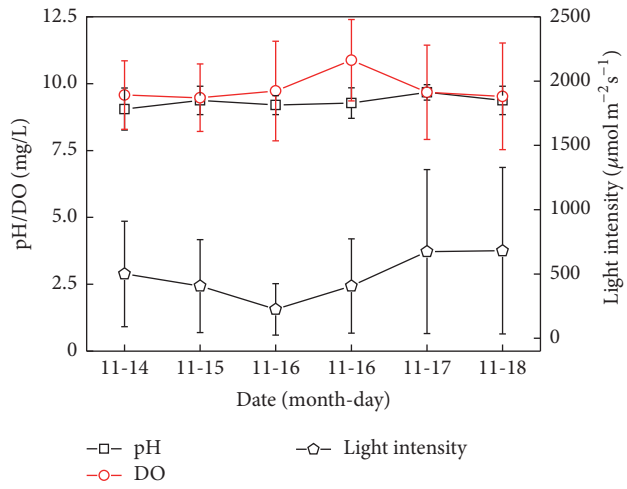

Figure 8: The fluctuation of light intensity, pH, and dissolved oxygen (DO) (the average value in the range of 8:00 am~5:00 pm) under outdoor conditions.

growth of single cells at the initial phase due to strong light. But in fact *Scenedesmus* sp. FS was still able to adapt to the environment of outdoor raceway pond. The growth and metabolism of *Scenedesmus* sp. FS was active, and the algae did not experience the lag phase and directly got into the logarithmic phase with a rapid growth rate.

In the experiment, light intensity and temperature in the outdoor changed obviously, and the highest light intensity reached more than 1500 μmol/(m^2·s), and water temperature ranged from 18.1 to 24.7°C. Sánchez et al. (2008) reported that the optimal growth temperature of *Scenedesmus almeriensis* was 35°C, and it could still survive at 48°C. This algae could tolerate high light intensity (1625 μmol/(m^2·s)) and could also accumulate 0.55% (wt%) lutein under this light intensity [16]. In this experiment, the wild algae *Scenedesmus* sp. FS was also able to tolerate similar light intensity. Additionally, the wild alga was able to grow under high alkaline condition with pH values between 9.0 and 9.7 (Figure 8). The dissolved oxygen changed between 9.5 and 10.9 mg/L daily, which was relatively stable. It can be seen that the wild algae *Scenedesmus* sp. FS could well adapt to the outdoor conditions in the process of cultivation. The pest pollution and other alien invasive algae in this experiment were not significant, which indicates the scale-up potential of the wild algae under outdoor culture conditions. In future studies, outdoor cultivation conditions need further optimization to obtain larger biomass and higher oil yield rate.

3.3. Oil Content and Fatty Acid Composition of Scenedesmus sp. FS. Numerous studies have shown that nitrogen deficiency can promote accumulation of oil in microalgae [17]. Goldberg and Cohen found that phosphorus deficiency could also significantly promote oil accumulation of *Monodus subterraneus* [18]. Under these conditions, the fixed CO_2 of algal cells would be converted with priority into lipid or carbohydrates, rather than proteins [8]. In normal culture condition, fatty acid synthesized was mainly used in the synthesis of membrane sugar-based glyceride and phospholipids, which accounted for about 5–20% of the dry weight of the algae cells. Under the nitrogen deficiency and other adverse environmental conditions, algae cell would change the oil synthesis route, beginning to accumulate neutral fat of about 20–50% of the dry weight, with triacylglycerol (TAG) as the main component. After 6 days of cultivation, the total nitrogen and phosphorus concentration in the pond were

Table 3: Fatty acid composition (wt%) of the wild *Scenedesmus* sp. FS cells.

Fatty acid	wt%
C16:0	24.55
C16:1	2.74
C18:0	2.56
C18:2	40.64
C18:3	9.19
C20:1	4.64
C20:2	4.53
C22:1	4.29
C24:1	2.45

70.8 ± 2.8 mg/L and 6.0 ± 0.1 mg/L, respectively, indicating a sufficient supply of nitrogen and phosphorus. Oil content in the algal cells increased slowly and oil content of *Scenedesmus* sp. FS was not high with fatty acid composition 22.0 ± 1.9% of the algal weight.

The compositions of fatty acid methyl esters (FAMEs) were shown in Table 3. The microalgal lipids mainly contained FAMEs with 16–18 carbons with a high cetane number. These lipids show better fuel properties and low temperature performance and were considered suitable for sustainable biodiesel production [19]. The content of FAMEs C16–C18 in the wild strain *Scenedesmus* sp. FS reached 79.68%, with C16:0 24.55% and C18:2 40.64%, showing good potential for development of biodiesel.

4. Conclusion

Using 18 s rDNA molecular technology, the dominant microalgae strain screened from contaminated *Chlorella zofingiensis* G1 in an outdoor photobioreactor was identified. The isolated species belonged to *Scenedesmus* genus, which was named *Scenedesmus* sp. FS. Under the conditions of a low concentration inoculation, this strain still had good alkali resistance and robust adaption to the stress of the outdoor environment. It had great potential as a large-scale cultivation strain for biodiesel production. Further research would be focused on the optimization of the culture conditions and the use of random mutagenesis technology, directed evolution method, or other technical means to obtain higher biomass and oil yield of the alga *Scenedesmus* sp. FS.

Competing Interests

The authors declare that they have no competing interests.

Authors' Contributions

Shuhao Huo, Changhua Shang, and Weizheng Zhou wrote the main part of the paper and performed the experiments. Zhongming Wang conceived the experiments. Others read and approved the manuscript. Shuhao Huo and Changhua Shang contributed equally to this work.

Acknowledgments

This research was funded by the National Natural Science Foundation of China (21506084, 21406093), the China Postdoctoral Science Foundation (2015T80502), the Natural Science Foundation of Jiangsu Province (BK20140540), the key Laboratory of Renewable Energy, Chinese Academy of Sciences (no. y507k11001), A Project Funded by the Priority Academic Program Development of Jiangsu Higher Education Institutions (PAPD), and the Training Project of the Young Core Instructor of Jiangsu University.

References

[1] Y. Chisti, "Biodiesel from microalgae," *Biotechnology Advances*, vol. 25, no. 3, pp. 294–306, 2007.

[2] J. Sheehan, T. Dunahay, J. Benemann, and P. Roessler, "A look back at the U.S. Department of Energy's aquatic species program: biodiesel from algae," NREL Report TP-580-24190, NREL, Golden, Colo, USA, 1998.

[3] L. Zhu, "Microalgal culture strategies for biofuel production: a review," *Biofuels, Bioproducts and Biorefining*, vol. 9, no. 6, pp. 801–814, 2015.

[4] L. Zhu, S. Huo, and L. Qin, "A microalgae-based biodiesel refinery: sustainability concerns and challenges," *International Journal of Green Energy*, vol. 12, no. 6, pp. 595–602, 2015.

[5] X. Miao and Q. Wu, "High yield bio-oil production from fast pyrolysis by metabolic controlling of *Chlorella protothecoides*," *Journal of Biotechnology*, vol. 110, no. 1, pp. 85–93, 2004.

[6] Z.-Y. Liu, G.-C. Wang, and B.-C. Zhou, "Effect of iron on growth and lipid accumulation in *Chlorella vulgaris*," *Bioresource Technology*, vol. 99, no. 11, pp. 4717–4722, 2008.

[7] W. Xiong, X. Li, J. Xiang, and Q. Wu, "High-density fermentation of microalga Chlorella protothecoides in bioreactor for microbio-diesel production," *Applied Microbiology and Biotechnology*, vol. 78, no. 1, pp. 29–36, 2008.

[8] L. Rodolfi, G. C. Zittelli, N. Bassi et al., "Microalgae for oil: strain selection, induction of lipid synthesis and outdoor mass cultivation in a low-cost photobioreactor," *Biotechnology and Bioengineering*, vol. 102, no. 1, pp. 100–112, 2009.

[9] A. Vonshak, G. Torzillo, J. Masojidek, and S. Boussiba, "Sub-optimal morning temperature induces photoinhibition in dense outdoor cultures of the alga *Monodus subterraneus* (Eustigmatophyta)," *Plant, Cell and Environment*, vol. 24, no. 10, pp. 1113–1118, 2001.

[10] N. R. Moheimani and M. A. Borowitzka, "The long-term culture of the coccolithophore *Pleurochrysis carterae* (Haptophyta) in outdoor raceway ponds," *Journal of Applied Phycology*, vol. 18, no. 6, pp. 703–712, 2006.

[11] R. Rippka, J. Deruelles, J. B. Waterbury, M. Herdman, and R. Y. Stanier, "Generic assignments, strain histories and properties of pure cultures of cyanobacteria," *Journal of General Microbiology*, vol. 111, no. 1, pp. 1–61, 1979.

[12] M. A. Saghai-Maroof, K. M. Soliman, R. A. Jorgensen, and R. W. Allard, "Ribosomal DNA spacer-length polymorphisms in barley: mendelian inheritance, chromosomal location, and population dynamics," *Proceedings of the National Academy of Sciences of the United States of America*, vol. 81, no. 24, pp. 8014–8018, 1984.

[13] J. Sambrook, E. F. Fritsch, and T. Maniatis, *Molecular Cloning, A Laboratory Manual*, Cold Spring Harbor Laboratory Press, 2nd edition, 1989.

[14] C. Bigogno, I. Khozin-Goldberg, S. Boussiba, A. Vonshak, and Z. Cohen, "Lipid and fatty acid composition of the green oleaginous alga Parietochloris incisa, the richest plant source of arachidonic acid," *Phytochemistry*, vol. 60, no. 5, pp. 497–503, 2002.

[15] C.-H. Hsieh and W.-T. Wu, "Cultivation of microalgae for oil production with a cultivation strategy of urea limitation," *Bioresource Technology*, vol. 100, no. 17, pp. 3921–3926, 2009.

[16] J. F. Sánchez, J. M. Fernández-Sevilla, F. G. Acién, M. C. Cerón, J. Pérez-Parra, and E. Molina-Grima, "Biomass and lutein productivity of *Scenedesmus almeriensis*: influence of irradiance, dilution rate and temperature," *Applied Microbiology and Biotechnology*, vol. 79, no. 5, pp. 719–729, 2008.

[17] Q. Hu, M. Sommerfeld, E. Jarvis et al., "Microalgal triacylglycerols as feedstocks for biofuel production: perspectives and advances," *The Plant Journal*, vol. 54, no. 4, pp. 621–639, 2008.

[18] I. Khozin-Goldberg and Z. Cohen, "The effect of phosphate starvation on the lipid and fatty acid composition of the fresh water eustigmatophyte *Monodus subterraneus*," *Phytochemistry*, vol. 67, no. 7, pp. 696–701, 2006.

[19] G. Huang, F. Chen, D. Wei, X. Zhang, and G. Chen, "Biodiesel production by microalgal biotechnology," *Applied Energy*, vol. 87, no. 1, pp. 38–46, 2010.

Hindawi Publishing Corporation
BioMed Research International
Volume 2016, Article ID 3856386, 9 pages
http://dx.doi.org/10.1155/2016/3856386

Research Article

Studies on the Ecological Adaptability of Growing Rice with Floating Bed on the Dilute Biogas Slurry

Qun Kang, Rui Li, Qi Du, Bowen Cheng, Zhiqi Liao, Chengcheng Sun, and Zhaohua Li

Faculty of Resources and Environmental Science, Hubei University, 368 Youyi Avenue, Wuhan, China

Correspondence should be addressed to Zhaohua Li; zli@hubu.edu.cn

Received 26 May 2016; Revised 25 August 2016; Accepted 5 September 2016

Academic Editor: Ningbo Gao

This study aimed to explore the ecological adaptability and the possibility of growing rice with floating bed on the dilute biogas slurry. The results of the experiments show that the growth stage, rice plant height, and rice yield and quality were significantly affected by multiple dilutions; rice plants cultivated with 45 multiple dilutions had better ecological adaptability than others. In the 45 multiple dilutions' group, the yield of rice was 13.3 g/bucket (8 rice plants), milled rice rate was 63.1%, and the content of crude protein in the rice was 6.3%. The concentrations of heavy metals in the rice cultivated with 30 multiple dilutions' slurry, such as total lead, cadmium, mercury, chromium, and arsenic, were all below the national standard. The study shows that it is possible and safe to cultivate rice plants with no soil but diluted biogas slurry. In the experiments, the yield, milled rice rate, and crude protein of the rice cultivated with slurry were not as much as those of rice cultivated with regular way in soil. This study provides the basic theoretical support for the development of biogas projects and the potential achievement of organic farming in special agricultural facilities and circular economy.

1. Introduction

Since the 21st century, energy shortage and environment pollution have become more severe. Due to the advantages in generating alternative energy and reducing environment pollution, the biogas projects developed rapidly in recent years. By the end of 2011, merely in China, 73032 biogas projects have already been established in large or medium scale [1]. For Mexico, the biogas generated from slurry has potential to produce 21 PJ per year, equivalent to 3.5% of natural gas consumption in 2013 [2]. Great attention has been paid to anaerobic digestion of animal waste, because it produces renewable energy in an environmentally friendly manner and therefore the construction of biogas plants is increasing around the world [3]. The biogas project not only reduces the agriculture waste but also produces clean bioenergy, which also contributes to considerable economic benefits.

The main problem about biogas projects is the large quantity of biogas slurry, the by-product of biogas production. Biogas slurry is a good source of plant nutrients and can improve soil properties [4–7]. The biogas slurry is normally slightly alkaline (pH 7.0–8.5). Despite the big carbon loss via methane and carbon dioxide generation, ninety percent of the raw nutrients remain in the slurry. It is estimated that the biogas slurry consists of 0.026%–0.081% total nitrogen (ammonia nitrogen 60%–75% and the rest is organic nitrogen), 0.02%–0.07% total phosphorus, and 0.047%–1.40% total potassium. In addition, biogas slurry is rich in trace elements (such as iron, zirconium, copper, boron, and molybdenum), auxins (such as gibberellin, indoleacetic acid), B group vitamins, and some antibiotics [8–10]. A tomato one-growing-season field study showed that the application of concentrated slurry can significantly bring up the total N, P, and K contents, conductivity, and fruit contents of amino acids, protein, soluble sugar, b-carotene, tannins, and vitamin C [11]. Zheng et al. found that biogas slurry-chemical fertilizers combination increased peanut grain yield and biomass, due to increases in soil N and P availability, microbial biomass C and N concentrations, and urease and dehydrogenase activities [12]. Win et al. concluded that the application of biogas slurry may be considered a substitute to the utilization of chemical

fertilizer without much greenhouse gas emission and heavy metal uptake [13]. Garg et al. applied fly ash and biogas slurry combination and found positive effects on the wheat yield and soil properties [6]. From past research, we find that biogas slurry does have the potential to improve soil properties and crop yield.

However, the problem is that there is no enough land for such large quantity of biogas slurry to utilize. With the surging development of collective livestock farms, around 2 hundred million tons of biogas slurry is produced every year only in China [14]. Owing to the propagation of household-scale anaerobic digesters and biogas plants in many Asian countries, including China, the amount of biogas slurry has drastically increased [15, 16]. Large livestock farm usually does not possess enough land space for the decomposition of biogas slurry. And the excessive discharge of biogas slurry not only changes the soil property but also causes secondary pollution [17–20]. Conventional wastewater treatment is not usually adopted to treat biogas slurry, due to its high costs and waste of nutrients [21]. The utilization of such large quantity of biogas slurry is of great significance in large-scale farming and biogas energy generation. At present, biogas fertilizer is mainly used for the relatively small size of more economic crops, such as vegetables, fruits, tobacco, and aquaculture. Rice is the most important staple food crop for the demand of the increasing population of the world and about 90% of world rice production comes from Asia [22]. Due to the position of rice in China's grain production (the largest total output and acreage), rice production is undoubtedly the largest biogas fertilizer consumed in China [23]. Many investigations focus on the rice field soil properties improvement or the environment affliction by biogas slurry [13, 24]. Song et al. studied growing rice with floating beds on natural waters [25]. Tian [26] studied growing rice with floating beds on the water of reservoirs. They all got good yields. Of all the research studies, few are about the direct utilization of rice soilless cultivation. This study's aim is to explore the ecological adaptability and the possibility of growing rice with floating bed on the dilute biogas slurry.

Artificial floating bed technology [27], which belongs to a surface soilless growing technology, has been recognized as a cost-effective and feasible process in wastewater treatment, especially for decentralized wastewater in rural areas. Currently, artificial floating beds have been widely used globally and often installed over waterbodies at weirs, ponds, rivers, reservoirs, and lakes [28]. In general, artificial floating beds have followed four main functions: water purification, habitat for fish and birds, improvement of landscape, and a break-water to protect the littoral zone. The function of water purification means to effectively and permanently remove excessive nutriments (mainly N and P) out of water volumes. The amount of time required to fulfill this purpose depends on the volumes and conditions of wastewater, the extent of active biofilms, and the maturity of bed plants as well as other environmental factors. Until now, despite numerous studies on floating plantation, most efforts have focused on wastewater treatment by cultivating plants on the beds. In contrast, using biogas slurry to cultivate economic plants on the floating bed has merely been studied. Thus, more empirical studies need to be conducted and the emphasis can be put on the factors that affect the growth of floating bed species.

In order to explore the feasibility of the direct utilization of biogas slurry in soilless rice production, this study conducted a floating bed rice planting experiment with diluted biogas slurry as medium. This study has the potential to provide the theoretical support for expanding the biogas utilization processes and developing the land-, water-, and fertilizer-saving facility agriculture.

2. Material and Methods

2.1. Materials and Planting Experiment. The planting experiment was carried out at the Hubei University, Wuhan, China, in a greenhouse with transparent rain shield cover on top.

The experimental biogas slurry was from a mesophilic biogas project in Tianmen City, Hubei Province, China. Its nutrient content and heavy metal concentration were measured. Before planting, the slurry was diluted by distilled water in descending dilution factor from 0 to 60 at intervals of 5. The diluted slurry is the medium for rice cultivation. At each dilution factor, 12-liter diluted slurry was collected and duplicates were applied. The slurry was kept into plastic buckets. 24 buckets were needed in total.

The experiment rice type is Ewan number 17. After 20 days of breeding in Tian Xin Zhou rice production area, the rice was ready for transplantation to the greenhouse. The foam board was cut into rounds with diameters slightly smaller than the buckets. Four equally spaced holes with diameters of around 2 cm were drilled on each of the foam boards. And all the foam boards were put in the buckets. Then, the rice seedlings were transplanted into the foam board of the buckets. Each small hole held two seedlings and each bucket contained eight seedlings. Seedlings were fixed with sponges. The planting experiment started on July 20th, 2015.

2.2. Sample Preparation and Analysis. After the seedlings were transplanted into the buckets, distilled water was added to each bucket to keep a relatively stable water volume. The slurry dilution medium in each bucket was changed every 15 days. The rice growth was observed and recorded from the beginning to the last day. The rice plants height and conductivity of the different multiple dilutions were measured. Plant height was measured with a ruler with accuracy to a millimeter, and conductivity was measured by portable conductivity meter (model: 320C-01A).

After the rice was mature, the rice panicle in each bucket was collected and the rice yield was measured. The rice husks were removed and the crude protein content and milled rice weight and rate were determined. Crude protein was measured by semimicro-Kjeldahl method. Heavy metals (copper, zirconium, lead, cadmium, and chromium) were determined by atomic absorption spectrophotometer (copper, zirconium by Flame method with model 4510; lead, cadmium, and chromium by graphite furnace method with model 4510F); Arsenic and mercury were determined by atomic fluorescence spectrometer (model: PF6-2).

Table 1: The conductivity value of different multiple dilutions biogas slurry (μs/cm).

Multiple dilutions	0	5	10	15	20	25	30	35	40	45	50	55	60
Conductivity (μs/cm)	3262	2480	1671	1192	974	872	784	719	638	605	566	532	438

2.3. Data Treatment and Analysis. Data are presented as mean ± standard deviation. Significant differences between and within multiple groups were examined using one-way ANOVA test followed by Tukey multiple comparisons test. The statistical analysis was performed by GraphPad Prism 6.0 software. A value of $P < 0.05$ was considered statistically significant.

3. Results and Analysis

3.1. Biogas Components and Conductivity. For nutrients, total nitrogen, phosphorus, and potassium were 0.13%, 0.023%, and 0.8% of the biogas slurry, respectively. The concentrations of the heavy metals, Zn, Cr, Cd, Pb, and Hg, were 3.33, 0.05, 0.001, 0.01, 0, and 0.004 mg/L, respectively. The pH of the slurry was 7.3 and COD_{Cr} concentration was 2,460 mg/L. The copper, zirconium, and COD_{Cr} concentrations exceeded the Chinese national standards for irrigation water quality (GB5084-1992). But when the slurry was diluted 2 times, the standards could be met.

According to Chinese national standards on the heavy metals and toxic substance in the water used in no-soil cultivation (Cu ≤ 0.1 mg/L, Zn ≤ 0.2 mg/L), the copper and zirconium concentrations exceeded the standard. When diluted 10 times, the standards could be met. In addition to the concentration of the nutrient components, either too high or too low conductivity of the culture solution used during no-soil-cultivation process can affect the growth of plants. Conductivity values of the different multiple dilutions were measured and shown in Table 1.

3.2. The Impact of Slurry Dilution Rate on Rice Growth Stages. The rice growth stages started from the day when it was sowed. The period of the first 20 days was a seedling stage. And, on the 20th day, rice was transplanted into the diluted slurry medium. The rice cultivated by normal way in soil usually experiences seedling stage, tillering stage, heading stage, flowering stage, grain filling stage, and fructicative stage. In the experiments, the rice cultivated with slurry of 30 to 55 multiple dilutions experienced tillering, heading, flowering, grain filling, and fructicative stages; the rice cultivated with slurry of 20, 25, and 60 multiple dilutions experienced only tillering, heading, and flowering stage. The rice cultivated with the 10 and 15 multiple dilutions' slurry experienced only tillering stage and heading stage. The relationship between the growth stages and the slurry dilution rate is shown in Table 2.

3.3. The Impact of Slurry Dilution Rate on Height of Rice Plants

3.3.1. The Height Change Trend during Rice Cultivated in Different Multiple Dilutions. After rice was transplanted into the diluted slurry medium, the height of the plants of all groups was measured on different growing days.

Figure 1(a) shows that the rice was alive when it was cultivated by the biogas slurry of 10 and 15 multiple dilutions in all days. On the 10th, 14th, 17th, 23rd, 36th, 60th, 90th, and 115th day, the height of rice plants cultivated by the biogas slurry of 15 multiple dilutions is greater than that cultivated by the biogas slurry of 10 multiple dilutions. On the 5th and 10th day, the rice died when cultivated by the biogas slurry of 0 and 5 multiple dilutions.

Figure 1(b) shows that the height of rice plants cultivated by the biogas slurry of 35 multiple dilutions is greater than that cultivated by the biogas slurry of 25 multiple dilutions on the 14th, 90th, and 115th day. On days 17, 25, 28, 34, 36, 60, 90, and 115, the height of rice plant which were cultivated with the biogas slurry of 35 multiple dilutions is greater than that with 20 multiple dilutions. There was no serious significance between the biogas slurries of 25 and 30 multiple dilutions in all days.

Figure 1(c) shows that all of the rice was alive cultivated with the biogas slurry of 40–55 dilutions, and the heights of rice plants have increased time-dependently.

3.3.2. The Relationship between Multiple Dilutions and the Height of Rice Plant on Days 28, 60, 90, and 115. The height of plant data on the 28th, 60th, 90th, and 115th day was selected and analyzed as follows.

(1) The Effect of the Biogas Slurry Multiple Dilutions on the Height of Rice Plant on the 28th Day. Figure 2 indicates that the multiple dilutions have obvious effects on the height of rice plants in the 10–30 multiple dilutions' group on the 28th day. The height of rice plants of 35 multiple dilutions was greater than that of 10, 20, 40, 50, 55, and 60. It is not statistically significant in the 40–60 multiple dilutions' groups.

(2) The Effect of the Biogas Slurry Multiple Dilutions on the Height of Rice Plant on the 60th Day. Figure 3 shows that there is positive relationship between 10–45 multiple dilutions of the biogas slurry and the height of rice plants, and the height of rice plants of 45 multiple dilutions was greater than that of 10, 15, 20, 25, 30, 35, and 40 multiple dilutions on the 60th day. After 45 multiple dilutions, the height of rice plants is decreased, but there is no obvious significance in 45–60 multiple dilutions.

(3) The Effect of the Biogas Slurry Multiple Dilutions on the Height of Rice Plants on the 90th Day. Figure 4 shows that there is a direct relationship between 10–45 multiple dilutions of the biogas slurry and the height of rice plants, and the height of rice plants of 45 multiple dilutions was greater than

Table 2: The growth stages of rice cultivated with different diluted biogas slurry.

Multiple dilutions	Duplication	Tillering stage	Heading stage	Flowering stage	Grain filling stage	Fructicative stage
10	1	√	√	×	×	×
	2	√	√	×	×	×
15	1	√	√	×	×	×
	2	√	√	×	×	×
20	1	√	√	√	×	×
	2	√	√	√	×	×
25	1	√	√	√	×	×
	2	√	√	√	×	×
30	1	√	√	√	√	√
	2	√	√	√	√	√
35	1	√	√	√	√	√
	2	√	√	√	√	√
40	1	√	√	√	√	√
	2	√	√	√	√	√
45	1	√	√	√	√	√
	2	√	√	√	√	√
50	1	√	√	√	√	√
	2	√	√	√	√	√
55	1	√	√	√	√	√
	2	√	√	√	√	√
60	1	√	√	√	×	×
	2	√	√	√	×	×

Note: √ shows the rice plants have ever experienced the growth.
× shows the rice plants have not experienced the growth.

that of 10, 15, 20, 25, 30, 35, and 40 multiple dilutions on the 90th day. After 45 multiple dilutions, there is a reverse relationship between multiple dilutions and the height of rice plants, and the height of rice plants of 60 multiple dilutions was less than that of 45 multiple dilutions.

(4) The Effect of the Biogas Slurry Multiple Dilutions on the Height of Rice Plants on the 115th Day. Figure 5 shows that there is a direct relationship between multiple dilutions and the height of rice plants in 10–45 dilutions' groups on the 115th day, and, specifically, the height of rice plants of 45 multiple dilutions was greater than that of 10, 15, 20, 25, and 30, and the height of rice plants of 35 and 40 multiple dilutions was greater than that of 30. After 45 multiple dilutions, there is a reverse relationship between multiple dilutions and the height of rice plants, and the height of rice plants of 45 and 50 multiple dilutions was greater than that of 60 multiple dilutions.

Based on Figure 5, the height of rice plants cultivated with 40, 45, and 50 multiple dilutions was obviously greater than that of other dilutions on 115th day.

The height of rice plants was affected significantly by multiple dilutions; the rice was not alive in the 0–5 multiple dilutions; however, it was alive in the 10–60 multiple dilutions. The height of rice plants shows the tendency from increase to decrease with the increase of multiple dilutions, and the height of the rice plant begins to decrease after 30 dilutions on the 30th day, and it tends to decrease after 45 dilutions on the 60th, 90th, and 115th day.

When the experiment was finished on the 115th day, the height of rice plants in 40, 45, and 50 dilutions was greater than that of other multiple dilutions.

3.4. The Effect of the Biogas Slurry Multiple Dilutions on the Yield and Quality of the Rice

3.4.1. The Effect of the Biogas Slurry Multiple Dilutions on the Yield of the Rice. Figure 6 shows that the rice plant produced rice with 30, 35, 40, 45, 50, and 55 multiple dilutions. There is a positive relationship between the production of rice and the multiple dilutions, and, specifically, the height in 45 multiple dilutions is the greatest one in all 30, 35, 40, and 45 multiple dilutions. There is a reverse relationship between the production of the rice and 45–55 dilutions, and moreover the production of the rice was the lowest in the 55 dilutions.

3.4.2. The Effect of the Biogas Slurry Multiple Dilutions on the Content of Crude Protein in the Rice. Figure 7 shows that there is reverse relationship between the multiple dilutions and the content of crude protein in the rice. Specifically, the

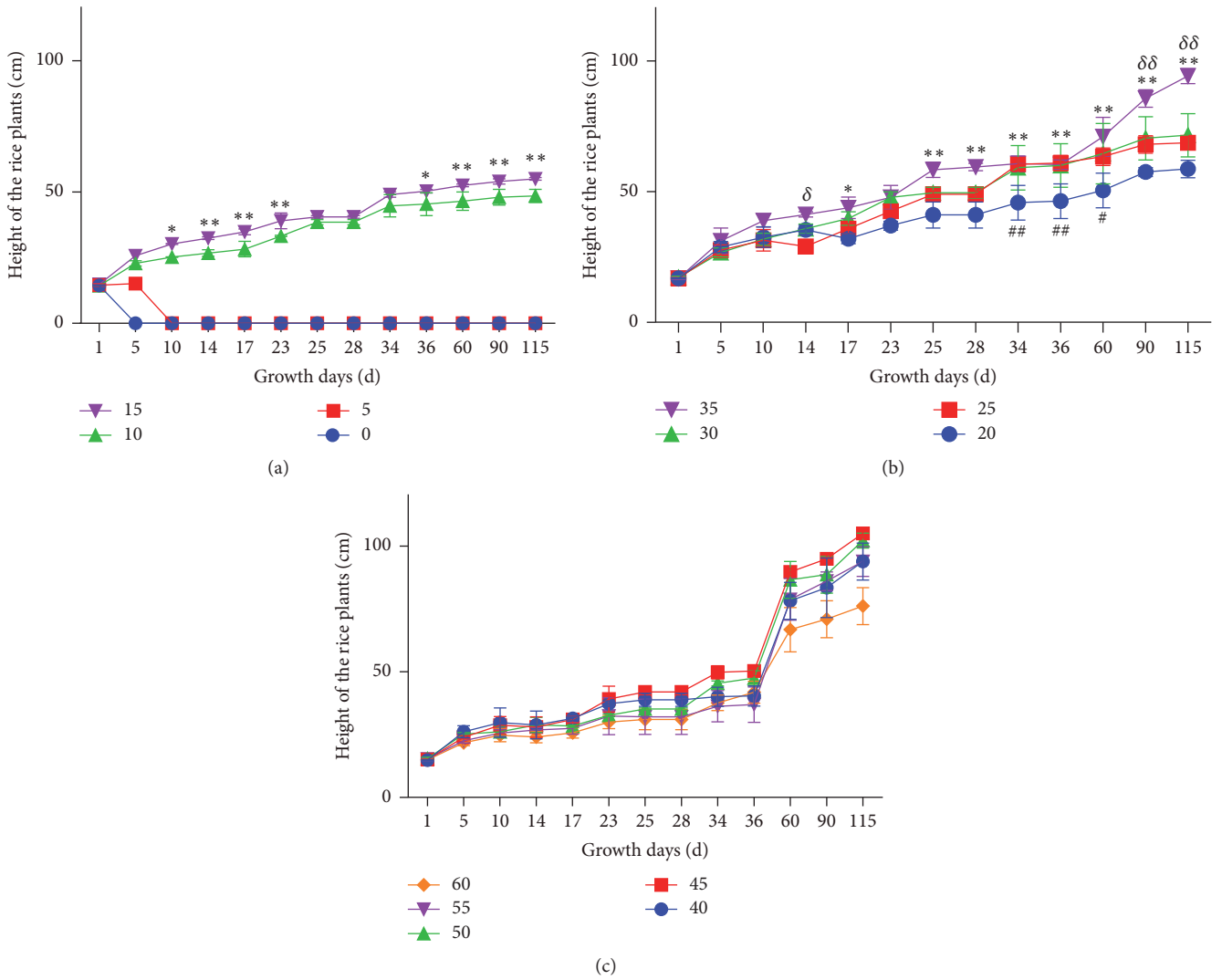

FIGURE 1: The relationship between the rice plant height and multiple dilutions during growth days. (a) represents the rice plants height of the 0, 5, 10, and 15 multiple dilutions' groups during growth days. $^{*}P < 0.05$, 15 *versus* 10 multiple dilutions' group. $^{**}P < 0.01$, 15 *versus* 10 multiple dilutions' group. (b) represents the rice plants height of the 20, 25, 30, and 35 multiple dilutions' groups during growth days, $^{*}P < 0.05$, 35 *versus* 20 multiple dilutions' group, $^{**}P < 0.01$, 35 *versus* 20 multiple dilutions' group, $^{\#}P < 0.05$, 25 *versus* 20 multiple dilutions' group, $^{**}P < 0.01$, 25 *versus* 20 multiple dilutions' group, $^{\delta}P < 0.05$, 35 *versus* 25 multiple dilutions' group, and $^{\delta\delta}P < 0.01$, 35 *versus* 25 multiple dilutions' group; (c) represents the rice plants height of the 40, 45, 50, 55, and 60 multiple dilutions' groups during growth days.

content of crude protein in the rice in the 30 dilutions was higher than that in 55. Moreover, there was no significant relationship between the contents of crude protein in 30, 35, 40, and 45 dilutions' groups. Finally, the content of crude protein in the 55 dilutions is the lowest.

3.4.3. The Effect of the Biogas Slurry Multiple Dilutions on the Milled Rice Rate. Figure 8 shows that there was a reversed relationship between the milled rice rate and multiple dilutions. Specifically, the milled rice rates in 30, 35, 40, and 45 dilutions' groups were higher than that in 55. Moreover, the milled rice rates in 30 and 35 dilutions were higher than that in 50. Finally, there were no obviously significant relationships both in 30, 35, 40, and 45 multiple dilutions' groups and in 50 or 55 groups.

3.5. Heavy Metal Concentration in the Rice. The heavy metals concentrations in the rice growing in the 30 times' dilution were measured. The total lead, cadmium, mercury, and arsenic concentrations were 0.02, 0.05, 0, and 0.02 mg/kg milled rice, respectively. All reached the Chinese Hygienic Standard for Grains (GB2715-2005). Total chromium concentration was 0.05 mg/kg, which also met the requirements of the standards for food safety (GB2762-2012).

The copper and zirconium concentrations were 1.02 and 1.51 mg/kg, respectively. Both were the nutrient elements in rice.

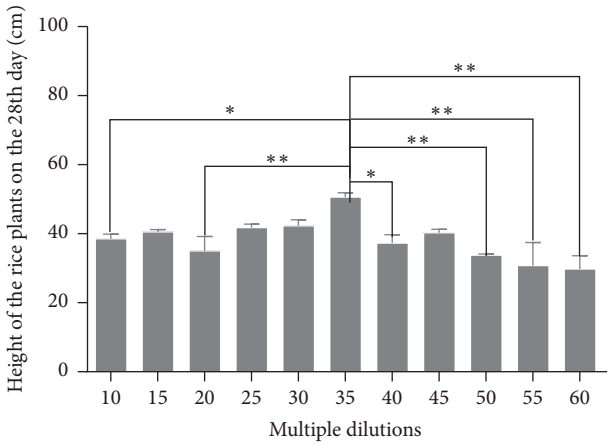

Figure 2: Height of the rice plant in different multiple dilutions on the 28th day. $^{*}P < 0.05$, *versus* 35 multiple dilutions' group. $^{**}P < 0.01$, *versus* 35 multiple dilutions' group.

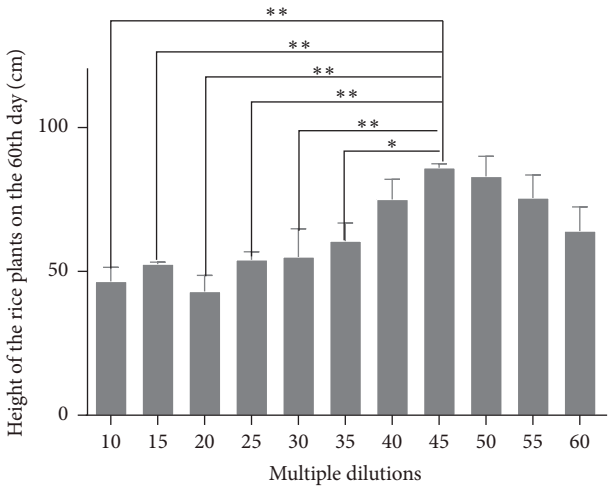

Figure 3: Height of rice plants in all different groups on the 60th day. $^{*}P < 0.05$, *versus* 45 multiple dilutions' group, $^{**}P < 0.01$, *versus* 45 multiple dilutions' group.

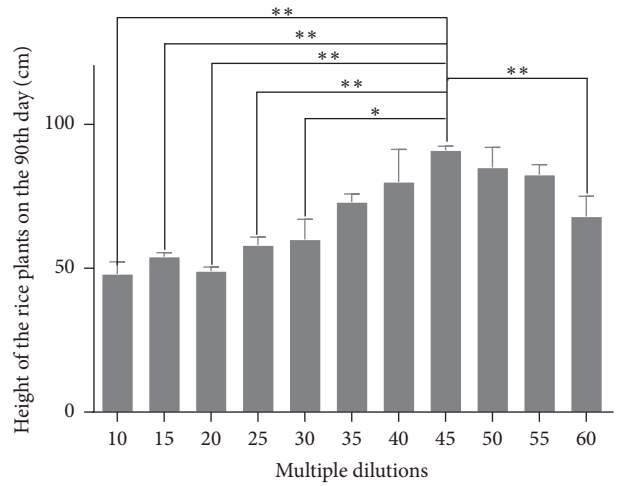

Figure 4: Height of rice plants in all different groups on the 90th day. $^{*}P < 0.05$ *versus* 45 multiple dilutions' group; $^{**}P < 0.01$ *versus* 45 multiple dilutions' group.

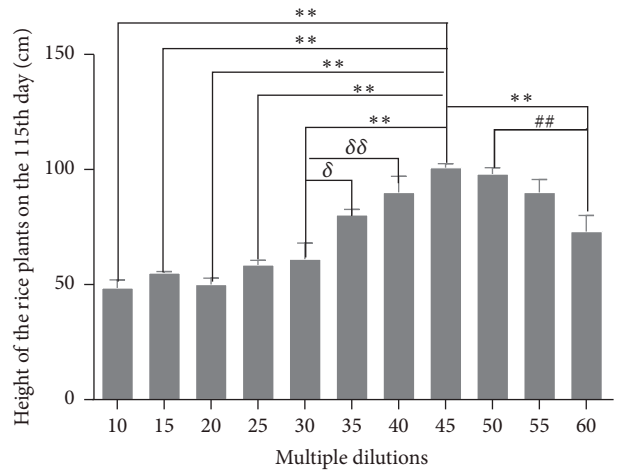

Figure 5: Height of rice plants in all different groups on the 115th Day. $^{*}P < 0.05$ *versus* 45 multiple dilutions' group; $^{**}P < 0.01$ *versus* 45 multiple dilutions' group; $^{\#\#}P < 0.01$, 50 *versus* 60 multiple dilutions' group; $^{\delta}P < 0.05$ 35 *versus* 30 multiple dilutions' group; and $^{\delta\delta}P < 0.01$ 40 *versus* 30 multiple dilutions' group.

4. Discussion

4.1. The Ecological Adaptability of Growing Rice with Diluted Biogas Slurry. The results show that the slurry dilution rate had a significant impact on the growth stages, plant height, and yield and quantity of rice. The reasons are as follows.

The plants cultivated in no soil absorb nutrition such as water and nitrogen and phosphorus and potassium elements and so on from the nutritive medium. So the nutritive medium is the key for the growth. When the dilution rate was 0 and 5, the conductivity value of the slurry was 3,262 μs/cm and 2,480 μs/cm, which is equal to 3/5 and 1/2 of the sea water. The inorganic salt concentration was so high that it was higher than that of plant cell fluid, which caused the death of the rice plants. When the dilution increased over 10 (the conductivity value was over 1,671 μs/cm), the plants were alive and grew.

When the dilution rates were 30 to 55, the conductivity value was from 784 μs/cm to 532 μs/cm and the rice plants produced rice. When the dilution rate was 60 (the conductivity value was 438 μs/cm) the rice plant did not grow or produce rice. The possible reason is that nutrient substance in the 60 dilutions' biogas slurry is too low. The yield of rice and height of the rice plants increased firstly and later decreased with the increase of dilutions. The possible reason is that, with the increase of dilutions, the conductivity value and nutrient substance reached a relatively suitable value for rice to grow well. But when the dilution increased, there was

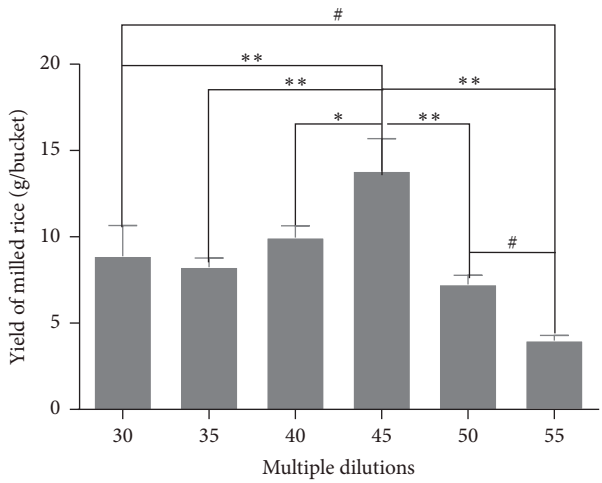

Figure 6: The relationship between the milled rice yield and multiple dilutions. $^{*}P < 0.05$ *versus* 45 multiple dilutions' group; $^{**}P < 0.01$ *versus* 45 multiple dilutions' group; and $^{\#}P < 0.05$ *versus* 55 multiple dilutions' group.

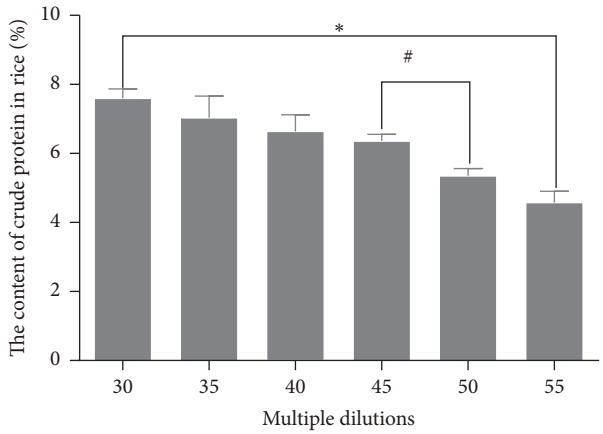

Figure 7: The relationship between the content of crude protein and multiple dilutions. $^{*}P < 0.05$ *versus* 55 multiple dilutions' group. $^{\#}P < 0.05$ *versus* 50 multiple dilutions' group.

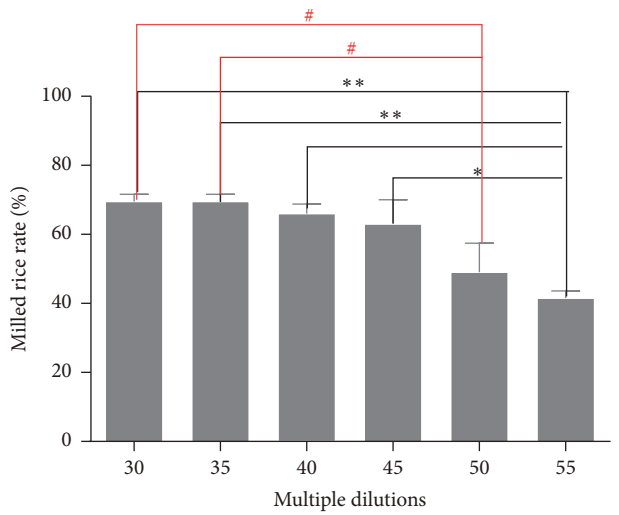

Figure 8: The relationship between the milled rice rate and multiple dilutions. $^{*}P < 0.05$ *versus* 55 multiple dilutions' group, $^{**}P < 0.01$ *versus* 55 multiple dilutions' group, and $^{\#}P < 0.05$ *versus* 50 multiple dilutions' group.

less of the nutrient substance in the slurry, which affects the yield of rice and height of the rice plants. Considering the situation of the yield, milled rate, and crude protein of the rice together, among all the dilutions, the 45 multiple dilutions are better than others. In the 45 multiple dilutions' group, the yield of rice was 13.3 g/bucket (8 rice plants); milled rice rate was 63.1%, which was 10% lower than that in average of rice cultivated by normal way in soil; the content of crude protein in the rice was 6.3%, which was also lower than that in average of rice cultivated by the normal way in soil (9.3%).

The concentrations of heavy metals in the rice, such as lead, chromium, and arsenate, cultivated with 30 dilutions reached the Chinese Hygienic Standard for Grains (GB2715-2005).

In this experiment, the rice yield was lower than the conventionally planted rice. The reason might be that when biogas slurry acts as the only nutrient source, the growing environment is not nutrients-balanced. When the rice fertilizer requirement increased, the biogas slurry concentration was not increased accordingly. Overall nutrients content of biogas slurry was relatively low [29]. Also the low iron content of the slurry contributed to the frequent rice iron deficiency during the experiment [30]. Regular addition of iron to the medium could maintain a stable growth of lettuce, celery, tomato, cucumber, and eggplant. This indicated that the addition of chelated iron was effective in solving biogas slurry iron shortage [31].

The heavy metals' concentrations in the rice growing in the 30 times' dilution were measured. The total lead, cadmium, mercury, and arsenic concentrations reached the Chinese Hygienic Standard for Grains (GB2715-2005). It shows cultivating rice in over 30 dilutions' biogas slurry is safe.

4.2. Swine Manure-Biogas Slurry-Rice-Biofuel Circle Mode. Scalable rice production with biogas slurry not only can bring economic benefits by harvesting rice but also can provide an economic production model with swine manure-biogas slurry-rice-biofuel biomass energy circle (Figure 9). As shown in Figure 7, rice could be obtained by the cultivation in biogas slurry, while rice straw could be used for the generation of biofuels such as bioethanol and biogas. The by-product of rice straw fermentation was biogas slurry, which can in turn be used to grow rice. Thus, a nitrogen circle was formed by this approach. The process also presented a highly viable measure for biogas upgrading, since CO_2 from crude biogas was consumed during the microalga photosynthesis. The production of straw-based biofuels in the form of bioethanol and biogas can compensate energy consumed in the system [32]. In other words, the biofuels

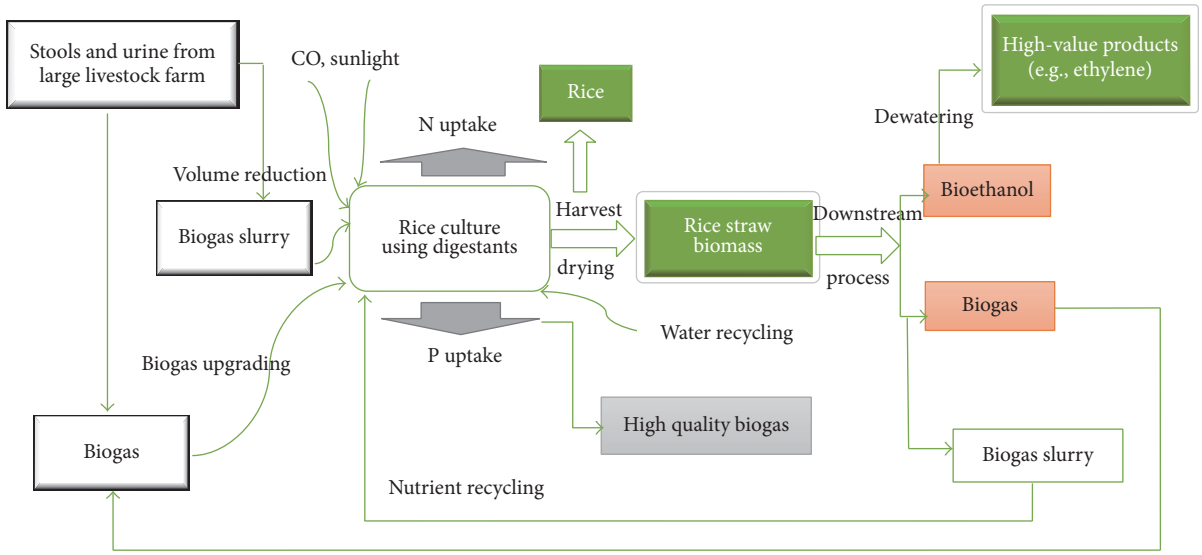

Figure 9: Swine manure-biogas slurry-rice-biofuel production circle.

generated can serve as the primary energy source for the operation of the whole process.

5. Conclusions

This study shows that it is possible and safe to cultivate rice plants on the floating bed with no soil but the diluted biogas slurry from by-products of biogas project. Among 0–60 multiple dilutions, rice plants cultivated with 45 multiple dilutions had better ecological adaptability than others. However the yield, crude protein, and milled rice rates of the rice plants cultivated with 45 multiple dilutions are not as much as those of rice cultivated in the regular way in soil.

The next research direction is comparing the nutrition components in the diluted biogas slurry with the nutrition components in the regular soil and adding extra nutrients or compound fertilizer to the biogas slurry in different rice growth stages for the purpose of increasing the rice yield and quantity.

This technique provides a problem solving approach to the big amount of slurry discharge in the livestock farms. Apart from economic benefits, the production circle of swine manure-biogas slurry-rice-biofuel has the potential to contribute to reducing the carbon footprint and protecting the environment.

Competing Interests

The authors declare that they have no competing financial interests.

References

[1] C. Chen, Z.-Y. Ruan, and J. Wu, "Research progress on the comprehensive disposal and utilization of biogas slurry from large scale biogas engineering," *China Biogas*, vol. 31, no. 1, pp. 25–28, 2013.

[2] E. C. Gutierrez, A. Xia, and J. D. Murphy, "Can slurry biogas systems be cost effective without subsidy in Mexico?" *Renewable Energy*, vol. 95, pp. 22–30, 2016.

[3] J. A. Alburquerque, C. de la Fuente, and M. P. Bernal, "Chemical properties of anaerobic digestates affecting C and N dynamics in amended soils," *Agriculture, Ecosystems and Environment*, vol. 160, pp. 15–22, 2012.

[4] J. L. Smith and L. F. Elliot, "Tillage and residue management effects on organic matter dynamics in semi-arid regions," *Advanced Soil Science*, vol. 88, no. 13, pp. 69–88, 1990.

[5] R. Prasad and J. F. Power, "Crop residue management," *Advanced Soil Science*, no. 15, pp. 205–251, 1991.

[6] R. N. Garg, H. Pathak, D. K. Das, and R. K. Tomar, "Use of flyash and biogas slurry for improving wheat yield and physical properties of soil," *Environmental Monitoring and Assessment*, vol. 107, no. 1–3, pp. 1–9, 2005.

[7] W. K. Liu, L. F. Du, and Q. C. Yang, "Biogas slurry added amino acids decreased nitrate concentrations of lettuce in sand culture," *Acta Agriculturae Scandinavica Section B: Soil and Plant Science*, vol. 59, no. 3, pp. 260–264, 2009.

[8] Y.-Y. Wang and R.-H. Liu, "Progress of comprehensive utilization of biogas slurry," *Journal of Anhui Agricultural Sciences*, vol. 35, no. 4, pp. 1089–1091, 2007.

[9] H.-X. Wang and Z.-S. Zhang, "Biogas chemicals and its application on agricultural production," *Shanxi Journal of Agricultural Sciences*, no. 3, pp. 89–91, 2006.

[10] Q. Guo, X.-L. Chai, and H.-J. Cheng, "Comprehensive utilizing of biogas liquid residue," *Recycling Research*, no. 6, pp. 37–41, 2005.

[11] F.-B. Yu, X.-P. Luo, C.-F. Song, and S.-D. Shan, "Concentrated biogas slurry enhanced soil fertility and tomato quality," *Acta Agriculturae Scandinavica Section B—Soil and Plant Science*, vol. 60, no. 3, pp. 262–268, 2010.

[12] X. Zheng, J. Fan, J. Cui et al., "Effects of biogas slurry application on peanut yield, soil nutrients, carbon storage, and microbial activity in an Ultisol soil in southern China," *Journal of Soils and Sediments*, vol. 16, no. 2, pp. 449–460, 2016.

[13] A. T. Win, K. Toyota, K. T. Win et al., "Effect of biogas slurry application on CH_4 and N_2O emissions, Cu and Zn uptakes by

whole crop rice in a paddy field in Japan," *Soil Science and Plant Nutrition*, vol. 60, no. 3, pp. 411–422, 2014.

[14] S.-W. Huang and X.-Y. Liao, "Progress and prospect of biogas fermentation residues (MFR) application on rice planting," *China Biogas*, vol. 3, no. 2, pp. 23–26, 2005.

[15] I. Angelidaki and L. Ellegaard, "Codigestion of manure and organic wastes in centralized biogas plants: status and future trends," *Applied Biochemistry and Biotechnology—Part A*, vol. 109, no. 1–3, pp. 95–105, 2003.

[16] E. R. Abraham, S. Ramachandran, and V. Ramalingam, "Biogas: can it be an important source of energy?" *Environmental Science and Pollution Research*, vol. 14, no. 1, pp. 67–71, 2007.

[17] M. Han, K.-F. Liu, and C.-D. Gao, "Review of biogas utilization harmless treatment and resource utilization," in *Proceedings of the Annual Conference of the Chinese Academy of Environmental Science*, pp. 3658–3671, 2014.

[18] S.-B. Wu, C. Cui, X.-Q. Zhang, W. Li, C.-L. Pang, and R.-J. Dong, "Effect of biogas slurry on yield increase, quality improvement, water and soil environment," *Chinese Journal of Agricultural Machinery*, vol. 44, no. 8, pp. 118–125, 2013.

[19] J.-F. Miao, J. Ye, Y.-M. Huang, Q. Kang, and Z.-H. Li, "Effects of biogas slurry irrigation on heavy metal contents in soils," *Agricultural Science & Technology*, vol. 15, no. 3, pp. 417–421, 2014.

[20] Y. E. Jing, J.-F. Miao, Y.-M. Huang, Y.-Q. Li, and Z.-H. Li, "Effects of biogas slurry irrigation on heavy metal content and Yield of lettuce," *Acta Agriculture Jiangxi*, vol. 26, no. 7, pp. 96–99, 2014.

[21] Q.-W. Sui, H.-M. Dong, Z.-P. Zhu, and H.-K. Huang, "Present status of biogas effluent treatment technology research and application," *Journal of Agricultural Science and Technology*, vol. 13, no. 1, pp. 83–87, 2013.

[22] J. Bruinsma, Ed., *World Agriculture: Towards 2015/2030 Summary Report*, Food and Agriculture Organization of the United Nations (FAO), Rome, Italy, 2002.

[23] S.-W. Huang and X.-Y. Liao, "Progress and prospect of biogas fermentation residues (MFR) application on RICE planting," *China Biogas*, vol. 23, no. 2, pp. 23–26, 2005.

[24] Y. Jia, G.-X. Sun, H. Huang, and Y.-G. Zhu, "Biogas slurry application elevated arsenic accumulation in rice plant through increased arsenic release and methylation in paddy soil," *Plant and Soil*, vol. 365, no. 1-2, pp. 387–396, 2013.

[25] X.-F. Song, Z.-M. Xiong, H.-D. Ying et al., "The technology of growing rice with floating bed on the natural waters," *Agricultural Science and Technology Communication*, no. 7, pp. 6–8, 1992.

[26] X.-M. Tian, "Study on the growing rice on the natual waters of Large reservoir," *Journal of Zhejiang Agricultural Sciences*, no. 5, pp. 211–214, 1993.

[27] L.-D. Zhu, J. Takala, E. Hiltunen, Z. H. Li, and Y. Kristianto, "Comparison of vertical-flow constructed wetlands with and without supplementary aeration treating decentralized domestic wastewater," *Environmental Technology*, vol. 34, no. 1, pp. 53–60, 2013.

[28] L. Zhu, Z. Li, and T. Ketola, "Biomass accumulations and nutrient uptake of plants cultivated on artificial floating beds in chinas rural area," *Ecological Engineering*, vol. 37, no. 10, pp. 1460–1466, 2011.

[29] J. Zhang, M.-X. Zhang, and S.-D. Shan, "Nutritional quality and yield of Pai-tsai (Brassica chinensis L.) as affected by biogas slurry application under soilless culture," *Bulletin of Science and Technology*, vol. 26, no. 3, pp. 407–412, 2010.

[30] S.-R. Xia, "The application and development of the domestic and foreign soilless cultivation," *Processing of Agricultural Products*, no. 3, pp. 35–37, 2009.

[31] X.-F. Zhou, L. Qiu, and Z.-L. Li, "The nutrient mechanism and technology optimization of soilless cultivation by biogas slurry medium," *Journal of Agricultural Mechanization Research*, vol. 35, no. 5, pp. 224–227, 2013.

[32] L.-D. Zhu and E. Hiltunen, "Application of livestock waste compost to cultivate microalgae for bioproducts production: a feasible framework," *Renewable and Sustainable Energy Reviews*, vol. 54, pp. 1285–1290, 2016.

Hindawi Publishing Corporation
BioMed Research International
Volume 2016, Article ID 4342892, 8 pages
http://dx.doi.org/10.1155/2016/4342892

Research Article

Isoprene Production on Enzymatic Hydrolysate of Peanut Hull Using Different Pretreatment Methods

Sumeng Wang,[1] Ruichao Li,[1] Xiaohua Yi,[1] Tigao Fang,[1] Jianming Yang,[1] and Hyeun-Jong Bae[2]

[1]*Key Lab of Plant Biotechnology in Universities of Shandong Province, College of Life Sciences, Qingdao Agricultural University, Qingdao 266109, China*
[2]*Bio-Energy Research Institute, Chonnam National University, Gwangju 500-757, Republic of Korea*

Correspondence should be addressed to Jianming Yang; yjming888@126.com and Hyeun-Jong Bae; baehj@chonnam.ac.kr

Received 21 June 2016; Revised 4 August 2016; Accepted 18 August 2016

Academic Editor: Liandong Zhu

The present study is about the use of peanut hull for isoprene production. In this study, two pretreatment methods, hydrogen peroxide-acetic acid (HPAC) and popping, were employed prior to enzymatic hydrolysis, which could destroy the lignocellulosic structure and accordingly improve the efficiency of enzymatic hydrolysis. It is proven that the isoprene production on enzymatic hydrolysate with HPAC pretreatment is about 1.9-fold higher than that of popping pretreatment. Moreover, through High Performance Liquid Chromatography (HPLC) analysis, the amount and category of inhibitors such as formic acid, acetic acid, and HMF were assayed and were varied in different enzymatic hydrolysates, which may be the reason leading to a decrease in isoprene production during fermentation. To further increase the isoprene yield, the enzymatic hydrolysate of HPAC was detoxified by activated carbon. As a result, using the detoxified enzymatic hydrolysate as the carbon source, the engineered strain YJM21 could accumulate 297.5 mg/L isoprene, which accounted for about 90% of isoprene production by YJM21 fermented on pure glucose (338.6 mg/L). This work is thought to be the first attempt on isoprene production by *E. coli* using peanut hull as the feedstock. More importantly, it also shows the prospect of peanut hull to be considered as an alternative feedstock for bio-based chemicals or biofuels production due to its easy access and high polysaccharide content.

1. Introduction

Isoprene (2-methylbuta-1,3-diene), as a polymer building block, plays a pertinent role in the synthetic chemistry industry and represents an important biological material. Isoprene could serve as the feedstock not only in industrial production of synthetic rubber or aviation fuel [1, 2] but also in the fields of isoprenoid medicines and fragrances [3]. Currently, industrial isoprene production mainly relies on fossil sources, achieved by means of chemical synthesis techniques [1, 4]. However, due to the decrease of petroleum reserve and the enhancement of environmental awareness, it becomes increasingly urgent and necessary to produce isoprene using renewable resources as an alternative to petroleum resource.

Although isoprene could be produced from many kinds of plants [5] or some microorganisms such as fungi, *Eurotium amstelodami* [6], both ways still sound impractical, since it is difficult to harvest isoprene from plant species [7], and the material shortage and low conversion efficiency are widely recognized as a bottleneck for isoprene production by microorganisms.

Today, millions of tons of agricultural lignocellulosic wastes are produced around the world annually. The abundant supply and low cost properties [8, 9] have made agricultural lignocellulosic wastes the most promising materials for substituting the dwindling fossil fuels. In China, the annual production of peanut could reach up to 1.3×10^7 tons, which accordingly resulted in 3.64×10^6 tons of peanut hull in 2008 [10]. Recently, the USDA reported that peanut production in China accounted for approximately 45% of the total yield of the world's peanut [11] (USDA 2015). As is shown in Figure 1, peanut hull consists of 46.8% holocellulose, 5.8% ash, 4.0%

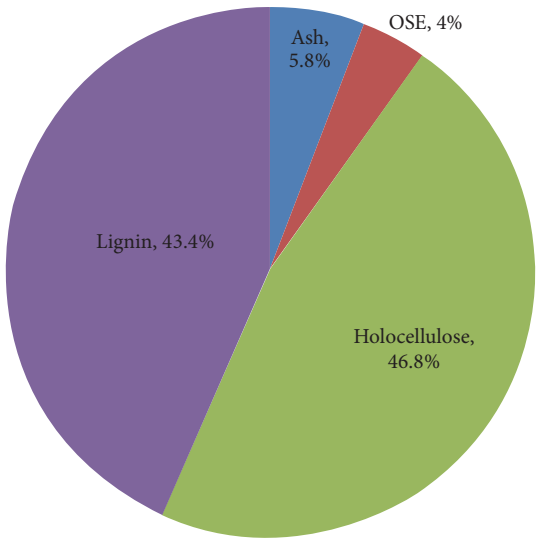

Figure 1: Chemical composition of peanut hull.

OSE, and 43.4% Klason lignin. Its high polysaccharide content makes peanut hull a suitable feedstock for the production of bio-based chemicals or biofuels including isoprene.

Since cellulose is usually surrounded by hemicellulose and lignin which would reduce the conversion rate of cellulose into fermentable sugar, it is vital to develop an economic pretreatment method to change the lignocellulosic biomass structure so as to improve degradation efficiency by cellulase to translate cellulose into fermentative saccharides. So far, various pretreatment techniques have been developed to disrupt the lignocellulosic structure prior to enzyme hydrolysis, including dilute acid, steam explosion, liquid hot water, ammonia pretreatments, and popping [12, 13]. Among them, the machine used in popping pretreatment is a very simple system consisting of direct burner and rotary reactor without steam generator [12], and this process has remarkable advantages including higher saccharification efficiency, cost effectiveness, and environmental safety [14]. Acetic acid might enhance the hydrolysis efficiency of hemicellulose [15], and hydrogen peroxide pretreatment has many advantages such as forming fewer inhibitors and generating more glucose yield in addition to lower toxicity and less environmental impact [15, 16].

Based on the above analysis, in this study, we introduced two pretreatment methods to treat peanut hull prior to hydrolysis by cellulase, popping [17] and HPAC [18], with HPAC being an efficient method, including hydrogen peroxide and acetic acid. Meanwhile, to further enhance the isoprene production, we detoxified the enzymatic hydrolysate of peanut hull pretreated by HPAC. We finally achieved the different isoprene production with several kinds of enzymatic hydrolysates. This work is the first attempt to produce isoprene by *E. coli* using the peanut hull as the feedstock. And, more importantly, this work provides evidence to show that another lignocellulose material, peanut hull, could be considered as a promising feedstock for industrial production of bio-based chemicals or biofuels.

2. Materials and Methods

2.1. HPAC Pretreatment and Popping Pretreatment. Peanut hull (PH) used in this experiment was collected from Shandong province, China. PH was milled and screened to a 40–60 mesh size and then was air-dried after its associated wastes were washed by running water. To be specific, ten-gram peanut hulls (PHs) were treated with 100 mL of HPAC solution, a mixture of hydrogen peroxide and acetic acid (1 : 1; v/v), and then incubated at 80°C for 3 h, after which materials were filtered to separate the HPAC solution from the solid residue, and they were washed 3 times by running water until neutral pH was reached [18].

A total of 100 g (dry weight) of PHs was treated using the popping equipment [17]. Filled with PHs (moisture content: 75%), the reactor was directly heated with a gas burner at a rate between 15 and 20°C/min and rapidly opened the hatch at 220°C and 1.47 MPa. After treatment, materials were recovered in a reactor and cooled at room temperature. And then HPAC and popping treated PHs were dried by a lyophilizer at −45°C for 5 days.

2.2. SEM Imaging. The surface morphologies of samples, including pretreated PHs by popping and HPAC and untreated PH, were analyzed using scanning election microscopy (SEM; JSM-7500F, Jeol, Japan). Imaging was captured at a beam voltage of 4 kV. Prior to observation and photography, biomass samples were dried at 50°C for 24 h and gold sputter-coated (20 nm).

2.3. Chemical Composition Analysis. Both 20 mg raw and pretreated PHs were used to analyze chemical composition. The structural carbohydrates, ash, and lignin analysis procedure of all biomass samples were measured according to the NREL Laboratory Analytical Procedure (LAP) [19]. And organic solvent extractives (OSE) were analyzed with TAPPI Standard Methods [20]. The raw and pretreated (HPAC and popping) PHs were analyzed for their neutral sugar content using gas chromatography (GC) [13]. The samples were analyzed via GC (GC-2010; Shimadzu, Otsu, Japan) using a DB-225 capillary column (30 m × 0.25 mm i.d., 0.25 μm film thickness, J&W; Agilent, Folsom, CA, USA) operated with helium. The operating conditions were as follows: injector temperature of 220°C, flame ionization detector (FID) at 250°C, and an oven temperature of 100°C for 1.5 min with a constant increase of 5°C/min to 220°C.

2.4. Enzymatic Hydrolysis. The PHs as 1% (w/v) substrate were treated in 50 mM sodium citrate buffer (pH 4.8) supplemented with 0.01% (w/v) sodium azide. Each of the enzymes, celluclast (Novozymes, Denmark) and xylanase (endo-1,4-β-xylanase from *Trichoderma longibrachiatum*, Sigma-Aldrich, USA), were loaded with 30 FPU per gram of glucan and 300 international units (IU)/mL, respectively. All samples were completely suspended in rotary shaker at 200 rpm at 37°C for 48 h. All enzymatic hydrolysis experiments were performed in triplicate.

2.5. Detoxification with Activated Carbon. The enzymatic hydrolysate of peanut hull (HPAC pretreated) along with 1% (w/v) activated carbon (05-690A, 50–200 mesh, Fisher Scientific Co., Pittsburgh, PA, USA) was mixed in 250 mL flask. And then the flask had been incubating at 30°C with shaking at the rate of 180 rpm for 10 h. After treatment, the activated carbon was removed from the mixture by centrifugation at 10000 rpm for 10 min. To get the detoxification hydrolysate, the supernate was finally filtered by using 0.2 μm filter membrane.

2.6. Shake Flask Fermentation. Shake flask experiments were carried out in triplicate using a series of 25 mL sealed shake flasks containing 5 mL fermentation medium including glucose 2 g/L or suitable concentration of enzymatic hydrolysate, K_2HPO_4 9.8 g/L, beef extract 9 g/L, ferric ammonium citrate 0.3 g/L, citric acid monohydrate 2.1 g/L, $MgSO_4$ 0.06 g/L, and 1 mL trace element solution, consisting of $(NH_4)_6Mo_7O_{24}{\cdot}4H_2O$ 0.37 g/L, $ZnSO_4{\cdot}7H_2O$ 0.29 g/L, H_3BO_4 2.47 g/L, $CuSO_4{\cdot}5H_2O$ 0.25 g/L, and $MnCl_2{\cdot}4H_2O$ 1.58 g/L. Meanwhile, the medium contained 34 mg/mL Cm and 100 mg/mL Amp. The engineered *E. coli* strain YJM21 [21] was inoculated to the culture broth and incubated in a gyratory shaker incubator at 37°C and 180 rpm. When OD_{600} reached 0.6, IPTG was added in final concentration of 0.5 mM, and the culture was further incubated at 30°C for 24 h.

2.7. Analytical Methods. Bacterial growth conditions were estimated from the optical density (OD) of the medium with a spectrophotometer (UV2310II, Shanghai Precision & Scientific Instrument Co., Ltd., China) at a wavelength of 600 nm. The concentration of isoprene was analyzed by a gas chromatograph (GC) equipped with a flame ionization detector (FID) and a TM-WAX column (25 m × 0.25 mm × 0.25 μm). N_2 was used as carrier gas. The initial column temperature was 50°C for 1 min and was increased at a rate of 6°C/min to a final temperature of 80°C, while the injector temperature was 140°C and the detector temperature was 230°C, respectively.

To identify bacterial isoprene production, peak retention times and mass spectra were compared with those of the standard. Concentrations of isoprene produced by bacterial cells were calculated by converting GC peak area to mg of isoprene via a calibration curve. Isoprene standard (TCI-EP, Tokyo, Japan) of various concentrations was added to 600 mL fermentation medium to construct a calibration curve.

3. Results and Discussion

3.1. Chemical Composition and Monosugar Composition Rate of Peanut Hull. In China, peanut hull, considered as the agricultural waste, was redundant and was not utilized very well. Meanwhile, its high polysaccharide content makes it a suitable feedstock for the production of bio-based chemicals or biofuels including isoprene. Figure 1 enumerates the chemical compositions of the peanut hull, such as ash, organic solvent extractives (OSE), holocellulose (glucose, xylose, arabinose, galactose, rhamnose, and mannose), and Klason lignin. The PH content contained 46.8% holocellulose, 5.8% ash, 4.0% OSE, and 43.4% Klason lignin. Although the lignin content of peanut hull was high and peanut hull also had significant amount of available sugars for bioconversion, this result still indicated that the lignin of PH sample needed to be removed via pretreatment process to enhance the enzymatic hydrolysis efficiency. Thus, two pretreatment methods (popping and HPAC) were conducted and the efficiency of lignin removed was evaluated. Figure 2 had shown the difference of lignin content between raw PH and pretreated PH. Compared with raw PH, the lignin content of PH pretreated by HPAC was reduced about 77.3%, while the lignin content of PH pretreated by popping was similar to raw PH. What is more, the recovery dry mass yield of each of the pretreated samples (popping and HPAC) was approximately 75.9% and 49.3%, respectively.

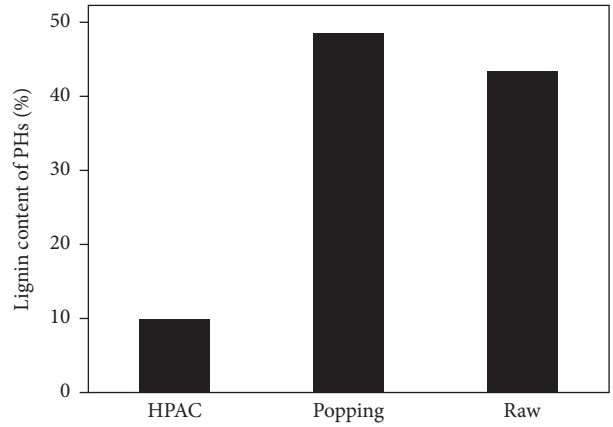

Figure 2: Lignin content of raw, popping, and HPAC pretreated PH.

The monosugar contents of different pretreated PHs were determined using GC (Figure 3). PH was mainly composed of 46.8% carbohydrates. In these carbohydrates, xylose and glucose were major components of sugar in raw PH, comprising approximately 14.5% and 26.6% of dry mass, respectively. After pretreatment, in comparison with raw PH, total carbohydrates of popping and HPAC PH were relatively increased about 1.6% and 27.3%, respectively. Some monosugar content was relatively reduced when compared with raw PH, but glucose content was significantly increased approximately 2 times in HPAC PH. Sugar (glucose) yield of each of the samples (popping and HPAC) was approximately 95.9% and 98.8%, respectively. It was safe to reach a conclusion that the HPAC pretreatment was more effective than the popping pretreatment to increase the sugar content in the hydrolysate.

3.2. Surface Morphology of Pretreated Peanut Hull. The hydrolysis efficiency is directly related to the contact between cellulase and cellulose. To investigate the PH physical changes before and after pretreatment, the physical structures of them were studied with SEM (Figure 4). In comparison with the smooth and integrated surface of raw PH (Figure 4(a)), pores were present in the pretreated PH (Figure 4(b)) on

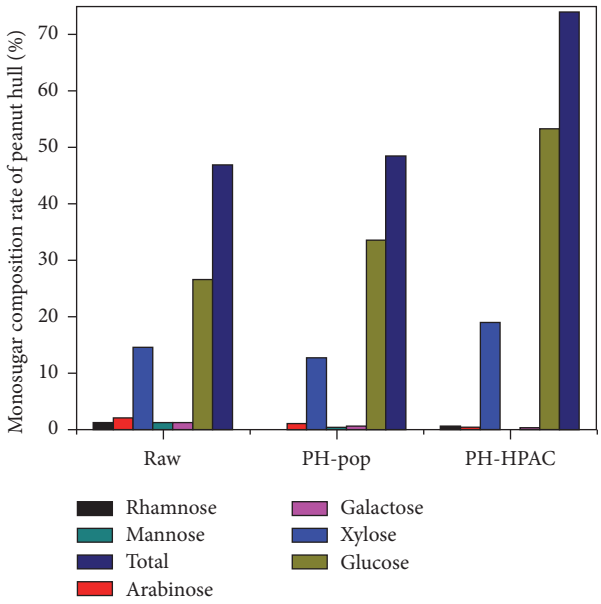

Figure 3: The monosugar contents of different pretreated PHs were determined using GC.

account of the high temperature and releasing the high pressure quickly, so that the structure of the PH was broken down. Figure 4(c) showed that the structure morphology of the HPAC pretreated PH was loosened and distortional, and the removed lignin might be viewed as the reason for the structure changes. No matter how destroyed the structure was or how removed the lignin was from PH, the surface area connecting cellulose and cellulose was increased. Consequently, the enzymatic hydrolysis efficiency might be increased dramatically with popping pretreatment and HPAC pretreatment.

3.3. Effect of Different Pretreated Methods of Peanut Hull on Isoprene Production. In our previous studies [4, 21, 22], we have engineered *E. coli* strains to biosynthesize isoprene using native MEP and exogenous MVA pathway. Compared with other studies, we found that the engineered *E. coli* strain is more effective to produce isoprene than other engineered strains such as *Cyanobacterium Synechocystis* [2], *Bacillus subtilis* [23], and *Saccharomyces cerevisiae* [24]. Hence, in this paper, we also choose the *E. coli* strain to evaluate the enzymatic hydrolysates of pretreated peanut hull.

Two pretreatment methods, popping and HPAC, were found to be able to destroy the lignocellulosic structure, which accordingly enhanced hydrolysis efficiency by cellulase. To ascertain the extent to which isoprene production could be influenced by these two pretreatment methods, the engineered strain was cultured in a fermentation medium with three kinds of carbon sources including pure glucose and two types of enzymatic hydrolysates using HPAC pretreatment and popping pretreatment, respectively. As was shown in Figure 5, the titer of isoprene produced by pure glucose (HPAC pretreatment and popping pretreatment) reached 338.6 mg/L, 211 mg/L, and 113.7 mg/L, respectively. The results demonstrated that the isoprene production from pure glucose fermentation was about 1.6 times and 3 times higher than that from HPAC and popping pretreatments, respectively, and using HPAC pretreatment cultures could produce approximately 1.9 times more isoprene production compared to using the popping pretreatment, with all the other conditions being the same.

Since lignocellulosic feedstocks mainly consist of cellulose, hemicellulose, and lignin [25], inhibitors exist in raw material and would be released during the course of pretreatment [26]. In addition, the concentration of inhibitors relied on the types of lignocellulosic feedstock and the different pretreatment methods utilized [26, 27]. Consequently, in this work, the reason leading to the significant difference in isoprene production among the three kinds of carbon sources would lie in the fact that inhibitors existed in two types of hydrolysates obtained by the HPAC and popping methods.

In this paper, to determine the categories and concentrations of inhibitors which were formed by HPAC and popping methods, two kinds of enzymatic hydrolysates were detected using HPLC method. Table 1 showed that there are four kinds of inhibitors (formic acid, acetic acid, hydroxymethylfurfural (HMF), and furfural) in the enzymatic hydrolysates with popping pretreatment, while only three kinds of inhibitors (acetic acid, furfural, and HMF) were measured in the enzymatic hydrolysate with HPAC pretreatment. Table 1 also notably indicated that the concentrations of acetic acid were approximated in two kinds of fermentation medium.

Different inhibitors have different detrimental effect on the cell growth and accordingly result in decrease in the yield of target product. Weak acid, such as formic acid and acetic acid, could cross the cell membrane, which resulted in the lower cell pH than normal and consequently inhibited cell growth [28, 29]. Mills et al. had also reported that formic acid had higher toxicity to *E. coli* than acetic acid [30]. Like furfural, HMF had a detrimental effect on DNA and would lead to single-strand breaks [29, 30]. Meanwhile, Martinez et al. had proven that the minimal inhibitory concentrations of furfural and HMF would attain 3.5 mg/mL and 4.0 mg/mL, respectively [31]. Thus, although the concentrations of HMF and furfural produced by popping pretreatment were higher than those of HPAC pretreatment, they were still too low to produce a significant impact on isoprene production.

Therefore, based on the above discussion, it can be concluded that formic acid in enzymatic hydrolysate of popping pretreatment would be the dominant factor for lower isoprene production. Additionally, acetic acid existed in HPAC hydrolysis which resulted in lower isoprene production by HPAC pretreatment than that by pure glucose.

3.4. Detoxification Effect of Enzymatic Hydrolysate of HPAC PH on Isoprene Production. To further enhance the production of isoprene, it is essential to remove inhibitors from enzymatic hydrolysate by using a proper method. Among various detoxification methods, activated charcoal claims the advantage of being cost effective and possessing higher capacity to absorb compounds, especially lignin-derived inhibitors and acetic acid, without affecting levels of sugar in

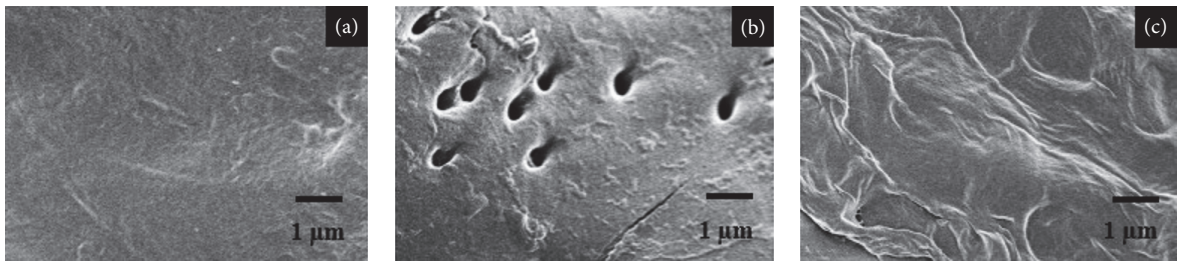

(a) (b) (c)

Figure 4: SEM images for raw (a), popping (b), and HPAC (c) pretreated PH.

Table 1: The types and concentrations of inhibitors in different fermentation medium.

Concentration (mg/mL)	HPAC (detoxified hydrolysate)	HPAC (raw hydrolysate)	Popping
Formic acid	0	0	0.2445
Acetic acid	0.004	0.01775	0.0229
HMF	1.18×10^{-5}	4.36×10^{-5}	0.0119
Furfural	2.15×10^{-5}	1.01×10^{-4}	1.42×10^{-3}

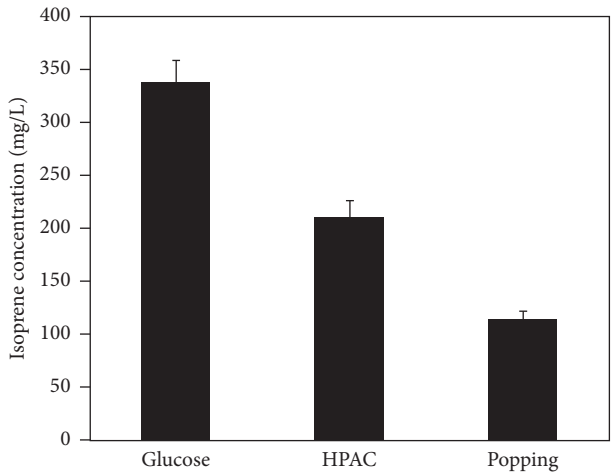

Figure 5: Effect of carbon sources on isoprene production. The engineered strain cultured in three different carbon sources including pure glucose, HPAC, and popping enzymatic hydrolysates. The cells were induced when OD_{600} reached about 0.6. The experiment was performed in triplicate.

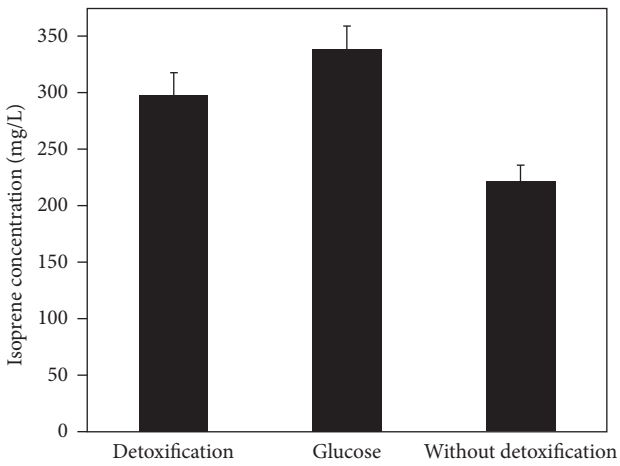

Figure 6: Detoxification effect of enzymatic hydrolysate of peanut hull on isoprene production. When OD_{600} reaches 0.6–0.9, cultures were induced at 30°C for 24 h using 0.5 mM IPTG. All the experiments were carried out in triplicate.

hydrolysate [13, 32, 33]. In addition, it is safe and easy to be manipulated using activated carbon.

After the HPAC pretreated hydrolysate was detoxified with activated charcoal, fermentation was performed with detoxification hydrolysate and raw hydrolysate, respectively. As was seen in Figure 6, the isoprene production of detoxification of HPAC hydrolysate reached 297.5 mg/L, with an increase of up to 41% compared with raw hydrolysate without detoxification. Based on the data shown in Table 1, through detoxification with activated charcoal, the concentrations of acetic acid, HMF, and furfural were reduced by 76.90%, 72.83%, and 78.77%, respectively. The results indicated that inhibitors, especially acetic acid in enzymatic hydrolysates of peanut hull, were inhibitory to engineering *E. coli*, and the removal of inhibitors from fermentation medium consequently led to a remarkable increase in the isoprene production.

3.5. The Difference in Gas Composition and Concentration between Glucose and Enzymatic Hydrolysis. To detect the variation of gas composition by different carbon sources during fermentation, the engineered strain YJM21 was cultured in the fermentation medium containing pure glucose or enzymatic hydrolysate with HPAC pretreatment as the carbon source. As shown in Figure 7 and Table 2, the gas composition

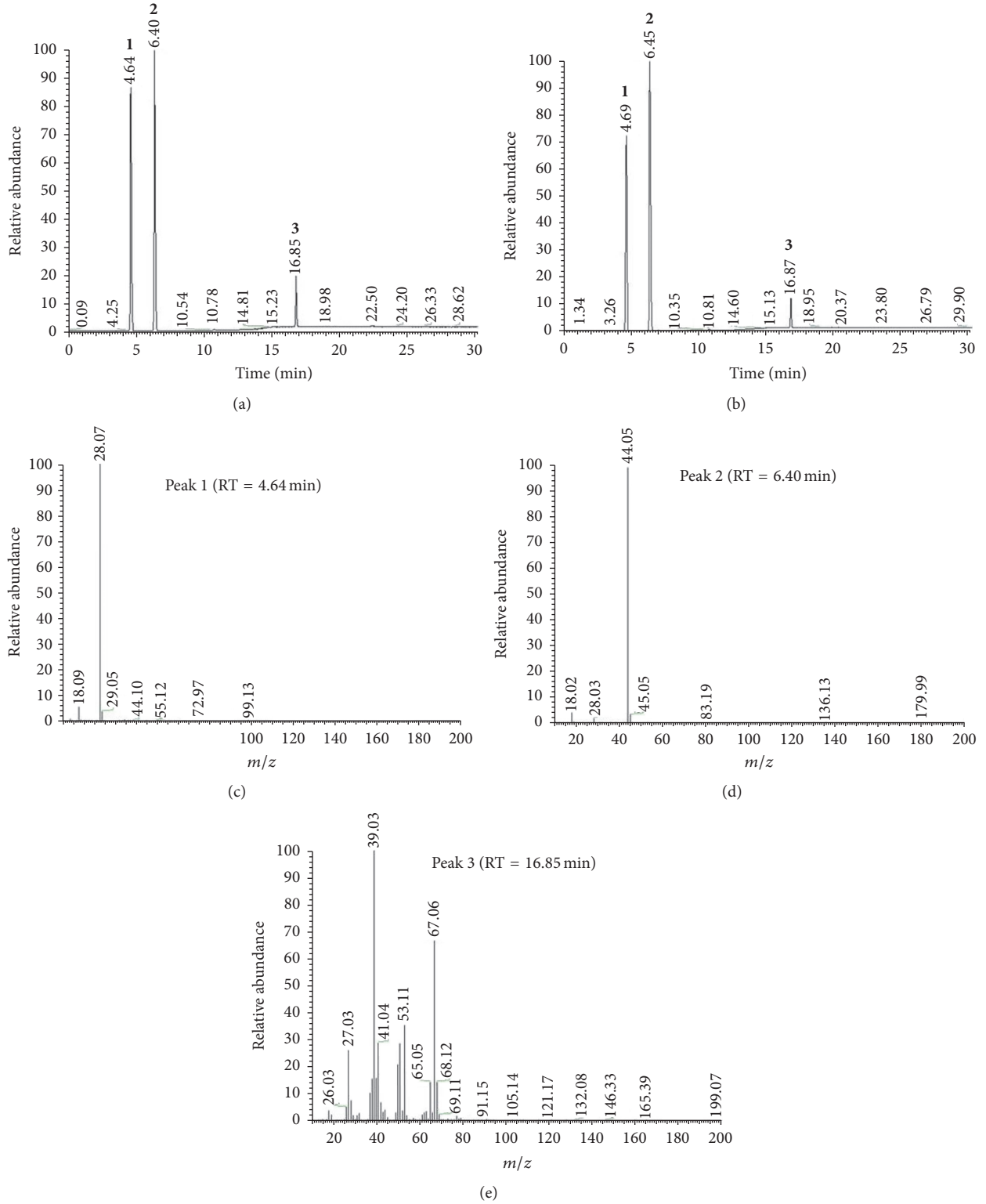

Figure 7: GC-MS analysis of fermentation gases. (a) GC map of gases composition of fermentation on glucose; (b) GC map of gases composition of fermentation on HPAC enzymatic hydrolysate; (c) MS map of peak 1 (N_2); (d) MS map of peak 2 (CO_2); (e) MS map of peak 3 (isoprene).

Table 2: Effect of different carbon sources on concentration of different fermentation gases.

Gas composition (%)	Glucose	HPAC enzymatic hydrolysate	Retention time (min)
N_2	42.13	39.34	4.69
CO_2	48.66	54.41	6.45
Unknown gas 1	0.24	0.19	10.78
Unknown gas 2	0.17	0.10	15.13
Isoprene	8.8	5.96	16.87

produced by pure glucose or enzymatic hydrolysis of peanut shell remained the same, while the gas concentration turned out to be different. The gas composition consisted of N_2, isoprene, CO_2, and a small amount of unknown gas. N_2, CO_2, isoprene, and the unknown gas which were produced by pure glucose accounted for 42.13%, 48.66%, 8.8%, and 0.41% of all gases, respectively, while those gases produced by enzymatic hydrolysate accounted for 39.34%, 54.41%, 5.96%, and 0.29%, respectively. The results indicated that though the fermentation medium constituted by enzymatic hydrolysate of peanut shell had no impact on the categories of gas composition, it could reduce the concentration of isoprene and increase the content of CO_2 in the whole fermented gases.

4. Conclusions

Peanut hull proves to be a promising feedstock to produce bio-based chemicals and biofuels due to its easy availability and polysaccharide content characteristics. In this study, the use of peanut hull for isoprene production was explored. Two pretreatment methods, HPAC and popping, were carried out prior to enzymatic hydrolysis, which could destroy the lignocellulosic biomass structure. The isoprene production using HPAC pretreatment was found to be about 1.9-fold higher than that using popping pretreatment. To further increase the isoprene yield, the enzymatic hydrolysate of HPAC was detoxified by activated carbon. The engineered strain YJM21 fermented on the detoxified enzymatic hydrolysate could accumulate 297.5 mg/L isoprene, which accounted for about 90% of isoprene production by YJM21 fermented on pure glucose (338.6 mg/L). This work is considered to be the first attempt to produce isoprene by *E. coli* using peanut hull as the feedstock, and it also provides evidence that another lignocellulose material, peanut hull, could be regarded as a promising feedstock for bio-based chemicals or biofuels of industrial production.

Competing Interests

The authors declare that they have no competing interests.

Acknowledgments

This work was financially supported by the Natural Science Foundation of Shandong Province, China (Grant no. ZR2015BM021), the National Natural Science Foundation of China (Grant no. 21572242), the Project of Science and Technology for People's Livelihood of Qingdao (no. 15-9-2-94-nsh), the special project of science and technology development for construction (Grant no. JK2015-22), the Talents of High Level Scientific Research Foundation (Grant no. 6631113326) of Qingdao Agricultural University, the National Natural Science Foundation of China (Grant no. 31300599), the Talents of High Level Scientific Research Foundation (Grant no. 6631113318) of Qingdao Agricultural University, and the National Natural Science Foundation of China (Grant no. 31172012/c1506).

References

[1] G. A. Alianell, F. Derwitsch, D. Wells, and T. Taylor, "Isoprene compositions and methods of use," Google Patents, 2009.

[2] P. Lindberg, S. Park, and A. Melis, "Engineering a platform for photosynthetic isoprene production in cyanobacteria, using *Synechocystis* as the model organism," *Metabolic Engineering*, vol. 12, no. 1, pp. 70–79, 2010.

[3] J. Kesselmeier and M. Staudt, "Biogenic volatile organic compounds (VOC): an overview on emission, physiology and ecology," *Journal of Atmospheric Chemistry*, vol. 33, no. 1, pp. 23–88, 1999.

[4] J. Yang, G. Zhao, Y. Sun et al., "Bio-isoprene production using exogenous MVA pathway and isoprene synthase in *Escherichia coli*," *Bioresource Technology*, vol. 104, pp. 642–647, 2012.

[5] T. D. Sharkey, S. Yeh, A. E. Wiberley, T. G. Falbel, D. Gong, and D. E. Fernandez, "Evolution of the isoprene biosynthetic pathway in kudzu," *Plant Physiology*, vol. 137, no. 2, pp. 700–712, 2005.

[6] J. Berenguer, V. Calderon, M. Herce, and J. Sanchez, "Spoilage of a bakery product (sobao pasiego) by isoprene-producing molds," *Revista de Agroquimica y Tecnologia de Alimentos*, vol. 31, pp. 580–583, 1991.

[7] A. Melis, "Solar energy conversion efficiencies in photosynthesis: minimizing the chlorophyll antennae to maximize efficiency," *Plant Science*, vol. 177, no. 4, pp. 272–280, 2009.

[8] P. Sassner, C.-G. Mårtensson, M. Galbe, and G. Zacchi, "Steam pretreatment of H_2SO_4-impregnated *Salix* for the production of bioethanol," *Bioresource Technology*, vol. 99, no. 1, pp. 137–145, 2008.

[9] C. Pothiraj, A. Arun, and M. Eyini, "Simultaneous saccharification and fermentation of cassava waste for ethanol production," *Biofuel Research Journal*, vol. 2, no. 1, pp. 196–202, 2015.

[10] Ministry of Agriculture of the People's Republic of China, *Law and Regulations*, 2009.

[11] United States Department of Agriculture (USDA), http://ndb.nal.usda.gov/ndb/foods/show/4800?fgcd=&manu=&lfacet=&format=&count=&max=35&offset=&sort=&qlookup=peanut.

[12] N. Mosier, C. Wyman, B. Dale et al., "Features of promising technologies for pretreatment of lignocellulosic biomass," *Bioresource Technology*, vol. 96, no. 6, pp. 673–686, 2005.

[13] I. S. Choi, S. G. Wi, S.-B. Kim, and H.-J. Bae, "Conversion of coffee residue waste into bioethanol with using popping pretreatment," *Bioresource Technology*, vol. 125, pp. 132–137, 2012.

[14] S. G. Wi, I. S. Choi, K. H. Kim, H. M. Kim, and H.-J. Bae, "Bioethanol production from rice straw by popping pretreatment," *Biotechnology for Biofuels*, vol. 6, no. 1, article 166, 2013.

[15] G. Banerjee, S. Car, T. Liu et al., "Scale-up and integration of alkaline hydrogen peroxide pretreatment, enzymatic hydrolysis, and ethanolic fermentation," *Biotechnology and Bioengineering*, vol. 109, no. 4, pp. 922–931, 2012.

[16] S. C. Rabelo, R. R. Andrade, R. Maciel Filho, and A. C. Costa, "Alkaline hydrogen peroxide pretreatment, enzymatic hydrolysis and fermentation of sugarcane bagasse to ethanol," *Fuel*, vol. 136, pp. 349–357, 2014.

[17] S. G. Wi, B. Y. Chung, Y. G. Lee, D. J. Yang, and H.-J. Bae, "Enhanced enzymatic hydrolysis of rapeseed straw by popping pretreatment for bioethanol production," *Bioresource Technology*, vol. 102, no. 10, pp. 5788–5793, 2011.

[18] S. G. Wi, E. J. Cho, D.-S. Lee, S. J. Lee, Y. J. Lee, and H.-J. Bae, "Lignocellulose conversion for biofuel: a new pretreatment greatly improves downstream biocatalytic hydrolysis of various lignocellulosic materials," *Biotechnology for Biofuels*, vol. 8, article 228, 2015.

[19] A. Sluiter, B. Hames, R. Ruiz et al., "Determination of structural carbohydrates and lignin in biomass," Tech. Rep. N TP-510-42618 2011:17, National Renewable Energy Laboratory, Golden, Colo, USA, 2010.

[20] TAPPI Standard, *Solvent Extractives of Wood and Pulp*, TAPPI, 1997.

[21] J. Yang, M. Xian, S. Su et al., "Enhancing production of bio-isoprene using hybrid MVA pathway and isoprene synthase in *E. coli*," *PLoS ONE*, vol. 7, no. 4, Article ID e33509, 2012.

[22] Y. Zhao, J. Yang, B. Qin et al., "Biosynthesis of isoprene in *Escherichia coli* via methylerythritol phosphate (MEP) pathway," *Applied Microbiology and Biotechnology*, vol. 90, no. 6, pp. 1915–1922, 2011.

[23] J. Xue and B. K. Ahring, "Enhancing isoprene production by genetic modification of the 1-deoxy-D-Xylulose-5-phosphate pathway in *Bacillus subtilis*," *Applied and Environmental Microbiology*, vol. 77, no. 7, pp. 2399–2405, 2011.

[24] S.-Y. Hong, A. S. Zurbriggen, and A. Melis, "Isoprene hydrocarbons production upon heterologous transformation of *Saccharomyces cerevisiae*," *Journal of Applied Microbiology*, vol. 113, no. 1, pp. 52–65, 2012.

[25] R. M. Rowell, *Handbook of Wood Chemistry and Wood Composites*, CRC Press, New York, NY, USA, 2012.

[26] M. Galbe and G. Zacchi, "Pretreatment of lignocellulosic materials for efficient bioethanol production," in *Biofuels*, L. Olsson, Ed., vol. 108 of *Advances in Biochemical Engineering/Biotechnology*, pp. 41–65, Springer, 2007.

[27] L. J. Jönsson, B. Alriksson, and N.-O. Nilvebrant, "Bioconversion of lignocellulose: inhibitors and detoxification," *Biotechnology for Biofuels*, vol. 6, no. 1, article 16, 2013.

[28] A. K. Chandel, S. S. da Silva, and O. V. Singh, "Detoxification of lignocellulose hydrolysates: biochemical and metabolic engineering toward white biotechnology," *BioEnergy Research*, vol. 6, no. 1, pp. 388–401, 2013.

[29] E. Palmqvist and B. Hahn-Hägerdal, "Fermentation of lignocellulosic hydrolysates. II: inhibitors and mechanisms of inhibition," *Bioresource Technology*, vol. 74, no. 1, pp. 25–33, 2000.

[30] T. Y. Mills, N. R. Sandoval, and R. T. Gill, "Cellulosic hydrolysate toxicity and tolerance mechanisms in *Escherichia coli*," *Biotechnology for Biofuels*, vol. 2, no. 1, article 26, 2009.

[31] A. Martinez, M. E. Rodriguez, S. W. York, J. F. Preston, and L. O. Ingram, "Effects of $Ca(OH)_2$ treatments ('overliming') on the composition and toxicity of bagasse hemicellulose hydrolysates," *Biotechnology and Bioengineering*, vol. 69, no. 5, pp. 526–536, 2000.

[32] R. E. Berson, J. S. Young, S. N. Kamer, and T. R. Hanley, "Detoxification of actual pretreated corn stover hydrolysate using activated carbon powder," *Applied Biochemistry and Biotechnology*, vol. 124, no. 1, pp. 923–934, 2005.

[33] W. Parawira and M. Tekere, "Biotechnological strategies to overcome inhibitors in lignocellulose hydrolysates for ethanol production: review," *Critical Reviews in Biotechnology*, vol. 31, no. 1, pp. 20–31, 2011.

Hindawi Publishing Corporation
BioMed Research International
Volume 2016, Article ID 8792548, 8 pages
http://dx.doi.org/10.1155/2016/8792548

Review Article

Strategies for Lipid Production Improvement in Microalgae as a Biodiesel Feedstock

L. D. Zhu,[1,2] Z. H. Li,[2] and E. Hiltunen[1]

[1] *Faculty of Technology, University of Vaasa and Vaasa Energy Institute, P.O. Box 700, 65101 Vaasa, Finland*
[2] *Hubei Collaborative Innovation Center for Green Transformation of Bio-Resources and Faculty of Resources and Environmental Science, Hubei University, Wuhan 430062, China*

Correspondence should be addressed to L. D. Zhu; zliand@uva.fi

Received 26 May 2016; Revised 20 July 2016; Accepted 25 July 2016

Academic Editor: Ramkrishna Sen

In response to the energy crisis, global warming, and climate changes, microalgae have received a great deal of attention as a biofuel feedstock. Due to a high lipid content in microalgal cells, microalgae present as a promising alternative source for the production of biodiesel. Environmental and culturing condition variations can alter lipid production as well as chemical compositions of microalgae. Therefore, application of the strategies to activate lipid accumulation opens the door for lipid overproduction in microalgae. Until now, many original studies regarding the approaches for enhanced microalgal lipid production have been reported in an effort to push forward the production of microalgal biodiesel. However, the current literature demonstrates fragmented information available regarding the strategies for lipid production improvement. From the systematic point of view, the review highlights the main approaches for microalgal lipid accumulation induction to expedite the application of microalgal biodiesel as an alternative to fossil diesel for sustainable environment. Of the several strategies discussed, the one that is most commonly applied is the design of nutrient (e.g., nitrogen, phosphorus, and sulfur) starvation or limitation. Other viable approaches such as light intensity, temperature, carbon dioxide, salinity stress, and metal influence can also achieve enhanced microalgal lipid production.

1. Introduction

Energy crisis, global warming, and climate changes have led to an ever-increasing concern on the sustainability issues of fossil fuels utilization as energy supply. Biofuels as types of renewable, alternative energy are recognized with the highest potential to satisfy the global energy demand. The biofuel feedstock mainly consists of the following sources: straw, wood materials, wood wastes, energy plants, sugarcane, manure, and many other agricultural coproducts or byproducts [1]. It is believed that biofuel production has several advantages such as reduction of country's reliance on crude oil imports, job creation, and farmers' income increase [2–4]. On the basis of feedstock differences, biofuels can be divided into three categories: the first generation, the second generation, and the third generation. First generation biofuels use edible feedstock such as soya beans, wheat, corn, rapeseed, oil crops, maize, sugarcane, and sugar beet, while second generation biofuels are derived from wastes and dedicated lignocellulosic feedstock such as switchgrass and jatropha [5]. One of the major disadvantages of both first and second generation biofuels is that the cultivation of these food or nonfood crops as biofuel feedstock might compete for limited arable farmland, which should be utilized to cultivate crops as food feedstock. Thus, biofuels are not considered renewable and sustainable if they are derived from food or nonfood crops [6]. Biofuel production from food crops grown in farmland will affect food security and prices, while the cultivation of nonfood energy crops will result in competition with food crops for farmland.

In response to the challenges outlined above, microalgae have received a global attention as a promising biofuel feedstock. Compared to first and second generation biofuel feedstock, microalgae as third generation biofuel feedstock have some distinguishable features, such as high photosynthetic efficiency, rapid growth, high lipid content, high CO_2 mitigation efficiency, noncompetition with food crops for farmland, and less water demand than land crops [5, 7–9].

As photosynthetic organisms, microalgae are able to capture solar energy and use water and atmospheric CO_2 to accumulate biomass in forms of organic ingredients such as lipids [10]. During the photosynthesis, neutral lipids are accumulated as triacylglycerols (TAGs) in microalgal cells [11]. Through transesterification, TAGs can be further transferred into various types of fatty acid methyl esters, the efficient compositions of biodiesel.

To generate large amount of microalgal biomass and meet the energy consumption demand, mass scale microalgal cultivation for biodiesel production is a plausible solution in the future [12]. Meanwhile, the improvement of lipid content in microalgal cells also presents a direction towards the sustainable development of microalgal biodiesel. Thus, it is extremely important to apply feasible strategies to induce microalgal lipid accumulation. The production and accumulation of microalgal lipids are found to be an indispensable buffer against the culturing conditions. Stored lipids not only ensure the survival of microalgal cells but also serve as a source of energy for cell multiplication such as nuclear division and DNA replication [11].

Objective and Structure of This Study. Plenty of original research articles that exactly investigate certain strategies for enhanced microalgal lipid production have been published. These strategies play crucial roles in triggering microalgal lipid accumulation. However, the current literature has not systematized all of the most promising strategies, and there is only fragmented information available. In other words, as yet, no comprehensive review has been published on those strategies for enhanced microalgal lipid production. Therefore, this review aims to bridge the gap and its objective is to systematically concentrate on the main lipid induction strategies that can evidently promote microalgal lipid production. The contribution of this review paper lies in the foundation for stakeholders, authorities, and practitioners to better understand microalgal lipid induction strategies and their significances in practice. In the coming parts, the authors first illustrate the metabolic pathways of lipid accumulation (Section 2), followed by the comprehensive discussion of approaches for lipid production improvement (Section 3). Finally, a summary of this article is concluded (Section 4).

2. Metabolic Pathways of Lipid Accumulation

The research on lipid-rich microalgal cultivation for biodiesel production has received an increased interest. Lipids and polyglucans are the energy and carbon reserves in microalgal cells, but polyglucans represent less concentrated stores of metabolic energy than lipids [11]. Both lipids and polyglucans not only ensure the survival of microalgal cells such as in night periods as well as in periods with variable light intensities but also supply energy for biological processes associated with the multiplication of microalgal cells, such as the replication of DNA, division of nuclear, cytokinesis, and formation and liberation of daughter cells. According to Berg et al. [13], the complete oxidation of fatty acids can generate energy at 9 kcal g^{-1} (38 kJ g^{-1}), compared to around 4 kcal g^{-1} (17 kJ g^{-1}) for carbohydrates. Lipids include two types: neutral lipids that serve as the energy reserves and polar lipids that are constituents of organelles and membranes. Microalgal cells accumulate and store neutral lipids in the form of triacylglycerols (TAGs).

Microalgal cell cycle contains several consecutive procedures, including cell growth, DNA replication, nuclear division, and cellular division. Metabolism of both starch and lipid begins with an identical initial pool of molecules containing three carbons such as glyceraldehyde 3-phosphate (GAP) and 3-phosphoglycerate (3PG) [14]. Figure 1 illustrates metabolic pathways that influence the accumulation of lipids by common C3 precursors. As for autotrophic microalgae, light capture for photosynthesis is crucial for microalgal growth to accumulate energy reserves such as lipids. As a result, DNA replication and nuclear and cellular division in cell cycle can be completed through the utilization of the reserves to meet requirements of carbon and energy [15].

The formation of both TAG and starch competes for carbon via common C3 precursors, resulting in carbon partitioning. However, the mechanism behind carbon partitioning together with the switch from starch towards the production of TAG has not been completely understood in the literature. When the route towards starch formation is inhibited, the pathway towards the formation of TAG molecules is improved [16]. Li et al. [17] suggested that the starch content of starchless mutants of microalgae *C. reinhardtii* was limited or even completely absent, leading to an increased TAG content in contrast to the wild type. Despite the increase in TAG content, Li et al. [18] found that growth of starchless microalgae *C. reinhardtii* was markedly inhibited by the inserted mutation, giving rise to the decrease of TAG productivity.

3. Approaches to Lipid Production Improvement

The composition and quantity of lipids are species-dependent and can be affected by external cultivation conditions, such as light intensity, temperature, carbon dioxide, nutrient starvation, salinity stress, and metal stress. The overproduction or overaccumulation of lipid reserves presents an indispensable buffer against changeable external cultivation conditions.

3.1. Light Intensity. Microalgal growth needs the input of light during the photosynthesis. As one of the key factors, light affects the performances of microalgal growth and the compositions [5]. Adequate light intensity favors the overproduction of microalgal lipids [19]. This might be because sufficient light intensity is beneficial to the storage of excess photoassimilates, which are further converted into chemical energy [20]. Microalga *Nannochloropsis* sp. experienced the accumulation of the highest amount of lipids (47% of DW) under the conditions with the highest light intensity (700 μmol photons s^{-1} m^{-2}) [21]. Takeshita et al. [22] found that *C. sorokiniana*, *C. viscosa*, *C. emersonii*, *C. vulgaris*, *P. beijerinckii*, and *P. kessleri* CCALA255, NIES-2152, and NIES-2159 were able to increase the productivity of lipids under high light intensity of 600 μmol photons m^{-2} s^{-1}. It has been

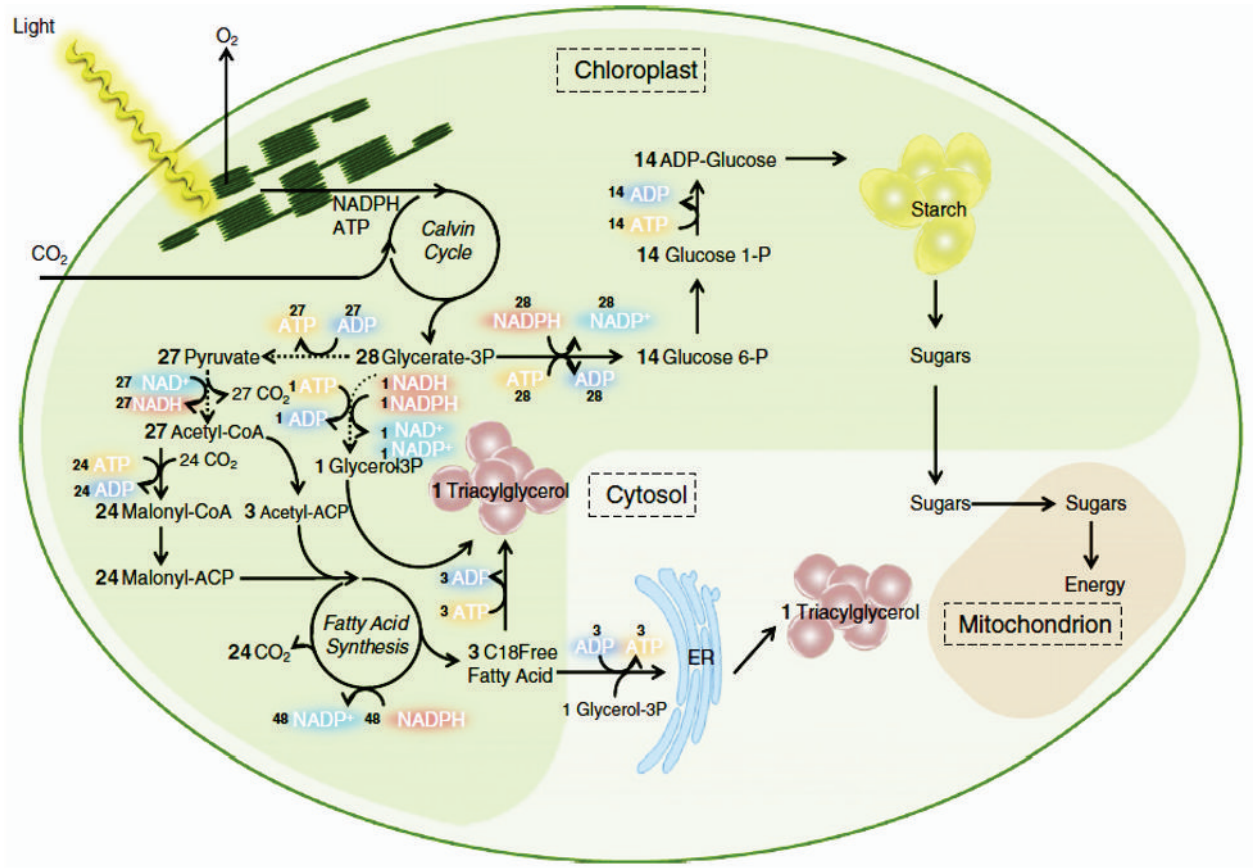

Figure 1: Simplified triacylglycerol (TAG) metabolism in green microalgae [14]. The dashed lines refer to the reactions that occur in the cytosol. The figure illustrates two possible pathways for TAG formation following the assumed route in the chloroplasts or over the endoplasmic reticulum (ER) membranes in the cytosol.

seen that the lipid content of the microalgae *Scenedesmus abundans* kept on rising as the light intensity increased from 3000 to 6000 lux [23]. The highest lipid content of 32.77% was achieved, when the culture was under the light intensity of 6000 lux, followed by 27.10 and 21.20% in the culture with 5000 and 3000 lux intensity, respectively. Another study indicated that *Botryococcus* sp. had shown the highest lipid percentage (35.9%) at 6000 lux [24]. However, Sun et al. [25] suggested that highest lipid percentage (33.0%) of microalgae *N. oleoabundans* HK-129 was achieved at 14,800 lux intensity. Thus, different microalgal species have the highest lipid content at variable light intensities, since they indicate different efficiencies in light utilization. From this point of view, the ability to use light is microalgae-specific.

Either limited or saturated light intensity cannot favor the growth of microalgae. When light intensity is fairly low, for example, below the compensation point, microalgal biomass concentration compromises, leading to poor growth and thus negatively impacting lipid accumulation [5]. After the compensation point, microalgae experience the increased growth as the light intensity increases, and the maximum photosynthetic efficiency occurs when it arrives at the light saturation point. Therefore, the positive effect of light intensity increases on lipid accumulation functions only up to a point [11]. Extremely high light intensity will cause photoinhibition, damage microalgal photosystems, and thus reduce lipid accumulation.

3.2. Temperature. The effect of temperature on microalgal growth and lipid production is similar to that of light intensity. Microalgal growth as well as lipid production exponentially increases to a certain extent as the temperature increases and reaches an optimal level [26]. The optimal value of temperature where the highest biomass production is achieved varies from species to species [27]. Microalgae *C. vulgaris* accumulated maximum lipids at 25°C, while the decrease of temperature resulted in an obvious decrease in the lipid content [28]. The temperature of 20°C was found to be the optimal temperature for microalgae *Scenedesmus* sp. to produce lipids [29]. The lipid concentration of microalgae *S. obliquus* ranged from 18 to 40% of DW, when the temperature ranged from 20 to 27.5°C [11]. Converti et al. [28] suggested that as the temperature increased from 20 to 25°C, the lipid content of *N. oculata* simultaneously increased from 7.9 to 14.9%. In another study, the optimum temperature of *C. minutissima* was found to be 20°C, where lipid productivity was the highest [30].

Increase of temperature to an optimal level causes the increase of total lipid content. However, it does not mean that all types of lipids experience the increase. Wei et al. [31] studied temperature effects on lipid properties of microalgae *Tetraselmis subcordiformis* and *Nannochloropsis oculata* and found that increased temperature led to a decrease in neutral lipids and polyunsaturated fatty acids but an increase in saturated and monounsaturated fatty acids. Likewise, James et al. [32] investigated temperature modulation of fatty acid profiles for microalgae *Chlamydomonas reinhardtii* and suggested that a switch to temperatures lower than 25°C could decrease the total amount of stored fatty acids but increase the content of unsaturated fatty acids.

3.3. Carbon Dioxide. As for phototrophic microalgae, CO_2 ensures carbon supply for photosynthesis. Optimal growth of microalgae needs adequate amount of dissolved CO_2. In general, as the quantity of CO_2 increases to an optimal level, the growth of microalgae and production of lipids increase. Aeration of gas mixture with a high concentration of CO_2 can meet the requirement for CO_2. The amount of CO_2 in atmospheric air is not sufficient. Li et al. [33] suggested that aeration with pure air resulted in a decrease in growth and lipid production of microalgae *Parachlorella kessleri*. Limited amount of CO_2 available in cultures slows down the metabolism of microalgae, causing reduced lipids [34]. To reduce costs, flue gas (rich in CO_2) can be introduced into microalgal culturing systems as a carbon source. However, high content of CO_2 will also affect the growth of microalgae. This is because unutilized CO_2 in culture will be converted to carbonic acid (H_2CO_3), reducing the pH value of the culture [27]. Therefore, to obtain enhanced biomass and lipid production requires optimal CO_2 levels.

The optimal amount of CO_2 varies among microalgal species. Cultivating microalgae *Chlorella vulgaris* under 8% (v/v) CO_2, Montoya et al. [35] achieved the maximum amount of saturated fatty acids and lipid productivity of 29.5 mg L^{-1} day^{-1}. Similarly, Widjaja et al. [36] reported that the growth and lipid production of *C. vulgaris* were enhanced with increased CO_2 concentration. The microalgae *Chlamydomonas* sp. JSC4 strain produced maximum lipid content (65.3%) and productivity (169.1 mg L^{-1} day^{-1}) at 4% (v/v) CO_2 [37]. Maximum lipid content (34% wt) was achieved, when microalgae *Chlorococcum littorale* were cultivated with 5% CO_2 concentration [38]. In another study, Ho et al. [39] grew green microalgae *S. armatus* at CO_2 concentration of 2% and obtained the highest lipid content of 22.4%.

3.4. Nutrient Starvation. Nutrient starvation or limitation is thought to be a feasible and environmentally friendly approach for the control of the cell cycle to enhance lipid productivity [40]. So far, nutrient starvation is recognized as the most successful strategy and most widely used. In an attempt to improve lipid productivity, it is important to obtain both substantial biomass yield and high lipid content of microalgal cells. In practice, algae are grown in media with sufficient nutrients in early stages to obtain higher biomass concentration as quickly as possible, while nutrient starvation is introduced in later stages for the overproduction of lipids.

Variation in macronutrients such as nitrogen, phosphorus, and sulfur in culturing media will lead to the alteration of macromolecular composition in microalgal cells. Under nutrient stress, lipid accumulation is favored, and TAG is formed as the dominant ingredient [27]. Plenty of studies have reported that most microalgal species can improve lipid accumulation and undergo transformation under nutrient stress [41–43]. Nevertheless, as for some species nutrient deficiency will not favor the accumulation of lipids. For instance, under nutrient deficiency the microalgae *Dunaliella salina* experienced lipid content decrease from 25 to 9% but carbohydrate increase from 16 to 56% [44].

Nitrogen, phosphorus, and/or sulfur starvation is widely recognized as a main lipid inducer for green microalgae species (Table 1). Ito et al. [45] reported that under nitrogen stress conditions the quantities of neutral lipids in microalgal cells were greatly increased, while amino acids were significantly reduced to 1/20 of the amount or even less. Mandal and Mallick [46] cultivated the microalgae *Scenedesmus obliquus* under phosphorus starvation and witnessed a lipid content increase from 10.0 to 29.5%. Sato et al. [47] suggested that sulfur starvation could trigger the microalgae *Chlamydomonas reinhardtii* to accumulate TAG in microalgal cells through the diversion of metabolic carbon-flow from protein to TAG synthesis. Apart from nitrogen, phosphorus, and sulfur starvation, depletion of nutrient medium during the growth of microalgal culture has also been found as another efficient starvation treatment for the production of lipids, since the starvation of all elements in nutrient media can be attained concurrently [11, 48]. For example, Přibyl et al. [49] found that the total extractable lipid content could reach up to 57.25%, when *C. vulgaris* was cultivated under nutrient depletion conditions for 7 days.

3.5. Salinity Stress. To resist osmotic pressure due to salinity stress, some metabolites in microalgal cells can be produced [50]. Surrounding salinity can affect the physiological and biochemical properties of microalgae. When microalgal cells are exposed to saline environment, recovery of turgor pressure, adjustment of the absorption and release of ions via cell membranes, and accumulation of osmosis-resisting matters are triggered [51, 52]. The salinity stress created inside the cells results in increment in the lipid content. Many microalgal species have been found to be subjected to the salinity stress. Yang et al. [53] applied NaCl induction with the optimal salt concentration at the late-exponential growth phase and found that the algae *Monoraphidium dybowskii* could increase total lipid content to 41.7% in a day. Pal et al. [21] investigated the effect of NaCl on the growth of *Nannochloropsis* sp. and reported that the highest total fatty acid (TFA) content of 47.0% DW and average lipid productivity of 360 mg TFA L^{-1} day^{-1} were achieved at 13 g L^{-1} NaCl. When exposed to salt pressure, *Scenedesmus* species experienced an obvious increase in lipid content [54]. Takagi et al. [55] studied the effect of salt concentration on intracellular accumulation of lipids and triacylglycerol in marine microalgae *Dunaliella* cells and found that as salt concentrations

Table 1: Lipid content of microalgae under the cultivation with nutrient stress factor.

Microalgae	Stress factor	Temperature (°C)	Culture time (d)	Metabolic type	Lipid content (%)	Reference
Chlorella vulgaris	Nitrogen starvation	25	10	Autotrophic	53	[61]
Chlorella vulgaris and *Chlorococcum oleofaciens*	Nitrogen starvation	25	12	Autotrophic	35 and 40	[62]
Monoraphidium sp.	Nitrogen starvation	25	5	Autotrophic	44.4	[63]
Chlorella zofingiensis	Nitrogen starvation; phosphorus starvation	25	28	Autotrophic	65.1; 44.7	[64]
Scenedesmus sp.	Nitrogen starvation	25	10	Mixotrophic	31	[65]
Chlorella zofingiensis	Nitrogen starvation; phosphorus starvation	25	8	Mixotrophic	41.2; 42.7	[41]
Chlorella zofingiensis	Nitrogen and phosphorus starvation	25	8	Mixotrophic	46.2	[41]
Ankistrodesmus falcatus	Nitrogen starvation; phosphorus starvation	20	16	Autotrophic	34.4; 45.9	[66]
Chlorella protothecoides	Phosphorus starvation	28	7	Mixotrophic	32.8	[42]
Parachlorella kessleri	Sulfur deprivation	20	14	Autotrophic	50.7	[67]
Chlorella lobophora	Sulfur deprivation	20	21	Autotrophic	50.0	[68]
Parachlorella kessleri	Depletion of diluted nutrient media	30	4	Autotrophic	60.0	[33]

increased intracellular lipid content increased and the final lipid content could reach up to 70%. Under salinity stress, *C. vulgaris* experienced a 21.1% increase of lipid yields [56].

Cultivation of microalgae under salt stress can also limit contaminants, invasive organisms, and competing microorganisms in microalgal systems, which presents another advantage. However, too high salinity introduced can inhibit the cell growth and change the shape and structure of microalgal cells, due to the water pressure between media and cells. Thus, an optimal range for salinity level is supposed to be determined.

3.6. Metal Stress. Metal ions can also affect the growth of microalgae and lipid production. Ren et al. [57] studied the effects of iron, magnesium, and calcium on biomass and lipid production of heterotrophic microalgae *Scenedesmus* sp. R-16 in a dark environment and found that the total lipid content increased to 43.2, 35.0, and 47.4%, respectively. Another study showed that *Chlorella minutissima* UTEX 2341 indicated strong resistance to copper and cadmium ions under heterotrophic culture conditions, and the lipid content was significantly increased by 93.9 and 21.1%, respectively [58]. Liu et al. [59] found that the total lipid content in cultures added with 1.2×10^{-5} mol L^{-1} $FeCl_3$ reached up to 56.6% of dry weight and was 3–7-fold higher than other media added with lower iron concentrations. Yeesang and Cheirsilp [24] cultivated microalgae *Botryococcus* spp. in cultures added with a high iron concentration (0.74 mM) and reported that the total lipid content was increased 1.4–2.5-fold. A study was carried out using *Chlorella* species under copper exposure to evaluate the metal stress on lipid contents, and it is found that higher lipid concentrations were observed in *C. protothecoides*, *C. vulgaris*, and *C. pyrenoidosa* in the presence of copper at 4.0 mg L^{-1} concentration. In addition, Li et al. [60] investigated the production of biomass and lipids by the microalgae *Chlorella protothecoides* under copper stress conditions and achieved the optimized biomass and lipid yield of 6.47 and 5.78 g L^{-1}, respectively.

4. Conclusions

Microalgae have been praised as a promising feedstock for the production of biodiesel. Lipids, which are energy reserves in microalgal cells, are the raw materials for biodiesel conversion. To promote microalgal biodiesel production during the scale-up process, the achievement of lipid overproduction is essential, and certain appropriate strategies can help realize the goal. Among all strategies, the most efficient and widely used one is to apply nutrient starvation. Other approaches for the induction of lipid overaccumulation include light intensity, temperature, carbon dioxide, salinity stress, and metal stress. In practice, the lipid-inducing strategies can also be combined in an effort to achieve lipid production optimization. This review paper provides stakeholders, authorities, and practitioners with the foundation for better understanding microalgal lipid induction strategies and their significances in practice. There is hope that microalgae-based lipid production can be promoted through the application of various strategies.

Competing Interests

The authors declare no competing interests regarding the publication of this paper.

Acknowledgments

This work was supported by the Kone Foundation in Finland. This work was also partially supported by the TransAlgae project funded by the Botnia-Atlantica programme and European Regional Development Fund.

References

[1] M. H. Langholtz, A. M. Coleman, L. M. Eaton, M. S. Wigmosta, C. M. Hellwinckel, and C. C. Brandt, "Potential land competition between open-pond microalgae production and terrestrial dedicated feedstock supply systems in the U.S.," *Renewable Energy*, vol. 93, pp. 201–214, 2016.

[2] H. Gunatilake, D. Roland-Holst, and G. Sugiyarto, "Energy security for India: biofuels, energy efficiency and food productivity," *Energy Policy*, vol. 65, pp. 761–767, 2014.

[3] L. Zhu, S. Huo, and L. Qin, "A microalgae-based biodiesel refinery: sustainability concerns and challenges," *International Journal of Green Energy*, vol. 12, no. 6, pp. 595–602, 2015.

[4] A. Chanthawong and S. Dhakal, "Stakeholders' perceptions on challenges and opportunities for biodiesel and bioethanol policy development in Thailand," *Energy Policy*, vol. 91, pp. 189–206, 2016.

[5] L. Zhu, "Microalgal culture strategies for biofuel production: a review," *Biofuels, Bioproducts and Biorefining*, vol. 9, no. 6, pp. 801–814, 2015.

[6] L. Zhu, H. Shuhao, S. Shakeel, and Z. Li, "Algal biorefinery for sustainable development and the challenges," *Proceedings of the Institution of Civil Engineers—Energy*, 2016.

[7] F. Han, H. Pei, W. Hu, L. Jiang, J. Cheng, and L. Zhang, "Beneficial changes in biomass and lipid of microalgae *Anabaena variabilis* facing the ultrasonic stress environment," *Bioresource Technology*, vol. 209, pp. 16–22, 2016.

[8] L. Zhu, "The combined production of ethanol and biogas from microalgal residuals to sustain microalgal biodiesel: a theoretical evaluation," *Biofuels, Bioproducts and Biorefining*, vol. 8, no. 1, pp. 7–15, 2014.

[9] S. R. Medipally, F. M. Yusoff, S. Banerjee, and M. Shariff, "Microalgae as sustainable renewable energy feedstock for biofuel production," *BioMed Research International*, vol. 2015, Article ID 519513, 13 pages, 2015.

[10] L. Zhu, "Biorefinery as a promising approach to promote microalgae industry: an innovative framework," *Renewable and Sustainable Energy Reviews*, vol. 41, pp. 1376–1384, 2015.

[11] M. Vitova, K. Bisova, S. Kawano, and V. Zachleder, "Accumulation of energy reserves in algae: from cell cycles to biotechnological applications," *Biotechnology Advances*, vol. 33, no. 6, pp. 1204–1218, 2015.

[12] L. D. Zhu, Z. B. Xu, L. Qin, Z. M. Wang, E. Hiltunen, and Z. H. Li, "Oil production from pilot-scale microalgae cultivation: an economics evaluation," *Energy Sources, Part B: Economics, Planning, and Policy*, vol. 11, no. 1, pp. 11–17, 2016.

[13] A. H. Berg, T. P. Combs, and P. E. Scherer, "ACRP30/adiponectin: an adipokine regulating glucose and lipid metabolism," *Trends in Endocrinology & Metabolism*, vol. 13, no. 2, pp. 84–89, 2002.

[14] L. de Jaeger, R. E. M. Verbeek, R. B. Draaisma et al., "Superior triacylglycerol (TAG) accumulation in starchless mutants of *Scenedesmus obliquus*: (I) mutant generation and characterization," *Biotechnology for Biofuels*, vol. 7, no. 1, article 69, 2014.

[15] K. Bišová and V. Zachleder, "Cell-cycle regulation in green algae dividing by multiple fission," *Journal of Experimental Botany*, vol. 65, no. 10, pp. 2585–2602, 2014.

[16] Z. T. Wang, N. Ullrich, S. Joo, S. Waffenschmidt, and U. Goodenough, "Algal lipid bodies: stress induction, purification, and biochemical characterization in wild-type and starchless *Chlamydomonas reinhardtii*," *Eukaryotic Cell*, vol. 8, no. 12, pp. 1856–1868, 2009.

[17] Y. T. Li, D. X. Han, G. R. Hu, M. Sommerfeld, and Q. A. Hu, "Inhibition of starch synthesis results in overproduction of lipids in *Chlamydomonas reinhardtii*," *Biotechnology and Bioengineering*, vol. 107, no. 2, pp. 258–268, 2010.

[18] Y. Li, D. Han, G. Hu et al., "*Chlamydomonas* starchless mutant defective in ADP-glucose pyrophosphorylase hyper-accumulates triacylglycerol," *Metabolic Engineering*, vol. 12, no. 4, pp. 387–391, 2010.

[19] P. C. Hallenbeck, M. Grogger, M. Mraz, and D. Veverka, "The use of Design of Experiments and Response Surface Methodology to optimize biomass and lipid production by the oleaginous marine green alga, *Nannochloropsis gaditana* in response to light intensity, inoculum size and CO_2," *Bioresource Technology*, vol. 184, pp. 161–168, 2015.

[20] A. E. Solovchenko, I. Khozin-Goldberg, S. Didi-Cohen, Z. Cohen, and M. N. Merzlyak, "Effects of light intensity and nitrogen starvation on growth, total fatty acids and arachidonic acid in the green microalga *Parietochloris incisa*," *Journal of Applied Phycology*, vol. 20, no. 3, pp. 245–251, 2008.

[21] D. Pal, I. Khozin-Goldberg, Z. Cohen, and S. Boussiba, "The effect of light, salinity, and nitrogen availability on lipid production by *Nannochloropsis* sp.," *Applied Microbiology and Biotechnology*, vol. 90, no. 4, pp. 1429–1441, 2011.

[22] T. Takeshita, S. Ota, T. Yamazaki, A. Hirata, V. Zachleder, and S. Kawano, "Starch and lipid accumulation in eight strains of six *Chlorella* species under comparatively high light intensity and aeration culture conditions," *Bioresource Technology*, vol. 158, pp. 127–134, 2014.

[23] S. K. Mandotra, P. Kumar, M. R. Suseela, S. Nayaka, and P. W. Ramteke, "Evaluation of fatty acid profile and biodiesel properties of microalga *Scenedesmus abundans* under the influence of phosphorus, pH and light intensities," *Bioresource Technology*, vol. 201, pp. 222–229, 2016.

[24] C. Yeesang and B. Cheirsilp, "Effect of nitrogen, salt, and iron content in the growth medium and light intensity on lipid production by microalgae isolated from freshwater sources in Thailand," *Bioresource Technology*, vol. 102, no. 3, pp. 3034–3040, 2011.

[25] X. Sun, Y. Cao, H. Xu et al., "Effect of nitrogen-starvation, light intensity and iron on triacylglyceride/carbohydrate production and fatty acid profile of *Neochloris oleoabundans* HK-129 by a two-stage process," *Bioresource Technology*, vol. 155, pp. 204–212, 2014.

[26] L.-D. Zhu and E. Hiltunen, "Methylation of *DACT2* accelerates esophageal cancer development by activating Wnt signaling," *Renewable and Sustainable Energy Reviews*, vol. 54, pp. 1285–1290, 2016.

[27] G. Sibi, V. Shetty, and K. Mokashi, "Enhanced lipid productivity approaches in microalgae as an alternate for fossil fuels—a review," *Journal of the Energy Institute*, vol. 89, no. 3, pp. 330–334, 2016.

[28] A. Converti, A. A. Casazza, E. Y. Ortiz, P. Perego, and M. Del Borghi, "Effect of temperature and nitrogen concentration on the growth and lipid content of *Nannochloropsis oculata* and

Chlorella vulgaris for biodiesel production," *Chemical Engineering and Processing: Process Intensification*, vol. 48, no. 6, pp. 1146–1151, 2009.

[29] L. Xin, H. Hong-ying, and Z. Yu-ping, "Growth and lipid accumulation properties of a freshwater microalga *Scenedesmus* sp. under different cultivation temperature," *Bioresource Technology*, vol. 102, no. 3, pp. 3098–3102, 2011.

[30] J. Cao, H. Yuan, B. Li, and J. Yang, "Significance evaluation of the effects of environmental factors on the lipid accumulation of *Chlorella minutissima* UTEX 2341 under low-nutrition heterotrophic condition," *Bioresource Technology*, vol. 152, pp. 177–184, 2014.

[31] L. Wei, X. Huang, and Z. Huang, "Temperature effects on lipid properties of microalgae *Tetraselmis subcordiformis* and *Nannochloropsis oculata* as biofuel resources," *Chinese Journal of Oceanology and Limnology*, vol. 33, no. 1, pp. 99–106, 2015.

[32] G. O. James, C. H. Hocart, W. Hillier, G. D. Price, and M. A. Djordjevic, "Temperature modulation of fatty acid profiles for biofuel production in nitrogen deprived *Chlamydomonas reinhardtii*," *Bioresource Technology*, vol. 127, pp. 441–447, 2013.

[33] X. Li, P. Přibyl, K. Bišová et al., "The microalga *Parachlorella kessleri*—a novel highly efficient lipid producer," *Biotechnology and Bioengineering*, vol. 110, no. 1, pp. 97–107, 2013.

[34] R. D. Gardner, E. Lohman, R. Gerlach, K. E. Cooksey, and B. M. Peyton, "Comparison of CO_2 and bicarbonate as inorganic carbon sources for triacylglycerol and starch accumulation in *Chlamydomonas reinhardtii*," *Biotechnology and Bioengineering*, vol. 110, no. 1, pp. 87–96, 2013.

[35] E. Y. O. Montoya, A. A. Casazza, B. Aliakbarian, P. Perego, A. Converti, and J. C. M. De Carvalho, "Production of *Chlorella vulgaris* as a source of essential fatty acids in a tubular photobioreactor continuously fed with air enriched with CO_2 at different concentrations," *Biotechnology Progress*, vol. 30, no. 4, pp. 916–922, 2014.

[36] A. Widjaja, C.-C. Chien, and Y.-H. Ju, "Study of increasing lipid production from fresh water microalgae *Chlorella vulgaris*," *Journal of the Taiwan Institute of Chemical Engineers*, vol. 40, no. 1, pp. 13–20, 2009.

[37] A. Nakanishi, S. Aikawa, S.-H. Ho et al., "Development of lipid productivities under different CO_2 conditions of marine microalgae *Chlamydomonas* sp. JSC4," *Bioresource Technology*, vol. 152, pp. 247–252, 2014.

[38] M. Ota, Y. Kato, H. Watanabe et al., "Fatty acid production from a highly CO_2 tolerant alga, *Chlorococcum littorale*, in the presence of inorganic carbon and nitrate," *Bioresource Technology*, vol. 100, no. 21, pp. 5237–5242, 2009.

[39] S.-H. Ho, C.-Y. Chen, and J.-S. Chang, "Effect of light intensity and nitrogen starvation on CO_2 fixation and lipid/carbohydrate production of an indigenous microalga Scenedesmus obliquus CNW-N," *Bioresource Technology*, vol. 113, pp. 244–252, 2012.

[40] G. Breuer, P. P. Lamers, D. E. Martens, R. B. Draaisma, and R. H. Wijffels, "Effect of light intensity, pH, and temperature on triacylglycerol (TAG) accumulation induced by nitrogen starvation in *Scenedesmus obliquus*," *Bioresource Technology*, vol. 143, pp. 1–9, 2013.

[41] L. D. Zhu, J. Takala, E. Hiltunen, and Z. M. Wang, "Recycling harvest water to cultivate *Chlorella zofingiensis* under nutrient limitation for biodiesel production," *Bioresource Technology*, vol. 144, pp. 14–20, 2013.

[42] Y. Li, F. Han, H. Xu et al., "Potential lipid accumulation and growth characteristic of the green alga *Chlorella* with combination cultivation mode of nitrogen (N) and phosphorus (P)," *Bioresource Technology*, vol. 174, pp. 24–32, 2014.

[43] I. Brányiková, B. Maršálková, J. Doucha et al., "Microalgae-novel highly efficient starch producers," *Biotechnology and Bioengineering*, vol. 108, no. 4, pp. 766–776, 2011.

[44] A. O. Alabi, M. Tampier, and E. Bibeau, "Microalgae technologies and processes for biofuels/bioenergy production in British Columbia," Current Technology, Suitability and Barriers to Implementation. Final Report, The British Columbia Innovation Council. Seed Science Press, 2009.

[45] T. Ito, M. Tanaka, H. Shinkawa et al., "Metabolic and morphological changes of an oil accumulating trebouxiophycean alga in nitrogen-deficient conditions," *Metabolomics*, vol. 9, no. 1, pp. 178–187, 2013.

[46] S. Mandal and N. Mallick, "Microalga *Scenedesmus obliquus* as a potential source for biodiesel production," *Applied Microbiology and Biotechnology*, vol. 84, no. 2, pp. 281–291, 2009.

[47] A. Sato, R. Matsumura, N. Hoshino, M. Tsuzuki, and N. Sato, "Responsibility of regulatory gene expression and repressed protein synthesis for triacylglycerol accumulation on sulfur-starvation in *Chlamydomonas reinhardtii*," *Frontiers in Plant Science*, vol. 5, article 444, 2014.

[48] B. Fernandes, J. Teixeira, G. Dragone et al., "Relationship between starch and lipid accumulation induced by nutrient depletion and replenishment in the microalga *Parachlorella kessleri*," *Bioresource Technology*, vol. 144, pp. 268–274, 2013.

[49] P. Přibyl, V. Cepák, and V. Zachleder, "Production of lipids in 10 strains of *Chlorella* and *Parachlorella*, and enhanced lipid productivity in *Chlorella vulgaris*," *Applied Microbiology and Biotechnology*, vol. 94, no. 2, pp. 549–561, 2012.

[50] A. Richmond, "Cell response to environmental factors," in *CRC Handbook of Microalgal Mass Culture*, A. Richmond, Ed., pp. 89–95, CRC Press, Florida, Fla, USA, 1986.

[51] F. Alkayal, R. L. Albion, R. L. Tillett, L. T. Hathwaik, M. S. Lemos, and J. C. Cushman, "Expressed sequence tag (EST) profiling in hyper saline shocked *Dunaliella salina* reveals high expression of protein synthetic apparatus components," *Plant Science*, vol. 179, no. 5, pp. 437–449, 2010.

[52] A. F. Talebi, M. Tabatabaei, S. K. Mohtashami, M. Tohidfar, and F. Moradi, "Comparative salt stress study on intracellular ion concentration in marine and salt-adapted freshwater strains of microalgae," *Notulae Scientia Biologicae*, vol. 5, no. 3, pp. 309–315, 2013.

[53] H. Yang, Q. He, J. Rong, L. Xia, and C. Hu, "Rapid neutral lipid accumulation of the alkali-resistant oleaginous *Monoraphidium dybowskii* LB50 by NaCl induction," *Bioresource Technology*, vol. 172, pp. 131–137, 2014.

[54] A. Kirrolia, N. R. Bishnoia, and N. Singh, "Salinity as a factor affecting the physiological and biochemical traits of *Scenedesmus quadricauda*," *Journal of Algal Biomass Utilization*, vol. 2, pp. 28–34, 2011.

[55] M. Takagi, Karseno, and T. Yoshida, "Effect of salt concentration on intracellular accumulation of lipids and triacylglyceride in marine microalgae *Dunaliella* cells," *Journal of Bioscience and Bioengineering*, vol. 101, no. 3, pp. 223–226, 2006.

[56] X. Duan, G. Y. Ren, L. L. Liu, and W. X. Zhu, "Salt-induced osmotic stress for lipid overproduction in batch culture of *Chlorella vulgaris*," *African Journal Biotechnology*, vol. 11, no. 27, pp. 7072–7078, 2012.

[57] H.-Y. Ren, B.-F. Liu, F. Kong, L. Zhao, G.-J. Xie, and N.-Q. Ren, "Enhanced lipid accumulation of green microalga *Scenedesmus*

sp. by metal ions and EDTA addition," *Bioresource Technology*, vol. 169, pp. 763–767, 2014.

[58] J. Yang, J. Cao, G. Xing, and H. Yuan, "Lipid production combined with biosorption and bioaccumulation of cadmium, copper, manganese and zinc by oleaginous microalgae *Chlorella minutissima* UTEX2341," *Bioresource Technology*, vol. 175, pp. 537–544, 2015.

[59] Z.-Y. Liu, G.-C. Wang, and B.-C. Zhou, "Effect of iron on growth and lipid accumulation in *Chlorella vulgaris*," *Bioresource Technology*, vol. 99, no. 11, pp. 4717–4722, 2008.

[60] Y. Li, J. Mu, D. Chen et al., "Production of biomass and lipid by the microalgae *Chlorella protothecoides* with heterotrophic-Cu(II) stressed (HCuS) coupling cultivation," *Bioresource Technology*, vol. 148, pp. 283–292, 2013.

[61] G. Mujtaba, W. Choi, C.-G. Lee, and K. Lee, "Lipid production by *Chlorella vulgaris* after a shift from nutrient-rich to nitrogen starvation conditions," *Bioresource Technology*, vol. 123, pp. 279–283, 2012.

[62] C. Adams, V. Godfrey, B. Wahlen, L. Seefeldt, and B. Bugbee, "Understanding precision nitrogen stress to optimize the growth and lipid content tradeoff in oleaginous green microalgae," *Bioresource Technology*, vol. 131, pp. 188–194, 2013.

[63] Y. Zhao, D. Li, K. Ding et al., "Production of biomass and lipids by the oleaginous microalgae *Monoraphidium* sp. QLY-1 through heterotrophic cultivation and photo-chemical modulator induction," *Bioresource Technology*, vol. 211, pp. 669–676, 2016.

[64] P. Feng, Z. Deng, L. Fan, and Z. Hu, "Lipid accumulation and growth characteristics of *Chlorella zofingiensis* under different nitrate and phosphate concentrations," *Journal of Bioscience and Bioengineering*, vol. 114, no. 4, pp. 405–410, 2012.

[65] L. Xin, H. Hong-ying, and Y. Jia, "Lipid accumulation and nutrient removal properties of a newly isolated freshwater microalga, *Scenedesmus* sp. LX1, growing in secondary effluent," *New Biotechnology*, vol. 27, no. 1, pp. 59–63, 2010.

[66] P. D. Álvarez-Díaz, J. Ruiz, Z. Arbib, J. Barragán, C. Garrido-Pérez, and J. A. Perales, "Lipid production of microalga *Ankistrodesmus falcatus* increased by nutrient and light starvation in a two-stage cultivation process," *Applied Biochemistry and Biotechnology*, vol. 174, no. 4, pp. 1471–1483, 2014.

[67] S. Ota, K. Oshima, T. Yamazaki et al., "Highly efficient lipid production in the green alga *Parachlorella kessleri*: draft genome and transcriptome endorsed by whole-cell 3D ultrastructure," *Biotechnology for Biofuels*, vol. 9, article 13, 2016.

[68] Y. Mizuno, A. Sato, K. Watanabe et al., "Sequential accumulation of starch and lipid induced by sulfur deficiency in *Chlorella* and *Parachlorella* species," *Bioresource Technology*, vol. 129, pp. 150–155, 2013.

Hindawi Publishing Corporation
BioMed Research International
Volume 2016, Article ID 3154929, 10 pages
http://dx.doi.org/10.1155/2016/3154929

Research Article

Simultaneous Saccharification and Fermentation of Sugar Beet Pulp for Efficient Bioethanol Production

Joanna Berłowska,[1] Katarzyna Pielech-Przybylska,[2] Maria Balcerek,[2] Urszula Dziekońska-Kubczak,[2] Piotr Patelski,[2] Piotr Dziugan,[1] and Dorota Kręgiel[3]

[1]*Department of Fermentation Technology, Institute of Fermentation Technology and Microbiology, Faculty of Biotechnology and Food Sciences, Lodz University of Technology, Wólczańska Str. 171/173, 90-924 Łódź, Poland*
[2]*Department of Spirit and Yeast Technology, Institute of Fermentation Technology and Microbiology, Faculty of Biotechnology and Food Sciences, Lodz University of Technology, Wólczańska Str. 171/173, 90-924 Łódź, Poland*
[3]*Department of Technical Microbiology, Institute of Fermentation Technology and Microbiology, Faculty of Biotechnology and Food Sciences, Lodz University of Technology, Wólczańska Str. 171/173, 90-924 Łódź, Poland*

Correspondence should be addressed to Katarzyna Pielech-Przybylska; katarzyna.pielech-przybylska@p.lodz.pl

Received 23 June 2016; Accepted 16 August 2016

Academic Editor: Liandong Zhu

Sugar beet pulp, a byproduct of sugar beet processing, can be used as a feedstock in second-generation ethanol production. The objective of this study was to investigate the effects of pretreatment, of the dosage of cellulase and hemicellulase enzyme preparations used, and of aeration on the release of fermentable sugars and ethanol yield during simultaneous saccharification and fermentation (SSF) of sugar beet pulp-based worts. Pressure-thermal pretreatment was applied to sugar beet pulp suspended in 2% w/w sulphuric acid solution at a ratio providing 12% dry matter. Enzymatic hydrolysis was conducted using Viscozyme and Ultraflo Max (Novozymes) enzyme preparations (0.015–0.02 mL/g dry matter). Two yeast strains were used for fermentation: Ethanol Red (*S. cerevisiae*) (1 g/L) and *Pichia stipitis* (0.5 g/L), applied sequentially. The results show that efficient simultaneous saccharification and fermentation of sugar beet pulp was achieved. A 6 h interval for enzymatic activation between the application of enzyme preparations and inoculation with Ethanol Red further improved the fermentation performance, with the highest ethanol concentration reaching 26.9 ± 1.2 g/L and 86.5 ± 2.1% fermentation efficiency relative to the theoretical yield.

1. Introduction

Sugar beet is grown and processed in all countries of the European Union (with the exception of Luxembourg) and plays an important role in sustaining jobs and local economies in many rural areas. Some 300,000 farms are involved in sugar beet production and the sugar industry is also a large employer [1]. Byproducts from the processing of sugar beet include beet leaves and sugar beet pulp. One ton of sugar beet yields on average 160 kg of sugar, 500 kg of wet pulp, and 38 kg of molasses. The exhausted beet material, which remains after diffusion with hot water to draw the sugar from the beets, is called pulp. It is usually pressed and/or dried for animal feed [2]. Annual production of beet pulp in the EU amounts to around 8 million tons of pressed and 5.5 million tons of dried product [1].

Lignocellulosic biomass, including sugar beet pulp (SBP), is a promising carbon source for the production of bio-based fuels and chemicals. SBP can be converted into fuel ethanol through chemical and/or enzymatic hydrolysis and via biochemical pathways. SBP consists mainly of polysaccharides such as cellulose (22–30%), hemicelluloses (24–32%), lignin (1-2%), and pectin (38–62%), which constitute up to 75–85% of the dry matter [3–5]. Before fermentation, the cell-wall material must be degraded into fermentable monosaccharides [6]. Before enzymatic hydrolysis of cellulose and hemicellulose into fermentable monosaccharides, lignocellulosic feedstocks are often structurally modified by

mild pretreatment. The goal is to break the lignin seal and disrupt the crystalline structure of the cellulose [6–8].

Cellulose and hemicellulose can be hydrolytically broken down into simple sugars by cellulases and hemicellulases, respectively, or by acids (e.g., sulfuric acid). Hexoses (glucose, galactose, and mannose) are fermented to ethanol by many naturally occurring microorganisms, but pentoses such as xylose and arabinose can be fermented to ethanol by relatively few native strains and usually at relatively low yields [9]. Xylose and arabinose generally comprise a significant fraction of agricultural residues and must be utilized to make biomass processing economically viable [10].

Saccharomyces cerevisiae, which remains the most widely used yeast for ethanol biosynthesis, produces ethanol by fermenting hexose sugars but is unable to ferment pentose sugars [11]. *S. cerevisiae* is incapable of growing on xylose and does not produce ethanol, although it does produce limited amounts of xylitol. A possible reason for this may be cofactor limitation. Xylose transport is also less efficient than glucose transport. Xylose is transported four times more slowly than glucose under aerobic conditions and twice as slowly under anaerobic conditions [12]. Some yeasts, such as *Candida shehatae*, *Candida tropicalis*, and *Pichia stipitis*, can ferment xylose and hexoses with relatively high yields [13] but have low ethanol tolerances, and ethanol concentrations over 30–35 g/L inhibit their metabolisms [14, 15]. The ability of these yeasts to metabolize xylose depends on culture oxygenation [16, 17].

When enzymatic hydrolysis is performed independently of the fermentation step (known as separate hydrolysis and fermentation, SHF), this results in high concentrations of lower saccharides, which expose the yeast to osmotic stress and even cause substrate inhibition. By adding the yeast and the enzymes which catalyze the hydrolysis of polysaccharides at the same time, so that the two processes occur simultaneously (simultaneous saccharification and fermentation, SSF), this effect can be reduced, since fermentable sugars are released and consumed continuously throughout the process [18, 19].

A number of reports in the literature discuss ethanol production using lignocellulosic biomass via simultaneous saccharification and fermentation [20]. However, few describe the utilization of SBP. With this substrate, however, costly thermochemical pretreatment might be avoided, due to its low lignin and high pectin contents. The proposed solution requires only simple and mild pretreatment procedures. Zheng et al. [21] report successful conversion of SBP into ethanol by SSF using several genetically modified ethanologenic bacteria, including *Escherichia coli* KO11, *Klebsiella oxytoca* P2, and *Erwinia chrysanthemi* EC16. In our study, only nonmodified yeasts strains were used. We also plan to conduct the bioconversion process using mixed cultures (conventional and nonconventional yeast), to solve the problem of xylose consumption.

The objective of this study was to determine the effects of various pretreatment methods and varying dosages of cellulase and hemicellulase enzyme preparations on polysaccharide hydrolysis and simultaneous saccharification and fermentation (SSF) of sugar beet pulp using two yeast strains applied sequentially: Ethanol Red (*S. cerevisiae*), recommended for hexose sugar fermentation, and *Pichia stipites*, which has good xylose fermentation ability. The effect of fermentation medium aeration after inoculation with *Pichia stipitis* on the efficiency of the process was also evaluated.

2. Materials and Methods

2.1. Feedstock. Fresh sugar beet pulp (SBP) was obtained from the Dobrzelin Sugar Factory (Poland) and stored at −20°C until used.

2.2. Enzymes. SBP was hydrolyzed using the commercial enzyme preparations Viscozyme (a multienzyme complex containing a wide range of carbohydrases, including arabanase, cellulase, β-glucanase, hemicellulase, and xylanase) and Ultraflo Max (endo-1,3(4)-β-glucanase; endo-1,4-xylanase) (Novozymes A/S, Denmark). Enzyme preparations were applied simultaneously, at loading rates ranging from 0.01 to 0.07 mL/g dry matter. Individual sugar yields were compared to determine the most effective dose for C6 and C5 sugar liberation.

2.3. Yeast Strains, Media, and Cultivation Conditions. Fermentation was carried out using a preparation of Ethanol Red dry distillery yeast (*S. cerevisiae*) (Fermentis Division S.I. Lesaffre, France) and *Pichia stipitis* NCYC 1541 (National Collection of Yeast Cultures, UK), applied sequentially. The process was initiated using yeast Ethanol Red (1 g d.m./L) and after 24 h the worts were inoculated with *Pichia stipitis* (0.5 g/L). *Pichia stipitis* was subcultured at 30°C on a solid YPG medium containing 1% yeast extract, 2% peptone, 2% glucose, and 2% agar. Two-step propagation was performed to obtain the *P. stipitis* inoculum. In the first step, stationary stage, inoculum cultures were grown for 24 h at 30°C in 100 mL Erlenmeyer flasks filled with 50 mL of liquid YPG medium supplemented with xylose (1%). The inoculum obtained was then transferred under sterile conditions into 1 L flasks containing 100 mL of the YPG medium and xylose. Propagation was carried out in shaken cultures for 48 hours at 30°C. The biomass obtained was centrifuged, washed twice with sterile physiological saline, and centrifuged again. After suspending the biomass in saline, the biomass yield was determined by drying the sample to a constant weight at 105°C. The yeast slurry was added to the worts at a ratio of 0.5 g d.m. of yeast/L wort.

2.4. Preparation of Worts. To prepare the worts for fermentation, SBP was milled to obtain 0.8–1.0 mm particles and a portion of the pulp (100 g) diluted with fresh water or with 2% w/w sulfuric acid (192 mL), to obtain mixtures with dry matter content ca. 12% w/w. Next, the mixtures were subjected to two types of pretreatment: (1) thermal pretreatment in a lab-scale autoclave by heating the sugar beet pulp to 121°C for 30 or 60 min at 0.1 MPa and (2) ultrasound pretreatment with a SONOPULS HD 2200 homogenizer in continuous mode, set to 50% or 100% amplitude (ultrasound power 400 W, 24 kHz) for 20 min. The control samples were not subjected to either thermal or ultrasound pretreatment. After pretreatment, the

worts were adjusted to pH 4.8 using 25% (w/w) sodium hydroxide before undergoing a process of simultaneous saccharification and fermentation, with or without the "activation" phase. Two variants of wort with "enzymatic activation" were prepared. In Variant I, the medium was digested with Viscozyme and Ultraflo Max enzyme preparations (each at a dose of 0.02 mL/g d.m.) and continually stirred and heated to 40°C for 6 h before inoculation with yeast. In Variant II, the medium was digested using the same preparations, each at doses of 0.015 mL/g d.m., stirred continuously, and heated to 48–50°C for 6 hours before inoculation with yeast. In Variant II, the worts were supplemented with $(NH_4)_2HPO_4$ (0.3 g/L) and inoculated with yeast. In fermentation trials without previous enzymatic activation, the samples were digested with enzyme preparations (each at doses of 0.02 mL/g d.m.), supplemented with $(NH_4)_2HPO_4$ (0.3 g/L), and immediately inoculated with yeast.

2.5. Fermentation. The fermentation experiments were carried out in 1 L glass flasks, each containing approximately 0.5 L of wort. Fermentation was initiated using 1 g of Ethanol Red distillery yeast (*S. cerevisiae*) per 1 L of wort. The yeast was first hydrated and acid-washed (15 min incubation of cells suspended in water with the addition of 25% w/w sulfuric acid solution, pH 2.5, at room temperature). The flasks were closed with stoppers equipped with fermentation pipes, filled with glycerol, and kept in a thermostat-regulated room at 37 ± 1°C. Fermentation was continued over 24 hours, at the end of which the specimens were inoculated with the *Pichia stipitis* yeast strain (0.5 g/L). In selected fermentation trials, after inoculation with *P. stipitis*, the effect of aeration was evaluated using a 0.3 vvm constant air supply. Fermentation was resumed for a further 48 hours, the entire process time amounting to 72 h. The process was controlled gravimetrically (a decrease in mass caused by the liberation of carbon dioxide). When the fermentation was complete, samples were collected to determine the ethanol, hexose, and pentose sugar concentrations.

2.6. Analytical Methods. The sugar beet pulp was analyzed following methods recommended for the sugar industry [22]. Solid substance was measured in a Radwag WPS-30S weighing dryer. Total nitrogen was determined using the Kjeldahl method. Reducing sugars and total sugars (after inversion with hydrochloric acid) were determined according to the Miller method [23], in g of invert sugar per kg of thick juice. The concentration of saccharose was calculated as the difference between the quantities of total sugars and reducing sugars (with a conversion coefficient of 0.95). Cellulose content was determined according to the Kürschner-Hoffer method [24], hemicellulose content using the Ernakow method [25], and lignin content following the method recommended by the National Renewable Energy Laboratory (NREL) [26]. The pH was also measured, using a digital pH meter.

The contents of glucose (GLC), fructose (FRU), galactose (GAL), xylose (XYL), arabinose (ARA), rhamnose (RHA), saccharose (SAC), cellobiose (CEL), raffinose (RAF), and galacturonic acid (GalA) in the media were determined before and after fermentation. The concentrations of ethanol in the media and in postfermentation effluents were determined using HPLC (Agilent 1260 Infinity, USA) on Hi-Plex Ca column (7.7 × 300 mm, 8 μm) (Agilent Technologies, USA) equipped with a refractive index detector (RID) at 55°C. Column temperature was maintained at 80°C. HPLC grade water was used as a mobile phase at a flow rate of 0.6 mL/min with a sample volume of 20 μL. Prior to analysis, samples of the worts were mixed with $ZnSO_4$ to final concentrations of 10% to induce protein precipitation. The solid debris was removed by centrifugation at 4,000 rpm for 20 min. Prior to analysis, all samples were filtered through 0.45 μm PES (polyethersulfone) membranes.

2.7. Evaluation of Hydrolysis and Fermentation. Hydrolysis yield (HY) was calculated according to the following formula:

$$\mathrm{HY} = \frac{C * 0.9}{\mathrm{RS} + \mathrm{SAC} + \mathrm{RAF} + P} * 100\%, \quad (1)$$

where C is the reducing pentose and hexose sugars concentration after hydrolysis [g/L]; RS are the reducing sugars in sugar beet pulp before hydrolysis [g/L]; SAC and RAF, respectively, are saccharose and raffinose contents [g/L]; P is polysaccharide (cellulose and hemicellulose) content [g/L]; and 0.9 is the conversion coefficient from polysaccharide (cellulose and hemicellulose) to pentose and hexose sugars (i.e., the molecular weight ratio of polysaccharide to hexose and pentose sugars).

The total sugar intake (percentage consumption of total sugars during fermentation) was calculated as the ratio of sugars used to their content in the wort prior to fermentation, expressed as a percentage.

Fermentation efficiency (FE) was calculated for fermentable sugars (using a stoichiometric equation) and expressed as a percentage of the theoretical yield, according to the following formula:

$$\mathrm{FE} = \frac{E}{\mathrm{FS} * 0.51} * 100\%, \quad (2)$$

where E is ethanol concentration in the fermented medium [g/L]; FS are fermentable sugars (glucose, fructose, galactose, and xylose); 0.511 is the constant which represents the theoretical yield of ethanol from glucose and xylose.

Ethanol yield was expressed as the amount of absolute ethanol (A_{100}) obtained from 100 kg of wet sugar beet pulp.

2.8. Statistical Analysis. All samples were prepared and analyzed in triplicate. Statistical calculations were performed using STATISTICA 9.0 software (StatSoft, USA). The results were evaluated using one-way analysis of variance (ANOVA) and two-way ANOVA with a significance level of 0.05. Where statistical differences were found ($p < 0.05$), post hoc analysis was conducted using Tukey's range test (with a significance level of 0.05) to determine which specific means were different.

3. Results and Discussion

3.1. Chemical Composition of Sugar Beet Pulp. The chemical composition of the sugar beet pulp used in this study was

Table 1: Chemical composition of raw material.

Physicochemical parameters	Sugar beet pulp
Dry mass (g/kg)	229.3 ± 11.5
pH	5.8 ± 0.2
Reducing sugars as invert sugar (g/kg d.m.)	9.8 ± 0.3
Saccharose (g/kg d.m.)	144.8 ± 12.5
Raffinose (g/kg d.m.)	2.4 ± 0.3
Cellulose (g/kg d.m.)	336.8 ± 15.2
Hemicellulose (g/kg d.m.)	405.5 ± 27.2
Lignin (g/kg d.m.)	1.4 ± 0.2
Protein ($N\times$ 6.25) (g/kg d.m.)	11.5 ± 0.25

Results expressed as mean values ± SE ($n = 3$).

typical for that of sugar beet byproducts of processing (see Table 1).

The high content of carbohydrates, in particular non-starch polysaccharides such as cellulose and hemicellulose, and low content of lignin are advantages from the technological point of view, enabling high yields of fermentable sugars (including glucose and xylose). Sugar beet pulp feedstock therefore has great potential for use in "second-generation" biofuel (ethanol) production. However, efficient hydrolysis and fermentation depend on the type of pretreatment, the conditions of enzymatic hydrolysis, and the microorganisms used for the fermentation of released hexose and pentose sugars.

Our results are similar to others reported in the literature [27, 28]. Any differences in the chemical composition of sugar beet pulp can be related to the varieties of sugar beet processed in sugar factories, to different conditions of sugar beet cultivation, and to the technologies used for processing.

3.2. Effect of Pretreatment Type and Enzyme Preparation Dosage on the Release of Fermentable Sugars. Different types of pretreatment and various dosages of the cellulase and hemicellulase preparations Viscozyme and Ultraflo Max (Novozymes) were investigated to determine their effects on the release of fermentable sugars. Thermochemical pretreatment is recommended to remove most of the lignin and facilitate the action of cellulases and hemicellulases on cellulose and hemicellulose, so that the microorganisms can use the liberated monosaccharides as a carbon source [7, 8].

Due to the fact that the tested feedstock contained a relatively low lignin content, the first batch of experiments was carried out without pretreatment. A mixture of SBP and water in a ratio providing a medium containing approx. 12% d.m. was digested using different doses of the enzyme preparations Viscozyme and Ultraflo Max, in a range from 0.01 to 0.07 mL/g d.m. The samples were then incubated at 37 ± 1°C for 72 h, but without yeast to determine the degree of polysaccharide hydrolysis. The goal of this stage of the study was to determine the amounts of sugars that could potentially be released under fermentation conditions. Due to the fact that the samples were not inoculated with yeast and there was no fermentation, the worts were supplemented with the antibiotics penicillin G sodium salt (100 000 U/L wort) and streptomycin sulfate salt (0.1 g/L wort) to protect the process from bacterial contamination and prevent microbial infections.

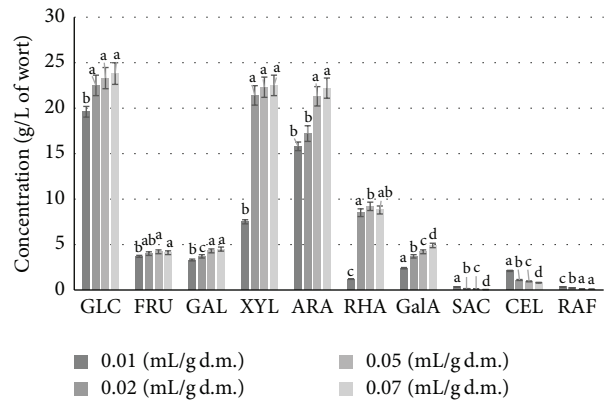

Figure 1: Qualitative and quantitative composition of carbohydrates in sugar beet pulp hydrolysate obtained after digestion of the feedstock (without pretreatment) with different dosage of Viscozyme and Ultraflo Max enzyme preparations. [a–c]Mean values for each sugar content with different letters are significantly different ($p < 0.05$, one-way ANOVA).

As shown in Figure 1, enzymatic hydrolysis of SBP in water with Viscozyme and Ultraflo Max preparations (each at a dose of 0.01 mL/g d.m.) resulted in the release of the following amounts of sugars (per liter): 19.6 g glucose, 3.3 g galactose, 3.7 g fructose, 7.5 g xylose, 15.8 g arabinose, 1.2 g rhamnose, and 2.4 g galacturonic acid. Saccharose (0.35 g/L), cellobiose (2.1 g/L), and raffinose (0.35 g/L) were also found. According to the literature [3, 29], these carbohydrates can be found in sugar beet roots, explaining their presence in the SBP. Rhamnose is bound to galacturonic acid by α-1-4-glycosidic bonds, which form long, "smooth" regions, and α-1-2-glycosidic bonds, which create branched regions in the chains that build pectins [30]. The remaining rhamnose is linked by α-1-5-glycosidic bonds to arabinose chains [28].

Increasing the dose of enzymatic preparations to 0.02 mL/g d.m. caused a relatively small rise (approx. 15%) in glucose concentration, to 22.5 g/L ($p > 0.05$), and significant increases in the concentration of xylose and rhamnose, to 21.4 g/L and 8.5 g/L, respectively ($p < 0.05$). Further increasing the enzyme preparation dosage to 0.05 mL/g d.m. of sugar beet pulp resulted in increased galactose, arabinose, and rhamnose contents ($p < 0.05$). However, a further increase to 0.07 mL/g d.m. did not significantly improve the efficiency with which sugars were released ($p > 0.05$).

The highest efficiency of hydrolysis (72 ± 3%) was observed in batches where the enzymatic preparations were applied in doses of 0.02 mL/g d.m. ($p < 0.05$). Higher doses of these preparations did not result in the release of greater amounts of glucose and xylose ($p > 0.05$). A significant increase occurred only in the case of arabinose ($p < 0.05$). The inhibition of cellulase and hemicellulase activities observed may have been caused by the rising concentration of sugars, as well as by the limited access of these enzymes to substrates contained in the feedstock.

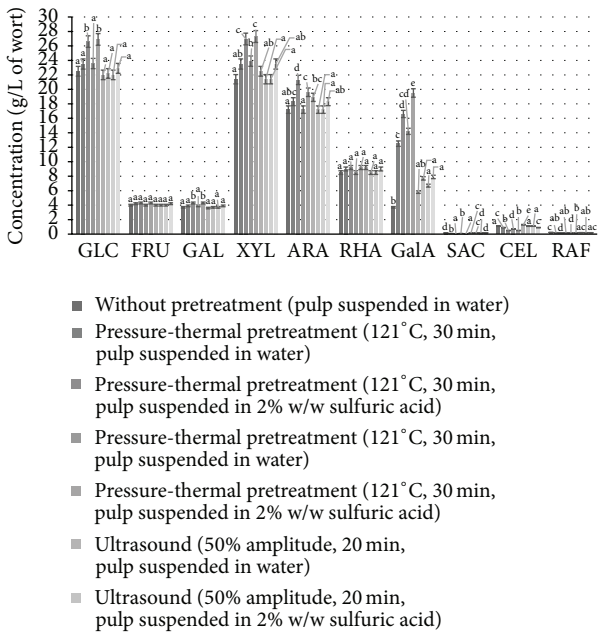

Figure 2: Qualitative and quantitative composition of carbohydrates in sugar beet pulp hydrolysate obtained after digestion of the sugar beet pulp with Viscozyme and Ultraflo Max enzyme preparations (each at a dose of 0.02 mL/g d.m.), preceded by different pretreatments. [a–e]Mean values for each sugar content with different letters are significantly different ($p < 0.05$, one-way ANOVA).

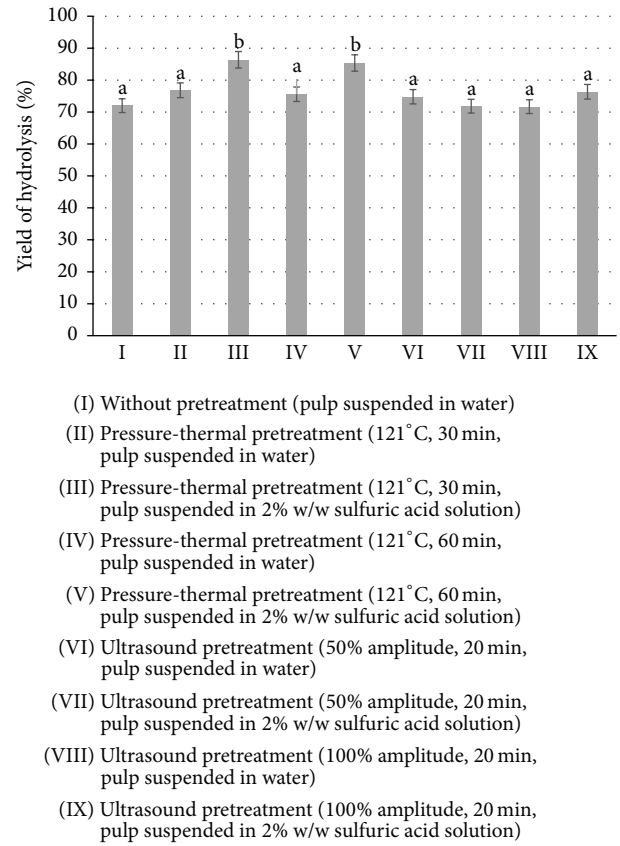

Figure 3: Yield of hydrolysis of polysaccharides in the tested SBP after pretreatment and enzymatic hydrolysis with Viscozyme and Ultraflo Max, each at a dose of 0.02 mL/g d.m., under fermentation conditions (37 ± 1°C, 72 h). [a-b]Mean values with different letters are significantly different ($p < 0.05$, one-way ANOVA).

The next stage of the investigation focused on whether pretreatment of the ground beet pulp improved the release of fermentable sugars. The following forms of pretreatment were considered: suspension in water or in 2% w/w sulfuric acid solution (ratio of the pulp to water or acid approx. 12% dry matter in the medium); pretreatment by autoclaving at 121°C for 30 or 60 min; ultrasound action (amplitude 50 or 100%, 20 min). Enzymatic hydrolysis was then performed with cellulase and hemicellulase preparations, each at doses of 0.02 mL/g d.m. The results are presented in Figure 2.

The highest release rate of fermentable sugars was observed after 30 minutes at 121°C from sugar beet pulp suspended in 2% w/w sulfuric acid solution. Most significantly, the concentration of glucose increased by 18% (from 22.5 to 26.6 g/L), and that of xylose increased by 26% (from 21.4 to 26.96 g/L) ($p < 0.05$). Conversely, the concentrations of cellobiose, raffinose, and saccharose dropped to 0.05–0.13 g/L of wort. The highest yield of polysaccharides and oligosaccharides was also observed with this variant of the experiment, reaching 86.4 ± 2.6% ($p < 0.05$). Neither increasing the time of thermal treatment to 60 minutes nor applying ultrasound treatment yielded higher concentrations of fermentable sugars (Figure 3) ($p < 0.05$). These results are in agreement with data obtained by Rezić et al. [31], which showed that pressure-thermal pretreatment had an effect on lignocellulosic substrates and favored the release of monosaccharides from cellulose and hemicellulose. Dilute acid hydrolysis treatment also caused disruption to the polymetric structure of the sugar beet pulp [32].

3.3. Results of Simultaneous Saccharification and Fermentation of Sugar Beet Pulp-Based Worts. Earlier research had demonstrated that conducting separate enzymatic hydrolysis of sugar beet pulp at elevated temperatures (approx. 48–50°C) for 48 hours increased the cost of the process and the risk of microbial infection, thereby lowering fermentation performance (data not shown). Therefore, this study focused on selecting optimal conditions for simultaneous saccharification and fermentation (SSF) of sugar beet pulp-based worts. SSF eliminates the time needed for separate hydrolysis of the polysaccharides present in sugar beet pulp. Consequently, it reduces the total time required for the process, from preparation of the feedstock to obtaining the final product. Based on our prior research, Ethanol Red distillery yeast was selected to ferment the hexose sugars. This strain exhibits tolerance to variable conditions (pH 3.5–6.0, temperature up to 40°C), which is especially important in SSF processes [33]. Also, in previous studies, the most efficient yeast for the fermentation of pentoses (e.g., xylose) had been found to be *Pichia stipitis* NCYC 1541 (the National Collection of Yeast Cultures, UK). Sequential inoculation was used, initiated with the dry distillery yeast (1 g d.m./L) followed by inoculation after 24 h with *Pichia stipitis* (0.5 d.m. g/L).

To investigate whether partial saccharification of the polysaccharides (so-called "enzymatic activation") had an impact on the effectiveness of the SSF process, we introduced an interval between the application of the enzymatic preparations (0.02 mL/g d.m.) and inoculation with yeast. After 6 hours of activation, the partially hydrolyzed biomass was inoculated with Ethanol Red yeast. After 24 h of fermentation, *P. stipitis* yeast inoculum was added. The results are presented in Table 2.

The lowest ethanol content (14.3 ± 0.6 g/L) was determined in the control sample, in which simultaneous saccharification and fermentation was performed without pretreatment ($p < 0.05$). When an analogous fermentation trial (pulp suspended in water, without pretreatment of SBP) was subjected to 6 h of enzymatic activation and then inoculated with yeast, the ethanol concentration after fermentation increased by 16.8% to 16.7 ± 0.5 g/L ($p < 0.05$). Fermentation efficiency rose from 54.2 ± 2.2% to 63.3 ± 1.8% of the theoretical yield.

The highest amount of ethanol ($p < 0.05$) was measured in the trial subjected to enzymatic activation (Variant I, inoculation with yeast Ethanol Red after 6 h action with Viscozyme 0.02 mL/g d.m. and Ultraflo Max 0.02 mL/g d.m. at 40°C), preceded by 30 min pressure-thermal pretreatment of the pulp suspended in 2% w/w sulfuric acid. Ethanol concentration in this wort reached 26.9±1.2 g/L, while the fermentation efficiency was 86.5 ± 2.1% of the theoretical yield. Intake of hexose sugars (i.e., glucose, fructose, and galactose) was 90.3 ± 2.2%, whereas 87.2 ± 1.9% of the xylose was used.

Similar fermentation factors were observed in Variant II of the experiment, in which enzymatic activation was performed for 6 h with lower doses of the preparations (0.015 mL/g d.m. Viscozyme and 0.015 mL/g d.m. Ultraflo Max), at higher temperatures (48–50°C) than in Variant I, but with analogous pretreatment (Table 2). Thermochemical pretreatment followed by activation using enzymatic preparations in doses between 0.015 and 0.02 mL/g d.m. of SBP and inoculation with yeast led to increased ethanol concentrations ($p < 0.05$) and more dynamic fermentation. As a consequence, the fermentation process was completed within 60 hours with no loss of CO_2.

Prolonging the period of pressure-thermal treatment from 30 to 60 min did not significantly improve the results for fermentation of SBP suspended in 2% w/w sulfuric acid ($p > 0.05$). Pretreatment with ultrasound before enzymatic hydrolysis did not improve the efficiency of fermentable sugar release or fermentation factors (Table 2) ($p > 0.05$). There was a statistically significant reduction in fermentation performance (i.e., ethanol concentration and process efficiency) with all fermentation batches of worts prepared from SBP pretreated with ultrasound waves, compared with those for analogous fermentation trials in which pressure-thermal pretreatment was applied ($p < 0.05$).

The most favorable variant was pressure-thermal pretreatment of SBP suspended in 2% w/w sulfuric acid, followed by simultaneous saccharification and fermentation of wort subjected to enzymatic activation. This variant enabled high utilization of fermentable sugars and maximal ethanol yield under the experimental conditions described above.

The concentrations of arabinose, rhamnose, and galacturonic acid reduced by similar proportions in all the fermentation trials, between 3 and 5% (data not shown), and did not differ statistically compared to the worts before fermentation. This indicates that the yeast strains used in our study did not assimilate these compounds. Patelski et al. [34], who investigated the bioconversion of sugar beet pulp into single-cell protein (SCP) using *Saccharomyces cerevisiae* and *Pichia stipitis* yeast strains, observed that glucose, fructose, and galactose were assimilated by all the tested strains. *S. cerevisiae* was not able to utilize xylose, arabinose, rhamnose, or galacturonic acid, while the *P. stipitis* strain utilized only approx. 15% of the arabinose and 40% of the rhamnose. It is notable that the *P. stipitis* yeast strain used by Patelski et al. was not found to utilize xylose as a carbon source for biomass production.

Recent research has investigated the possibility of improving the fermentation of arabinose by using recombinant yeast strains [35]. Bettiga et al. [36] investigated pentose fermentation using recombinant *S. cerevisiae* strains. Under anaerobic conditions, a yeast strain containing a complete L-arabinose pathway fermented L-arabinose in the presence of glucose. The authors observed minor coconsumption of L-arabinose in the presence of glucose, but after glucose depletion the consumption rate was higher and subsequently pentose fermentation was observed.

According to the literature, the ability of *Pichia stipitis* yeast to metabolize xylose is dependent on culture oxygenation [16, 17]. It has been reported that ethanol yield can be significantly increased when qO2 (the specific oxygen uptake rate) is adjusted to the optimum oxygen level for the type of sugar consumed [37]. According to our results, aeration did not improve the effectiveness of SBP fermentation. However, statistically significant increases in the consumption of hexose sugars and xylose were observed ($p < 0.05$), and as a consequence we noted an approximately threefold increase in the yeast biomass ($p < 0.05$) (see Figure 4). The recovery of so-called postfermentation yeast, which is a valuable source of protein (over 50% d.m.), can significantly improve the economic viability of the entire process.

Gutiérrez-Rivera et al. [38] observed that, in coculture experiments (simultaneous inoculation of *S. cerevisiae* ITV-01 and *P. stipitis* NRRL Y-7124), ethanol production did not depend on the level of aeration, while ethanol productivity was higher in cocultures with an air supply compared to those without (1.26 and 0.38 $g\,L^{-1}\,h^{-1}$, resp.). Moreover, ethanol productivity from aerated cocultures was greater than with *P. stipitis* NRRL Y-7124 alone under the same conditions (0.24 and 1.26 $g\,L^{-1}\,h^{-1}$, resp.). Yet, whereas with *P. stipitis* NRRL Y-7124 100% of the xylose was used, with aerated cocultures xylose uptake was incomplete (79.6%). Gutiérrez-Rivera et al. conclude that it is probable that *S. cerevisiae* ITV-01 and *P. stipitis* NRRL Y-7124 adversely affect each other. This may be due to the limited oxygen available for *P. stipites*, as a result of oxygen utilization by *S. cerevisiae*.

On the basis of our fermentation results, we calculated the quantity of ethanol obtained from 100 kg of sugar beet pulp-based wort. Our study shows that 6.8 ± 0.3 kg absolute ethanol can be produced from 100 kg of wet sugar beet pulp

Table 2: Effect of simultaneous saccharification and fermentation conditions on sugar beet pulp-based wort fermentation factors and intake of sugars.

Fermentation trial	Parameters	Pretreatment								
			Pressure-thermal pretreatment				Ultrasound pretreatment			
			30 min		60 min		50% amplitude, 20 min		100% amplitude, 20 min	
		Without pretreatment, pulp suspended in water	Pulp suspended in water	Pulp suspended in 2% w/w sulfuric acid solution	Pulp suspended in water	Pulp suspended in 2% w/w sulfuric acid solution	Pulp suspended in water	Pulp suspended in 2% w/w sulfuric acid solution	Pulp suspended in water	Pulp suspended in 2% w/w sulfuric acid solution
Initial fermentable sugar content as sum of glucose, fructose, galactose, saccharose, and xylose [g/L]		51.75 ± 1.55^{a}	55.18 ± 1.65^{a}	62.21 ± 1.86^{b}	55.45 ± 1.65^{a}	62.85 ± 1.90^{b}	52.23 ± 1.40^{a}	51.43 ± 1.54^{a}	51.27 ± 1.54^{a}	54.67 ± 1.64^{a}
Without enzymatic activation*	Ethanol content (g/L)	14.3 ± 0.6^{a}	19.9 ± 0.7^{efgh}	22.5 ± 1.1^{hij}	20.5 ± 0.8^{fghi}	22.7 ± 0.9^{ij}	15.8 ± 0.4^{ab}	16.3 ± 0.5^{abc}	16.2 ± 0.5^{abc}	17.5 ± 0.7^{bcde}
	Fermentation efficiency (% of the theoretical yield)	54.2 ± 2.2^{a}	70.7 ± 2.3^{cdefgh}	70.9 ± 3.5^{defgh}	72.5 ± 2.8^{fghi}	80.3 ± 3.1^{ij}	59.4 ± 1.5^{ab}	62.2 ± 1.9^{abcd}	62.1 ± 1.9^{abc}	62.7 ± 2.5^{abcde}
	Intake of hexoses (%)	85.1 ± 2.4^{abcdef}	83.2 ± 2.5^{abc}	83.8 ± 2.2^{abcd}	84.2 ± 2.6^{abcde}	83.8 ± 2.5^{abcd}	82.1 ± 2.4^{a}	82.8 ± 2.5^{ab}	85.2 ± 2.5^{abcdef}	85.1 ± 2.4^{abcdef}
	Intake of xylose (%)	65.3 ± 1.5^{a}	75.2 ± 1.8^{cdef}	77.2 ± 1.5^{defgh}	76.2 ± 1.4^{cdefg}	77.5 ± 1.6^{defgh}	67.3 ± 1.5^{ab}	74.5 ± 1.5^{cd}	76.2 ± 1.5^{cdefg}	71.3 ± 1.5^{bc}
Enzymatic activation, Variant I**	Ethanol content (g/L)	16.7 ± 0.5^{abcd}	22.5 ± 0.7^{hij}	26.9 ± 1.2^{k}	23.6 ± 0.9^{j}	27.1 ± 1.2^{k}	17.5 ± 0.6^{bcde}	18.3 ± 0.7^{bcdef}	18.1 ± 0.6^{bcdef}	18.7 ± 0.8^{cdef}
	Fermentation efficiency (% of the theoretical yield)	63.3 ± 1.8^{bcde}	80.1 ± 2.3^{ij}	86.5 ± 2.1^{j}	83.4 ± 3.2^{j}	84.4 ± 3.7^{j}	65.8 ± 2.2^{bcdefg}	69.8 ± 2.7^{cdefgh}	69.3 ± 2.3^{cdefg}	67.0 ± 2.9^{bcdefg}
	Intake of hexoses (%)	91.6 ± 2.5^{efgh}	88.2 ± 2.2^{abcdefgh}	90.3 ± 2.4^{bcdefgh}	90.5 ± 2.5^{cdefgh}	95.5 ± 2.6^{h}	89.2 ± 2.5^{abcdefgh}	88.6 ± 2.2^{abcdefgh}	88.2 ± 2.2^{abcdefgh}	87.5 ± 2.5^{abcdefg}
	Intake of xylose (%)	74.5 ± 2.5^{cd}	86.5 ± 2.6^{jkl}	88.2 ± 1.9^{kl}	87.5 ± 1.8^{kl}	89.5 ± 1.5^{l}	83.5 ± 1.6^{ijk}	80.5 ± 1.2^{efghi}	82.5 ± 1.5^{hijk}	81.5 ± 1.4^{ghij}
Enzymatic activation, Variant II**	Ethanol content (g/L)	16.9 ± 0.5^{abcd}	22.1 ± 0.8^{ghij}	26.6 ± 1.5^{k}	22.7 ± 0.8^{ij}	26.9 ± 1.5^{k}	18.1 ± 0.6^{bcdef}	18.6 ± 0.8^{cdef}	19.2 ± 0.7^{def}	19.6 ± 0.7^{efg}
	Fermentation efficiency (% of the theoretical yield)	64.3 ± 1.6^{bcdef}	78.5 ± 2.8^{hij}	83.8 ± 4.7^{j}	80.3 ± 2.7^{ij}	83.8 ± 4.2^{j}	68.0 ± 2.3^{bcdefg}	71.0 ± 2.8^{efgh}	73.6 ± 2.6^{ghi}	70.3 ± 2.5^{cdefgh}
	Intake of hexoses (%)	91.3 ± 2.2^{defgh}	88.2 ± 2.6^{abcdefgh}	92.0 ± 2.5^{fgh}	89.5 ± 1.8^{abcdefgh}	93.0 ± 1.5^{gh}	88.3 ± 2.2^{abcdefgh}	88.5 ± 2.2^{abcdefg}	86.2 ± 2.5^{abcdefg}	88.2 ± 2.4^{abcdefgh}
	Intake of xylose (%)	74.9 ± 1.9^{cde}	83.3 ± 2.2^{ijk}	88.1 ± 2.2^{kl}	85.2 ± 2.2^{ijkl}	89.5 ± 2.2^{l}	74.9 ± 1.9^{cde}	80.8 ± 1.5^{fghi}	80.3 ± 2.0^{efghi}	80.5 ± 1.5^{efghi}

Results expressed as mean values ± SE ($n = 3$); $^{a-b}$mean values for initial fermentable sugar content with different letters are significantly different ($p < 0.05$, one-way ANOVA); $^{a-l}$mean values for ethanol content, fermentation efficiency, intake of hexoses, and intake of xylose with different letters are significantly different ($p < 0.05$, two-way ANOVA).

*Without enzymatic activation: inoculation with yeast Ethanol Red immediately after application of enzyme preparations.

**Enzymatic activation, Variant I: inoculation with yeast Ethanol Red after 6 h of enzymatic preparations action (Viscozyme 0.02 mL/g d.m.; Ultraflo Max 0.02 mL/g d.m., 40°C). Enzymatic activation, Variant II: inoculation with yeast Ethanol Red after 6 h of enzymatic preparations action (Viscozyme 0.015 mL/g d.m.; Ultraflo Max 0.015 mL/g d.m., 48–50°C).

Table 3: Ethanol yield (kg absolute ethanol) from 100 kg of wet (ca. 23% d.m.) sugar beet pulp.

Fermentation trial	Pretreatment								
		Pressure-thermal pretreatment				Ultrasound pretreatment			
		30 min		60 min		50% amplitude, 20 min		100% amplitude, 20 min	
	Without pretreatment, pulp suspended in water	Pulp suspended in water	Pulp suspended in 2% w/w sulfuric acid solution	Pulp suspended in water	Pulp suspended in 2% w/w sulfuric acid solution	Pulp suspended in water	Pulp suspended in 2% w/w sulfuric acid solution	Pulp suspended in water	Pulp suspended in 2% w/w sulfuric acid solution
Without enzymatic activation*	3.6 ± 0.2^{a}	5.0 ± 0.2^{efgi}	5.6 ± 0.3^{ijk}	5.1 ± 0.2^{ghij}	5.7 ± 0.2^{jk}	3.9 ± 0.1^{ab}	4.1 ± 0.2^{abc}	4.1 ± 0.1^{abc}	4.4 ± 0.2^{bcdef}
Enzymatic activation, Variant I**	4.2 ± 0.1^{abcd}	5.6 ± 0.2^{ijk}	6.7 ± 0.3^{h}	5.9 ± 0.2^{k}	6.8 ± 0.3^{l}	4.4 ± 0.2^{bcdef}	4.6 ± 0.2^{cdefg}	4.5 ± 0.2^{bcdefg}	4.7 ± 0.2^{cdefg}
Enzymatic activation, Variant II**	4.2 ± 0.1^{abcd}	5.5 ± 0.2^{hijk}	6.7 ± 0.4^{jk}	5.7 ± 0.2^{jk}	6.7 ± 0.4^{bcdefg}	4.5 ± 0.2^{bcdefg}	4.7 ± 0.2^{cdefg}	4.8 ± 0.2^{defg}	4.9 ± 0.2^{efg}
Enzymatic activation, Variant I & aeration	4.3 ± 0.1^{bcde}	5.7 ± 0.2^{bcde}	6.6 ± 0.3^{jk}	5.6 ± 0.2^{ijk}	6.6 ± 0.3^{l}	4.7 ± 0.1^{cdefg}	4.9 ± 0.2^{efg}	4.9 ± 0.2^{efg}	5.0 ± 0.2^{fghi}

Results expressed as mean values ± SE ($n = 3$); $^{a–l}$mean values with different letters are significantly different ($p < 0.05$, two-way ANOVA).

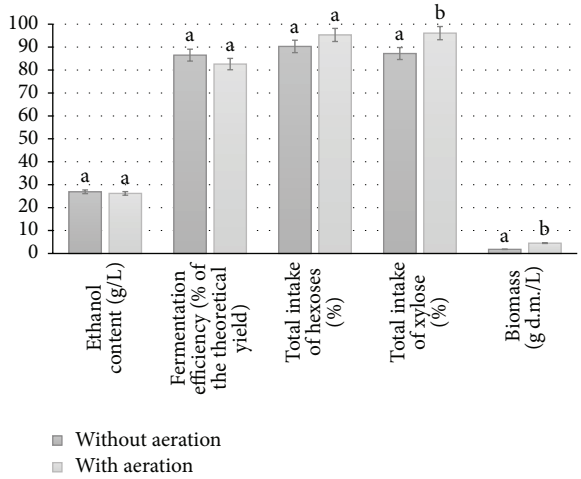

Figure 4: Effect of aeration on efficiency of simultaneous saccharification and fermentation of sugar beet pulp (fermentation Variant I with enzymatic activation: inoculation with yeast Ethanol Red after 6 h of enzymatic action (Viscozyme 0.02 mL/g d.m.; Ultraflo Max 0.02 mL/g d.m., 40°C), preceded by 30 min pressure-thermal pretreatment of SBP suspended in 2% w/w sulfuric acid solution). [a-b]Mean values for each index with different letters are significantly different ($p < 0.05$, one-way ANOVA).

(approx. 23% d.m.) under the most favorable conditions, as established in our experiments (see Table 3).

4. Conclusions

The results of our study suggest that sugar beet pulp, an inexpensive byproduct of sugar beet processing, could provide an alternative feedstock for second-generation ethanol production. To ensure the effectiveness of simultaneous saccharification and fermentation, enzymatic hydrolysis should be preceded by pressure-thermal pretreatment (121°C, 30 min) of sugar beet pulp suspended in 2% w/w sulphuric acid in a ratio providing 12% dry matter. A 6 h interval for enzymatic activation between the start of digestion with enzyme preparations and inoculation with the yeast strain may improve fermentation performance. Fermentation of progressively released fermentable hexose (glucose, fructose, and galactose) and pentose (xylose) sugars by two yeast strains applied sequentially, Ethanol Red (*S. cerevisiae*) and *Pichia stipitis* NCYC 1541, yielded 6.8 ± 0.3 kg absolute ethanol from 100 kg of wet sugar beet pulp (approx. 23% dry matter). To increase the intake of released monomer sugars, strains of yeast able to ferment rhamnose, arabinose, and galacturonic acid should also be added.

Abbreviations

SSF: Simultaneous saccharification and fermentation
SBP: Sugar beet pulp
vvm: Aeration rate = gas volume flow per unit of liquid volume per minute (volume per volume per minute)
d.m.: Dry matter
GLC: Glucose
GAL: Galactose
FRU: Fructose
XYL: Xylose
ARA: Arabinose
RHA: Rhamnose
GalA: Galacturonic acid
SAC: Saccharose
CEL: Cellobiose
RAF: Raffinose.

Competing Interests

The authors declare that they have no competing interests.

Acknowledgments

This research was financed by a grant from NCBiR (Polish National Centre for Research and Development) implemented within the framework of the Programme of Applied Research, PBS1/B8/3/2012 "Biomass Sugar Beet Pulp as a New Feedstock for the Production of Fermentation Substrates."

References

[1] J.-L. Barjol, H. Chavanes, A. Krick et al., "Environmental report. Beet growing and sugar production in Europe," Monography of CIBE (the International Confederation of European Beet growers) & CEFS (the European Committee of Sugar Manufacturers), 2003, http://www.comitesucre.org/userfiles/environ(5)(3).pdf.

[2] "Sugar Beet. White Sugar," Agribusiness Handbook, http://www.eastagri.org/publications/pub_docs/4_Sugar_web.pdf.

[3] V. Micard, C. M. G. C. Renard, and J.-F. Thibault, "Enzymatic saccharification of sugar-beet pulp," *Enzyme and Microbial Technology*, vol. 19, no. 3, pp. 162–170, 1996.

[4] R. M. McCready, "Polysaccharides of sugar beet pulp. A review of their chemistry," *Journal of Sugarbeet Research*, vol. 14, no. 3, pp. 260–270, 1966.

[5] F. Michel, J. Thibault, J. Barry, and R. de Baynast, "Preparation and characterisation of dietary fibre from sugar beet pulp," *Journal of the Science of Food and Agriculture*, vol. 42, no. 1, pp. 77–85, 1988.

[6] P. Alvira, E. Tomás-Pejó, M. Ballesteros, and M. J. Negro, "Pretreatment technologies for an efficient bioethanol production process based on enzymatic hydrolysis: a review," *Bioresource Technology*, vol. 101, no. 13, pp. 4851–4861, 2010.

[7] A. Pessoa Jr., I. M. Mancilha, and S. Sato, "Cultivation of *Candida tropicalis* in sugar cane hemicellulosic hydrolyzate for microbial protein production," *Journal of Biotechnology*, vol. 51, no. 1, pp. 83–88, 1996.

[8] A. Pessoa Jr., I. M. de Mancilha, and S. Sato, "Evaluation of sugar cane hemicellulose hydrolyzate for cultivation of yeasts and filamentous fungi," *Journal of Industrial Microbiology & Biotechnology*, vol. 18, no. 6, pp. 360–363, 1997.

[9] C. S. Gong, "Recent advances in D-xylose conversion by yeasts," in *Annual Reports of Fermentation Processes*, G. T. Tsao, Ed., pp. 253–291, Academic Press, New York, NY, USA, 1983.

[10] L. R. Lynd, R. T. Elander, and C. E. Wyman, "Likely features and costs of mature biomass ethanol technology," *Applied Biochemistry and Biotechnology*, vol. 57-58, no. 1, pp. 741–761, 1996.

[11] F. W. Bai, W. A. Anderson, and M. Moo-Young, "Ethanol fermentation technologies from sugar and starch feedstocks," *Biotechnology Advances*, vol. 26, no. 1, pp. 89–105, 2008.

[12] C. A. Batt, S. Carvallo, D. D. Easson Jr., M. Akedo, and A. J. Sinskey, "Direct evidence for a xylose metabolic pathway in *Saccharomyces cerevisiae*," *Biotechnology and Bioengineering*, vol. 28, no. 4, pp. 549–553, 1986.

[13] J. D. McMillan, "Xylose fermentation to ethanol: a review," National Renewable Energy Laboratory, http://www.nrel.gov/docs/legosti/old/4944.pdf.

[14] H. Rouhollah, N. Iraj, E. Giti, and A. Sorah, "Mixed sugar fermentation by *Pichia stipitis, Sacharomyces cerevisiaea*, and an isolated xylosefermenting *Kluyveromyces marxianus* and their cocultures," *African Journal of Biotechnology*, vol. 6, no. 9, pp. 1110–1114, 2007.

[15] J. M. Laplace, J. P. Delgenes, R. Moletta, and J. M. Navarro, "Combined alcoholic fermentation of D-xylose and D-glucose by four selected microbial strains: process considerations in relation to ethanol tolerance," *Biotechnology Letters*, vol. 13, no. 6, pp. 445–450, 1991.

[16] J. P. Delgenes, R. Moletta, and J. M. Navarro, "The ethanol tolerance of *Pichia stipitis* Y 7124 grown on a D-xylose, D-glucose and L-arabinose mixture," *Journal of Fermentation Technology*, vol. 66, no. 4, pp. 417–422, 1988.

[17] J. C. du Prezz, B. van Driessel, and B. A. Prior, "The fermentation of D-xylose by *Candida shehatae* and *Pichia stipitis* at low dissolved oxygen level," *Yeast*, vol. 5, pp. 129–139, 1989.

[18] C.-G. Hounsa, E. V. Brandt, J. Thevelein, S. Hohmann, and B. A. Prior, "Role of trehalose in survival of *Saccharomyces cerevisiae* under osmotic stress," *Microbiology*, vol. 144, no. 3, pp. 671–680, 1998.

[19] R. Thatipamala, S. Rohani, and G. A. Hill, "Effects of high product and substrate inhibitions on the kinetics and biomass and product yields during ethanol batch fermentation," *Biotechnology and Bioengineering*, vol. 40, no. 2, pp. 289–297, 1992.

[20] K. Olofsson, M. Bertilsson, and G. Lidén, "A short review on SSF—an interesting process option for ethanol production from lignocellulosic feedstocks," *Biotechnology for Biofuels*, vol. 1, article 7, 2008.

[21] Y. Zheng, C. Yu, Y.-S. Cheng et al., "Integrating sugar beet pulp storage, hydrolysis and fermentation for fuel ethanol production," *Applied Energy*, vol. 93, pp. 168–175, 2012.

[22] *AOAC Official Methods of Analysis of AOAC International*, vol. 2, AOAC International, Maryland, Md, USA, 16th edition, 1995.

[23] G. L. Miller, "Use of dinitrosalicylic acid reagent for determination of reducing sugar," *Analytical Chemistry*, vol. 31, no. 3, pp. 426–428, 1959.

[24] K. Kurschner and A. Hoffer, "A new quantitative cellulose determination," *Chemie in unserer Zeit*, vol. 161, no. 55, p. 1811, 1931.

[25] V. V. Arasimovich and A. I. Ermakov, "Measurement of the total content of hemielluloses," in *Methods for Biochemical Studies of Plants*, A. I. Ermakov, Ed., pp. 164–165, Agropromizdat, Saint Petersburg, Russia, 1987.

[26] D. Templeton and T. Ehrman, "Determination of acid-insoluble lignin in biomass," Chemical Analysis and Testing Task, Laboratory Analytical Procedure LAP-003, National Renewable Energy Laboratory (NREL), Golden, Colo, USA, 1995.

[27] P. Wolak and A. Złocińska, "Examination of the chemical composition of sugar beet pulp-a by-product of sugar industry," *Engineering Sciences and Technologies*, vol. 2, no. 5, pp. 109–119, 2012 (Polish).

[28] S. Kühnel, H. A. Schols, and H. Gruppen, "Aiming for the complete utilization of sugar-beet pulp: examination of the effects of mild acid and hydrothermal pretreatment followed by enzymatic digestion," *Biotechnology for Biofuels*, vol. 4, article 14, 2011.

[29] Y. Lin and S. Tanaka, "Ethanol fermentation from biomass resources: current state and prospects," *Applied Microbiology and Biotechnology*, vol. 69, no. 6, pp. 627–642, 2006.

[30] C. M. G. C. Renard, M.-J. Crépeau, and J.-F. Thibault, "Structure of the repeating units in the rhamnogalacturonic backbone of apple, beet and citrus pectins," *Carbohydrate Research*, vol. 275, no. 1, pp. 155–165, 1995.

[31] T. Rezić, D. Oros, I. Marković, D. Kracher, R. Ludwig, and B. Šantek, "Integrated hydrolyzation and fermentation of sugar beet pulp to bioethanol," *Journal of Microbiology and Biotechnology*, vol. 23, no. 9, pp. 1244–1252, 2013.

[32] H. G. Yücel and Z. Aksu, "Ethanol fermentation characteristics of *Pichia stipitis* yeast from sugar beet pulp hydrolysate: use of new detoxification methods," *Fuel*, vol. 158, pp. 793–799, 2015.

[33] M. Balcerek and K. Pielech-Przybylska, "Effect of simultaneous saccharification and fermentation conditions of native triticale starch on the dynamics and efficiency of process and composition of the distillates obtained," *Journal of Chemical Technology and Biotechnology*, vol. 88, no. 4, pp. 615–622, 2013.

[34] P. Patelski, J. Berlowska, P. Dziugan et al., "Utilisation of sugar beet bagasse for the biosynthesis of yeast SCP," *Journal of Food Engineering*, vol. 167, article 8118, pp. 32–37, 2015.

[35] B. Wiedemann and E. Boles, "Codon-optimized bacterial genes improve L-arabinose fermentation in recombinant Saccharomyces cerevisiae," *Applied and Environmental Microbiology*, vol. 74, no. 7, pp. 2043–2050, 2008.

[36] M. Bettiga, O. Bengtsson, B. Hahn-Hägerdal, and M. F. Gorwa-Grauslund, "Arabinose and xylose fermentation by recombinant *Saccharomyces cerevisiae* expressing a fungal pentose utilization pathway," *Microbial Cell Factories*, vol. 8, article 40, 2009.

[37] M. Taniguchi, T. Tohma, T. Itaya, and M. Fujii, "Ethanol production from a mixture of glucose and xylose by co-culture of *Pichia stipitis* and a respiratory-deficient mutant of *Saccharomyces cerevisiae*," *Journal of Fermentation and Bioengineering*, vol. 83-84, no. 4, pp. 364–370, 1997.

[38] B. Gutiérrez-Rivera, K. Waliszewski-Kubiak, O. Carvajal-Zarrabal, and M. G. Aguilar-Uscanga, "Conversion efficiency of glucose/xylose mixtures for ethanol production using *Saccharomyces cerevisiae* ITV01 and *Pichia stipitis* NRRL Y-7124," *Journal of Chemical Technology and Biotechnology*, vol. 87, no. 2, pp. 263–270, 2012.

Hindawi Publishing Corporation
BioMed Research International
Volume 2016, Article ID 6197867, 11 pages
http://dx.doi.org/10.1155/2016/6197867

Review Article

Copyrolysis of Biomass and Coal: A Review of Effects of Copyrolysis Parameters, Product Properties, and Synergistic Mechanisms

Cui Quan and Ningbo Gao

Department of Environmental Science and Engineering, School of Energy and Power Engineering, Xi'an Jiaotong University, Xi'an, Shaanxi 710049, China

Correspondence should be addressed to Ningbo Gao; nbogao@xjtu.edu.cn

Received 6 May 2016; Revised 19 July 2016; Accepted 3 August 2016

Academic Editor: Xiaoling Miao

Concerns in the last few decades regarding the environmental and socioeconomic impacts of the dependence on fossil fuels have resulted in calls for more renewable and alternative energy sources. This has led to recent interest in copyrolysis of biomass and coal. Numerous reviews have been found related to individual pyrolysis of coal and biomass. This review deals mainly with the copyrolysis of coal and biomass and then compares their results with those obtained using coal and biomass pyrolysis in detail. It is controversial whether there are synergistic or additive behaviours when coal and biomass are blended during copyrolysis. In this review, the effects of reaction parameters such as feedstock types, blending ratio, heating rate, temperature, and reactor types on the occurrence of synergy are discussed. Also, the main properties of the copyrolytic products are pointed out. Some possible synergistic mechanisms are also suggested. Additionally, several outlooks based on studies in the literature are also presented in this paper.

1. Introduction

Coal is the most abundant fossil fuel energy source available to the world economy and its reserve was expected to last for up to 200 years compared to about 65 years and 40 years for natural gas and crude oil, respectively. The pyrolysis of coal is a good method for producing liquid fuels and other chemicals; however, the yields of these products are limited due to low content of hydrogen in coal. Hydropyrolysis, a pyrolysis process under hydrogen, is an effective method to improve tar yield and quality, but high cost of pure hydrogen hinders its industrial application. Accordingly, it is necessary to supply H_2 for coal from other hydrogen-rich materials, such as plastic wastes, polymers, petroleum residues, and coke-oven gas.

Compared with plastic wastes and so forth biomass is a perspective source to replace fossil fuels in the future, as it is abundant, renewable, clean, and carbon dioxide neutral. Both biomass and coal are carriers of accumulated solar energy. The formation profile, however, changes the nature and availability of the two fuels. The difference in composition from biomass to coal is illustrated using a Van Krevelen diagram in terms of hydrogen/carbon (H/C) and oxygen/carbon (O/H) ratios as described in Figure 1 [1]. It could be clearly observed that, in comparison to coal, biomass has a higher value of H/C ratio (1.26–1.58) and O/C ratio (0.4–0.8). Higher hydrogen contents in biomass indicated that biomass could act as hydrogen donors in copyrolysis with coal. In addition, pyrolysis is inherently meant to be completed in an inert atmosphere, while the presence of higher oxygen content in biomass actually provides a significant increase in reactivity of the pyrolysis environment, facilitating the conversion of coal. Thus, some synergy effect may be expected when coprocessing biomass with coal.

Recently, many researchers used different fuels (such as sawdust, legume straw, lignite, and bituminous coal) and different reactors (such as TGA, fluidized bed reactor, fixed-bed reactor, and free fall reactor) under various operating parameters (such as temperature, heating rate, blending ratio, particle size, and contacting way of particles) to study the copyrolysis behaviors focusing on product distribution and product characteristics, as well as the possible existing

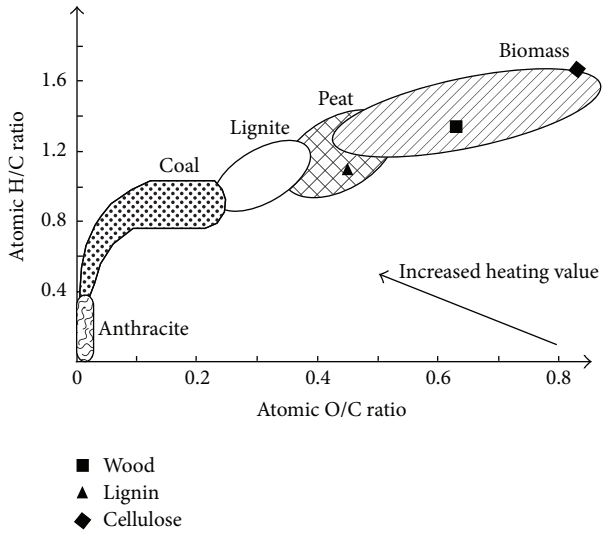

Figure 1: Van Krevelen's diagram showing the various H/C ratios and O/C ratios for different feedstocks [1].

synergetic effects. In general, to evaluate the interaction between biomass and coal blend, the experimental values were compared with the theoretical values which are sum of the values of individual samples in proportion to their blending values. The percentage of increasing or decreasing of the experimental values with respect to the theoretical values is called synergetic effects. The lack of synergy between the two fuels during copyrolysis is indicated by the linear relationship between the volatile matter release/product yield and the percentage of biomass added to the mixture. Given such a wide range of variables involved, the results obtained by different groups are sometimes conflicting. That is to say, synergistic or additive behaviors were reported to occur for copyrolysis processes of biomass/coal blends. In a study by Vuthaluru [2], the pyrolysis of biomass and coal blends by thermogravimetric analysis (TG) in different biomass/coal ratios showed no synergy effect, and there is a linear relationship between the char yield and the amount of biomass in the blend. Pan et al. [3] and Kastanaki et al. [4] also confirmed that no interaction took place between biomass and coal in a blend during pyrolysis. More recent efforts by Aboyade et al. [5], Chen et al. [6], Shui et al. [7], Park et al. [8], Ulloa et al. [9], and Haykiri-Acma and Yaman[10] have challenged this view, and they show that there are significant interactions between the coal and biomass fractions during pyrolysis in TG. Onay et al. [11], Sonobe et al. [12], Zhang et al. [13], Wei et al. [14, 15], Yuan et al. [16], and Li et al. [17] also verified the occurrence of synergy effect on the yields of the major pyrolytic products, gaseous component, tar components, and the reactivities of the chars. Interestingly, Park et al. [8] observed that synergy occurs on both TG and fixed-bed reactor, while Sonobe et al. [12], who conducted the copyrolysis of Thai lignite and corncob, verified the presence of synergy effect on a fixed-bed reactor rather than a TG apparatus. In addition, researchers who study the distribution of major products such as char, liquid, and gas tend to find no evidence of synergy effect [18], while those who study the composition of the volatiles tend to conclude the opposite [12, 19]. The occurrence of synergy during copyrolysis is generally not conclusive, and it depends on the pyrolysis technique and fuels used. These conflicting conclusions are intriguing and need to be clarified. Numerous reviews have been found related to individual studies on coal pyrolysis and biomass pyrolysis [20–22]. To our knowledge, little reviews are available on copyrolysis of coal/biomass blends [23, 24].

In this paper, a comprehensive overview on copyrolysis of coal and biomass was presented. The interest is to focus on the synergistic effects or the additive effect between coal and biomass in their copyrolysis. The effects of reaction parameters such as feedstock types, blending ratio, heating rate, temperature, and reactor types on the occurrence of synergy and on the distribution and properties of copyrolytic products are pointed out. Moreover, some possible synergistic mechanisms during copyrolysis of coal/biomass blends were also presented.

2. Copyrolysis Reaction Parameters

Copyrolysis of biomass and coal blend generally goes through a series of extremely complex reactions. Many pyrolysis process parameters such as feedstock types, blending ratio, heating rate, temperature, and reactor types may strongly affect the yield and properties of the products.

2.1. Effect of Feedstock Types. The types of blending fuels ought to be a major factor that can intrigue the synergy. It has been shown that many blends of biomass species and coal, such as hazelnut shell and coal [25], legume straw and coal [13], sawdust and coal [26], microalgae and coal [6], corncob and coal [12], and corn stalk and subbituminous coal [27], exhibit synergetic effects during copyrolysis process.

Biomass is mainly composed of several chemical constituents: cellulose, hemicellulose, lignin, some extractives, and minerals [28]. Cellulose, hemicellulose, and lignin could create synergistic effects on thermal behavior of the coal [29]. It is believed that H and OH radicals released from biomass during pyrolysis can promote cracking of the aromatic rings of coal [12, 30, 31]. Some researchers also stated that catalytic effects of the minerals in biomass promoted synergy effects between biomass and coal [32]. Yuan et al. [33] conclude that hemicellulose provides strongest promotion effect on the coal conversion during copyrolysis. The holocellulose (cellulose and hemicellulose) components of biomass are mainly responsible for the volatiles of the pyrolysis, which can further produce hydrogen by secondary reactions. Thus, the synergy effect in the presence of legume straw with higher holocellulose and ash content is more significant than that in the presence of pine sawdust with copyrolysis of biomass and coal in a free fall reactor [14]. Lignin in biomass may cause some polymerizing reactions in the low-temperature range, resulting in the formation of resonance stabilized phenoxy radical and other reactive radicals [34–36]. Such radicals are effective and active intermediates to depolymerize coal by cleaving methylene bridges. Nevertheless, the lignin-derived intermediates are short-lived as compared to the time needed for complete coal depolymerization.

Coal is mainly formed as the results of slow metamorphosis of biomass over a long period of time. The degree of that metamorphosis is among the criteria used to determine coal rank. Many researchers [10, 25, 33, 37, 38] found that, during copyrolysis, low rank coals could easily create synergies with biomass and interactions between biomass and low rank coal are more pronounced than those between biomass and high rank coal. They considered that the higher structure similarity between biomass and low-rank coal than that between biomass and high rank coal was the reason. Additionally, as the coal rank decreases, the major pyrolytic decomposition regions of coal shifted to lower temperatures. Biomass reacted in a temperature region close to low-rank coal and this could allow interactions to occur between the components [39]. Simultaneously, hydrogen acceptor ability of low-rank coal was stronger than high-rank coal [40]. During pyrolysis process, the lamellae of the coal cross-linked network is disturbed, causing much fragmentation of coal into hydrogen deficient active sites. Biomass has a higher H/C ratio than coal; the availability of hydrogen around the coal particles would be increased during copyrolysis. There exists hydrogen transfer reaction from biomass to coal. Usually the synergistic positive effect is observed preferentially with low rank coals also due to their stronger ability of capturing hydrogen.

2.2. The Influence of Blending Ratio. The proportion of biomass in the blend had a significant influence on product distribution of solid, liquid, and gas [19]. With the increase of biomass blending ratio, the char yield decreases, while the yields of liquid and gas increase [27, 41]. Copyrolysis experiments performed on TG revealed that percent residual mass decreased with increasing biomass content in blends [2, 6, 11, 12, 42, 43]. Typical TG curves for biomass, coal, and their mixtures are presented in Figure 2 [11]. The immobile phase of the coal structure mostly comprises highly cross-linked aromatics, held together by significantly stronger C=C bonds with bond energy of 1000 kJ/mol [19]. These bonds are more difficult to rupture under the heat than the macromolecular structure of cellulose, hemicelluloses, and lignin in biomass, which are linked together by relatively weak ether bonds (R–O–R) with bond energy of about 380–420 kJ/mol. Thus, biomass decomposes much faster than coal. Additionally, biomass undergoes higher weight loss than coal as indicated in Figure 2, and the curve for each biomass/coal blend lies between the curves of the single component.

High thermochemical reactivity and the high volatile content of biomass facilitate the conversion of coal [9, 12]. The degree of synergistic effects was dependent on many factors, that is, coal type, blending ratio, and reactor type [43]. Generally, synergy effect is more pronounced under the higher biomass blending ratio, due to the fact that the presence of sufficient amount of biomass could offer plenty of hydrogen donors to coal [8, 11, 13, 42]. However, degree of synergy effect was not linearly dependent on the amount of biomass in the blends [8, 14, 45]. Since packing density and thermal conductivity of biomass are lower than those of coal, the increase in proportions of biomass would decrease the heating rate of the blends and result in longer releasing time

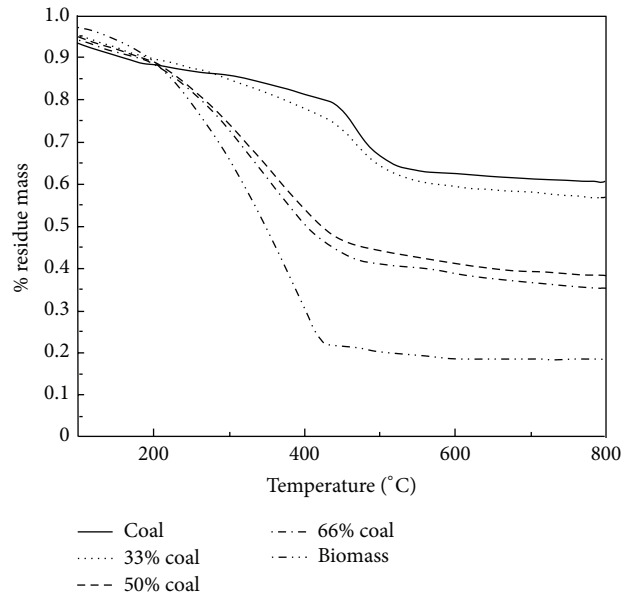

Figure 2: Percent residual mass versus the temperature for raw materials and coal/biomass blends [11].

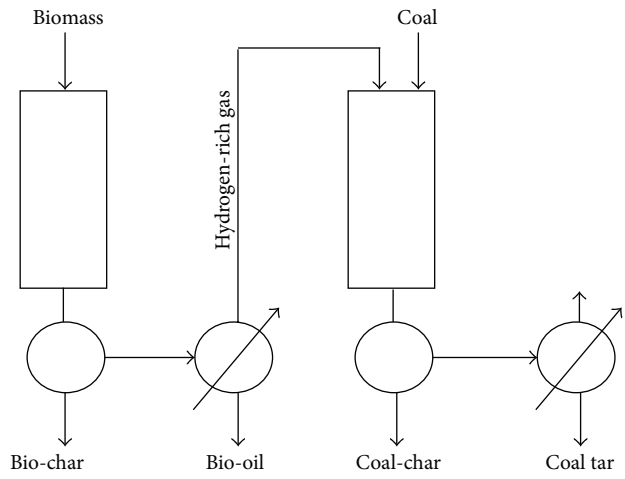

Figure 3: Flow-chart of two-stage copyrolysis process [44].

of the volatiles from both biomass and coal [8]. Therefore, OH and H radicals are released more slowly from biomass to enhance the cracking of coal tar [12, 46], and more tar is converted to gaseous products [7]. In addition, biomass char residues formed during copyrolysis are easy to accumulate on the molecules' surface of coal which block the pores of coal molecule through which the volatile matters generated by coal pyrolyzing are driven out. That is to say, the interaction between the solid phases sometimes presents an inhibitive effect on thermal decomposition [6, 11, 47, 48]. In order to avoid accumulating of biomass char on coal surface, Li and Xu [44] proposed two-stage copyrolysis process as illustrated in Figure 3. Fast pyrolysis of biomass and coal was conducted in an individual reactor which was separated from each other in series space, thus making it easy to achieve the best process control of each reactor. The hydrogen-rich gas produced from

biomass pyrolysis was then used as a hydrogen source for the coal hydropyrolysis.

2.3. The Influence of Heating Rate. The temperature ranges for pyrolysis of biomass and coal differ considerably and it is known that these processes can be distinguished if the heating rate was sufficiently low so only additive behavior can be observed [49]. In view of the different temperature ranges required for the devolatilisation of coal and biomass, the utility of slow heating experiments in looking for synergetic effects appears limited. If the heating rate is increased, the intrinsic devolatilization becomes slower compared with the sample heat up. It could be expected that the pyrolysis processes of biomass and coal could happen simultaneously under very fast heating rate, and, therefore, volatile release from biomass and coal overlapped [13]. Coal pyrolysis yields and products could be different in the case of high heating rates since the reaction atmosphere also involves noninert species [50]. That is to say, copyrolysis of biomass/coal blends at high heating rate favoured the synergism [13, 16, 33, 51]. Suelves et al. [38, 52] report synergy when using pyrolysis-GC (pyroprobe). In this technique, the fuels are blended and contained in a small thin-walled silica tube and a moderate high rate is applied (typical nominal rates of 10^3 K/s). Yuan et al. [33, 51, 53] conducted rapid pyrolysis of biomass/coal blends on a drop style high-frequency magnetic field based furnace with heating rate higher than 10^3 K/s. Synergy effect can be found to promote nitrogen release from fuel samples and decrease char-N yields. Zhang et al. [13, 41, 54], who conducted fast pyrolysis experiments in a free fall reactor, also observed appearance of synergy during the copyrolysis of biomass and coal. However, Meesri and Moghtaderi[49] confirmed the lack of synergistic effects on pyrolytic products yields as well as gas composition from pyrolysis of coal/sawdust blends under high heating rate ($10^{4\circ}$C/s) in a drop-tube reactor, with short residence time and limited particle-particle contact.

When copyrolyzing biomass with coal, coal and biomass are heated together in an inert atmosphere, creating a joint volatile stream and solid char as products. Therefore, the synergistic effect observed during copyrolysis might be due to volatile-volatile interaction and volatile-char interaction [55, 56]. A higher heating rate led to the formation of higher yields of volatile [49, 57, 58]. These increase the probability of gas phase reactions between the volatiles coming from coal and biomass, enhancing the intensity of the synergism. Many authors had confirmed that there was significant synergy in the vapor phase during copyrolysis of coal and biomass [12, 19, 27, 59]. Simultaneously, the volatilization amount of alkali and alkaline earth metallic (AAEM) species at fast heating rates is higher than those at slow heating rate. Such volatilized species may contribute catalytic activity to coal pyrolysis as well as gas phase reactions, resulting in significant synergy or chemical interactions in the vapor phase [9, 12, 60].

2.4. The Influence of Temperature. It is known from the literature survey and previous studies that pyrolysis temperature plays an important role on product distribution of coal/biomass blend [8, 11–13, 16]. Pyrolysis of coal yields mainly solid with moderate production of liquid and gas, as opposite to biomass pyrolysis in which liquid and solid equally dominated the products. The experimental yields of solid, liquid, and gas for coal/biomass blend lay between those of coal and biomass; however, appearance of synergy makes them deviate from the calculated yields [12].

With increasing temperature, char yield decreased but volatile matter yield increased [8, 11]. In other words, pyrolysis conversion increased as the temperature increased. Many researchers conclude that biomass may promote devolatilization of the coal at lower temperatures [61]; however, manifestations of the synergies between biomass and coal varied with temperature. Aboyade et al. [5] reported that the interactions occurred between 300 and 500°C, corresponding to the end of biomass devolatilization and the start of coal decomposition. Ulloa et al. [9] considered that interactions detected in the blends were produced at pyrolysis temperatures over 400°C, when most of the components in the blend are devolatilized, and are attributed to secondary reactions that inhibit the formation of char. Park et al. [8] observed that from copyrolysis of sawdust and coal blend in TG the synergy effect to produce more volatiles from coal pyrolysis is pronounced above 400°C. In a fixed bed at isothermal condition, the synergy effects to produce more volatiles appear at 500–700°C, and the maximum synergy exhibits at sawdust blending ratio of 0.6 at 600°C. In a study of Zhang et al. [13], they concluded that the optimum condition for synergy effect in copyrolysis of lignite and legume straw blend in a free fall reactor is 600°C at which enough free radical and hydrogen donors are generated. From the above, it is deduced that 400–600°C may be the optimal temperature range for the synergy occurrence. With further increasing temperature, the synergy effect decreases because of the increased pyrolysis rate and lack of hydrogen donating ability, resulting in the increased retrogressive condensation reactions. Some researchers [8, 12] reported that the increase in temperature to 800°C makes the difference between the experimental yield and the calculated yield decrease or even converge.

2.5. The Influence of Reactor Types. Many types of reactors including TG, fixed-bed reactor, fluidized-bed reactor, drop style high-frequency magnetic field based furnace, and free fall reactor have been involved to investigate copyrolysis behavior of biomass and coal. TG is most commonly used. Early reports have concluded that no interactions between the biomass and coal exist during copyrolysis [2–4, 12, 31, 50, 64–66]. Lacks of synergies are mainly due to the low heating rate used in the TG runs (which allowed the different devolatilization phases of both components in the blend to be easily separated) and to the relatively high nitrogen flow rate in the apparatus (which prevented volatile species to remain close to the devolatilizing particles in the crucible, ensuring an inert atmosphere on the sample during the run) [50]. More recent efforts by Aboyade et al. [5], Chen et al. [6], Shui et al. [7], Park et al. [8], Ulloa et al. [9], Yangali et al. [61], and Haykiri-Acma and Yaman [10] have challenged this view, showing that there are indeed significant interactions between coal and biomass fractions during copyrolysis in TG.

Table 1: Co-pyrolysis studies of coal/biomass blends performed on TG.

1st author	HR (°C/min)	Temp. (°C)	Fuels[a,b]	Coal to biomass blend ratio (w/w)	Publishing year
			Synergistic behaviors		
Haykiri-Acma [10]	20	900	li-hs	98-96-94-90-80	2007
Chen [6]	10-20-40	1000	semi-cv	30-50-70	2012
Park [8]	15	900	sub-sd	60	2010
Shui [7]	10	800	sub-sd	50	2011
Aboyade [5]	5-10-50	900	hc-bg-cc	90-80-70-60-50	2012
Song [62]	10	1000	sd-li	20-50-80	2014
Ulloa [9]	10-30-50	1200	sub-bit-sd	50	2009
Li [42]	10-15-20-25-30	900	bit-sd	20-40-60-80	2015
Wu [63]	10-20-40	950	ce-bit	25-50-75	2016
			Additive behaviors		
Vuthaluru [2]	20	1250	sub-ww-ws	10-20-30-50	2003
Jones [31]	25	900	bit-hvb-li-pw	25-50-75	2005
Sonobe [12]	10	600	li-cc	90-50-10	2008
Kastanaki [4]	10	850	li-oc-fr-cr	95-90-80	2002
Biagini [50]	20	900	hv-lv-sd-ss	15 to 60	2002
Pan [3]	100	900	bl-lq-pc	80-60-40-20	1996
Vamvuka [64]	10	850	li-oc-fr-cr	95-90-80	2003
Sadhukhan [65]	40	1000	li-ww	50-40-10	2008
Idris [66]	10-20-40-60	900	sub-op	80-60-50-40-20	2010

[a]Coals: sub, subbituminous; li, lignite; hvb, high-volatile bituminous; bit, bituminous; semi: semianthracite; bl, black; lq, low-quality; hv, high-volatile; lv, low-volatile; hc, hard coal.
[b]Biomass: ww, wood waste; ws, wheat straw; hs, hazelnut shell; pi, pinewood; cc, corncob; cv: chlorella vulgaris; sd: sawdust; oc, olive cake; fr, forest residue; cr, cotton residue; pc, pine chips; op, oil palm; ss, sewage sludge; ce, cellulose.

An overview of the existing literature performed on TG is summarized in Table 1.

Fixed-bed reactors using a relatively large amount of sample would provide intimate contact between neighbouring fuel particles and their volatiles, resulting in the occurrence of the synergy effect for both pyrolysis product yield and gas product compositions [8, 11, 12, 32, 62, 67]. However, intimate contact between biomass and coal particles during copyrolysis does not necessarily mean the occurrence of synergy during copyrolysis [68, 69]. Compared with atmospheric fixed-bed reactor, pressurized pyrolysis and vacuum pyrolysis of coal and biomass also verified the existence of significant synergistic behavior [19, 59]. However, tube furnaces used for pyrolysis usually have long high-temperature zones; volatiles must go through the long high-temperature zone before escaping from the reactors. The extended residence time of intraparticle volatiles allows for increased extraparticle secondary reactions (tar cracking, char-forming) [70]. Therefore, it is difficult to distinguish that the synergies in these reactors are mainly caused by primary pyrolysis process or the second reaction of volatiles [31].

Recently, many varieties of fast pyrolysis reactors have been developed and used to carry out copyrolysis experiment of coal/biomass mixture. These included fluidized beds, drop style high-frequency magnetic field based furnace, and free fall reactor. Some researchers considered that fluidized-bed reactors are not suitable to investigate interactions since near total segregation of sample particles in this apparatus could result in lack of synergies between biomass and coal particles [32]. Yuan et al. [16, 33, 51, 53] conducted rapid pyrolysis of biomass/coal blends on a drop style high-frequency magnetic field based furnace at 600–1200°C, and the nitrogen conversion characteristics of biomass/coal blends were investigated. Synergies can be found to promote nitrogen release from fuel samples and decrease char-N yields under all conditions. Xu et al. [13, 14, 41] had performed copyrolysis of coal and biomass in a free-fall reactor, and they concluded that both the higher blending ratio (around 70 wt.%) and the relatively lower temperature (around 600°C) are more favourable to synergy effects during the copyrolysis of biomass and coal in the free fall reactor. Nowadays, some specially designed reactors, that is, a single-particle reactor system [69], a microfluidized bed reactor [71], and congruent-mass TGA [72, 73], were also applied to study the copyrolysis behaviour of coal/biomass blends.

3. Characteristics of Biomass and Coal Copyrolysis Products

The products from copyrolysis of coal and biomass included liquid, char, and gas. The influence of synergy effects on the yield and composition of pyrolysis products would be presented in the following discussion.

3.1. Liquid

3.1.1. Liquid Yield. The relatively high content of H_2 in biomass may play a synergistic role as H_2 donor during

copyrolysis with coal, resulting in more liquid product than that from additive model [11, 13, 14, 56]. Wei et al. [14] reported that the liquid yield was in the range of 25.1–40.9% during copyrolysis of biomass and coal in a free fall reactor from 500 to 700°C, with incremental deviations ranging from 0.9 to 8.0% in the amount of liquid. Onay et al. [11] found that the maximum pyrolysis oil yield reached 39.5% with 5% of lignite mixed with safflower seed during the copyrolysis in a fixed-bed reactor at 550°C; the pyrolysis oil yield increased by about 17% compared to the expected ones. However, in a study by Park et al. [8], even though synergy effect can be found to promote the release of volatiles under all conditions, tar yields are lower than the calculated ones. The lower-than-expected tar yield may be due to the interactions between biomass and coal that promote an additional decomposition of tar to enhance gas yield. As a result, the ratio of tar to the total volatiles decreases.

3.1.2. Liquid Property. Copyrolysis could enhance the transfer of coal hydrogen to valuable petrochemical produced that otherwise would be transferred to molecular hydrogen if coal was pyrolyzed alone [74]. Jones et al. [31] concluded that the pyrolysis oils from biomass/coal blends became poor in aromatics and rich in phenols. Onay et al. [11] reported that the copyrolysis oils contained a greater concentration of single-ring aromatic compounds and aliphatic group rings than biomass pyrolysis oil. Wei et al. [15] also found that the yield of light molecular weight phenols, methylphenol, dimethylphenol, and their derivatives increased at about 5 wt% during the copyrolysis. Song et al. [62] also reported that copyrolysis promoted the yields of phenols and guaiacols in tar. Due to the higher O/C ratio of biomass, the pyrolysis of biomass should produce more oxygenated free radicals. The reactive oxygenated free radicals from biomass react with the unsaturated aromatics from coal and prevent them from recombining to form long chain hydrocarbons [19]. However, high O content of biomass may result in a waste of H, yielding more water. How to transfer H efficiently into oil is a challenge. In order to realize the directional transformation of H and O during copyrolysis of biomass and coal, Zhang et al. [54] constructed a specially designed free fall reactor, where a controlled recontact of volatile with char from primary pyrolysis could be achieved, causing volatile-char interaction, and their results revealed that the recontact of the volatiles-char effectively enhanced tar generation and suppressed water formation during copyrolysis.

3.2. Gas

3.2.1. Gas Yield. Sonobe et al. [12] reported that the gas yields are higher than expected from the calculated value based on individual material during copyrolysis of 50 : 50 lignite/corncob blend in a fixed bed reactor, and the gas yield discrepancies took place in the temperature zones of 350–500°C. In the experiments of Yuan et al. [16], who carried out rapid copyrolysis of rice straw and bituminous coal in a high-frequency furnace, they found that gas yield increased with the increasing temperatures. Experimental gas yields were slightly lower than the calculated values in the low temperature range. As the temperature increased, experimental gas yields became higher than the calculated values. They considered that synergy effect promoted gas yields mainly within the high-temperature range. Park et al. [8] found that the gas yield from sawdust and coal pyrolysis at a blending ratio of 0.6 in a fixed bed reactor monotonically increased from 21.2% to 35.7% as the temperature increased from 400 to 800°C, the gas yields are higher than expected by the calculation, and the maximum difference of gas yields between the experimental and calculated ones could reach 6.0% at 400°C. Interactions between biomass and coal promote an additional decomposition of tar to enhance gas yield.

3.2.2. Gas Composition. The abundant gaseous compounds produced from both coal and biomass pyrolysis were mainly CO_2, CO, CH_4, and H_2 [12, 13]. The experimental results showed that the compositions of the gaseous products from blended samples are not all in accordance with those of their parent fuels. Sonobe et al. [12] reported that the experimental yields of CO and CO_2 of the lignite/corncob blend were more or less identical to the calculated yields at all temperatures. However, Wei et al. [14] found that the experimental yields of CO and CO_2 are lower than the calculated values. They inferred that, in the copyrolysis, the carbon elements in feedstock have the tendency to move toward tar or char instead of gas. Yuan et al. [16] reported that the experimental CO yields are very close to the calculated values at low temperature. As the temperature increased, experimental yields of CO were higher than the calculated values. Experimental yields of CO_2 were almost the same as the calculated values. Significant synergy effect in product gas composition was highly pronouncing for CH_4 formation [12, 14], that is, twice or even three times higher than the calculated values. Sonobe et al. [12] considered that water, one of the major components in biomass volatiles, can be expected to act as a reactive agent to promote the secondary tar cracking producing more CH_4. It is also suggested that the water could react with the CO to produce active hydrogen, that is, water gas shift reaction (WGSR):

$$CO + H_2O = CO_2 + H_2. \quad (1)$$

The new-formed hydrogen produced by WGSR has a higher hydrogenation activity and thus improves the copyrolysis performance [75]. The positive influence of water on copyrolysis of coal and biomass is very useful for practical industrial utilization. It allows the use of the coal and biomass contained large amount of moisture with partial dryness or even without further predrying.

3.3. Char

3.3.1. Char Yield. From copyrolysis of biomass and coal, char yields are lower than that from the additive model due to the synergy effect on the additional degradation of the blends by H_2 supply from biomass pyrolysis with the catalytic effect of inorganic species in biomass ash [8]. There are several factors affecting the extent of the decrease in the char yield. The heat release by secondary reactions is reported to promote

the volatilization of primary tars which in turn reduces the char yield [76]. However, some researchers considered that interaction between solid phases presents an inhibitive effect on thermal decomposition during copyrolysis, leading to higher than expected char yield [6, 48]. There are several investigations in which char yields from copyrolysis were found different than expected. Park et al. [8] reported that the maximum difference of char yields between the experimental and calculated ones could reach 8.3% during copyrolysis of sawdust and coal in a fixed bed reactor. Sonobe et al. [12] reported that the solid yield of the lignite/corncob blend was much lower (i.e., 9%) than expected from the calculated value based on individual materials under the range of temperatures studied. In an experiment carried out by Fei et al. [67], the char yield determined experimentally was 1.08–2.88% higher than the calculated values.

3.3.2. Char Property. The pyrolysis conditions determine the chemical composition of the solid products. The volatile-char interaction occurring during copyrolysis has the potential to affect the amount of AAEM in char, the development of char structure, and therefore char reactivity [56]. The biomass blending ratio also significantly affected the copyrolysis char structure evolution, and the addition of biomass could also promote the uniformity degree of the copyrolysis char [43, 63]. AAEM species retained in char during copyrolysis are important catalysts for the gasification/combustion of char. Generally, the in situ pyrolyzed char from the coal/biomass blend exhibited a higher reactivity than that from the coal or the biomass [43, 77, 78]. Zhang et al. [13] found that the CO_2 reactivity of the chars obtained from the copyrolysis under the higher blending ratio (around 70 wt.%) conditions is about twice as high as those of coal char alone, even higher than those of biomass alone. Nevertheless, Yuan et al. [16] considered that a low biomass/coal mass ratio increases the gasification reactivity of the residual char. The char obtained from copyrolysis can be used in the preparation of active carbon if its pore structure and surface area are appropriate. Additionally, char from copyrolysis of coal and biomass could be used to produce a smokeless solid fuel. Blesa et al. [30] prepared smokeless fuel briquettes from copyrolysis of a low-rank coal and biomass at 600°C with the aim to reduce both the volatile matter and the sulphur content and to increase the high calorific value. Cordero et al. [79] found that the chars resulting from copyrolysis of coal and lignocellulosic wastes show heating values within the range of high-quality solid fuels whereas the ash contents remain in the vicinity of that of the starting coal, which can be used as smokeless.

4. Environmental Benefits

Coprocessing of coal and biomass for energy and chemical production will not just reduce fossil-derived CO_2 emissions, but also limit the discharge of local air pollutants such as SO_x and NO_x. Blesa et al. [30] studied low-temperature copyrolysis of a low-rank coal and biomass and reported a synergetic effect on the desulphurization of coal. Similarly, Cordero et al. [79] reported that the presence of biomass improved the removal of sulfur from the coal structure when a high sulfur coal was subjected to copyrolysis using waste biomass materials. They explained this mechanism by the hydrogen donor property of biomass, which makes sulfur release from coal easier in the form of H_2S during copyrolysis. However, some other researchers [10, 46] claimed that additional presence of calcium coming from biomass during copyrolysis should have increased the sulfur fixing potential of char in the form of CaS and $CaSO_4$ rather than releasing it and thus leading to a lower sulphur release. The higher the amount of calcium, the higher the amount of sulphur in the cocarbonised material. As for N-containing compounds, Yuan et al. [33] found that, during copyrolysis of biomass and coal, synergies can be found to promote nitrogen release from fuel samples, decreased char-N yields, and increased volatile-N yields.

5. Possible Synergistic Mechanisms

Synergistic effects on the copyrolysis can be complicatedly varied depending on the type of blending stock and the pyrolysis condition. Jones et al. [31] outlined some parameters for the synergy. The contact time of fuel particles was well proved to be important for the occurrence of synergy. Some studies also reported the synergistic mechanisms which presumably involved the free radical reactions when lignite and biomass were copyrolyzed. However, knowledge of the synergistic effect remains inadequate. The actual mechanism by which interactions between coal and biomass cause synergy effect during copyrolysis is still not very clear.

5.1. Hydrogen Transfer Reaction. One of the main differences in characteristics of biomass as compared to coal is that biomass possesses a higher value of H/C ratio. Under the same pyrolysis condition, the H_2 yield generated from biomass is about 5–16 times as high as that generated from coal [13]. The pyrolysis of coal may be influenced by the presence of hydrogen-rich light molecules (CO, CO_2, H_2, CH_4, H_2O, etc.) which are rapidly evolved from biomass at high temperature. These pyrolysis gases may take part in volatile-coal interactions and modify the thermal behavior of coal, especially in the temperature range between 400 and 500°C, where the coal exists in a plastic state.

The transferable hydrogen contained in the coal itself plays an important role for coal plasticity. Actual active methylene carbons such as the naphthenic carbons and ethylene carbons between aromatic moieties might act as hydrogen donor sites. Amount of transferable hydrogen in coal itself was dramatically decreased in the temperature range of 350–500°C [80].

Nevertheless, with copyrolysis of coal with biomass, in the temperature range of 300–600°C, the gas formation rate of H_2 from biomass pyrolysis was maintained at a constant value [12], thus increasing availability of hydrogen around the coal particles. There are external hydrogen donors to interfere with the chain radical processes between the coal and biomass radicals; chemical interactions therefore occurred. In order to evaluate the degree of hydrogen transfer reaction, two parameters, hydrogen donor ability (HDA) and hydrogen

acceptor ability (HAA), of biomass from coal should be evaluated.

5.2. Catalytic Effects of AAEM. The presence of AAEM species (mainly K, Na, Ca, and Mg) is in greater abundance in biomass relative to coal. During pyrolysis, volatilization of AAEM species will occur [81]. Such volatilized species may contribute catalytic activity to coal pyrolysis as well as gas phase reactions [9, 12, 60]. To determine the effect of sawdust ash on coal pyrolysis, copyrolysis experiment of sawdust ash/(sawdust ash + coal) blend ratio of 0.2 was carried out on TG by Park et al. [8]. They observed a noticeable DTG peak at around 700°C, which is not observed from the individual thermal decomposition of coal and sawdust. At this temperature, most of volatile matters are removed and residue was mainly composed of coal char and sawdust ash. Therefore, weight loss at this temperature would be the additional decomposition of char by the catalytic effect of inorganic species from sawdust ash. AAEM species present in the biomass, mostly Ca and K, promote demethoxylation reactions. Under normal conditions, these compounds, particularly the methoxyphenols, are precursors to the formation of the aromatic structures of biomass char. However in the presence of aliphatics found in evolved coal volatiles, the methoxyphenols are thought to undergo secondary reactions that produce volatiles instead [5, 9, 45]. At the same time, there have also been suggestions that demineralisation of coal through acid treatment influences the degree of synergy observed [52]. The result may be due to removal of the mineral matter as well as the changes in porosity of coal by the acid treatment. Fei et al. [67] reported that the blends of two original coals synergistically showed a decrease in the tar yield and an increase in the char yield, whereas for the blends using one or two acid-washed coals, the synergy gave rise to increases in both the tar yield and the char yield.

5.3. Heat Transfer. Some researchers confirmed that the synergy effect is also caused by heat transfer during the copyrolysis. Thermal decomposition process of lignite was highly endothermic, especially for the reactions occurring between 250 and 475°C during which extensive thermal decomposition of macromolecular chains took place. Thermal decomposition of corncob, on the other hand, was an exothermic process. It is noticed that corncob strongly dominated the behaviour of the blend, observing that the heat profile of the blend followed closely that of corncob especially at temperatures around 250–450°C, suggesting the occurrence of the synergistic activities at around that temperature range [12]. The exothermic heat from corncob pyrolysis could promote the low-temperature thermal decomposition of lignite to form more liquid product.

6. Conclusions and Outlook

While facing fossil fuels shortage and severe environmental pollution, biomass, as a clean, storable, and transmittable renewable energy resource, has caught the attention of the world. It is desirable to have coutilization of biomass and coal as a step towards sustainable energy supply system and minimize the impact on the environment by the use of coal. The copyrolysis process and the possible synergy are significantly affected by feedstock type, blending ratio, heating rate, temperature, and reactor types. The synergetic effect could be explained by the transferring of active H radicals from biomass to coal, the catalytic role of AAEM from the biomass, and the heat transfer during copyrolysis. Although the conclusions whether there are synergistic or additive behaviours during copyrolysis are sometimes conflicting, there are some certain laws: higher biomass reactivity and higher structure similarity between biomass and coal could enhance the synergy effect. In addition, under the condition of fast heating rate, the synergistic effects are obvious. Copyrolysis of biomass and coal offers simplicity and effectiveness to produce high-grade pyrolysis oil and higher reactivity char. However, in most published literature, the degree of synergy is judged according to the changes on product yield and product composition. Element migration is the essence of synergy effects during copyrolysis. Therefore, much attention should be paid on the migration regularity and directional control mechanism of hydrogen, oxygen, and other elements during copyrolysis process.

Competing Interests

The authors declared that there is no conflict of interests related to this paper.

Acknowledgments

This work was supported by the National Natural Science Foundation of China (nos. 51306029 and 51476023) and New Teachers' Scientific Research Support Program of Xi'an Jiaotong University. The authors also thank Professor Shaoping Xu from Dalian University of Technology and Eugene Leung from ECO Environmental Energy Research Institute Limited for the advice about this manuscript.

References

[1] D. W. Van Krevelen, *Coal: Typology-Physics-Chemistry-Constitution*, Elsevier Science, Amsterdam, The Netherlands, 1993.

[2] H. B. Vuthaluru, "Thermal behaviour of coal/biomass blends during co-pyrolysis," *Fuel Processing Technology*, vol. 85, no. 2-3, pp. 141–155, 2004.

[3] Y. G. Pan, E. Velo, and L. Puigjaner, "Pyrolysis of blends of biomass with poor coals," *Fuel*, vol. 75, no. 4, pp. 412–418, 1996.

[4] E. Kastanaki, D. Vamvuka, P. Grammelis, and E. Kakaras, "Thermogravimetric studies of the behavior of lignite-biomass blends during devolatilization," *Fuel Processing Technology*, vol. 77-78, pp. 159–166, 2002.

[5] A. O. Aboyade, J. F. Görgens, M. Carrier, E. L. Meyer, and J. H. Knoetze, "Thermogravimetric study of the pyrolysis characteristics and kinetics of coal blends with corn and sugarcane residues," *Fuel Processing Technology*, vol. 106, pp. 310–320, 2013.

[6] C. Chen, X. Ma, and Y. He, "Co-pyrolysis characteristics of microalgae *Chlorella vulgaris* and coal through TGA," *Bioresource Technology*, vol. 117, pp. 264–273, 2012.

[7] H. Shui, C. Shan, Z. Cai et al., "Co-liquefaction behavior of a sub-bituminous coal and sawdust," *Energy*, vol. 36, no. 11, pp. 6645–6650, 2011.

[8] D. K. Park, S. D. Kim, S. H. Lee, and J. G. Lee, "Co-pyrolysis characteristics of sawdust and coal blend in TGA and a fixed bed reactor," *Bioresource Technology*, vol. 101, no. 15, pp. 6151–6156, 2010.

[9] C. A. Ulloa, A. L. Gordon, and X. A. García, "Thermogravimetric study of interactions in the pyrolysis of blends of coal with radiata pine sawdust," *Fuel Processing Technology*, vol. 90, no. 4, pp. 583–590, 2009.

[10] H. Haykiri-Acma and S. Yaman, "Synergy in devolatilization characteristics of lignite and hazelnut shell during co-pyrolysis," *Fuel*, vol. 86, no. 3, pp. 373–380, 2007.

[11] Ö. Onay, E. Bayram, and Ö. M. Kocükar, "Copyrolysis of seyitömer-lignite and safflower seed: influence of the blending ratio and pyrolysis temperature on product yields and oil characterization," *Energy and Fuels*, vol. 21, no. 5, pp. 3049–3056, 2007.

[12] T. Sonobe, N. Worasuwannarak, and S. Pipatmanomai, "Synergies in co-pyrolysis of Thai lignite and corncob," *Fuel Processing Technology*, vol. 89, no. 12, pp. 1371–1378, 2008.

[13] L. Zhang, S. Xu, W. Zhao, and S. Liu, "Co-pyrolysis of biomass and coal in a free fall reactor," *Fuel*, vol. 86, no. 3, pp. 353–359, 2007.

[14] L.-G. Wei, L. Zhang, and S.-P. Xu, "Effects of feedstock on co-pyrolysis of biomass and coal in a free-fall reactor," *Journal of Fuel Chemistry and Technology*, vol. 39, no. 10, pp. 728–734, 2011.

[15] L. G. Wei, L. Zhang, and S. P. Xu, "Synergetic effects on tar components from co-pyrolysis of biomass and coal in a free fall reactor," *Journal of Fuel Chemistry and Technology*, vol. 40, pp. 519–525, 2012.

[16] S. Yuan, Z.-H. Dai, Z.-J. Zhou, X.-L. Chen, G.-S. Yu, and F.-C. Wang, "Rapid co-pyrolysis of rice straw and a bituminous coal in a high-frequency furnace and gasification of the residual char," *Bioresource Technology*, vol. 109, pp. 188–197, 2012.

[17] S. Li, X. Chen, L. Wang, A. Liu, and G. Yu, "Co-pyrolysis behaviors of saw dust and Shenfu coal in drop tube furnace and fixed bed reactor," *Bioresource Technology*, vol. 148, pp. 24–29, 2013.

[18] B. Moghtaderi, C. Meesri, and T. F. Wall, "Pyrolytic characteristics of blended coal and woody biomass," *Fuel*, vol. 83, no. 6, pp. 745–750, 2004.

[19] A. O. Aboyade, M. Carrier, E. L. Meyer, H. Knoetze, and J. F. Görgens, "Slow and pressurized co-pyrolysis of coal and agricultural residues," *Energy Conversion and Management*, vol. 65, pp. 198–207, 2013.

[20] F.-X. Collard and J. Blin, "A review on pyrolysis of biomass constituents: mechanisms and composition of the products obtained from the conversion of cellulose, hemicelluloses and lignin," *Renewable and Sustainable Energy Reviews*, vol. 38, pp. 594–608, 2014.

[21] L. Zhang, R. Liu, R. Yin, and Y. Mei, "Upgrading of bio-oil from biomass fast pyrolysis in China: a review," *Renewable and Sustainable Energy Reviews*, vol. 24, pp. 66–72, 2013.

[22] J. Lédé, "Cellulose pyrolysis kinetics: an historical review on the existence and role of intermediate active cellulose," *Journal of Analytical and Applied Pyrolysis*, vol. 94, pp. 17–32, 2012.

[23] F. Abnisa and W. M. A. Wan Daud, "A review on co-pyrolysis of biomass: an optional technique to obtain a high-grade pyrolysis oil," *Energy Conversion and Management*, vol. 87, pp. 71–85, 2014.

[24] F. Mushtaq, R. Mat, and F. N. Ani, "A review on microwave assisted pyrolysis of coal and biomass for fuel production," *Renewable and Sustainable Energy Reviews*, vol. 39, pp. 555–574, 2014.

[25] H. Haykiri-Acma and S. Yaman, "Interaction between biomass and different rank coals during co-pyrolysis," *Renewable Energy*, vol. 35, no. 1, pp. 288–292, 2010.

[26] J.-Y. Lee, C. Yoo, S.-Y. Jun, C.-Y. Ahn, and H.-M. Oh, "Comparison of several methods for effective lipid extraction from microalgae," *Bioresource Technology*, vol. 101, no. 1, pp. S75–S77, 2010.

[27] M. Guo and J.-C. Bi, "Characteristics and application of co-pyrolysis of coal/biomass blends with solid heat carrier," *Fuel Processing Technology*, vol. 138, pp. 743–749, 2015.

[28] B. C. Gates, G. W. Huber, C. L. Marshall, P. N. Ross, J. Siirola, and Y. Wang, "Catalysts for emerging energy applications," *MRS Bulletin*, vol. 33, no. 4, pp. 429–435, 2008.

[29] Z. Wu, S. Wang, J. Zhao, L. Chen, and H. Meng, "Synergistic effect on thermal behavior during co-pyrolysis of lignocellulosic biomass model components blend with bituminous coal," *Bioresource Technology*, vol. 169, pp. 220–228, 2014.

[30] M. J. Blesa, J. L. Miranda, R. Moliner, M. T. Izquierdo, and J. M. Palacios, "Low-temperature co-pyrolysis of a low-rank coal and biomass to prepare smokeless fuel briquettes," *Journal of Analytical and Applied Pyrolysis*, vol. 70, no. 2, pp. 665–677, 2003.

[31] J. M. Jones, M. Kubacki, K. Kubica, A. B. Ross, and A. Williams, "Devolatilisation characteristics of coal and biomass blends," *Journal of Analytical and Applied Pyrolysis*, vol. 74, no. 1-2, pp. 502–511, 2005.

[32] A.-G. Collot, Y. Zhuo, D. R. Dugwell, and R. Kandiyoti, "Co-pyrolysis and co-gasification of coal and biomass in bench-scale fixed-bed and fluidized bed reactors," *Fuel*, vol. 78, no. 6, pp. 667–679, 1999.

[33] S. Yuan, X.-L. Chen, W.-F. Li, H.-F. Liu, and F.-C. Wang, "Nitrogen conversion under rapid pyrolysis of two types of aquatic biomass and corresponding blends with coal," *Bioresource Technology*, vol. 102, no. 21, pp. 10124–10130, 2011.

[34] J. W. Kim, S. B. Lalvani, C. B. Muchmore, and B. A. Akash, "Coliquefaction of coal and black liquor to environmentally acceptable liquid fuels," *Energy Sources*, vol. 21, no. 9, pp. 839–847, 1999.

[35] R. W. Coughlin and F. Davoudzadeh, "Coliquefaction of lignin and bituminous coal," *Fuel*, vol. 65, no. 1, pp. 95–106, 1986.

[36] S. B. Lalvani, C. B. Muchmore, J. A. Koropchak, B. Akash, C. Chavez, and P. Rajagopal, "Coal liquefaction in lignin-derived liquids under low severity conditions," *Fuel*, vol. 70, no. 12, pp. 1433–1438, 1991.

[37] Z. Miao, G. Wu, P. Li, X. Meng, and Z. Zheng, "Investigation into co-pyrolysis characteristics of oil shale and coal," *International Journal of Mining Science and Technology*, vol. 22, no. 2, pp. 245–249, 2012.

[38] I. Suelves, M. J. Lázaro, and R. Moliner, "Synergetic effects in the co-pyrolysis of samca coal and a model aliphatic compound studied by analytical pyrolysis," *Journal of Analytical and Applied Pyrolysis*, vol. 65, no. 2, pp. 197–206, 2002.

[39] E. Kastanaki and D. Vamvuka, "A comparative reactivity and kinetic study on the combustion of coal-biomass char blends," *Fuel*, vol. 85, no. 9, pp. 1186–1193, 2006.

[40] K. Kidena, S. Murata, and M. Nomura, "Studies on the chemical structural change during carbonization process," *Energy and Fuels*, vol. 10, no. 3, pp. 672–678, 1996.

[41] C. Quan, S. Xu, Y. An, and X. Liu, "Co-pyrolysis of biomass and coal blend by TG and in a free fall reactor," *Journal of Thermal Analysis and Calorimetry*, vol. 117, no. 2, pp. 817–823, 2014.

[42] S. Li, X. Chen, A. Liu, L. Wang, and G. Yu, "Co-pyrolysis characteristic of biomass and bituminous coal," *Bioresource Technology*, vol. 179, pp. 414–420, 2015.

[43] H. Meng, S. Wang, L. Chen, Z. Wu, and J. Zhao, "Thermal behavior and the evolution of char structure during co-pyrolysis of platanus wood blends with different rank coals from northern China," *Fuel*, vol. 158, pp. 602–611, 2015.

[44] S. Li and S. Xu, "Co-pyrolysis of coal and biomass," *Coal Conversion*, vol. 25, pp. 7–12, 2002.

[45] A. O. Aboyade, M. Carrier, E. L. Meyer, J. H. Knoetze, and J. F. Görgens, "Model fitting kinetic analysis and characterisation of the devolatilization of coal blends with corn and sugarcane residues," *Thermochimica Acta*, vol. 530, pp. 95–106, 2012.

[46] M. J. Blesa, V. Fierro, J. L. Miranda, R. Moliner, and J. M. Palacios, "Effect of the pyrolysis process on the physicochemical and mechanical properties of smokeless fuel briquettes," *Fuel Processing Technology*, vol. 74, no. 1, pp. 1–17, 2001.

[47] W.-P. Yan and Y.-Y. Chen, "Experimental study on co-pyrolysis characteristics of lignite mixed with biomass mixture," *Journal of Power Engineering*, vol. 26, no. 6, pp. 865–893, 2006.

[48] H. Darmstadt, M. Garcia-Perez, A. Chaala, N.-Z. Cao, and C. Roy, "Co-pyrolysis under vacuum of sugar cane bagasse and petroleum residue: properties of the char and activated char products," *Carbon*, vol. 39, no. 6, pp. 815–825, 2001.

[49] C. Meesri and B. Moghtaderi, "Lack of synergetic effects in the pyrolytic characteristics of woody biomass/coal blends under low and high heating rate regimes," *Biomass and Bioenergy*, vol. 23, no. 1, pp. 55–66, 2002.

[50] E. Biagini, F. Lippi, L. Petarca, and L. Tognotti, "Devolatilization rate of biomasses and coal-biomass blends: an experimental investigation," *Fuel*, vol. 81, no. 8, pp. 1041–1050, 2002.

[51] S. Yuan, Z.-J. Zhou, J. Li, X.-L. Chen, and F.-C. Wang, "HCN and NH_3 released from biomass and soybean cake under rapid pyrolysis," *Energy and Fuels*, vol. 24, no. 11, pp. 6166–6171, 2010.

[52] I. Suelves, R. Moliner, and M. J. Lázaro, "Synergetic effects in the co-pyrolysis of coal and petroleum residues: influences of coal mineral matter and petroleum residue mass ratio," *Journal of Analytical and Applied Pyrolysis*, vol. 55, no. 1, pp. 29–41, 2000.

[53] S. Yuan, Z.-J. Zhou, J. Li, X.-L. Chen, and F.-C. Wang, "HCN and NH_3 (NOx precursors) released under rapid pyrolysis of biomass/coal blends," *Journal of Analytical and Applied Pyrolysis*, vol. 92, no. 2, pp. 463–469, 2011.

[54] J. Zhang, C. Quan, Y. Qiu, and S. Xu, "Effect of char on co-pyrolysis of biomass and coal in a free fall reactor," *Fuel Processing Technology*, vol. 135, pp. 73–79, 2015.

[55] N. T. Weiland, N. C. Means, and B. D. Morreale, "Product distributions from isothermal co-pyrolysis of coal and biomass," *Fuel*, vol. 94, pp. 563–570, 2012.

[56] M. Wang, J. Tian, D. G. Roberts, L. Chang, and K. Xie, "Interactions between corncob and lignite during temperature-programmed co-pyrolysis," *Fuel*, vol. 142, pp. 102–108, 2015.

[57] D. Mohan, C. U. Pittman Jr., and P. H. Steele, "Pyrolysis of wood/biomass for bio-oil: a critical review," *Energy & Fuels*, vol. 20, no. 3, pp. 848–889, 2006.

[58] A. Demirbas, "Pyrolysis of ground beech wood in irregular heating rate conditions," *Journal of Analytical and Applied Pyrolysis*, vol. 73, no. 1, pp. 39–43, 2005.

[59] X. Yang, C. Yuan, J. Xu, and W. Zhang, "Co-pyrolysis of Chinese lignite and biomass in a vacuum reactor," *Bioresource Technology*, vol. 173, pp. 1–5, 2014.

[60] W. Zhu, W. Song, and W. Lin, "Catalytic gasification of char from co-pyrolysis of coal and biomass," *Fuel Processing Technology*, vol. 89, no. 9, pp. 890–896, 2008.

[61] P. Yangali, A. M. Celaya, and J. L. Goldfarb, "Co-pyrolysis reaction rates and activation energies of West Virginia coal and cherry pit blends," *Journal of Analytical and Applied Pyrolysis*, vol. 108, pp. 203–211, 2014.

[62] Y. Song, A. Tahmasebi, and J. Yu, "Co-pyrolysis of pine sawdust and lignite in a thermogravimetric analyzer and a fixed-bed reactor," *Bioresource Technology*, vol. 174, pp. 204–211, 2014.

[63] Z. Wu, S. Wang, J. Zhao, L. Chen, and H. Meng, "Thermochemical behavior and char morphology analysis of blended bituminous coal and lignocellulosic biomass model compound co-pyrolysis: effects of cellulose and carboxymethylcellulose sodium," *Fuel*, vol. 171, pp. 65–73, 2016.

[64] D. Vamvuka, E. Kakaras, E. Kastanaki, and P. Grammelis, "Pyrolysis characteristics and kinetics of biomass residuals mixtures with lignite," *Fuel*, vol. 82, no. 15–17, pp. 1949–1960, 2003.

[65] A. K. Sadhukhan, P. Gupta, T. Goyal, and R. K. Saha, "Modelling of pyrolysis of coal-biomass blends using thermogravimetric analysis," *Bioresource Technology*, vol. 99, no. 17, pp. 8022–8026, 2008.

[66] S. S. Idris, N. A. Rahman, K. Ismail, A. B. Alias, Z. A. Rashid, and M. J. Aris, "Investigation on thermochemical behaviour of low rank Malaysian coal, oil palm biomass and their blends during pyrolysis via thermogravimetric analysis (TGA)," *Bioresource Technology*, vol. 101, no. 12, pp. 4584–4592, 2010.

[67] J. Fei, J. Zhang, F. Wang, and J. Wang, "Synergistic effects on co-pyrolysis of lignite and high-sulfur swelling coal," *Journal of Analytical and Applied Pyrolysis*, vol. 95, pp. 61–67, 2012.

[68] M. Montiano, E. Díaz-Faes, and C. Barriocanal, "Kinetics of co-pyrolysis of sawdust, coal and tar," *Bioresource Technology*, vol. 205, pp. 222–229, 2016.

[69] K. Wan, Z. Wang, Y. He et al., "Experimental and modeling study of pyrolysis of coal, biomass and blended coal-biomass particles," *Fuel*, vol. 139, pp. 356–364, 2015.

[70] W. S.-L. Mok and M. J. Antal Jr., "Effects of pressure on biomass pyrolysis. I. Cellulose pyrolysis products," *Thermochimica Acta*, vol. 68, no. 2-3, pp. 155–164, 1983.

[71] Y. Mao, L. Dong, Y. Dong et al., "Fast co-pyrolysis of biomass and lignite in a micro fluidized bed reactor analyzer," *Bioresource Technology*, vol. 181, pp. 155–162, 2015.

[72] Y. Zhang, D. Fan, and Y. Zheng, "Comparative study on combined co-pyrolysis/gasification of walnut shell and bituminous coal by conventional and congruent-mass thermogravimetric analysis (TGA) methods," *Bioresource Technology*, vol. 199, pp. 382–385, 2016.

[73] Y. Zhang, Y. Zheng, M. Yang, and Y. Song, "Effect of fuel origin on synergy during co-gasification of biomass and coal in CO_2," *Bioresource Technology*, vol. 200, pp. 789–794, 2016.

[74] M. J. Lázaro, R. Moliner, and I. Suelves, "Co-pyrolysis of coals and lube oil wastes in a bench-scale unit," *Energy & Fuels*, vol. 13, no. 4, pp. 907–913, 1999.

[75] Z. Guo, Z. Bai, J. Bai, Z. Wang, and W. Li, "Co-liquefaction of lignite and sawdust under syngas," *Fuel Processing Technology*, vol. 92, no. 1, pp. 119–125, 2011.

[76] S. Völker and T. Rieckmann, "Thermokinetic investigation of cellulose pyrolysis—impact of initial and final mass on kinetic results," *Journal of Analytical and Applied Pyrolysis*, vol. 62, no. 2, pp. 165–177, 2002.

[77] S. Krerkkaiwan, C. Fushimi, A. Tsutsumi, and P. Kuchonthara, "Synergetic effect during co-pyrolysis/gasification of biomass and sub-bituminous coal," *Fuel Processing Technology*, vol. 115, pp. 11–18, 2013.

[78] M. Yilgin, N. D. Duranay, and D. Pehlivan, "Co-pyrolysis of lignite and sugar beet pulp," *Energy Conversion and Management*, vol. 51, no. 5, pp. 1060–1064, 2010.

[79] T. Cordero, J. Rodríguez-Mirasol, J. Pastrana, and J. J. Rodríguez, "Improved solid fuels from co-pyrolysis of a high-sulphur content coal and different lignocellulosic wastes," *Fuel*, vol. 83, no. 11-12, pp. 1585–1590, 2004.

[80] K. Kidena, K. Matsumoto, M. Katsuyama, S. Murata, and M. Nomura, "Development of aromatic ring size in bituminous coals during heat treatment in the plastic temperature range," *Fuel Processing Technology*, vol. 85, no. 8–10, pp. 827–835, 2004.

[81] J. Long, H. Song, X. Jun et al., "Release characteristics of alkali and alkaline earth metallic species during biomass pyrolysis and steam gasification process," *Bioresource Technology*, vol. 116, pp. 278–284, 2012.

Hindawi Publishing Corporation
BioMed Research International
Volume 2016, Article ID 7263974, 9 pages
http://dx.doi.org/10.1155/2016/7263974

Research Article

Inhibitory Effect of Long-Chain Fatty Acids on Biogas Production and the Protective Effect of Membrane Bioreactor

Kris Triwulan Dasa,[1] Supansa Y. Westman,[2] Ria Millati,[1] Muhammad Nur Cahyanto,[1] Mohammad J. Taherzadeh,[2] and Claes Niklasson[3]

[1]*Department of Food and Agricultural Product Technology, Universitas Gadjah Mada, Yogyakarta 55281, Indonesia*
[2]*Swedish Center for Resource Recovery, University of Borås, 50190 Borås, Sweden*
[3]*Department of Chemistry and Chemical Engineering, Chalmers University of Technology, 41296 Gothenburg, Sweden*

Correspondence should be addressed to Ria Millati; ria_millati@ugm.ac.id

Received 27 May 2016; Revised 26 July 2016; Accepted 23 August 2016

Academic Editor: Ningbo Gao

Anaerobic digestion of lipid-containing wastes for biogas production is often hampered by the inhibitory effect of long-chain fatty acids (LCFAs). In this study, the inhibitory effects of LCFAs (palmitic, stearic, and oleic acid) on biogas production as well as the protective effect of a membrane bioreactor (MBR) against LCFAs were examined in thermophilic batch digesters. The results showed that palmitic and oleic acid with concentrations of 3.0 and 4.5 g/L resulted in >50% inhibition on the biogas production, while stearic acid had an even stronger inhibitory effect. The encased cells in the MBR system were able to perform better in the presence of LCFAs. This system exhibited a significantly lower percentage of inhibition than the free cell system, not reaching over 50% at any LCFA concentration tested.

1. Introduction

Comprising mainly methane, biogas is a renewable energy source that can be directly used as a car fuel, for heating, or indirectly used to generate electricity [1]. Biogas production through anaerobic digestion involves four crucial steps including hydrolysis, acidogenesis, acetogenesis, and methanogenesis. Each step is carried out by different consortia of microorganisms, partly standing in syntrophic interrelation with each other [2]. Biogas can be produced from various kinds of waste materials, including municipal solid waste (MSW), industrial waste, and agricultural waste. Among waste materials, lipid-rich wastes, which are released from, for example, dairy products industry, slaughterhouses, edible oil processing industry, olive oil mills, and wool scouring facilities are produced in high amounts each year [3–6]. Accumulation of this waste creates a serious problem to the environment such as heavy odor and plenty of leachate; hence, a sustainable handling of this waste is highly desirable.

Lipids, the main constituent in lipid-rich wastes, play the most significant role in anaerobic digestion for biogas production due to their high energy content [7]. Lipids are long-chain fatty acids (LCFAs) bonded to glycerol, alcohols, or other groups by an ester or ether linkage. During hydrolysis, lipids are rapidly degraded into monomers such as glycerol and LCFAs which are further converted into short organic acids via β-oxidation [7]. The short organic acids are subsequently converted into acetate and hydrogen which are eventually converted into methane and carbon dioxide [1]. Biogas derived from lipid have higher methane content compared to that derived from carbohydrates and proteins [7].

Albeit the higher quality of biogas produced from lipid, biogas production from lipid is hampered by excessive organic loading or LCFAs [8, 9]. It has been reported that LCFAs inhibited several reactions during the anaerobic degradation process [10]. The inhibitory effects of LCFA are already visible at concentrations as low as 50 mg/L [11]. LCFAs also have severe inhibitory effects on the microorganisms in anaerobic digestion, particularly for methanogens and acetogens [11].

Another challenge in the anaerobic digestion process of lipid-containing wastes is washout of methanogens at high organic loading rates. Methanogens grow very slow and sensitive in the harsh process conditions. As a result, methanogens require longer retention time in the digesters [12]. In addition, methanogens is also sensitive to inhibitor compound. Sousa et al. [13] reported that methanogens in the anaerobic digestion of lipid-containing wastes are sensitive to the LCFAs derived from the lipid hydrolysis. A great reduction of methanogen population results in a decreased methane production [12, 14].

Retaining and protecting anaerobic digesting microbial cells inside a membrane bioreactor (MBR) can be a potential solution to overcome the problems of washout and inhibition. It has been reported that using the microorganisms encased in a semipermeable polyvinylidene fluoride (PVDF) membrane, the biogas production could be improved [15–17]. MBR was able to retain the cells; hence, it provides a better system for preventing cell washout in semicontinuous digestion processes at high organic loading rate [16, 18]. Furthermore, MBR has shown a protective effect on substrates containing inhibitors such as fruit-flavor compounds [19]. In searching the literature, no report on application of MBR to overcome LCFAs inhibition on biogas production has been found. Therefore, the objective of this work was to investigate the inhibitory effect of LCFAs on biogas production under thermophilic condition and the protective performance of MBR against LCFAs. Saturated (palmitic acid, $C_{16:0}$, and stearic acid, $C_{18:0}$) and unsaturated (oleic acid, $C_{18:1}$) LCFAs were used as models of LCFA inhibitors.

2. Materials and Methods

2.1. Anaerobic Culture Preparation. An anaerobic culture with 22 g VS/L was obtained from thermophilic biogas plant at Borås Energy and Environment AB, Sweden. The culture was acclimated in an incubator at 55°C for 3 days prior to use. The acclimated sludge was homogenized and filtered through a sieve with a pore size of 1.0 mm in order to remove any remaining large particles. The sludge was thereafter centrifuged (Carl Padberg 77933 LE, Huber and Moser, Germany) at 30,000 rpm for 15 minutes and the supernatant was discarded. The suspended sludge was later used as an inoculum for cell containment in membrane sachets, or as free cells.

2.2. Synthetic Medium, Membrane, and Inhibitors. The synthetic medium was prepared as previously described [19]. It contained D-glucose, yeast extract, and nutrient broth with a concentration of 20 g/L in distilled water. The nutrient broth contained 1 g/L D(+)-glucose, 15 g/L peptone, 6 g/L sodium chloride, and 3 g/L yeast extract. The solution was homogenized and filtered using 0.2 μm membrane filters. Flat plain PVDF (polyvinylidene fluoride, Durapore®) membranes were obtained from Thermo Fisher Scientific Inc. (Sweden) and used for cell encasement. PVDF membranes have a hydrophilic surface, with pore size and thickness of 0.1 μm and 125 μm, respectively.

Palmitic, stearic, and oleic acid were used as model LCFA inhibitors and were purchased from Sigma Aldrich (Sweden). These inhibitors were first dissolved in 2.5 mL methanol (reagent grade) in order to obtain a homogeneous solution in the reactors; thereafter, they were added to the reactors at concentrations of 0, 1.5, 3.0, and 4.5 g/L.

2.3. Membrane Sachet Preparation and Cell Containment Procedure. A cell containment technique was conducted following the method described in a previous study [16]. In this work, the cells were encased inside the membrane, which according to Mahboubi et al. [20] is referred to as reverse membrane bioreactor. The PVDF membranes were cut into rectangular shapes 6 × 6 cm and folded to create membrane pockets of 3 × 6 cm. The pockets were heat-sealed (HPL 450 AS, Hawo, Germany) on two sides with heating and cooling times of 4.0 and 3.5 s, leaving one side open for insertion of the inoculums. Three grams of solid inoculums was injected into the synthetic membrane pockets. The remaining open side of the sachet was sealed and the inoculum inside was carefully spread out. The inoculum containing sachets were immediately used for biogas production.

2.4. Anaerobic Batch Digestion Process Setup. The experiments were carried out in thermophilic batch digestion. The LCFAs were added to the reactor at concentrations of 1.5, 3, and 4.5 g/L. Reactor without addition of inhibitors was used as controls. The reactors of the free cells were performed in parallel, with otherwise identical conditions to compare the performance of membrane bioreactor in the presence of inhibitor. The experiment was conducted using 100 mL serum glass bottles with total working volume of 43.5 mL. Each reactor contained 1 mL of synthetic medium, 3 g of free cell or encased cell, 40 mL distilled water, and 2.5 mL of inhibitor solution or 2.5 mL of methanol for the control. The reactors were sealed and flushed with 80% N_2 and 20% CO_2 gas mix to obtain anaerobic conditions. During the biogas production process, the digesters were shaken twice a day.

2.5. Analytical Methods. Methane production was measured by Varian 450 gas chromatograph with a capillary column equipped with a thermal conductivity detector (TCD). N_2 was used as a carrier gas, and the instrument was operated with injector and oven temperature at 75°C and 50°C, nitrogen column flow 2.0 mL/min and detector temperature at 250°C. A 0.25 mL pressure lock syringe (VICI, USA) was used for the gas sampling.

Methane production was determined as previously described by Hansen et al., 2004 [21]. The measurement of methane production was based on gas composition, releasing the gas from the reactor, changing the reactor pressure to normal pressure, and another GC measurement at this normal pressure of the reactor. The syringe used for gas sampling has a valve and, therefore, the gas inside the syringe has the same pressure as the reactor vessel in both of the measurements. The methane production was calculated from the difference of peak sizes between two measurements.

The percentage of inhibition from each treatment was used as an indicator of the inhibitory effects caused by the LCFA and calculated according to the following equation:

$$\text{Inhibition } (\%) = \frac{(x - y)}{x} \times 100, \quad (1)$$

where x is methane production from control reactor and y is methane production from samples.

Volatile fatty acids (VFAs) were analyzed using a Waters® High Performance Liquid Chromatography (HPLC) system with a BIORAD Aminex® HPX-87H, 300 mm × 7.8 mm column, and 5 mM of sulphuric acid as mobile phase. It was operated at 0.6 mL/min isocratic mobile phase flow; the column temperature was set at 50°C and the VFAs were detected using a UV detector at a wavelength of 210 nm. The experiment was performed in triplicate, and the results were presented in average.

3. Results and Discussion

3.1. Inhibitory Effects of LCFAs on Biogas Production. Palmitic and stearic acids are the principal saturated LCFAs to be accumulated in anaerobic digestion process. They are known to be degraded five times slower than unsaturated acids [22]. Oleic acid is one of the most common LCFAs [23] and has the highest toxicity level among the various kinds of LCFAs, with a minimum inhibitory concentration (MIC) of 50–75 mg/L under mesophilic conditions [24–27]. However, inhibitory effects of the aforementioned LCFAs have not yet been examined under thermophilic anaerobic digestion. In this experiment, the possible inhibition effects of palmitic, stearic, and oleic acid were investigated at three different concentrations, that is, 1.5, 3, and 4.5 g/L in batch thermophilic anaerobic digestion. Reactor without addition of LCFAs was used as control. The cumulative methane productions of control as well as reactor with addition of palmitic, stearic, and oleic acid at three different concentrations are shown in Figures 1(a)–1(c), respectively.

Figure 1(a) shows that the methane production increased sharply in all the reactors during the first 6 days of incubation. After six days, the methane production continued at a lower rate. This indicates that the more biodegradable material was consumed within the first 6 days. The methane production started to decrease on day 4 with addition of 3 and 4.5 g/L of palmitic acid and on day 8 with addition of 1.5 g/L palmitic acid. At the end of digestion, the accumulation of methane yield with addition of palmitic acid at 0, 1.5, 3, and 4.5 g/L was 1.4, 1.1, 0.6, and 0.6 Nm^3/kg VS, respectively. The methane production decreased by 21, 57, and 57% compared to control with addition of 1.5, 3, and 4.5 g/L. The specific methanogenic activities of control as well as reactors with addition of 1.5, 3, and 4.5 g/L palmitic acid were 0.115, 0.100, 0.055, and 0.061 Nm^3 CH_4/kg VS/d, respectively. A shorter time required to affect the methane production that resulted in lower cumulative methane productions at all the concentration tested compared to that of control confirmed that palmitic acid has an inhibitory effect on the thermophilic anaerobic digestion process. It has been reported that the addition of palmitic acid at a concentration of >1.1 g/L inhibited the performance of anaerobic digestion by about 50% under mesophilic conditions [28]. The result of this work shows that under thermophilic condition, methane reduction exceeding 50% was obtained when palmitic acid was added at concentration of 3 g/L. Furthermore, the maximum methane reduction was obtained with the addition of 3 g/L of palmitic acid as increasing concentration of palmitic acid up to 4.5 g/L had a similar effect with that of 3 g/L.

Effect of stearic acid on methane production is presented in Figure 1(b). Initially, methane was produced in all of the reactors showing that the microorganisms were able to perform at all concentrations of stearic acid added. The cumulative methane productions of reactors with addition of all tested concentrations were similar to that of control until day 4. Subsequently, the methane was produced in a lower rate compared to that of control until the end of digestion. On the last day of the digestion, the accumulated methane yield from control and the media containing stearic acid at 1.5, 3.0, and 4.5 g/L were 3.4, 1.5, 1.2, and 0.9 m^3/kg VS, respectively. The accumulated methane yields from the media containing LCFAs correspond to 56, 65, and 74% of methane reduction with respect to control. Addition of stearic acid to the reactor also decreased the specific methanogenic activity of the reactor. The specific methanogenic activities of control were 0.181, whereas for reactors with addition of 1.5, 3, and 4.5 g/L stearic acid the specific methanogenic activities were 0.121, 0.089, and 0.078 Nm^3 CH_4/kg VS/d, respectively. The result shows that higher concentration of stearic acid resulted in lower methane production, which indicates an inhibitory activity of stearic acid towards anaerobic digesting microorganism. In this work, stearic acid at concentration of 1.5% is enough to reduce 50% of methane production under thermophilic condition. This is in accordance with a previous finding stating that stearic acid at a concentration of 1.5 g/L could inhibit 50 percent of the anaerobic performance under mesophilic conditions [28].

Meanwhile, the results of the effect of oleic acid study are presented in Figure 1(c). Addition of oleic acid at all tested concentration did not affect methane production until day 6 as the level of methane production was the same with that of control. Similar to those of palmitic and stearic acid, addition of oleic acid at all tested concentrations to the anaerobic digesters resulted in a lower specific methanogenic activity and a lower accumulated methane yield compared to that of control. The specific methanogenic activities of control as well as reactors with addition of 1.5, 3, and 4.5 g/L oleic acid were 0.341, 0.165, 0.067, and 0.079 Nm^3 CH_4/kg VS/d, respectively. The accumulated methane yields produced in the reactor with addition of oleic acid at concentrations of 0, 1.5, 3.0, and 4.5 g/L were 6.7, 3.5, 1.8, and 2.0 m^3/kg VS, respectively. The result shows that addition of oleic acid at concentration of 1.5 g/L caused 48% reduction of methane under thermophilic condition. This concentration is higher compared to that of previous work that reported oleic acid at a concentration of 0.05–0.07 g/L could inhibit the digestion performance by about 50 percent under mesophilic conditions [26]. Oleic acid at 3 g/L exhibited strong inhibitory activity as shown by 73% methane reduction compared to that of control.

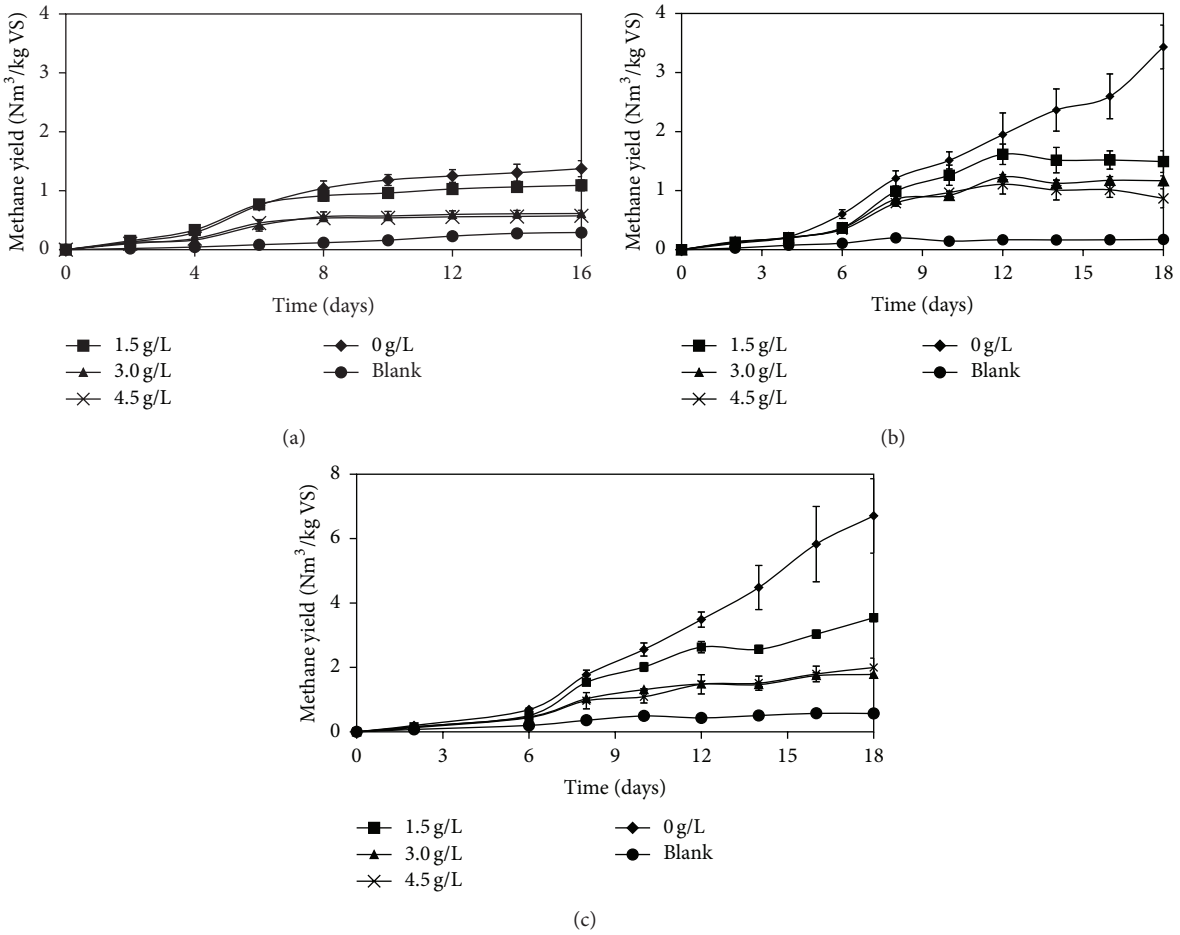

Figure 1: Accumulated methane yield from reactors of free cells containing the LCFAs. (a) Palmitic acid, (b) stearic acid, and (c) oleic acid.

The results from the current work show that all the tested LCFAs reduced methane production by 50% at concentration of 1.5–3 g/L. Sousa et al. [13] reported that oleic acid had more severe effects on the methanogens than the saturated LCFAs. Furthermore, Shin et al., 2003, [24] reported that unsaturated oleic acid was more inhibitory than the saturated stearate and palmitate on the acetate degradation. The inhibitory effects of major long-chain fatty acids (LCFAs), which have 16 or 18 carbons, did not only have an effect on the acetate degradation, but also on the propionate degradation and β-oxidation. The adsorption of LCFAs onto the microbial cell wall or the membrane that causes damage in the microorganism's transport and protective functions is suggested to be the mechanism underlying the inhibition effect of LCFAs.

3.2. Performance of the Membrane Bioreactor (MBR) with Encased Cells in the Presence of Inhibitory LCFAs for Biogas Production. The MBR has been intensively studied in both batch and continuous digestion processes in order to improve the process efficiency and biogas productivity under harsh anaerobic process conditions [15–18]. The previous section showed inhibition of LCFAs on methane production under thermophilic digestion. In this work, the encased cells in the MBR system were studied in batch digestion processes, in order to investigate the potential application of this system in overcoming the inhibitory effects of LCFAs. Experiment with MBR without addition of LCFAs was used as control. Furthermore, to evaluate the performance of MBR, a conventional reactor containing free cells which run under identical condition was used as comparison. Percentage of inhibition, the accumulation of VFAs and pH were used as parameters indicating the performance of the system.

3.2.1. Percentage of Inhibition. The accumulated methane yield of MBR with addition of palmitic acid is presented in Figure 2(a). As can be seen, accumulated methane yields of reactor with addition of 1.5 and 3 g/L were similar to that of control which indicates addition of palmitic acid at concentration up to 3 g/L did not affect the methane production in MBR system. However, higher concentration of palmitic acid at 4.5 g/L resulted in lower accumulated methane yield compared to that of control. The specific methanogenic activities of MBR with addition of palmitic acid were in the range of 0.032–0.049 Nm^3 CH_4/kg VS/h. The percentage of inhibition in the MBR with encased cells was 1.4, 5.0, and 42.3% at palmitic acid concentrations of 1.5, 3.0, and 4.5 g/L, respectively, whereas the percentage of inhibition in the reactors with free cells containing palmitic

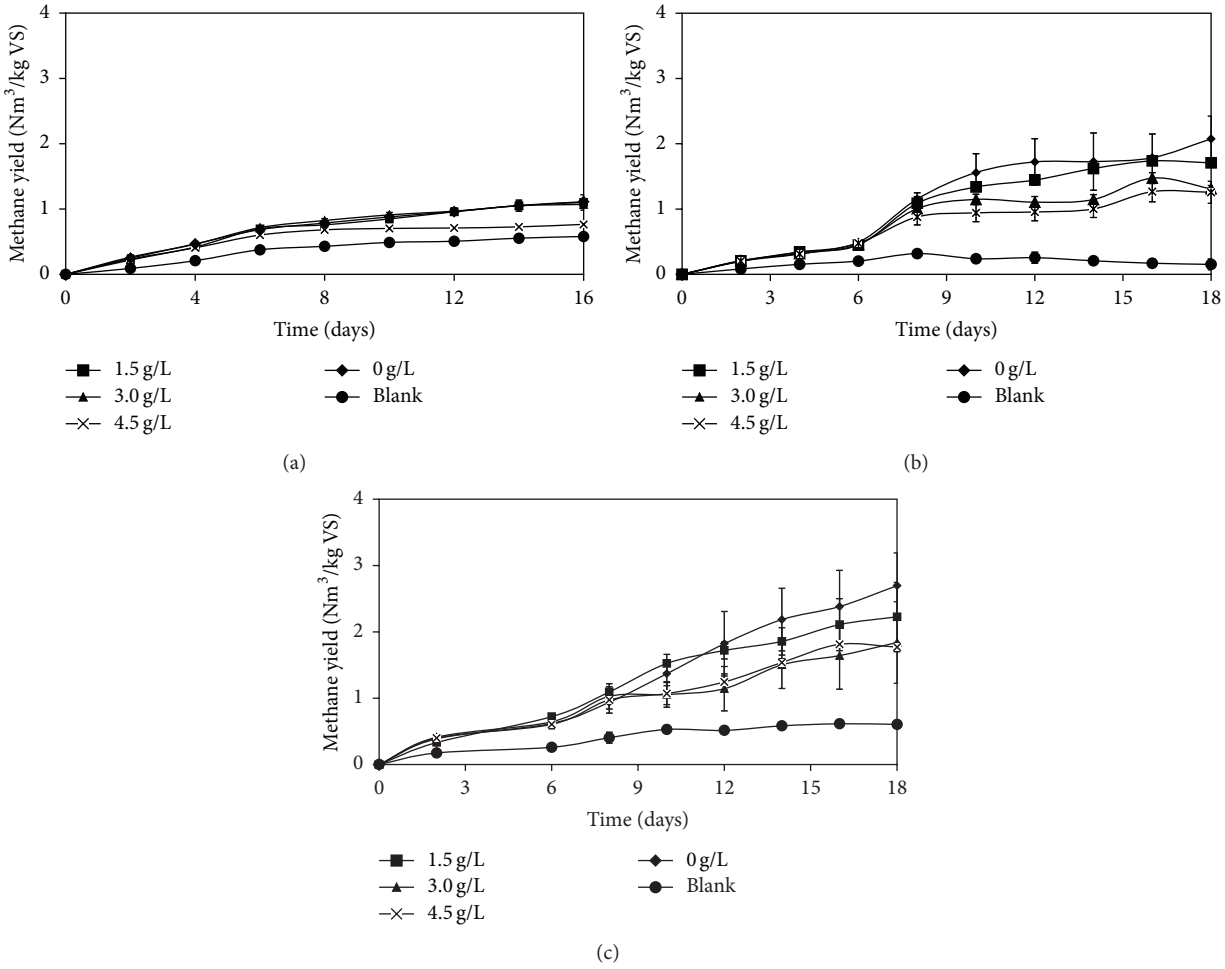

Figure 2: Accumulated methane yield from the MBR with the encased cells containing the LCFAs. (a) Palmitic acid, (b) stearic acid, and (c) oleic acid.

acid at concentrations of 1.5, 3.0, and 4.5 g/L was 26.1%, 70.2%, and 73.9%, respectively (Figure 3(a)). The results show that percentages of inhibition in all tested concentrations of MBR were lower than that of free cells. And this explains that MBR system was significantly less affected by the presence of palmitic acid compared to the conventional system with free cells. In addition, the inhibitory concentration (IC_{50}) that reduces 50% of methane production was obtained at less than 3 g/L in free cells whereas the IC_{50} of MBR was higher than 4.5 g/L.

The accumulated methane yield of MBR with addition of different concentration of stearic acid is shown in Figure 2(b). The accumulated methane yield in the MBR containing stearic acid of 1.5 g/L was not significantly different with that of control. This showed that MBR could tolerate stearic acid with a concentration of 1.5 g/L, while free cells failed under the same condition (Figure 1(b)). The specific methanogenic activities of MBR with addition of stearic acid were in the range of 0.069–0.098 Nm^3 CH_4/kg VS/h. Furthermore, the percentage of inhibition in the bioreactor with addition of stearic acid at 1.5, 3.0, and 4.5 g/L was 54.8, 63.6, and 69.0%, respectively, for free cells and 9.1, 30.0, and 38.2%, respectively, for MBR (Figure 3(b)). The results show that IC_{50} of MBR system (>4.5 g/L) was approximately three times higher than that of free cells (<1.5 g/L).

Similar to palmitic and stearic acids, the accumulated methane yield in the MBR system with addition of oleic acid at concentration of 1.5 g/L was not significantly different with that of control (Figure 2(c)). In comparison with free cells, addition of oleic acid at the same concentration already caused 48% methane reduction. Addition of oleic acid at concentration higher than 3 g/L decreased the methane production by 33.3%. The specific methanogenic activities of MBR with addition of oleic acid were in the range of 0.065–0.090 Nm^3 CH_4/kg VS/h. When the performance of MBR was presented in the percentage of inhibition, the results showed that the percentage of inhibition in MBR containing oleic acid was less than 50% at all concentrations of the oleic acid. The free microbial cells in the conventional system were more severely affected by the oleic acid already at a concentration of 1.5 g/L. The inhibition was more than 50% when oleic acid concentration was increased to 3.0 and 4.5 g/L (Figure 3(c)). Hence the IC_{50} of MBR was higher than 4.5 g/L, whereas the IC_{50} of free cells was less than 1.5 g/L.

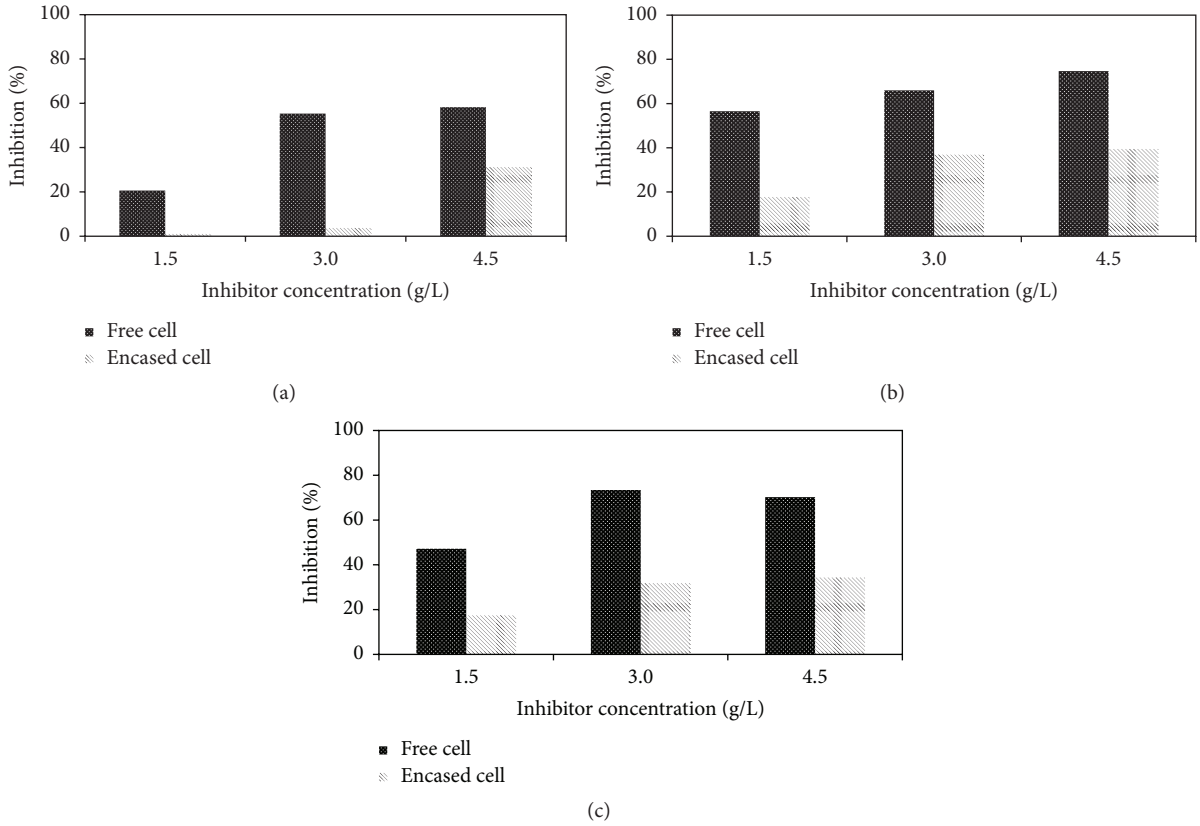

Figure 3: Percentage of inhibition in the reactors with the free cells and MBR with the encased cells in the presence of LCFAs. (a) Palmitic acid, (b) stearic acid, and (c) oleic acid.

In general, the specific methanogenic activities of free cells were higher than that of MBR. This is most likely due to the extra resistance to the mass transfer of the substrate through the membrane. However, it did not reduce the accumulated methane yield as higher accumulated methane yield was obtained from MBR.

The results of the current work emphasize the benefit of encased cells in MBR over free cells system. In MBR system, the cells were encased in a hydrophilic PVDF membrane which theoretically is impermeable to hydrophobic compound such as LCFA. Besides, encasement increases the cell density inside the membrane which might enhance cell tolerance against the inhibitor. In addition, MBR system offers an advantage in having easier cell recovery from the bioreactor in the downstream processing unit [29].

3.2.2. Volatile Fatty Acid and pH. In an anaerobic treatment, lipids are first hydrolyzed to glycerol and free LCFAs by the acidogenic bacteria. Glycerol is further converted into acetate by acidogenesis, while the LCFAs are converted into hydrogen, acetate, and/or propionate through the β-oxidation pathway (syntrophic acetogenesis) [30]. During the last stage of methanogenesis, the products of the previous stage are further degraded to principally carbon dioxide and methane. Under ideal operating conditions, the acid production and gas production are in balance, with the volatile acids being broken down as quickly as they are produced [31]. Thus, VFAs and pH have been widely used as fast indicators of unstable anaerobic digestion processes. Therefore, in this work, VFAs and pH were analyzed in order to investigate the performance of the encased cells in MBR system in comparison to free cells.

Tables 1 and 2 show total VFA concentrations and pH on the last day of digestion in both free cells and MBR system. The total VFA concentration and the pH in both systems were not different from the control for both free cells and MBR with addition of palmitic acid at all tested concentrations. The VFA concentrations in MBR systems with encased cells were in the range of 2.4–2.8 g/L, while the reactors with free cells were in the range of 2.1–3.2 g/L.

In the case of stearic acid, addition of LCFA at concentration higher than 3 g/L increased VFA for both free cells and MBR. The increase of VFA was followed with the decrease of pH as can be seen in Table 2. However, VFAs in free cells at addition of 4.5 g/L were two times higher than that of control, whereas under the same condition, only 25% increase of VFA was observed in MBR system. It has been reported that accumulation of VFAs above 4 g/L in the digester leads to an imbalance of anaerobic digestion process [10, 12]. In this experiment, with the addition of stearic acid at concentrations of 3.0 and 4.5 g/L the reactor with free cells resulted in an accumulation of VFA compounds to 4.4 and 5.4 g/L, respectively. In the MBR reactor, on the other hand, the VFA concentrations of 2.6 and 2.4 g/L were measured

Table 1: Total VFA concentration on the last day of the experiment in the reactors with the free cells and the MBR with the encased cells containing different LCFAs at different concentrations.

LCFAs	Conc. (g/L)	Total VFA concentration (g/L)	
		Free cells	Encased cells
Palmitic acid	0	2.1 ± 0.6[a]	2.4 ± 0.1[a]
	1.5	2.5 ± 0.0[a]	2.6 ± 0.0[a]
	3.0	2.6 ± 0.0[a]	2.8 ± 0.2[a]
	4.5	3.2 ± 0.0[a]	2.8 ± 0.1[a]
Stearic acid	0	2.6 ± 0.5[a]	1.8 ± 0.1[a]
	1.5	2.7 ± 0.1[a]	1.9 ± 0.0[a]
	3.0	4.4 ± 0.1[b]	2.6 ± 0.0[b]
	4.5	5.4 ± 0.2[b]	2.4 ± 0.0[b]
Oleic acid	0	4.0 ± 0.5[a]	3.4 ± 1.1[a]
	1.5	4.6 ± 0.5[a]	3.8 ± 0.1[a]
	3.0	4.5 ± 0.1[a]	4.0 ± 0.4[a]
	4.5	5.1 ± 0.2[b]	4.2 ± 1.2[b]

[a]Not significantly different from control.
[b]Significantly different from the control, $p < 0.05$, $n = 3$.

Table 2: pH value on the last day of the experiment in the reactors with the free cells and the MBR with the encased cells containing different LCFAs at different concentrations.

LCFAs	Conc. (g/L)	pH	
		Free cells	Encased cells
Palmitic acid	0	5.65	5.38
	1.5	5.29	5.11
	3.0	5.14	5.10
	4.5	5.18	4.90
Stearic acid	0	5.97	6.23
	1.5	5.75	6.01
	3.0	5.48	5.72
	4.5	4.81	5.79
Oleic acid	0	5.12	5.84
	1.5	5.61	5.76
	3.0	5.27	5.16
	4.5	5.25	5.20

at the same concentrations of stearic acid added. In both systems with the stearic acid, the pH decreased during the incubation period (Table 2), following the concentration of VFAs (Table 1). Higher pH values were found in MBR system compared to the free cell system. The addition of stearic acid at different concentrations to the bioreactor with the free cell led to decrease in the pH from 5.97 in the control to 4.81 in the reactors with addition of 4.5 g/L stearic acid. The pH in the reactors with the encased cells, however, decreased only from 6.23 in the control to 5.79 in the reactor with the highest concentration of stearic acid.

Similar to stearic acid, increasing the concentration of the oleic acid added to both the systems led to an increase in the total VFA concentration. As for the other LCFAs investigated, and probably for the same reasons, the VFA accumulation was higher in the conventional system with free cells compared to MBR system with encased cells. The VFA concentrations of free cells were higher than 4 g/L in all tested concentrations. In contrast, VFA concentrations higher than 4 g/L in the MBR reactors were observed only in the reactors containing oleic acid at concentrations of 3.0 and 4.5 g/L. However, the pH values measured at the end of the incubations in both systems were not different. These results prove that MBR system with encased cells was superior to the conventional system with free cells as it shows lower percentage of inhibition, lower VFA production, and stabil pH in the presence of all tested LCFA.

In this study, the microbial cells encased in the PVDF membranes displayed less inhibition with palmitic, stearic, and oleic acid compared to the free cells. In the conventional system, the free microbial cells probably had a more direct contact with the inhibitors leading to an adsorption of the inhibitors onto the cell membrane. Gerardi [12] reported that the cell walls of methanogens lacking protective envelopes resulted in inhibitor sensitive cells. This can cause damage to the cells and lead to an unstable digestion process with a low biogas production [7]. At the end of the digestion, the higher VFA concentration in the reactor with the free cells can also be due to the fast degradation by the free cells, being readily exposed to the substrates, including the LCFAs. This resulted in high VFA concentrations in the end, since the more sensitive methanogens could not convert the VFAs as fast as they were produced by the less sensitive acid-forming bacteria. High VFA concentrations in the reactors can inhibit the activity of the methane-forming microorganisms leading to unstable digestion processes [5, 10, 24].

The encased cells in MBR, on the other hand, were protected by a polymeric membrane enclosing the microorganisms. The membrane could likely limit the diffusion of the inhibitors to the cells. Thereby, the microorganisms had a longer time to detoxify the medium by utilizing the LCFAs and VFAs for biogas production and maintaining them at a low concentration close to the cells. At the end of digestion, the lower VFAs concentration allowed the encased cells to perform efficiently without any negative effect from the high concentrations of VFAs; thus, a stable digestion process could be maintained. In addition, method of retaining microbial cells in the membranes provides a high cell density, meaning that the cells-to-LCFA ratio is high, thus, enabling a better acclimatization and detoxification. Alves et al. [25, 32] studied an anaerobic fixed-bed reactor that was used to prevent cells washout. It was shown that retention of cells improved the tolerance of the system in the presence of high concentrations of LCFAs in the wastewater.

It is also possible that the inhibitors could not pass through the cell pellet inside the pouches of the MBR easily, meaning that only a portion of the cells were affected by the adsorption of the inhibitors onto the cell membrane. Protection by the outer layer of cells in a dense cell pellet has previously been reported as a reason for the higher tolerance of encapsulated and flocculating yeast cells to convertible inhibitors during a second generation bioethanol production [33, 34]. Similar phenomena are likely to be present also for the encased anaerobic sludge, tightly packed in between the membrane layers.

At the same time, using membranes as cell supporting material in the MBR may lead to mass transfer limitations during the biodegradation process, especially so in static reactors only shaken once per day. This was evident from the results, with lower accumulated methane yields in the MBR compared to the reactors with free cells. MBR in continuous processes, or in batch reactors with continuous flow of the medium, would however likely display a better performance, enhancing biogas productivity in the presence of LCFAs compared to free cells, as previously observed for other inhibitory substances [15–18].

From the above results, it can be concluded that using PVDF membrane to enclose microbial cells in MBR reduced the inhibitory effects of palmitic, stearic, and oleic acid on the performance of microbial cells in thermophilic anaerobic degradation systems for biogas production. Thus, the degradation of lipid-containing wastes for biogas production can be run in a better balanced system as compared to the conventional system with free cells.

4. Conclusion

Increasing the concentration of LCFAs (palmitic, stearic, and oleic acid) to thermophilic anaerobic batch digesters led to stronger inhibitory effects on the microorganisms. Retaining cells in a membrane bioreactor (MBR) was a successful approach to decreasing the inhibitory effect of LCFAs, since a lower percentage of inhibition and more stable VFA concentration and pH value were found in MBR compared to the conventional system with free cells.

Competing Interests

The authors declare that they have no competing interests.

Acknowledgments

This work was financially supported by the Directorate of Research and Community Service, Ministry of Research, Technology and Higher Education of the Republic of Indonesia through international research collaboration and scientific publication (Grant no. 309/LPPM/2015) and the Swedish Research Council. The authors would like to thank Dr. Johan Westman for his useful discussions.

References

[1] S. G. Pavlostathis, G. Misra, M. Prytula, and D. Yeh, "Anaerobic processes," *Water Environment Research*, vol. 68, no. 4, pp. 479–497, 1996.

[2] I. Angelidaki and B. K. Ahring, "Thermophilic anaerobic digestion of livestock waste: the effect of ammonia," *Applied Microbiology and Biotechnology*, vol. 38, no. 4, pp. 560–564, 1993.

[3] P. Becker, D. Köster, M. N. Popov, S. Markossian, G. Antranikian, and H. Märkl, "The biodegradation of olive oil and the treatment of lipid-rich wool scouring wastewater under aerobic thermophilic conditions," *Water Research*, vol. 33, no. 3, pp. 653–660, 1999.

[4] S.-H. Kim, S.-K. Han, and H.-S. Shin, "Two-phase anaerobic treatment system for fat-containing wastewater," *Journal of Chemical Technology and Biotechnology*, vol. 79, no. 1, pp. 63–71, 2004.

[5] M. Quéméneur and Y. Marty, "Fatty acids and sterols in domestic wastewaters," *Water Research*, vol. 28, no. 5, pp. 1217–1226, 1994.

[6] S. Sayed, J. van der Zanden, R. Wijffels, and G. Lettinga, "Anaerobic degradation of the various fractions of slaughterhouse wastewater," *Biological Wastes*, vol. 23, no. 2, pp. 117–142, 1988.

[7] K. Hanaki, M. O'Nagase, and T. Matsuo, "Mechanism of inhibition caused by long-chain fatty acids in anaerobic digestion process," *Biotechnology and Bioengineering*, vol. 23, no. 7, pp. 1591–1610, 1981.

[8] O. Stabnikova, S.-S. Ang, X.-Y. Liu, V. Ivanov, J.-H. Tay, and J.-Y. Wang, "The use of hybrid anaerobic solid-liquid (HASL) system for the treatment of lipid-containing food waste," *Journal of Chemical Technology and Biotechnology*, vol. 80, no. 4, pp. 455–461, 2005.

[9] L.-J. Wu, T. Kobayashi, Y.-Y. Li, and K.-Q. Xu, "Comparison of single-stage and temperature-phased two-stage anaerobic digestion of oily food waste," *Energy Conversion and Management*, vol. 106, pp. 1174–1182, 2015.

[10] I. W. Koster and A. Cramer, "Inhibition of methanogenesis from acetate in granular sludge by long-chain fatty acids," *Applied and Environmental Microbiology*, vol. 53, no. 2, pp. 403–409, 1987.

[11] A. Rinzema, M. Boone, K. Van Knippenberg, and G. Lettinga, "Bactericidal effect of long chain fatty acids in anaerobic digestion," *Water Environment Research*, vol. 66, no. 1, pp. 40–49, 1994.

[12] M. H. Gerardi, *The Microbiology of Anaerobic Digesters*, John Wiley & Sons, Hoboken, NJ, USA, 2003.

[13] D. Z. Sousa, A. F. Salvador, J. Ramos et al., "Activity and viability of methanogens in anaerobic digestion of unsaturated and saturated long-chain fatty acids," *Applied and Environmental Microbiology*, vol. 79, no. 14, pp. 4239–4245, 2013.

[14] D. Deublein and A. Steinhauser, *Biogas from Waste and Renewable Resources*, Wiley-VCH, Weinheim, Germany, 2008.

[15] R. Wikandari, S. Youngsukkasem, R. Millati, and M. J. Taherzadeh, "Performance of semi-continuous membrane bioreactor in biogas production from toxic feedstock containing d-Limonene," *Bioresource Technology*, vol. 170, pp. 350–355, 2014.

[16] S. Youngsukkasem, J. Akinbomi, S. K. Rakshit, and M. J. Taherzadeh, "Biogas production by encased bacteria in synthetic membranes: protective effects in toxic media and high loading rates," *Environmental Technology*, vol. 34, no. 13-14, pp. 2077–2084, 2013.

[17] S. Youngsukkasem, K. Chandolias, and M. J. Taherzadeh, "Rapid bio-methanation of syngas in a reverse membrane bioreactor: membrane encased microorganisms," *Bioresource Technology*, vol. 178, pp. 334–340, 2015.

[18] S. Youngsukkasem, H. Barghi, S. K. Rakshit, and M. J. Taherzadeh, "Rapid biogas production by compact multilayer membrane bioreactor: efficiency of synthetic polymeric membranes," *Energies*, vol. 6, no. 12, pp. 6211–6224, 2013.

[19] R. Wikandari, S. Gudipudi, I. Pandiyan, R. Millati, and M. J. Taherzadeh, "Inhibitory effects of fruit flavors on methane production during anaerobic digestion," *Bioresource Technology*, vol. 145, pp. 188–192, 2013.

[20] A. Mahboubi, P. Ylitervo, W. Doyen, H. De Wever, and M. J. Taherzadeh, "Reverse membrane bioreactor: introduction to a new technology for biofuel production," *Biotechnology Advances*, vol. 34, no. 5, pp. 954–975, 2016.

[21] T. L. Hansen, J. E. Schmidt, I. Angelidaki et al., "Method for determination of methane potentials of solid organic waste," *Waste Management*, vol. 24, no. 4, pp. 393–400, 2004.

[22] G. Silvestre, J. Illa, B. Fernández, and A. Bonmatí, "Thermophilic anaerobic co-digestion of sewage sludge with grease waste: effect of long chain fatty acids in the methane yield and its dewatering properties," *Applied Energy*, vol. 117, pp. 87–94, 2014.

[23] J. A. Lalman and D. M. Bagley, "Anaerobic degradation and inhibitory effects of linoleic acid," *Water Research*, vol. 34, no. 17, pp. 4220–4228, 2000.

[24] H.-S. Shin, S.-H. Kim, C.-Y. Lee, and S.-Y. Nam, "Inhibitory effects of long-chain fatty acids on VFA degradation and β-oxidation," *Water Science and Technology*, vol. 47, no. 10, pp. 139–146, 2003.

[25] M. M. Alves, J. A. Mota Vieira, R. M. Alvares Pereira, M. A. Pereira, and M. Mota, "Effects of lipids and oleic acid on biomass development in anaerobic fixed-bed reactors. Part II: oleic acid toxicity and biodegradability," *Water Research*, vol. 35, no. 1, pp. 264–270, 2001.

[26] C.-S. Hwu, B. Donlon, and G. Lettinga, "Comparative toxicity of long-chain fatty acid to anaerobic sludges from various origins," *Water Science and Technology*, vol. 34, no. 5-6, pp. 351–358, 1996.

[27] A. Pereira, M. Mota, and M. Alves, "Degradation of oleic acid in anaerobic filters: the effect of inoculum acclimatization and biomass recirculation," *Water Environment Research*, vol. 73, no. 5, pp. 612–621, 2001.

[28] M. A. Pereira, O. C. Pires, M. Mota, and M. M. Alves, "Anaerobic biodegradation of oleic and palmitic acids: evidence of mass transfer limitations caused by long chain fatty acid accumulation onto the anaerobic sludge," *Biotechnology and Bioengineering*, vol. 92, no. 1, pp. 15–23, 2005.

[29] D. Traversi, S. Villa, E. Lorenzi, R. Degan, and G. Gilli, "Application of a real-time qPCR method to measure the methanogen concentration during anaerobic digestion as an indicator of biogas production capacity," *Journal of Environmental Management*, vol. 111, pp. 173–177, 2012.

[30] D. G. Cirne, X. Paloumet, L. Björnsson, M. M. Alves, and B. Mattiasson, "Anaerobic digestion of lipid-rich waste-effects of lipid concentration," *Renewable Energy*, vol. 32, no. 6, pp. 965–975, 2007.

[31] C.-N. Weng and J. S. Jeris, "Biochemical mechanisms in the methane fermentation of glutamic and oleic acids," *Water Research*, vol. 10, no. 1, pp. 9–18, 1976.

[32] M. M. Alves, J. A. M. Vieira, R. M. Á. Pereira, M. A. Pereira, and M. Mota, "Effect of lipids and oleic acid on biomass development in anaerobic fixed-bed reactors. Part I: biofilm growth and activity," *Water Research*, vol. 35, no. 1, pp. 255–263, 2001.

[33] J. O. Westman, N. Bonander, M. J. Taherzadeh, and C. J. Franzén, "Improved sugar co-utilisation by encapsulation of a recombinant *Saccharomyces cerevisiae* strain in alginate-chitosan capsules," *Biotechnology for Biofuels*, vol. 7, no. 1, article 102, 2014.

[34] J. O. Westman, V. Mapelli, M. J. Taherzadeh, and C. J. Franzén, "Flocculation causes inhibitor tolerance in *Saccharomyces cerevisiae* for second-generation bioethanol production," *Applied and Environmental Microbiology*, vol. 80, no. 22, pp. 6908–6918, 2014.

Hindawi Publishing Corporation
BioMed Research International
Volume 2016, Article ID 7631458, 12 pages
http://dx.doi.org/10.1155/2016/7631458

Research Article

Complex Approach to Conceptual Design of Machine Mechanically Extracting Oil from *Jatropha curcas* L. Seeds for Biomass-Based Fuel Production

Ivan Mašín and Michal Petrů

Institute for Nanomaterials, Advanced Technologies and Innovation, Technical University of Liberec, 46117 Liberec, Czech Republic

Correspondence should be addressed to Michal Petrů; michal.petru@tul.cz

Received 27 May 2016; Accepted 5 July 2016

Academic Editor: Rong-Gang Cong

One of important sources of biomass-based fuel is *Jatropha curcas* L. Great attention is paid to the biofuel produced from the oil extracted from the *Jatropha curcas* L. seeds. A mechanised extraction is the most efficient and feasible method for oil extraction for small-scale farmers but there is a need to extract oil in more efficient manner which would increase the labour productivity, decrease production costs, and increase benefits of small-scale farmers. On the other hand innovators should be aware that further machines development is possible only when applying the systematic approach and design methodology in all stages of engineering design. Systematic approach in this case means that designers and development engineers rigorously apply scientific knowledge, integrate different constraints and user priorities, carefully plan product and activities, and systematically solve technical problems. This paper therefore deals with the complex approach to design specification determining that can bring new innovative concepts to design of mechanical machines for oil extraction. The presented case study as the main part of the paper is focused on new concept of screw of machine mechanically extracting oil from *Jatropha curcas* L. seeds.

1. Introduction

The use of bioenergy as energy derived from biofuels in the world permanently increases [1, 2]. Biomass-based fuels as renewable organic source of bioenergy have advantages (e.g., no harmful carbon dioxide emissions, reduction of dependency on fossil fuels, and versatility) and some disadvantages (e.g., requiring more land, relative ineffectiveness when compared to gasoline, and problematic supply chain) as well [3–6]. One of important sources of biomass-based fuel is *Jatropha curcas* L. [7–10]. *Jatropha curcas* L. is crop with inconsiderable potential due to its high oil content, rapid growth, easy propagation, drought tolerant nature, ability to grow and reclaim various types of land, need for less irrigation and less agricultural inputs, pest resistance, short gestation periods, and suitable traits for easy harvesting enumerated [11]. Biooil extracted from *Jatropha curcas* L. seeds has positive chemical properties (e.g., better oxidative stability compared to soybean oil, lower viscosity than castor oil, and lower pour point than palm oil) [12]. *Jatropha* significant advantage is that it is one of the cheapest sources for biodiesel production (compared to palm oil, soybean, or rapeseed) [13]. On the other hand former and recent findings [14–17] also show that researchers, economists, biochemists, farmers, machine designers, and biofuel producers should not just automatically follow the initial *Jatropha* hype but critically reflect on, for example, current economic situation, state biofuel policy, institutional factors, labour costs, water irrigation, local differences, and last but not least farmer's needs. The evaluations [15], for example, opened many questions connecting with *Jatropha* processing profitability. One of the recommendations in [15] mentioned mechanised extraction as the most efficient and feasible method for oil extraction for small-scale farmers. Consequently one of the strategies of how to produce biofuel from *Jatropha curcas* L. in more efficient manner is to increase the effectiveness of oil pressing process, which would increase the benefits of small-scale farmers. This objective can be achieved through the further innovations of mechanical expellers or presses for small-scale farmers. Due to the great attention paid to

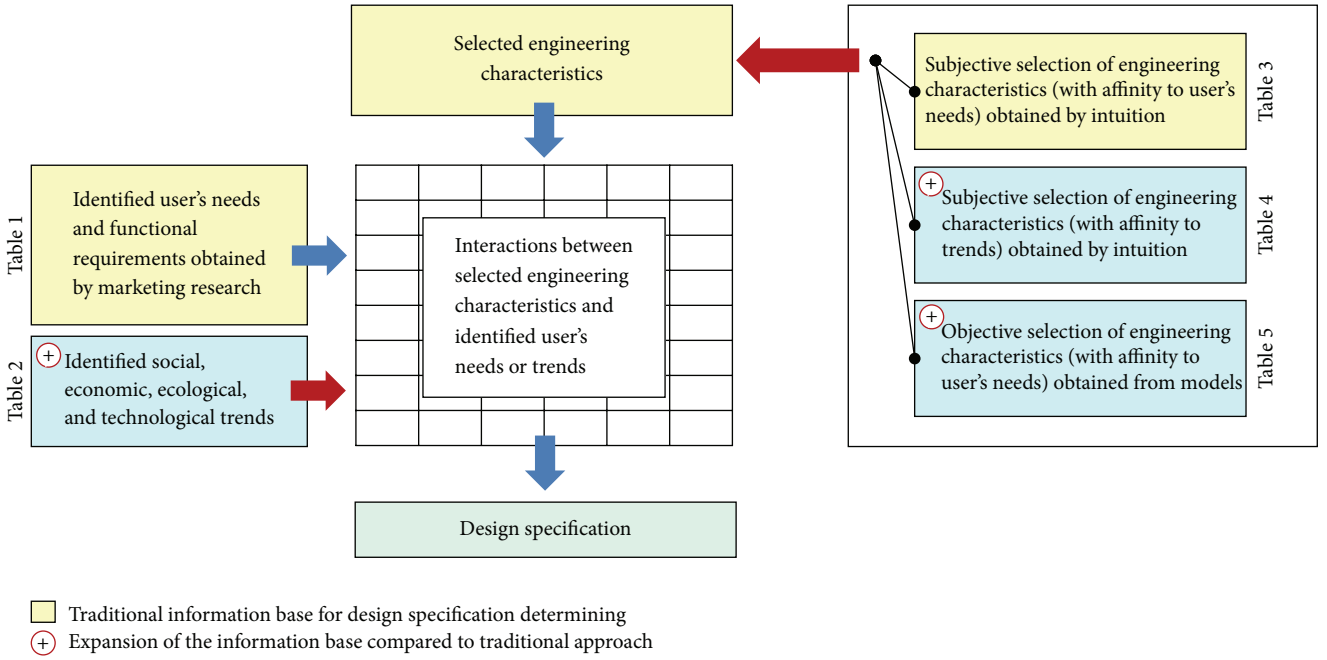

Figure 1: Complex approach to design specification determining with expanded information base.

this issue [18–26] innovators should be aware that further *Jatropha*-presses development is possible only when applying the systematic approach and design methodology in all stages of engineering design as an essential part of *Jatropha*-press life-cycle. Systematic approach in this case means that designers and development engineers rigorously apply scientific knowledge, integrate different constraints and user priorities, carefully plan product and activities, and systematically solve technical problems. Basic phases of the engineering design process have been in the past developed into more detailed procedures focused on the systematic development [27–33], on creative solution of technical problems [34–37], or on the preliminary and detailed embodiment design [38–40]. The correct definition of the right problem in the form of design specifications is widely regarded as a decisive step towards the effective implementation of all engineering design procedures [41–43]. Two information transformations are required to determine design specification. During the first information transformation the user's needs are translated to functional requirements. The second information transformation takes place when converting the functional requirements to machine characteristics (design specifications) that have been selected to ensure fulfilment of specified functional requirements. By performing these transformations design assignment is then defined as an information input to concept generation phase and subsequent detailed designing. During this process various methods such as marketing research [44, 45], voice of customer (VOC) [46, 47], usability testing (thinking aloud protocol) [48, 49], Kansei engineering [50, 51], or quality function deployment (QFD) [52–54] are systematically utilized. Innovation science using function-object analysis [55, 56] or main parameter value [57] is also important to mention. For the conceptual design phase of innovation process is suitable to use modern creative techniques supporting idea generation and overcoming technical and physical contradictions based on TRIZ [58–61]. The process of concept generation is finished by choosing between concept alternatives by simple evaluation charts [28] or advanced techniques or analytic hierarchy process [4]. Since the above methods are becoming standards when upgrading technical products in 21st century it is clear that further development and innovation of machine for mechanical extraction of oil from *Jatropha curcas* L. require similar advanced techniques and methods.

2. Complex Approach to Design Specification and Concept Generation

Generation of the new technical product concept is in general carried out in the following two steps:

1st step: target design specification determining

2nd step: system or components concept(s) generation

In the first step the information transformations described in the Introduction take place. Abovementioned approaches [42, 44–54] to these transformations of needs to design specification are often focused only on the transformation of the primary needs formulated intuitively and subjectively by users during marketing research or on the evaluation of attributes of competing products (Figure 1).

In today's world of technology, which leads to accelerated development, for example, in technologies or material science, to include to the mentioned transformations only information from users (farmers) or information about other similar products is insufficient. That is because users do not have

Figure 2: Typical machines mechanically extracting oil from *Jatropha curcas* L. seeds.

and cannot have sufficient knowledge of the possibilities of current technologies or have not access to information about trends in the relevant fields of technology. Users (farmers) can only guess at what is possible in present and near future design. For that reason it is necessary to enrich traditional approach to determination of the design specification. First technological, ecological, economic, and social trends should be included in a set of functional requirements (needs)—Figure 1. Second relevant engineering characteristics with affinity to technological, social, or economic trends should be involved into process of design specification determining as well (Figure 1). Third designers should additionally include information obtained by modelling that can objectively on the basis of physical and chemical laws extend set of suitable engineering characteristics describing future machine (Figure 1).

After design specification determining logical process of problem solving or progressive techniques supporting designer's creativity should be used to obtain a concept of innovative solution. Among these techniques we can include

(i) function oriented search [62] or function-behaviour oriented search [63],

(ii) 40 inventive principles and heuristics [64, 65],

(iii) laws or trends of evolution of technical systems [66, 67],

(iv) multilevel system thinking [68, 69],

(v) morphological matrix [70] or solution catalogue [71].

Utilization of the described complex approach to design specification and concept generation will be partially demonstrated on machine extracting oil from *Jatropha curcas* L. seeds for small-scale producers or farmers.

3. Case Study: Conceptual Design of Machine Mechanically Extracting Oil from *Jatropha curcas* L. Seeds in Small-Scale

Basic functions of the mechanical extraction machine consist in separating the solid component (structures) and liquid component (oil). Linear or nonlinear pressing (vertical, horizontal, or angled) by a sliding piston or rotary screw is frequently used for small-scale production. As the technological set-up for *Jatropha* processing is not yet fully developed and progress may be made in terms of mechanisation [15] we present mentioned complex approach in the following case study focused on conceptual design of screw extractor press extracting biooil from *Jatropha curcas* L. seeds for small-scale production. First, the research team analysed sources [7–9, 13–17, 19] and information obtained during interview realized in Sumatra and Java (Indonesia)—Figure 2. Low production cost [14], high productivity [16], and higher oil yield [19] were considered as essential extracting machines user's needs (Table 1).

In accordance with the principles described in Section 2 (Figure 1) the set of primary user's needs was subsequently extended by trends in the production of oil and biofuel from *Jatropha curcas* L. At extraction machine attributes determining process not only the primary user's needs, but also "unexpected" needs based on technological, economic, social, or ecological trends were taken into account. By the research of [7, 16, 18, 19] and by interviews made in Indonesia we identified the following trends:

(i) Trend to higher degree of cleaning of crude oil from solid particles (husks) [7, 19]

(ii) Trend to lower oil content in the seed cake [8]

(iii) Trend to necessary competition with big corporations [16]

(iv) Trend to commercial use of the seed cake after oil extraction [18]

(v) Trend to mechanical separating kernels and husks [19]

(vi) Trend to more profitable technology [19]

Interpretation of these trends upon their integration is shown in Table 2.

The next step in the process of design specification determination was to select appropriate engineering characteristics with affinity to identified primary user's needs and trends. First measurable engineering characteristics of the innovated extraction machine with affinity to interpreted user's needs were subjectively and intuitively selected by traditional approach (Table 3).

Table 1: Decomposition and interpretation of primary user's needs (machines mechanically extracting oil).

Primary user's need	Need decomposition	Interpretation of need (requirement)
Low operational cost	Operated by unskilled worker	Low demand for qualification
	Low energy consumption	Low power (fuel) consumption
	High availability	Low failure rate
	Long lifetime	Long lifetime of machine parts
High productivity	High labour productivity	Low manual work intensity
	Fast filling up of machine	Fast filling up of machine bin
	Fast and easy cleaning	Fast and easy cleaning of chamber
	Easy spare parts replacement	Quick parts disassembly or assembly
High yield of quality oil	High oil yield	High efficiency of extraction
	Low waste	High degree of seeds utilization
	Clean oil	Low volume of impurities

Table 2: Decomposition and interpretation of identified trends.

Identified trend	Trend decomposition	Interpretation of trend (requirement)
Husks removal	Husks separation	Stop husk
	Husks removing	Move husk
	Impurities separation	Stop impurity
Better utilization of seed cake	Obtain oil from seed cake	Wring out seed cake
	Control of the seed cake composition	Bind enzymes in the seed cake
	Seed cake processing	Form seed cake
More profitable oil extraction	Reduce operational costs	Run autonomously
	Integrate activities	Integrate operations

Table 3: Selected engineering characteristics with affinity to interpreted user's needs.

Engineering characteristic	Unit
Extraction capacity	kg/hr
Relative manual operation time	min/t
Seeds silo volume	m^3
Oil tank volume	m^3
Active/loaded part (dis)assembly time	min
Relative energy consumption	kW/t
Oil yield	%
Mean time to failure	hr
Time for chamber cleaning	min

Table 4: Selected engineering characteristics with affinity to interpreted trends.

Engineering characteristic	Unit
Seed cake thickness	mm
Volume of the husks elements in the oil	%
Time of autonomous machine run	min
Volume of impurities in the oil	%
Volume of residual oil in seed cake	%
Volume of enzymes in the seed cake	%

Consequently measurable engineering characteristics of the innovated machine for oil extraction from *Jatropha curcas* L. with affinity to interpreted trends were subjectively and intuitively selected (Table 4).

As mentioned in Section 2, it is important to include phenomena occurring during oil extraction into process of design specification setting (Figure 1). Intuitively and subjectively selected engineering characteristics listed in Tables 3 and 4 were subsequently extended by set of characteristics obtained during an objective study of appropriate physical and mathematical models describing relevant phenomena and processes. In that case we use the following models:

Model Nr. 1: model for pressing the seeds in a container (Figure 3)

Model Nr. 2: Perzyna model for the study of the deformation and compression of seed (Figure 4)

Model Nr. 3: determination of oil region for maximum oil yield (Figure 5)

Model Nr. 4: determination of compressive force to press different state seeds (Figure 6)

Model Nr. 5: representation of the volume strain, the compressive energy, and volume compressibility during seeds pressing (Figure 7)

It is known that the volumetric strain and deformation of seeds increase the stress and energy intensity. Petrů et al. and Herak et al. [24, 72] set bound of oil region between

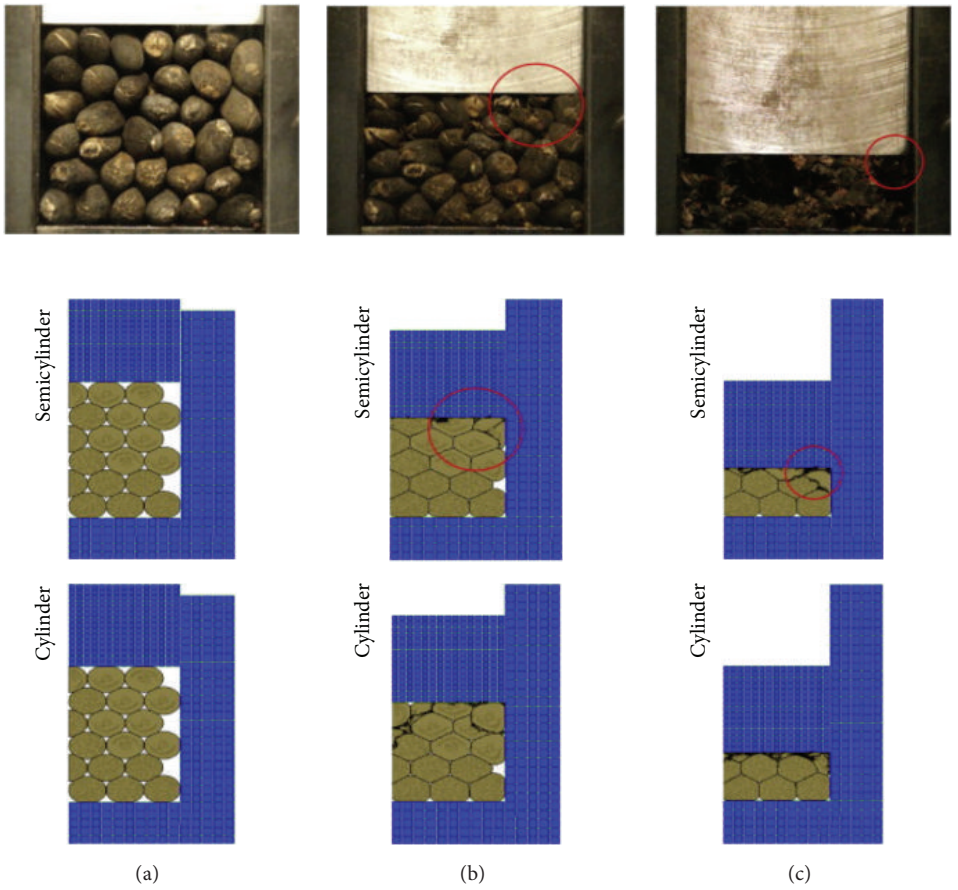

Figure 3: FEM model for pressing the seeds in a container [24].

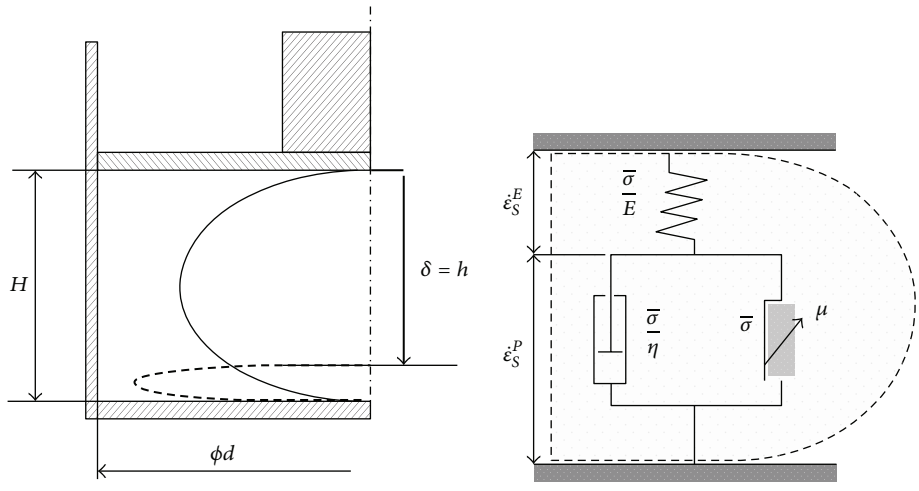

Figure 4: Perzyna model for the study of the deformation and compression of seed [23].

lower oiliness point (LOP = 40%) and upper oiliness point (UOP = 80%)—Figure 5. From Figures 5 and 6 it is apparent that the increase in oil yield is possible by increasing the compressive force.

Based on the analysis of enumerated physical and mathematical models other important engineering characteristics were identified. These characteristics used for the complex approach to design specification determination are summarized in Table 5.

The number of identified engineering characteristics (Tables 3, 4, and 5) was then reduced by characteristics of integration (e.g., silo and tank volume and autonomous

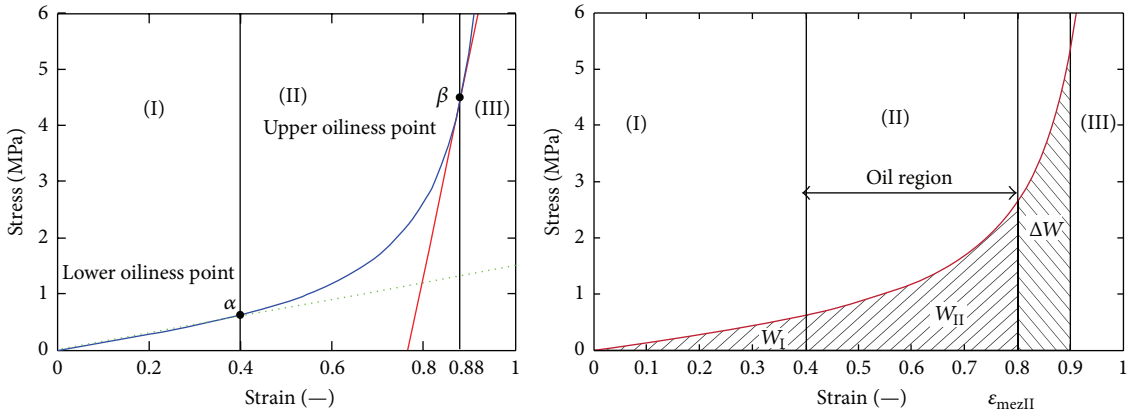

Figure 5: Oil region for maximum oil yield [72].

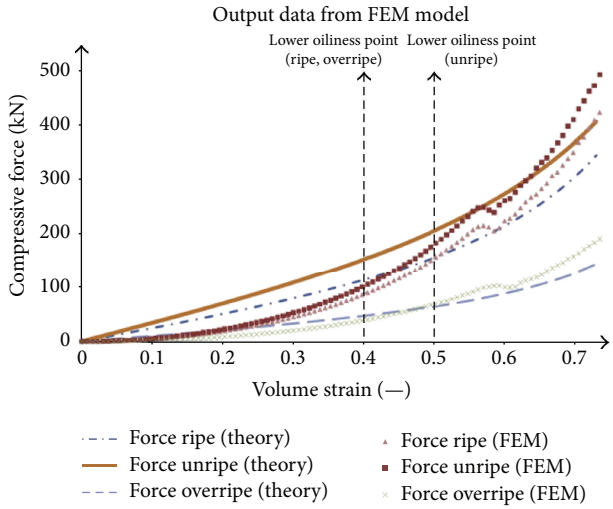

Figure 6: Determination of compressive force to press the seed (ripe, unripe, and overripe) [23].

Table 5: Engineering characteristics determined by analysis of physical and mathematical models.

Engineering characteristic	Unit
Friction between the wall of the chamber and the seed	—
Surface friction between the tool and the seed	—
Angle between the longitudinal axis of the seed and the surface of the tool	∘
Compressive stress during pressing ripe seeds	MPa
Compressibility	MPa^{-1}
Compressive force for pressing seeds	kN
Volume compressive energy	$J\,mm^3 \cdot 10^{-3}$
Average diameter of the solid particles in the oil	μm
Degree of degradation of the oil	Mw

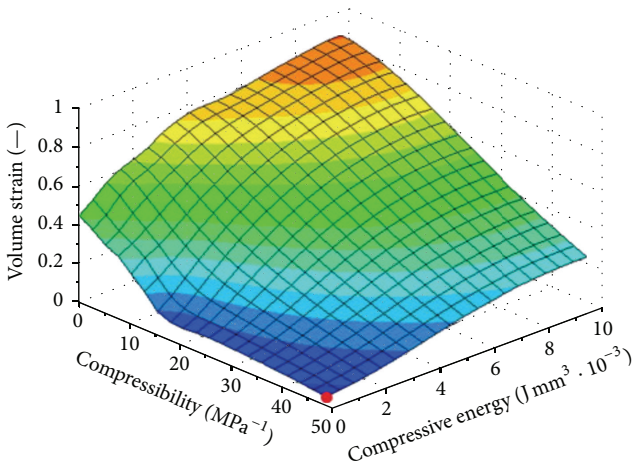

Figure 7: Parametric representation of the volume strain, the compressive energy, and volume compressibility during pressing seeds [24].

machine run) or by review of their affinity to identified requirements. Selected characteristics should have to ensure that the new innovated machine will better satisfy small-scale producers or farmers. In accordance with the complex approach described in Section 2 correlation matrix for detection and evaluation of interactions between engineering characteristics and requirements (interpreted needs or trends) was prepared (Figure 8). This matrix indicates how engineering characteristics affect the satisfaction of each requirement. Compared to the standardized QFD method [52–54] a comparison with competing products both in terms of information from the market and in the context of comparing engineering characteristics has not been conducted. The degree of importance (1 = min, 10 = max) of small-scale farmers individual requirement was based on expert subjective opinion of research team members which is the usual procedure.

The significance of individual engineering characteristics was calculated by standard manner as the sum of the products of the degree of importance of requirement and correlation intensity (e.g., strong, medium, weak, or nonexistent). The

Requirements	Degree of importance	Engineering characteristics: Extraction capacity	Relative manual operation time	Active/loaded part (dis)assembly time	Relative energy consumption	Oil yield	Mean time to failure	Time for chamber cleaning	Seed cake thickness	Volume of the husks elements in the oil	Time of autonomous machine run	Volume of impurities in the oil	Volume of residual oil in seed cake	Volume of enzymes in the seed cake	Friction between the wall of the chamber and the seed	Surface friction between the tool and the seed	Angle between the long axis of seed and surface of the tool	Compressive stress during pressing seeds	Compressibility	Compressive force for pressing seeds	Volume compressive energy	Average diameter of the solid particles in the oil	Degree of degradation of the oil
Low demand for qualification	7	1	3	9	0	1	9	9	0	1	9	3	1	1	0	0	0	1	0	1	0	1	3
Low power consumption (fuel)	8	3	1	1	9	9	3	1	3	1	1	3	3	3	3	3	9	9	9	9	9	3	3
Low failure rate	6	3	1	3	1	1	9	3	3	3	9	3	1	1	3	3	3	9	3	9	9	1	0
Long lifetime of machine parts	6	3	1	3	1	0	9	1	3	3	3	1	1	1	3	3	3	9	3	9	9	1	0
Low manual work intensity	10	9	9	9	3	9	9	9	3	9	9	3	3	3	1	1	3	9	9	9	9	3	3
Fast filling up of machine bin	6	3	9	0	0	0	0	1	0	0	3	0	0	0	0	0	1	0	3	1	0	0	0
Fast and easy cleaning of chamber	6	1	9	1	0	1	1	9	1	3	3	3	0	1	9	3	3	3	3	3	3	3	1
Quick parts disassembly or assembly	6	1	9	9	0	0	1	1	0	1	3	0	0	0	1	1	1	1	3	1	1	3	0
High efficiency of extraction	10	9	3	1	3	9	3	1	3	3	1	9	3	3	1	1	3	9	9	9	9	3	3
High degree of seeds utilization	10	3	1	0	0	9	0	1	9	3	1	3	3	3	3	3	3	9	9	9	9	3	9
Low volume of impurities	8	3	0	0	0	3	1	3	1	3	0	9	1	1	3	3	3	3	3	3	3	9	3
Stop husk	8	3	3	0	0	3	0	0	1	9	0	3	1	1	3	3	1	3	3	3	1	3	1
Move husk	4	1	3	0	3	1	3	0	1	9	0	1	0	0	3	3	1	3	3	1	1	0	0
Stop impurity	8	3	3	0	0	3	0	0	1	3	0	9	1	1	1	1	1	3	1	1	1	9	1
Wring out seed cake	5	3	1	0	3	9	0	0	9	1	0	1	9	3	3	3	3	9	9	9	9	1	3
Bind enzymes in the seed cake	4	0	0	0	3	1	0	0	3	1	0	0	3	9	3	3	1	3	3	3	3	3	3
Form seed cake	3	1	1	0	3	3	0	0	9	1	1	0	9	3	3	3	3	9	9	9	9	1	1
Run autonomously	7	3	9	3	3	3	9	3	1	3	9	1	1	3	0	0	0	1	3	1	0	3	1
Integrate operations	5	3	3	1	3	1	3	3	3	9	9	1	1	3	1	1	1	1	3	+3	3	3	1
	Importance	437	479	293	228	521	425	331	350	459	418	426	253	259	279	243	305	661	620	653	617	393	283
	Relative importance	4.9%	5.4%	3.3%	2.6%	5.8%	4.8%	3.7%	3.9%	5.1%	4.7%	4.8%	2.8%	2.9%	3.1%	2.7%	3.4%	7.4%	6.9%	7.3%	6.9%	4.4%	3.2%
	Direction of improvement	↑	↓	↓	↓	↑	↑	↓	↓	↓	↑	↓	↓	↑	↓	↓	•	↓	↓	↓	↓	↓	↓
	Target value					72												1.4	0.21	70	3.5		
	Unit	kg/hr	min/t	min	kW/t	%	hr	min	mm	%	min	%	%	%	—	—	∘	MPa	MPa^{-1}	kN	$Jmm^3 \cdot 10^{-3}$	μm	Mw

Correlation intensity
9 pts: strong
3 pts: medium
1 pt: low
0 pts: none

Figure 8: Correlation matrix used for design specification of machine mechanically extracting oil from *Jatropha curcas* L. seeds.

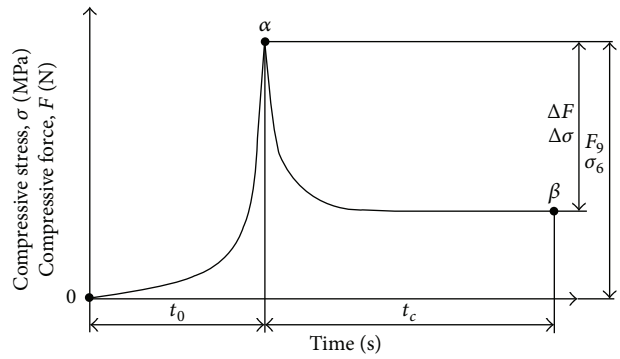

Figure 9: Compression and relaxation during oil seeds pressing [72].

resulting correlation matrix (Figure 8) showed that in terms of the functional requirements imposed on the machine mechanically extracting oil from seeds of *Jatropha curcas* L. the most important engineering characteristics are

(i) compressive stress during pressing seeds (absolute importance 661),

(ii) compressive force for pressing seeds (absolute importance 653),

(iii) compressibility (absolute importance 620),

(iv) volume compressive energy (absolute importance 617),

(v) oil yield (absolute importance 551).

These important engineering characteristics were considered by the research team as the essential and relevant target numeric values were set as design specification for upgrading the machine mechanically extracting oil from *Jatropha curcas* L. seeds. As the design of the proper screw (chamber) plays the most important role in the oil extraction efficiency we will pay in next part of the paper attention to the new concept of screw design.

It is known [72] that the process of oil extraction from *Jatropha curcas* L. seeds can be streamlined by using changes of pressing force at a time, that is, by compression and subsequent relaxation (Figure 9). This can be technically ensured by designing the various pressing chambers known [73] and by changing the geometry of the screw as shown in Figure 10. The distribution of oil yield in individual chambers of the press machine is also illustrated in Figure 10.

However, the problem arises due to enormous rise of temperature caused by the friction among seeds, chamber walls, and tool and especially due to increase of the compression energy required for the extraction of oil regarding the maximum compressive space in maximum recovery of oil (Figures 11 and 12).

For assessment and visualization of maximum theoretical volumetric oil yield the numerical model was created (Figure 11). The model shows the unit distribution of oil yield (max = 1, min = 0) in the individual chambers of the press, whose design is similar to press in Figure 10. The model illustrates one of the principal problems of mechanical oil pressing that occurs when the compression energy necessary for extruding the oil is increasing beyond a certain limit. According to the presented numerical model (Figure 11) it is ideally apparent that minimum oil yield can be achieved in the chambers with a lower filling and vice versa maximum oil yield (97.5%) can be achieved in the chambers with a higher filling. In real conditions of oil extraction this maximal oil yield is not achieved due to the fact that standard extraction presses are not able to provide the required compression energy. The reason for this oil yield limitation is that forces and stress exponentially increase in relation to the compression (Figures 5 and 6). From the point of view of oil extraction efficiency a new concept of machine mechanically extracting oil from *Jatropha curcas* L. seeds should therefore solve technical problems rising in the chamber with the largest filling where compressive stress and compressive energy are the highest. Unequal loading of the individual chambers of the oil extracting machine is also seen from streamlines courses in Figure 12. Low compression energy will be generated on the left side of the working zone (area A in Figure 12), while the highest compression energy will be generated on the right side of the working zone close to the outlet nozzle of oil extracting machine (area B in Figure 12).

Not only do the above phenomena cause technical problems (maximum force acting on parts of the machine), but increased temperature also causes oil degradation, change in its chemical composition, and the subsequent quality deterioration of the oil for the production of biofuel. Due to these phenomena design of the extraction machine screw and chamber shown in Figure 10 cannot be fully used and therefore maximum oil recovery cannot be achieved by this solution (we gain yield around 40–65%).

To solve this technical problem we used the following two techniques of innovation science:

(i) Trends of evolution of technical systems—statistically authentic evolution lines describing the regular evolutionary transition of systems from one specified state to another, being true for all technical (engineering) systems [58].

(ii) Inventive principles—each inventive principle represents concept or idea that may be applied to solve the problem situation; it means to remove technical contradiction [64, 68]. Technical contradiction is formed when there is an obstacle to making an improvement.

Using these techniques following directions of solution have been identified:

(i) Asymmetry (symmetry change): change the shape or properties of an object from symmetrical to asymmetrical or change the shape of an object to suit external asymmetries.

(ii) Dynamics: change the object (or outside environment) for optimal performance at every stage of operation, divide an object into parts capable of movement

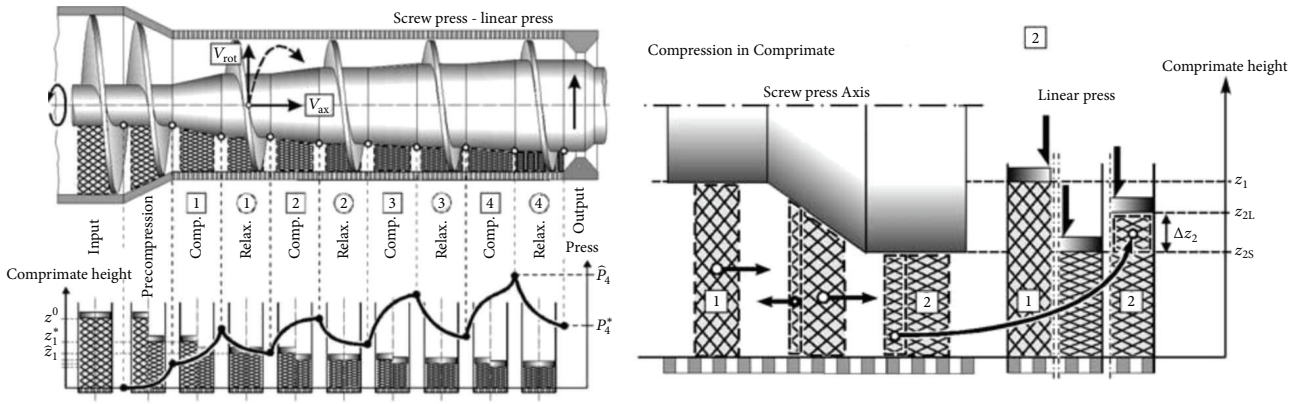

Figure 10: Variable geometry of compression chamber geometry and screw [73].

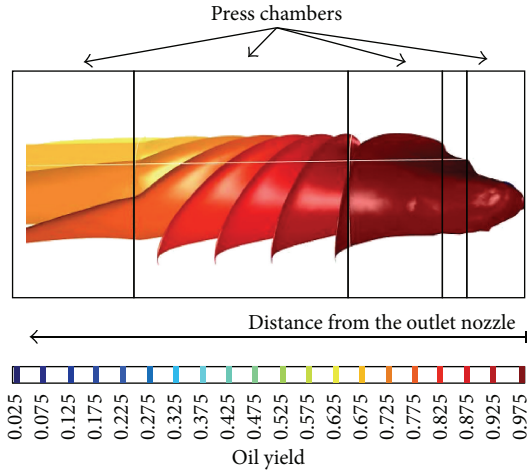

Figure 11: Visualization of the oil yield depending on the compression volume of chambers.

relative to each other, or increase the degree of free motion.

(iii) Another dimension: move into an additional dimension—from one to two—from two to three or use the other side.

(iv) Periodic action: instead of continuous action, use periodic or pulsating action.

(v) Porosity: make an object porous or add porous elements.

With creative support of these heuristics a concept of solution of mentioned problem was prepared. Problem and cause of lower oil yield could be resolved by automatically opening one or more grooves for discharging solid particles (hulks, impurities) in the body of the screw (Figure 13). The grooves would be opened when compressive energy is high and the grooves would be closed automatically when the compressive power is under certain level. A conceptual comparison of traditional screw design and two variants of innovated screw is illustrated in Figure 13. Effects of presented new variants of screw geometry and the number of grooves are shown in Figures 14 and 15.

4. Conclusions

Big attention should be paid to the systematic design of machines used in the process-chain for biomass fuel production. Without a more complex approach to design specification and concept generation machines for mechanical extracting oil from seeds (biospecies) cannot accomplish the necessary efficiency or productivity and in particular small-scale producers cannot achieve desired profitability. It is useful to include extended information base into determination of design specification. Standard information base should be enriched by technological, ecological, economic, and social trends and by information obtained by modelling that can objectively on the basis of physical and chemical laws extend set of suitable engineering characteristics describing parameters of future machines. In the case of machine mechanically extracting oil from *Jatropha curcas* L. seeds concept generation known and entirely new models were employed. These models refined original theoretical considerations and were consequently used to illustrate the relationship between compression force, compression energy, and new shapes of extraction machine screw. Using the model shows new possibilities for improving the pressing process towards a maximum yield of oil for biomass-based fuel production. It was also confirmed that it is appropriate and necessary to use advanced tools of innovation science as inventive principles or trends of evolution of technical systems. By the complex approach to design specification and concept generation the new concept of screw shape was proposed. Since presented case study shows the big potential in terms of utilization modelling and innovation science techniques it is necessary to continue with focused research to improve machinery performance and thus support small-scale farmers or biomass-based fuel produces.

Competing Interests

The authors declare that they have no competing interests.

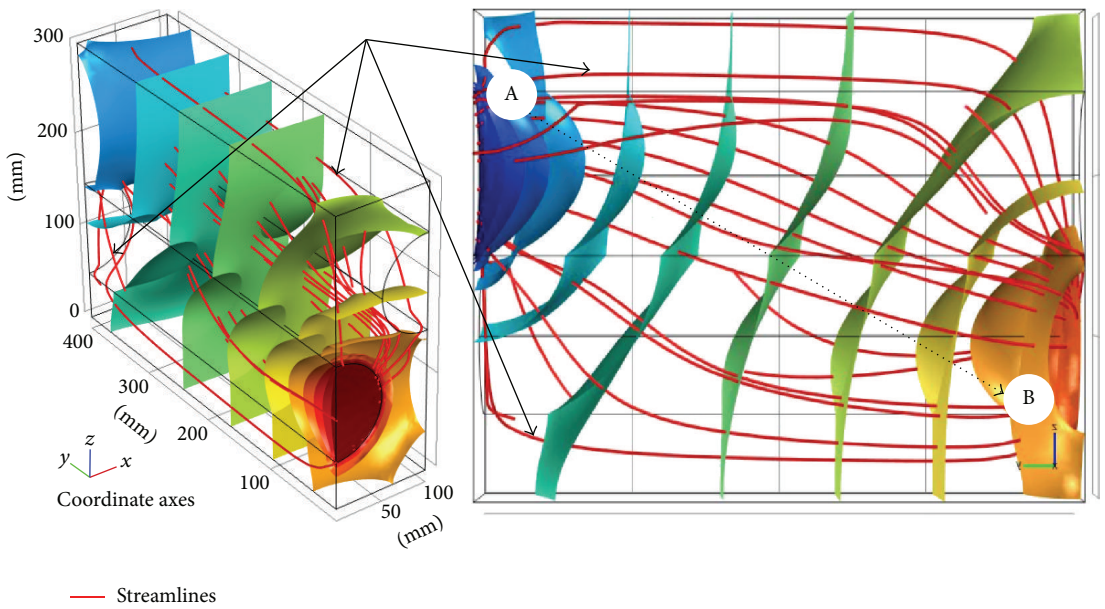

Figure 12: Numerical model—visualization of the maximum compressive energy required in the oil extracting machine depending on the compression volume of chamber (A—area with the lowest compressive energy and stress distribution in the working zone of oil extracting machine; B—area with the highest compressive energy and stress distribution in the working zone of oil extracting machine).

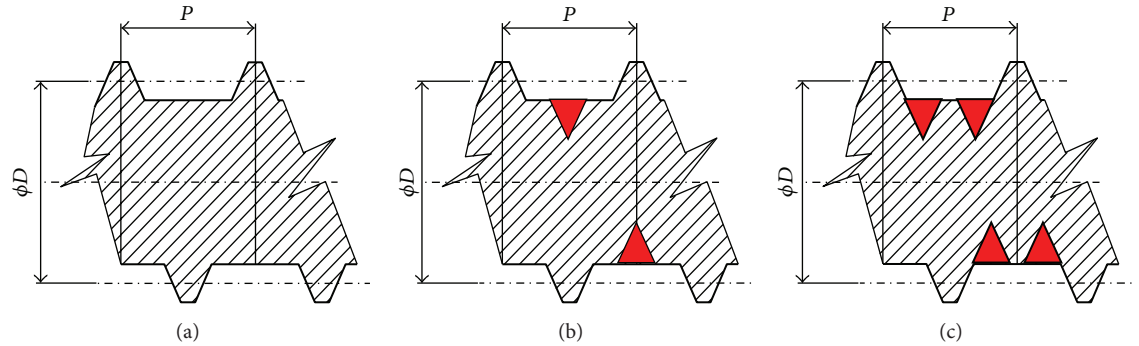

Figure 13: Traditional solution of screw and new concept of screw for machine mechanically extracting oil from *Jatropha curcas* L. seeds: (a) standard screw design, (b) screw design with one groove for decrease of compressive force and expended energy reduction, and (c) screw design with two grooves for decrease of compressive force and expended energy reduction.

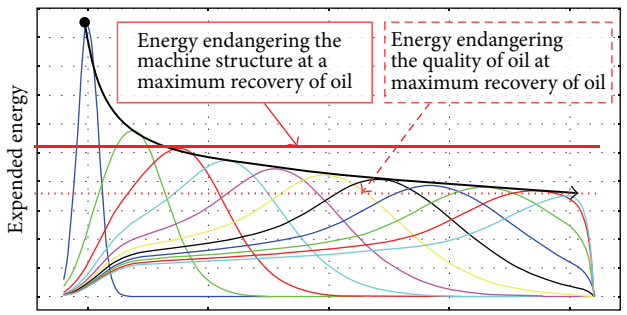

Figure 14: Courses of expended energy using the original screw geometry (dark blue) and using the new design concept with modified geometry of the screw with one groove in multiple variations of groove shape (other colours).

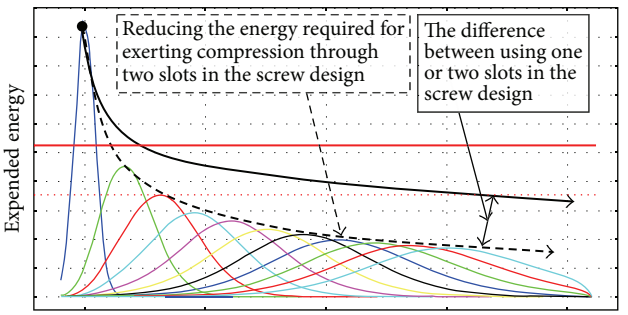

Figure 15: Courses of expended energy using the original screw geometry (dark blue) and using the new design concept with modified geometry of the screw with two grooves in multiple variations of groove shape (other colours).

Acknowledgments

The activities of this project LO1201 were financed with cofunding from the Ministry of Education, Youth and Sports (Czech Republic) as part of targeted support from the "National Sustainability Program I" programme.

References

[1] M. K. Alavijeh and S. Y. Yaghmaei, "Biochemical production of bioenergy from agricultural crops and residue in Iran," *Waste Management*, vol. 52, no. 6, pp. 375–394, 2016.

[2] C. M. T. Johnston and G. C. van Kooten, "Global trade impacts of increasing Europe's bioenergy demand," *Journal of Forest Economics*, vol. 23, no. 2, pp. 27–44, 2016.

[3] E. J. S. Mitchell, A. R. Lea-Langton, J. M. Jones, A. Williams, P. Layden, and R. Johnson, "The impact of fuel properties on the emissions from the combustion of biomass and other solid fuels in a fixed bed domestic stove," *Fuel Processing Technology*, vol. 142, no. 2, pp. 115–123, 2016.

[4] Z. Wang, T. Lei, X. Chang et al., "Optimization of a biomass briquette fuel system based on grey relational analysis and analytic hierarchy process: a study using cornstalks in China," *Applied Energy*, vol. 157, pp. 523–532, 2015.

[5] Berkeley Biodiesel, "Advantages and disadvantages of biodiesel fuel," 2016, http://www.berkeleybiodiesel.org/advantages-and-disadvantages-of-biodiesel.html.

[6] A. Rimkus, J. Žaglinskis, P. Rapalis, and P. Skačkauskas, "Research on the combustion, energy and emission parameters of diesel fuel and a biomass-to-liquid (BTL) fuel blend in a compression-ignition engine," *Energy Conversion and Management*, vol. 106, no. 12, pp. 1109–1117, 2015.

[7] N. Contran, L. Chessa, M. Lubino, D. Bellavite, P. P. Roggero, and G. Enne, "State-of-the-art of the *Jatropha curcas* productive chain: from sowing to biodiesel and by-products," *Industrial Crops and Products*, vol. 42, no. 1, pp. 202–215, 2013.

[8] A. S. Silitonga, A. E. Atabani, T. M. I. Mahlia, H. H. Masjuki, I. A. Badruddin, and S. Mekhilef, "A review on prospect of *Jatropha curcas* for biodiesel in Indonesia," *Renewable and Sustainable Energy Reviews*, vol. 15, no. 8, pp. 3733–3756, 2011.

[9] F. Deeba, V. Kumar, K. Gautam, R. K. Saxena, and D. K. Sharma, "Bioprocessing of *Jatropha curcas* seed oil and deoiled seed hulls for the production of biodiesel and biogas," *Biomass and Bioenergy*, vol. 40, no. 5, pp. 13–18, 2012.

[10] F. S. Navarro-Pineda, S. A. Baz-Rodríguez, R. Handler, and J. C. Sacramento-Rivero, "Advances on the processing of *Jatropha curcas* towards a whole-crop biorefinery," *Renewable and Sustainable Energy Reviews*, vol. 54, no. 2, pp. 247–269, 2016.

[11] M. Moniruzzaman, Z. Yaakob, and R. Khatun, "Biotechnology for *Jatropha* improvement: a worthy exploration," *Renewable and Sustainable Energy Reviews*, vol. 54, no. 2, pp. 1262–1277, 2016.

[12] S. Nithiyanantham, P. Siddhuraju, and G. Francis, "Potential of *Jatropha curcas* as a biofuel, animal feed and health products," *Journal of the American Oil Chemists' Society*, vol. 89, no. 6, pp. 961–972, 2012.

[13] S. Lim and L. K. Teong, "Recent trends, opportunities and challenges of biodiesel in Malaysia: an overview," *Renewable and Sustainable Energy Reviews*, vol. 14, no. 3, pp. 938–954, 2010.

[14] K. Goswami, J. Saikia, and H. K. Choudhury, "Economic benefits and costs of jatropha plantation in North-East India," *Agricultural Economics Research Review*, vol. 24, no. 1, pp. 99–108, 2011.

[15] "Perspectives of Jatropha Production and Processing for Small-scale Producers," Jatropha Expert Meeting—Conference report, https://hivos.org/sites/default/files/publications/20121129conferencereportjatrophaexpertmeeting.pdf.

[16] U. S. Malik, M. Ahmed, M. A. Sombilla, and S. L. Cueno, "Biofuels production for smallholder producers in the Greater Mekong Sub-region," *Applied Energy*, vol. 86, supplement 1, pp. S58–S68, 2009.

[17] K. Goswami and H. K. Choudhury, "To grow or not to grow? Factors influencing the adoption of and continuation with Jatropha in North East India," *Renewable Energy*, vol. 81, pp. 627–638, 2015.

[18] A. S. Silitonga, A. E. Atabani, T. M. I. Mahlia, H. H. Masjuki, I. A. Badruddin, and S. Mekhilef, "Main technologies in biodiesel production: state of the art and future challenges," *Renewable and Sustainable Energy Reviews*, vol. 15, no. 8, pp. 3733–3756, 2011.

[19] B. Y. Lim, R. Shamsudin, B. T. H. T. Baharudin, and R. Yunus, "A review of processing and machinery for *Jatropha curcas* L. fruits and seeds in biodiesel production: harvesting, shelling, pretreatment and storage," *Renewable and Sustainable Energy Reviews*, vol. 52, no. 12, pp. 991–1002, 2015.

[20] A. N. Siregar, W. M. F. W. Mahmod, J. A. Ghani, C. H. C. Haron, and M. Riza, "Design and analysis of single screw extruder for jatropha seeds using finite element method," *Research Journal of Applied Sciences, Engineering and Technology*, vol. 7, no. 10, pp. 2098–2105, 2014.

[21] C. Bi and B. Jiang, "Study of residence time distribution in a reciprocating single-screw pin-barrel extruder," *Journal of Materials Processing Technology*, vol. 209, no. 8, pp. 4147–4153, 2009.

[22] R. Akinoso, A. O. Raji, and J. C. Igbeka, "Effects of compressive stress, feeding rate and speed of rotation on palm kernel oil yield," *Journal of Food Engineering*, vol. 93, no. 4, pp. 427–430, 2009.

[23] M. Petrů, O. Novák, D. Herák, and S. Simanjuntak, "Finite element method model of the mechanical behaviour of *Jatropha curcas* L. seed under compression loading," *Biosystems Engineering*, vol. 111, no. 4, pp. 412–421, 2012.

[24] M. Petrů, O. Novák, D. Herák, I. Mašín, P. Lepšík, and P. Hrabě, "Finite element method model of the mechanical behaviour of *Jatropha curcas* L. bulk seeds under compression loading: study and 2D modelling of the damage to seeds," *Biosystems Engineering*, vol. 127, no. 1, pp. 50–66, 2014.

[25] P. Sirisomboon and P. Kitchaiya, "Physical properties of Jatropha curcas L. kernels after heat treatments," *Biosystems Engineering*, vol. 102, no. 2, pp. 244–250, 2009.

[26] W. M. J. Achten, L. Verchot, Y. J. Franken et al., "Jatropha biodiesel production and use," *Biomass and Bioenergy*, vol. 32, no. 12, pp. 1063–1084, 2008.

[27] G. Pahl, W. Beitz, J. Feldhusen, and K. H. Grote, *Engineering Design. A Systematic Approach*, Springer, Berlin, Germany, 2007.

[28] S. Pugh, *Total Design. Integrated Methods for Successful Product Engineering*, Prentice Hall, 1991.

[29] N. P. Suh, *Axiomatic Design Advances and Application*, Oxford University Press, 2001.

[30] W. Eversheim, Ed., *Innovation Management for Technical Products. Systematic and Integrated Product Development and Production Planning*, Springer, Berlin, Germany, 2009.

[31] V. Hubka and W. E. Eder, *Theory of Technical Systems: A Total Concept Theory for Engineering Design*, Springer, 1988.

[32] W. E. Eder and S. Hosnedl, *Introduction to Design Engineering Systematic Creativity and Management*, CRC Press/Balkema, London, UK, 2010.

[33] M. Baxter, *Product Design: Practical Methods for the Systematic Development of New Products*, Chapman & Hall, London, UK, 1995.

[34] G. S. Altshuller, *Creativity as an Exact Science*, Gordon and Breach, 1988.

[35] J. Terninko, A. Zusman, and B. Zlotin, *Systematic Innovation: An Introduction to TRIZ (Theory of Inventive Problem Solving)*, CRC Press, New York, NY, USA, 1998.

[36] M. A. Orloff, *Inventive Thinking through TRIZ: A Practical Guide*, Springer, Berlin, Germany, 2006.

[37] J. Goldenberg and D. Mazursky, *Creativity in Product Innovation*, Cambridge University Press, Cambridge, Uk, 2002.

[38] G. Boothroyd, P. Dewhurst, and W. Knight, *Product Design for Manufacture and Assembly*, Marcel Dekker, 2002.

[39] D. M. Anderson, *Design for Manufacturability*, CRC Press, 2014.

[40] B. Bergman, J. de Mare, T. Svensson, and S. Loren, *Robust Design Methodology for Reliability: Exploring the Effects of Variation and Uncertainty*, John Wiley & Sons, 2009.

[41] K. T. Ulrich and S. D. Eppinger, *Product Design and Development*, McGraw-Hill Education, New York, NY, USA, 2015.

[42] A. Chakrabarti, *Engineering Design Synthesis. Understanding, Approaches and Tools*, Springer, New York, NY, USA, 2010.

[43] D. F. Ciambrone, *Effective Transition from Design to Production*, Taylor and Francis, 2008.

[44] N. Bradley, *Marketing Research: Tools and Techniques*, Oxford University Press, 2013.

[45] D. Bridger, *Decoding the Irrational Consumer: How to Commission, Run and Generate Insights from Neuromarketing Research*, Marketing Science, Kogan Page, 2015.

[46] K. Yang, *Voice of the Customer Capture and Analysis*, McGraw-Hill, New York, NY, USA, 2008.

[47] R. F. Mateo Ferrús and M. D. Somonte, "Design in robotics based in the voice of the customer of household robots," *Robotics and Autonomous Systems*, vol. 79, no. 5, pp. 99–107, 2016.

[48] D. Ruiz, D. Jain, and K. Grayson, "Subproblem decomposition: an exploratory research method for effective incremental new product development," *Journal of Product Innovation Management*, vol. 29, no. 3, pp. 385–404, 2012.

[49] C. Barnum, *Usability Testing Essentials*, Morgan Kaufmann, 2010.

[50] M. Nagamachi, Ed., *Kansei/Affective Engineering*, CRC Press, New York, NY, USA, 2011.

[51] P. Tarantino, *Kansei Engineering: Statistical Approaches for Innovation and Early Product Development*, LAP Lambert Academic Publishing, 2013.

[52] Y. Akao, Ed., *Quality Function Deployment. Integrating Customer Requirements into Product Design*, Productivity Press, 1990.

[53] J. P. Ficalora and L. Cohen, *Quality Function Deployment and Six Sigma. A QFD Handbook*, Prentice Hall, Upper Saddle River, NJ, USA, 2010.

[54] F. Francessini, *Advanced Quality Function Deployment*, St. Lucia Press, 2002.

[55] K. M. Kamarudin, K. Ridgway, and M. R. Hassan, "Modelling the conceptual design process with hybridization of TRIZ methodology and systematic design approach," *Procedia Engineering*, vol. 131, pp. 1064–1072, 2015.

[56] L. S. Chechurin, W. W. Wits, H. M. Bakker, and T. H. J. Vaneker, "Introducing trimming and function ranking to solidworks based on function analysis," *Procedia Engineering*, vol. 131, pp. 184–193, 2015.

[57] What Are Main Parameters of Value (MPV's)?, http://www.gen3partners.com/methodology/innovation-processes/main-parameters-of-value.

[58] K. Gadd, *TRIZ for Engineers. Enabling Inventive Problem Solving*, Wiley, 2011.

[59] Z. A. Rahim, I. L. S. Sheng, and A. B. Nooh, "TRIZ methodology for applied chemical engineering: a case study of new product development," *Chemical Engineering Research and Design*, vol. 103, pp. 11–24, 2015.

[60] G. Cameron, *Trizics: Teach Yourself Triz, How to Invent, Innovate and Solve Impossible Technical Problems Systematically*, Createspace, 2010.

[61] M. A. Orloff, *Modern Triz: A Practical Course with Easy Triz Technology*, Springer, New York, NY, USA, 2012.

[62] S. S. Litvin, "New TRIZ-based tool—Function-Oriented Search (FOS)," in *Proceedings of the ETRIA Conference: TRIZ Future*, pp. 505–509, Florence, Italy, November 2004.

[63] T. Montecchi and D. Russo, "FBOS: function/behaviour–oriented search," *Procedia Engineering*, vol. 131, pp. 140–149, 2015.

[64] 40 Principles: Triz Keys to Technical Innovation, Technical Innovation Ctr, 1997.

[65] M. A. de Carvalho, S. D. Savransky, and T. Wei, *121 Heuristics for Solving Problems*, Lulu.com, Raleigh, NC, USA, 2004.

[66] S. Filippi and D. Barattin, "Definition and exploitation of trends of evolution about interaction," *Technological Forecasting and Social Change*, vol. 86, pp. 216–236, 2014.

[67] D. Zouaoua, P. Crubleau, D. Choulier, and S. Richir, "Application of evolution laws," *Procedia Engineering*, vol. 131, pp. 922–932, 2015.

[68] S. D. Savransky, *Introduction to TRIZ Methodology of Inventive problem Solving*, CRC Press, Boca Raton, Fla, USA, 2000.

[69] D. Mann, *Hands on Systematic Innovation: For Business and Management*, Edward Gaskell, 2004.

[70] V. Hubka, M. M. Andreasen, and W. E. Eder, *Practical Studies in Systematic Design*, Butterworths, 1988.

[71] N. Cross, *Engineering Design Methods*, John Wiley & Sons, New York, NY, USA, 1995.

[72] D. Herak, A. Kabutey, R. Choteborsky, M. Petru, and R. Sigalingging, "Mathematical models describing the relaxation behaviour of *Jatropha curcas* L. bulk seeds under axial compression," *Biosystems Engineering*, vol. 131, pp. 77–83, 2015.

[73] M. Raß, "Einstellung der verarbeitungseigenschaften von rapssaat für das trennpressen," in *Dezentrale Ölsatenverarbeitung, Warum und Wie?* KTBL-Arbeitspapier 167, pp. 46–58, KTBL, Darmstadt. Landwirtschaftsverlag GmbH, Münster, Germany, 1999.

Hindawi Publishing Corporation
BioMed Research International
Volume 2016, Article ID 8568604, 7 pages
http://dx.doi.org/10.1155/2016/8568604

Research Article

Structural Changes of Lignin after Liquid Hot Water Pretreatment and Its Effect on the Enzymatic Hydrolysis

Wen Wang,[1] Xinshu Zhuang,[1] Zhenhong Yuan,[1,2] Wei Qi,[1] Qiang Yu,[1] and Qiong Wang[1]

[1]*Key Laboratory of Renewable Energy and Guangdong Key Laboratory of New and Renewable Energy Research and Development, Guangzhou Institute of Energy Conversion, Chinese Academy of Sciences, Guangzhou 510640, China*
[2]*Collaborative Innovation Center of Biomass Energy, Zhengzhou 450002, China*

Correspondence should be addressed to Zhenhong Yuan; yuanzh@ms.giec.ac.cn

Received 14 March 2016; Accepted 13 June 2016

Academic Editor: Encarnación Ruiz

During liquid hot water (LHW) pretreatment, lignin is mostly retained in the pretreated biomass, and the changes in the chemical and structural characteristics of lignin should probably refer to re-/depolymerization, solubilization, or glass transition. The residual lignin could influence the effective enzymatic hydrolysis of cellulose. The pure lignin was used to evaluate the effect of LHW process on its structural and chemical features. The surface morphology of LHW-treated lignin observed with the scanning electron microscopy (SEM) was more porous and irregular than that of untreated lignin. Compared to the untreated lignin, the surface area, total pore volume, and average pore size of LHW-treated lignin tested with the Brunner-Emmet-Teller (BET) measurement were increased. FTIR analysis showed that the chemical structure of lignin was broken down in the LHW process. Additionally, the impact of untreated and treated lignin on the enzymatic hydrolysis of cellulose was also explored. The LHW-treated lignin had little impact on the cellulase adsorption and enzyme activities and somehow could improve the enzymatic hydrolysis of cellulose.

1. Introduction

Bioethanol production from lignocellulosic biomass has gained focus for easy availability of feedstock, no competition with the food supply, and reduction in net carbon emission [1, 2]. Cellulose, hemicellulose, and lignin which are the main components of lignocellulosic materials form complex and compact structure via covalent and noncovalent bonds to make lignocellulose resist the microbial and enzymatic attack [1]. Pretreatment followed by enzymatic hydrolysis and fermentation is an essential process for the effective bioconversion of lignocellulose to ethanol. The pretreatment can lead to changes in the structure and chemical composition of biomass and thus create new features for the pretreated biomass [3]. Liquid hot water (LHW) which is a hydrothermal pretreatment makes the pretreated biomass mainly composed of cellulose and lignin [4]. The residual lignin in the pretreated lignocellulose can negatively influence the enzymatic hydrolysis of cellulose via physical barrier and enzyme adsorption [4–6], and its chemical and structural characteristics are changed due to depolymerization and condensation reactions during LHW pretreatment [7]. Ko et al. [7] extracted lignin from LHW-pretreated hardwoods at four different severities through extensive enzymatic hydrolysis and found that lignin that suffered at more severity of LHW pretreatment exhibited more significant inhibition on enzymatic hydrolysis. The pretreatment type, biomass source, and isolation method determined the characteristics of lignin which would exhibit various impacts on enzymatic hydrolysis [8].

The authors found that a part of cellulose always existed in lignin extractive through the extensive enzymatic hydrolysis of LHW-treated lignocellulose. The residual cellulose in lignin extractive may influence the following research such as enzyme adsorption and enzymatic hydrolysis. In general, the milled wood lignin (MWL) and cellulolytic enzyme lignin (CEL) have been thought to nearly resemble the native lignin. However, the ball-milling process for isolating MWL could result in β-ether cleavage [9], and the isolation procedure for CEL could increase phenolic β-O-4 content [10] and

reduce molecular weight [11]. Recently, She et al. [12] reported that alkali could not change the main structural feature of lignin preparations isolated with 50% dioxane. Although the MWL and CEL have been used as representative sources for structural and chemical analysis of lignin, the application of alkali lignin for further analysis might provide compensatory research. Alkali lignin has seldom been used for characteristic analysis of lignin mainly due to its high amount of nonlignin components, especially hemicellulose [13]. In this study, the relative pure alkali lignin was used to investigate the effect of LHW pretreatment on structural and chemical changes of lignin. The effect of LHW-treated lignin on enzymatic hydrolysis of pure cellulose was investigated. This study was a preliminary try to explore the structural and chemical changes of lignin in the LHW process and would provide useful information for the future research.

2. Materials and Methods

2.1. Materials. The alkali lignin with 5% moisture (Product ID: 370595) was purchased from Sigma-Aldrich (Shanghai) Trading Co., Ltd. It was composed of 85.0% lignin, 1.3% glucan, and 1.3% xylan. Whatman number 1 filter papers were purchased from Guangzhou Maolin Instrument Co., Ltd. (China). Cellulase whose filter paper activity was 151.7 FPU/g powder was purchased from Imperial Jade Bio-technology Co. Ltd. (China).

2.2. Pretreatment. The alkali lignin was pretreated by liquid hot water under the condition of 180°C, 4 MPa, 20 min, which was the optimized operation in the previous study [14]. The ratio of lignin to water was 1 : 20 (g : mL). After pretreatment, the solid residue was air-dried at room temperature and then stored in the desiccator. The LHW-treated lignin was composed of 90.7% lignin and 1.4% glucan.

Whatman number 1 filter papers were cut into pieces in size of less than 1 cm × 1 cm. The pieces were ground at 25000 rpm for 1 min with the swing pulverizer (Guangzhou Daxiang Electronic Machinery Co., Ltd., China) and then stored in the desiccator.

2.3. Enzymatic Hydrolysis. The filter paper and lignin mixed in the mass ratio of 0.1 : 0.03 were loaded into a 5 mL Eppendorf tube containing 2.6 mL 0.05 M citrate buffer (pH 4.8). The tubes were sealed with parafilm and fixed on a salver and then placed into a rotatory shaker which was set at 50°C, 150 rpm. The hydrolysis was performed for 72 h with the cellulase loadings of 5, 10, 20, and 40 FPU/g filter paper. The filter papers hydrolyzed under the same conditions without lignin addition were used as the controls. Meanwhile, the filter paper mixing with lignin in the mass ratio of 0.1 : 0.05 was also hydrolyzed with 15 FPU/g filter paper cellulase loadings under the same condition.

2.4. Enzyme Activity Assay. The enzyme solution was prepared with 0.198 g cellulase and 10 mL 0.05 M citrate buffer (pH 4.8). The Eppendorf tubes containing 3 mL enzyme solution with and without 30 mg lignin were sealed with parafilm and taped on a salver and then placed into a rotatory shaker at the speed of 150 rpm. After incubating at 50°C for 60 min, the filter paper and CMCase activities of the samples were assayed according to the described methods [15]. The β-glucosidase activity was assayed with p-nitrophenyl-β-D-glucopyranoside (pNPG) method described in [16].

2.5. Adsorption. The filter paper, lignin, and their mixture in the mass ratio of 0.6 : 0.3 were loaded into 50 mL conical flasks containing 20 mL enzyme solution, respectively. The cellulase loading was 20 FPU/g filter paper. The flasks were placed into a rotatory shaker under the condition of 50°C, 150 rpm. The solutions with volume of 200 μL were taken at 5, 10, 15, 20, 40, 60, 80, 100, 120, and 180 min. The protein content was quantified according to the previous method [4]. All of the experiments in this study were in duplicate.

2.6. Analytic Methods. Compositional analysis was carried out as the procedure described by the National Renewable Energy Laboratory (NREL) [17]. Lignin treated with and without LHW was coated with a thin layer of gold and then observed with a scanning electron microscope (SEM, S-4800, Hitachi) under an accelerating voltage of 2.0 kV. FTIR test was conducted according to the described KBr pellet technique with a TENSOR 27 Fourier transform infrared spectrometer (Bruker Optics, Germany) [18]. The special surface area, pore size, and total pore volume of lignin were analyzed with the automated surface and porosity analyzer (SI-MP-10/PoreMaster 33, Quantachrome Instruments, USA). Sulfur content of lignin was determined with the elemental analyzer (vario EL cube, Germany). The HPLC system (Waters 2698, USA) equipped with a sugar column (SH1011, Shodex) was applied to measure the sugar concentrations at 50°C with 5 mM H_2SO_4 used as the mobile phase at the flow rate of 0.5 mL/min.

3. Results and Discussion

3.1. Surface Structure. Liquid hot water is a promising green pretreatment. LHW-treated biomass is mainly composed of cellulose and lignin. LHW pretreatment caused the redistribution of lignin which could influence the enzymatic hydrolysis [19]. In order to discover the changes of lignin during LHW pretreatment, pure alkali lignin was used in this study to avoid the interruption from cellulose and hemicellulose. The pure lignin which was pretreated at 180°C, 4 MPa, for 20 min was air-dried at room temperature to alleviate the influence of high oven temperature on the surface structure [20]. The photographs and SEM observed morphologies of untreated and treated lignin were shown in Figure 1. The untreated lignin was brown and granular (Figure 1(a)), while the treated lignin was yellow and powdered (Figure 1(b)). As for the SEM observed morphologies, the untreated lignin was smooth (Figure 1(c)), while the treated lignin was porous and irregular (Figure 1(d)). These indicated that changes happened to lignin during LHW pretreatment. It was reported that lignin can be melted at temperatures from 170°C to 180°C and redeposited with the temperature decreasing [21].

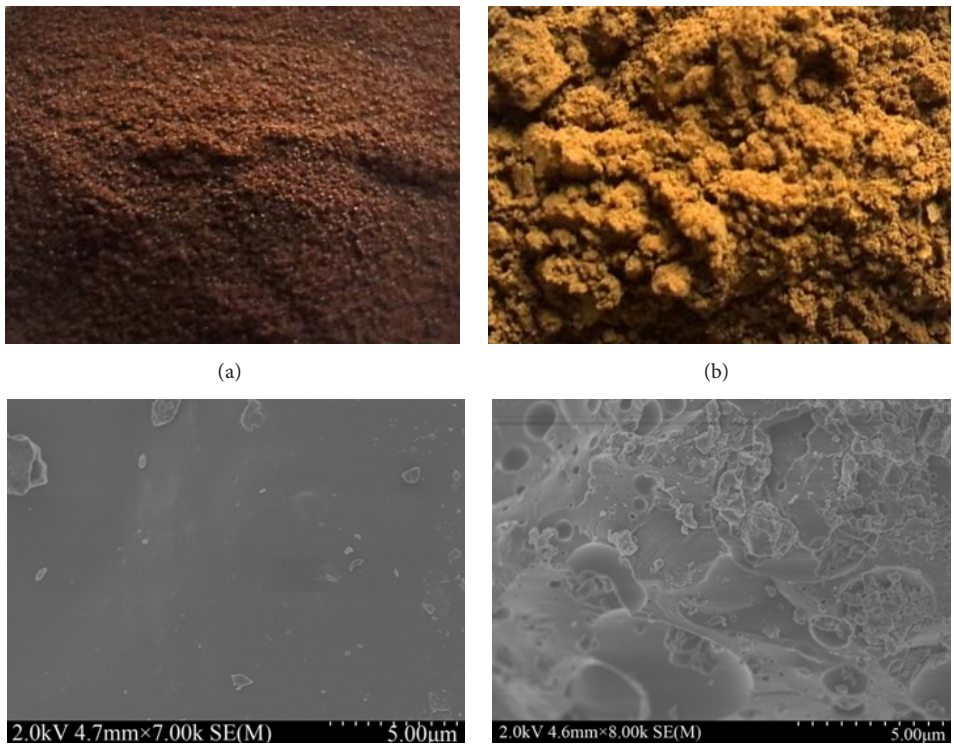

FIGURE 1: Photographs and SEM observed morphologies of LHW-untreated and LHW-treated lignin, (a) photograph of untreated lignin, (b) photograph of treated lignin, (c) SEM observed untreated lignin, and (d) SEM observed treated lignin.

The surface changes of lignin were quantified with the BET analysis. The BET results of untreated and treated lignin were shown in Table 1. Compared with the untreated lignin, the surface area, total pore volume, and average pore size of treated lignin were raised nearly four times, eight times, and one time, respectively. The increase of surface area meant that the adsorption of cellulase to lignin might be improved. The increase in total pore volume and average pore size might contribute to the access of cellulase to cellulose. It might be deduced that there might be double effects of LHW-treated lignin on the enzymatic hydrolysis. One was that the lignin reduced the cellulolytic efficiency through adsorbing cellulase; the other was that the increase in the pore size of lignin could improve the access of cellulase to cellulose.

3.2. FTIR Analysis. The changes of the chemical groups were analyzed with FTIR method. The result was presented in Figure 2. The spectrogram shape of the untreated and treated lignin was almost the same, but the absorbance of treated lignin was stronger than that of untreated lignin, which meant that either new chemical groups were formed or new connections of chemical bonds were built in the LHW process. The band at 3600–3050 cm^{-1} is assigned to O-H stretching vibration which is attributed to the aliphatic and phenolic hydroxyl groups in lignin [22]. The intermolecular and intramolecular hydrogen bonds existed in the aliphatic and phenolic hydroxyl groups, such as O(2)H$\cdots$O(6) intramolecular H-bond, O(3)H$\cdots$O(5) intramolecular H-bond, and O(6)H$\cdots$O(3′) intermolecular H-bond. The stronger absorbance of LHW-treated lignin indicated that, after LHW pretreatment, the H-bond connections of the aliphatic and phenolic hydroxyl groups might be improved or new free hydroxyl groups might be formed in the

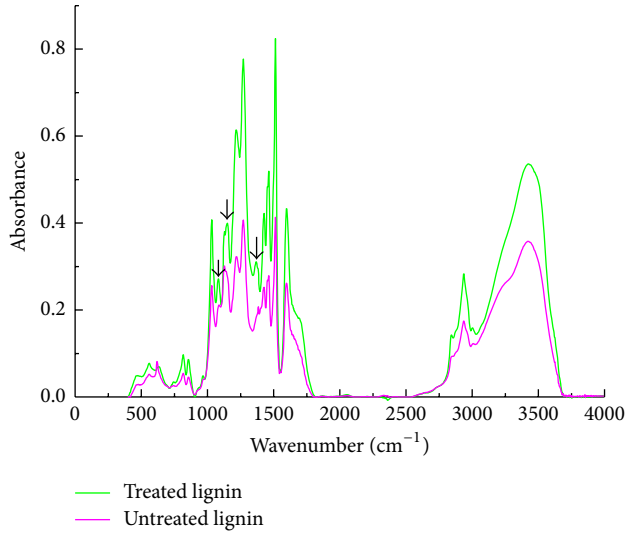

FIGURE 2: FTIR spectrograms of LHW-untreated and LHW-treated lignin.

Table 1: BET measurements of the LHW-untreated and LHW-treated lignin.

	Surface area (m^2/g)	Total pore volume (cc/g)	Average pore diameter (nm)
Untreated lignin	27.12	0.06	8.78
Treated lignin	125.81	0.53	16.87

Table 2: Assignments of characteristic peaks in FTIR spectrogram.

Wavenumber (cm^{-1})	Assignments of characteristic peaks
2937	C-H stretching vibrations in methyl and methylene
1597	Stretching vibrations of aromatic skeleton and C=O
1514	Vibrations of aromatic skeleton
1463	C-H deformations in methyl
1427	Plane deformation of C-H in aromatic skeleton
1271	Stretching vibrations of guaiacyl ring and C=O
1217	Stretching vibrations of C-C, C-O, and C=O
1032	Plane deformations of aromatic C-H, C-O deformations in primary alcohols, and C=O stretching vibrations
856	C-H vibrations in the positions of 2, 5, and 6 out of the plane of guaiacyl units

LHW process. It could be seen from Figure 2 that, after LHW pretreatment, the peaks of lignin at the bands of 1082, 1151, and 1367 cm^{-1} which were marked with the arrows appeared. The bands at 1082, 1151, and 1367 cm^{-1} are assigned to C-O deformation in the secondary alcohols and aliphatic ethers, C-O stretching vibration in the tertiary alcohols, and C-H stretching vibration in the aliphatic methyl and phenol OH, respectively. The assignments of other characteristic peaks were summarized in Table 2. According to the enhanced absorbance of LHW-treated lignin, it could be inferred that some connections of chemical bonds in lignin were broken down, and some new free chemical groups were generated in the process of LHW pretreatment.

3.3. The Effect of Lignin on the Enzyme Activity and Adsorption. The main inhibition of lignin on enzymatic hydrolysis was thought to be the nonproductive adsorption of cellulase. Figure 3 showed the adsorption of cellulase to cellulose and treated lignin. The mixture of untreated lignin and citrate buffer presented brown color which interrupted the testing result. Therefore, the adsorption of cellulase to untreated lignin was not shown here. As time goes on, the adsorption of cellulase to treated lignin was at around 5%, while the adsorption of cellulase to filter paper increased from 6.3% to 52.6%. The adsorption of cellulase to the mixture of filter paper and treated lignin was nearly equal to the summation of individual adsorption from filter paper and treated lignin. It meant that the adsorption of cellulase was mainly attributed to the cellulose, which was corresponding to the previous research [23]. Zheng et al. [23] also found that the lignin imposed little impact on the apparent enzyme activity. The same phenomenon was observed in this study and presented in Figure 4. The enzyme activities with and without addition of lignin were measured. The relative enzyme activities were calculated as the ratio of enzyme activities with lignin to that without lignin. After adding untreated and treated lignin, the relative enzyme activities retained more than 90%. The treated lignin hardly put impact on the CMCase activity. The little impact on the enzyme activities might be caused by the little adsorption of cellulase to lignin.

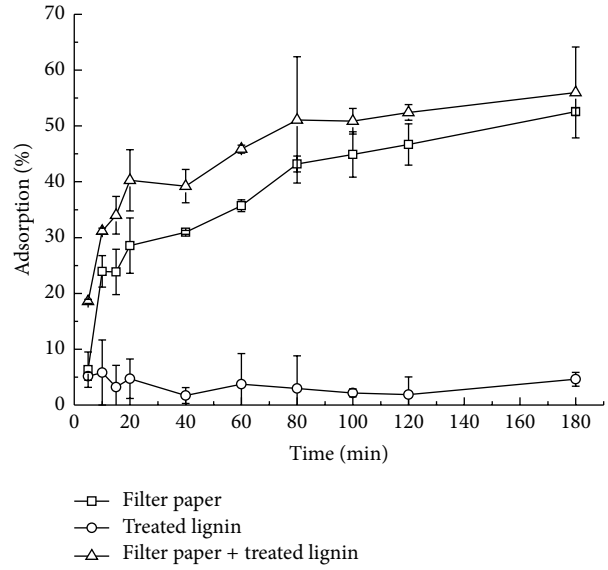

Figure 3: Adsorption of cellulase to LHW-treated lignin, filter paper, and their mixture.

3.4. Enzymatic Hydrolysis. The effect of untreated and treated lignin on the enzymatic hydrolysis of cellulose was carried out in the 5 mL Eppendorf tubes which were sealed with parafilms to avoid the water evaporation. The mass ratio of lignin to cellulose was from 30% to 50% which was in

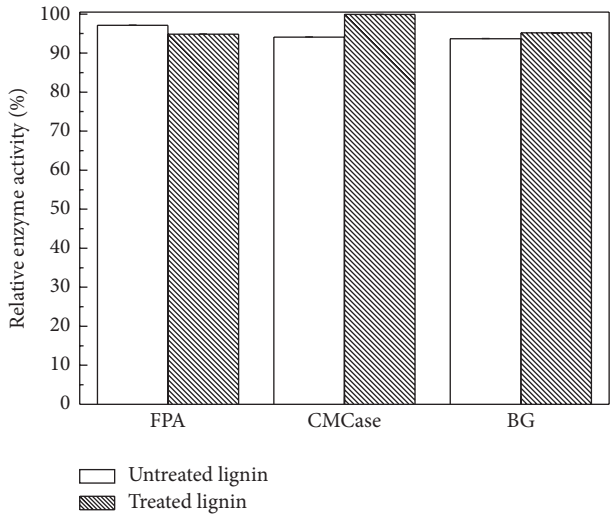

Figure 4: The effect of LHW-untreated and LHW-treated lignin on enzyme activities.

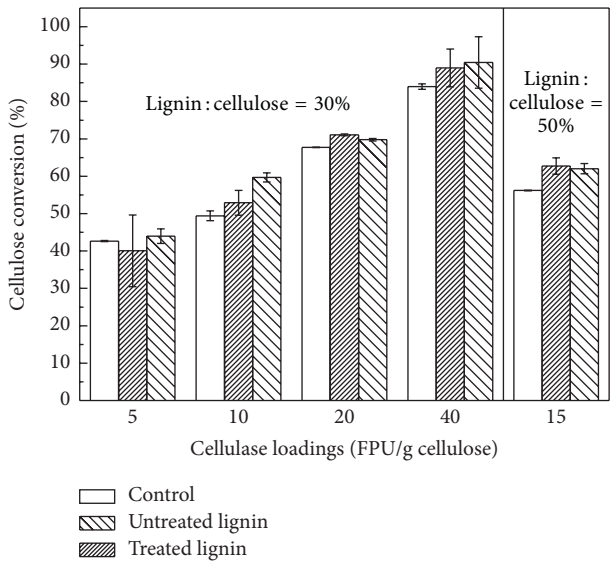

Figure 5: Enzymatic hydrolysis of filter paper in the presence of LHW-untreated and LHW-treated lignin at 50°C for 72 h.

analogy to the contents of lignin and cellulose in the LHW-treated biomass [18]. The ratio of solid to liquid was 5% to relieve the negative effect of viscosity on the enzymatic hydrolysis. The effects of lignin and cellulase loadings on the enzymatic hydrolysis were explored, and the 72-hour enzymatic hydrolyzed results were shown in Figure 5.

Both untreated and treated lignin could improve the enzymatic hydrolysis of cellulose at the lignin loadings of 30% and 50% and cellulase loadings of 5, 10, 20, and 40 FPU/g cellulose. These were contradictory with the previous researches which reported that lignin could inhibit the enzymatic hydrolysis of cellulose [24, 25]. Recently, several researches had reported that lignosulfonate could reduce the nonproductive adsorption of cellulase to lignin through the electrostatic repulsion or acting as the surfactant to enhance the enzymatic hydrolysis of lignocellulose [26–28]. Considering the isolation procedure of alkali lignin, the sulfur content of the alkali lignin used in this study was detected. It showed that the untreated and treated lignin had 1.83% and 1.23% sulfur content, respectively, which were lower than the least sulfur content of the lignosulfonate (5.27%) used in Zhou's research [26]. The improvement of lignin on the enzymatic hydrolysis of cellulose might originate from the small part of lignosulfonate existing in the lignin. Although the treated lignin adsorbed a little cellulase and thus slightly reduced the enzyme activities (Figures 3 and 4), the enzymatic hydrolysis of cellulose was improved (Figure 5). This meant that the negative effect of LHW-treated lignin on the enzymatic hydrolysis could be neglected.

From Figure 5, it also could be seen that the cellulose conversion was increased with the cellulase loading increasing. Whatman number 1 filter paper was used as the pure cellulose to assay the enzyme activity of cellulase in Ghose's method [14]. When the cellulase loading achieved 40 FPU/g cellulose, the conversion of filter paper (the control in Figure 5) did not reach 100% but was just close to 85%. It suggested that the lignin was not the main factor influencing the enzymatic hydrolysis. Although several researches had reported that the removal of lignin could enhance the enzymatic hydrolysis of lignocellulose [29–31], the methods used to remove lignin in their research could induce the structural changes of the lignocellulose. It would be not accurate to only discuss the effect of lignin removal on the enzymatic hydrolysis of lignocellulose. The crystallinity, particle size, nature of the residual lignin and substrate loading, and cellulose accessibility were reported to affect the enzymatic hydrolysis of cellulose [32–36]. The method to extract lignin from lignocellulose could more or less change the native structural characteristics of lignin. The investigation on the impact of lignin extractive on the enzymatic hydrolysis of cellulose may never reflect the real influence mechanism of lignin in the lignocellulose, but it can push the way to discover the truth. A method of reconstructing individual lignin, cellulose, and hemicellulose into a complex should be developed to simulate the lignocellulose. Through the reconstruction, the influence mechanism of lignocellulosic components and structure on enzymatic hydrolysis should be finally disclosed.

4. Conclusion

The research on the untreated and treated alkali lignin suggested that the chemical and structural characteristics of lignin were changed in the LHW process. The residual lignin in the LHW-treated lignocellulose which had similar structural and chemical features with the LHW-treated alkali lignin might put its impact on enzymatic hydrolysis of cellulose not via the nonproductive adsorption of cellulase.

Competing Interests

The authors declare that there is no conflict of interests regarding the publication of this paper.

Acknowledgments

This study was financially supported by the National Basic Research Program of China (973 Program, 2012CB215300), the National Natural Science Foundation of China (21476233, 51176196, 21206163, and 21506216), and the President Innovation Foundation of Guangzhou Institute of Energy Conversion (y207r1).

References

[1] A. R. C. Morais, A. M. Da Costa Lopes, and R. Bogel-Łukasik, "Carbon dioxide in biomass processing: contributions to the green biorefinery concept," *Chemical Reviews*, vol. 115, no. 1, pp. 3–27, 2015.

[2] L. Paulova, P. Patakova, B. Branska, M. Rychtera, and K. Melzoch, "Lignocellulosic ethanol: technology design and its impact on process efficiency," *Biotechnology Advances*, vol. 33, no. 6, pp. 1091–1107, 2015.

[3] M. Shafiei, K. Karimi, H. Zilouei, and M. J. Taherzadeh, "Enhanced ethanol and biogas production from pinewood by NMMO pretreatment and detailed biomass analysis," *BioMed Research International*, vol. 2014, Article ID 469378, 10 pages, 2014.

[4] W. Wang, X. Zhuang, Z. Yuan, Q. Yu, and W. Qi, "Investigation of the pellets produced from sugarcane bagasse during liquid hot water pretreatment and their impact on the enzymatic hydrolysis," *Bioresource Technology*, vol. 190, pp. 7–12, 2015.

[5] J. K. Ko, E. Ximenes, Y. Kim, and M. R. Ladisch, "Adsorption of enzyme onto lignins of liquid hot water pretreated hardwoods," *Biotechnology and Bioengineering*, vol. 112, no. 3, pp. 447–456, 2015.

[6] Y. Kim, T. Kreke, J. K. Ko, and M. R. Ladisch, "Hydrolysis-determining substrate characteristics in liquid hot water pretreated hardwood," *Biotechnology and Bioengineering*, vol. 112, no. 4, pp. 677–687, 2015.

[7] J. K. Ko, Y. Kim, E. Ximenes, and M. R. Ladisch, "Effect of liquid hot water pretreatment severity on properties of hardwood lignin and enzymatic hydrolysis of cellulose," *Biotechnology and Bioengineering*, vol. 112, no. 2, pp. 252–262, 2015.

[8] S. Nakagame, R. P. Chandra, J. F. Kadla, and J. N. Saddler, "The isolation, characterization and effect of lignin isolated from steam pretreated Douglas-fir on the enzymatic hydrolysis of cellulose," *Bioresource Technology*, vol. 102, no. 6, pp. 4507–4517, 2011.

[9] A. Fujimoto, Y. Matsumoto, H.-M. Chang, and G. Meshitsuka, "Quantitative evaluation of milling effects on lignin structure during the isolation process of milled wood lignin," *Journal of Wood Science*, vol. 51, no. 1, pp. 89–91, 2005.

[10] T. Ikeda, K. Holtman, J. F. Kadla, H.-M. Chang, and H. Jameel, "Studies on the effect of ball milling on lignin structure using a modified DFRC method," *The Journal of Agricultural and Food Chemistry*, vol. 50, no. 1, pp. 129–135, 2002.

[11] H. M. Chang, E. B. Cowling, W. Brown, E. Adler, and G. Miksche, "Comparative studies on cellulolytic enzyme lignin and milled wood lignin of sweetgum and spruce," *Holzforschung*, vol. 29, pp. 153–159, 1975.

[12] D. She, F. Xu, Z. Geng, R. Sun, G. L. Jones, and M. S. Baird, "Physicochemical characterization of extracted lignin from sweet sorghum stem," *Industrial Crops and Products*, vol. 32, no. 1, pp. 21–28, 2010.

[13] R. Sun, J. M. Lawther, and W. B. Banks, "Effects of extraction time and different alkalis on the composition of alkali-soluble wheat straw lignins," *The Journal of Agricultural and Food Chemistry*, vol. 44, no. 12, pp. 3965–3970, 1996.

[14] Q. Yu, X. Zhuang, Q. Wang, W. Qi, X. Tan, and Z. Yuan, "Hydrolysis of sweet sorghum bagasse and eucalyptus wood chips with liquid hot water," *Bioresource Technology*, vol. 116, pp. 220–225, 2012.

[15] K. Ghose T, "Measurement of cellulose activities," *Pure & Applied Chemistry*, vol. 59, pp. 257–268, 1987.

[16] W. Wang, X. Zhuang, Z. Yuan et al., "Highly efficient conversion of sugarcane bagasse pretreated with liquid hot water into ethanol at high solid loading," *International Journal of Green Energy*, vol. 13, no. 3, pp. 298–304, 2016.

[17] A. Sluiter, B. Hames, R. Ruiz et al., "Determination of structural carbohydrates and lignin in biomass," Tech. Rep. NREL/TP-510-42618, 2008.

[18] W. Wang, X. Zhuang, Z. Yuan et al., "Effect of structural changes on enzymatic hydrolysis of eucalyptus, sweet sorghum bagasse, and sugarcane bagasse after liquid hot water pretreatment," *Bioresources*, vol. 7, no. 2, pp. 2469–2482, 2012.

[19] B. S. Donohoe, S. R. Decker, M. P. Tucker, M. E. Himmel, and T. B. Vinzant, "Visualizing lignin coalescence and migration through maize cell walls following thermochemical pretreatment," *Biotechnology and Bioengineering*, vol. 101, no. 5, pp. 913–925, 2008.

[20] X. Luo and J. Y. Zhu, "Effects of drying-induced fiber hornification on enzymatic saccharification of lignocelluloses," *Enzyme and Microbial Technology*, vol. 48, no. 1, pp. 92–99, 2011.

[21] M. Zeng, E. Ximenes, M. R. Ladisch et al., "Tissue-specific biomass recalcitrance in corn stover pretreated with liquid hot-water: SEM imaging (part 2)," *Biotechnology and Bioengineering*, vol. 109, no. 2, pp. 398–404, 2012.

[22] M. Poletto, A. J. Zattera, and R. M. C. Santana, "Structural differences between wood species: evidence from chemical composition, FTIR spectroscopy, and thermogravimetric analysis," *Journal of Applied Polymer Science*, vol. 126, no. 1, pp. E336–E343, 2012.

[23] Y. Zheng, S. Zhang, S. Miao, Z. Su, and P. Wang, "Temperature sensitivity of cellulase adsorption on lignin and its impact on enzymatic hydrolysis of lignocellulosic biomass," *Journal of Biotechnology*, vol. 166, no. 3, pp. 135–143, 2013.

[24] A. Várnai, M. Siika-aho, and L. Viikari, "Restriction of the enzymatic hydrolysis of steam-pretreated spruce by lignin and hemicellulose," *Enzyme and Microbial Technology*, vol. 46, no. 3-4, pp. 185–193, 2010.

[25] J. L. Rahikainen, R. Martin-Sampedro, H. Heikkinen et al., "Inhibitory effect of lignin during cellulose bioconversion: the effect of lignin chemistry on non-productive enzyme adsorption," *Bioresource Technology*, vol. 133, pp. 270–278, 2013.

[26] H. Zhou, H. Lou, D. Yang, J. Y. Zhu, and X. Qiu, "Lignosulfonate to enhance enzymatic saccharification of lignocelluloses: role of molecular weight and substrate lignin," *Industrial & Engineering Chemistry Research*, vol. 52, no. 25, pp. 8464–8470, 2013.

[27] Z. Wang, J. Y. Zhu, Y. Fu et al., "Lignosulfonate-mediated cellulase adsorption: Enhanced enzymatic saccharification of lignocellulose through weakening nonproductive binding to lignin," *Biotechnology for Biofuels*, vol. 6, article 156, 2013.

[28] H. Lou, M. Wang, H. Lai et al., "Reducing non-productive adsorption of cellulase and enhancing enzymatic hydrolysis of lignocelluloses by noncovalent modification of lignin with

lignosulfonate," *Bioresource Technology*, vol. 146, pp. 478–484, 2013.

[29] S. I. Mussatto, M. Fernandes, A. M. F. Milagres, and I. C. Roberto, "Effect of hemicellulose and lignin on enzymatic hydrolysis of cellulose from brewer's spent grain," *Enzyme and Microbial Technology*, vol. 43, no. 2, pp. 124–129, 2008.

[30] G. J. M. Rocha, V. F. N. Silva, C. Martín, A. R. Gonçalves, V. M. Nascimento, and A. M. Souto-Maior, "Effect of xylan and lignin removal by hydrothermal pretreatment on enzymatic conversion of sugarcane bagasse cellulose for second generation ethanol production," *Sugar Tech*, vol. 15, no. 4, pp. 390–398, 2013.

[31] S. Lv, Q. Yu, X. Zhuang et al., "The influence of hemicellulose and lignin removal on the enzymatic digestibility from sugarcane bagasse," *Bioenergy Research*, vol. 6, no. 4, pp. 1128–1134, 2013.

[32] L. Rosgaard, P. Andric, K. Dam-Johansen, S. Pedersen, and A. S. Meyer, "Effects of substrate loading on enzymatic hydrolysis and viscosity of pretreated barley straw," *Applied Biochemistry and Biotechnology*, vol. 143, no. 1, pp. 27–40, 2007.

[33] M. Yoshida, Y. Liu, S. Uchida et al., "Effects of cellulose crystallinity, hemicellulose, and lignin on the enzymatic hydrolysis of *Miscanthus sinensis* to monosaccharides," *Bioscience, Biotechnology and Biochemistry*, vol. 72, no. 3, pp. 805–810, 2008.

[34] S. Nakagame, R. P. Chandra, and J. N. Saddler, "The effect of isolated lignins, obtained from a range of pretreated lignocellulosic substrates, on enzymatic hydrolysis," *Biotechnology and Bioengineering*, vol. 105, no. 5, pp. 871–879, 2010.

[35] A.-I. Yeh, Y.-C. Huang, and S. H. Chen, "Effect of particle size on the rate of enzymatic hydrolysis of cellulose," *Carbohydrate Polymers*, vol. 79, no. 1, pp. 192–199, 2010.

[36] J. A. Rollin, Z. Zhu, N. Sathitsuksanoh, and Y.-H. P. Zhang, "Increasing cellulose accessibility is more important than removing lignin: a comparison of cellulose solvent-based lignocellulose fractionation and soaking in aqueous ammonia," *Biotechnology and Bioengineering*, vol. 108, no. 1, pp. 22–30, 2011.